Spring 4-29-2013

Characterization of the Placenta-Specific 8.1 Gene Function during Zebrafish Embryogenesis

Haiting Ma
Washington University in St. Louis

WASHINGTON UNIVERSITY IN ST. LOUIS

Division of Biology and Biomedical Sciences
Developmental, Regenerative and Stem Cell Biology

Dissertation Examination Committee:
Lilianna Solnica-Krezel, Chair
Philip V. Bayly
Robert J. Coffey
Susan K. Dutcher
Raphael Kopan
Gregory D. Longmore

Characterization of the Placenta-Specific 8.1 Gene Function during Zebrafish Embryogenesis

by

Haiting Ma

A dissertation presented to the
Graduate School of Arts and Sciences
of Washington University in
partial fulfillment of the
requirements for the degree
of Doctor of Philosophy

May 2013

St. Louis, Missouri

TABLE OF CONTENTS

PAGE

LIST OF FIGURES

LIST OF TABLES

LIST OF ABBREVIATIONS

µg	Microgram
µm	Micrometer
µM	Micromole
Am	Axial mesoderm
Ap	Animal pole
AP	Anteroposterior
Ap	Animal pole
APC	*ADENOMATOUS POLYPOSIS COLI*
Bmp	Bone morphogenetic protein
bp	Base pair
C&E	Convergence and Extension
CC	Cystic colonies
CFTR	*CYSTIC FIBROSIS TRANSMEMBRANE CONDUCTANCE REGULATOR*
COP	Constitutive photomorphogenesis
CRC	Colorectal cancer
cyc	*cyclops*
DIC	differential interference contrast
dkk	Dickkopf (Wnt signaling antagonist)
dpf	Days post fertilization
Dsh	Dishevelled
DV	dorsal-ventral
ECM	Extracellular matrix
EGFP	Enhanced green fluorescent protein
EGFR	Epithelial growth factor receptor
EMS	Ethyl methanesulfonate

EMT	Epithelial-mesenchymal transition
ENU	N-ethyl N-nitrosourea
EVL	Enveloping layer
FGF	Fibroblast growth factor
G protein	Guanine nucleotide-binding proteins
GFP	Green fluorescent protein
GOF	gain-of-function
GPCR	G protein coupled receptor
GPCR	G protein-coupled receptors
GTP	Guanosine triphosphate
GTPase	guanosine triphosophatase
H&E	Hematoxylin and eosin
HEK293T	Human embryonic kidney 293T cells
Hg	Hatching gland
Hh	Hedgehog
hpf	Hours post fertilization
HRAS	*Harvey rat sarcoma viral oncogene homolog*
IFT	Intraflagellar transport
JAK	Janus kinases
JNK	Jun N-terminal kinase
KLH	Keyhole limpet hemocyanin
kny	*knypek/glypican4*
KV	Kupffer's vesicle
L/R	Left-right
LOF	loss-of-function
LWR	Length-to-width ratio
MBT	Mid-blastrula transition
mCherry	monomeric Cherry (a red fluorescent protein)

ML	Mediolateral
MO	Morpholino oligonucleotide
NC	Notochord
ng	nanogram
NT	Neural tube
ntl	*no tail*
papc	*paraxial protocadherin*
PBS	phosphate buffered saline
PCP	Planar cell polarity
PDC	plasmacytoid dendritic cells
PFA	paraformaldehyde
pg	picogram
PGE2	prostaglandin E2
PKC	Protein kinase C
Plac8	Placenta-specific gene 8
Pp	Prechordal plate
PSM	Presomitic mesoderm
RAS	*rat sarcoma viral oncogene homolog*
RNA	ribonucleatic acid
Sc	Spinal Cord
SC	spiky colonies
So	Somite
spw	*southpaw*
sqt	*squint*
Stat3	Signal transducer and activator of transcription 3
TALENs	Transcription Activator-Like Effector Nucleases
TB	Tailbud
TGF	Transforming growth factor

TMA	Tissue microarray
TILLING	Targeting Induced Local Lesions in Genomes
tri	*trilobite*
Vg	Vegetal pole
WT	Wild-type
Y	Tyrosine
YAMC	Young adult mice colon cells
YSL	Yolk syncytial layer

ACKNOWLEDGEMENTS

This work would have been impossible without the tremendous supports from my mentors Dr. Lilianna Solnica-Krezel and Dr. Robert Coffey. Thank you both for providing the best possible PhD experience I could ever hope for. It is a great privilege to be a graduate student, and it is more so to be a student under the guidance of the two great mentors. I would like to thank Dr. Solnica-Krezel for giving me the opportunity to pursue a risky project. She leads by example as a brilliant and persistent scientist, a visionary leader, and a kind, generous, and supportive person. She always inspires me and other lab members to carry out careful research on important biological questions, to pursue better results with better approaches. She teaches me to be a careful, critical thinker and experimentalist, which is a life-long lesson for me to appreciate. I also would like to thank Dr. Coffey who is inspiring as a dedicated physician scientist leading cutting edge translational research. I learnt from their untiring contributions to science that what scientists ought to do is to push the boundaries on the frontiers for knowledge, insights, and advancement of human health. I am indebted to their coordinated efforts to make the transition from Vanderbilt University to Washington University smooth, and their continuing efforts and commitments to make this collaborative thesis project continue as if we had not moved.

I am also extremely grateful to my committee members Dr. Greg Longmore, Dr. Susan Dutcher, Dr. Philip Bayly, and Dr. Raphael Kopan at Washington University, and Dr. Jim Patton, Dr. Joshua Gamse, and Dr. Albert Reynolds at Vanderbilt University for their constructively critical comments and insightful discussions in my continual journal as a scientist. In addition, I would like to express my deep appreciation to Dr. Andrzej Krezel for sharing his knowledge, expertise, and equipment for expression and purification of the Plac8.1 protein.

The friendly and knowledgeable colleagues in both Dr. Solnica-Krezel's laboratory and Dr. Coffey's laboratory make me feel exceptional fortunate and resourceful. My deep gratitude goes to all former and current members of both laboratories. In particular, I would like to thank Dr. Terry Van Raay, Dr. Cunxi Li, and Dr. Zheng Cao for bringing me the wonderful rotation student's experiences in both laboratories. Also I wound like to thank Dr. Cunxi Li for being a long-time collaborator and friend. The boundary-free data sharing, and your patience for endless discussions and communications are essential for this collaborative project. Also I would like to thank Dr. Diane Sepich for all the discussions and help

with experiments, thank Jiakun Chen, Dr. Jimman Shin, and Yinzi Liu for their help with the TALEN experiments, thank Robert Zhang for his help with protein purification, thank Anna Hindes for her efforts to look for *plac8.1* mutant fish and to order reagents and equipment, and thank Eric Sanders, Steve Canters, Amy Bradshaw, Heidi Beck, and so many people for taking care of the fish.

I am fortunate to experience the great training opportunities at Washington University and Vanderbilt University. I would like to thank Dr. Jim Skeath, Dr. Tim Schedl, and Dr. Jim Patton for their help. I would also like to thank the supporting staff: Kim Smith, Stacy Kiel, Linda Lobos, Leslie Maxwell, and many others.

Finally, I specially thank my wife who is my soul mate in life and science, and our parents for being the caring, understanding, patient, and perpetual providers of the unconditional love that makes this and beyond possible.

ABSTRACT OF THE DISSERTATION

Characterization of the Placenta-Specific 8.1 Gene Function during Zebrafish Embryogenesis

Haiting Ma

Doctor of Philosophy in Developmental, Regenerative and Stem Cell Biology

Washington University in St. Louis, 2013

Dr. Lilianna Solnica-Krezel, Chair

The *PLAC8* gene encodes for a small, cysteine-rich protein conserved in vertebrates that is a member of a large family of PLAC8-motif containing proteins with diverse functions in animals, plants, and algae. Recently, high levels of *PLAC8* expression have been detected in aggressive colorectal cancer and invasive breast cancer, and potentially contributing to the cancer pathogenesis. However, the molecular and cellular functions of PLAC8 in vertebrate development, homeostasis, and disease remain unclear. To determine the function of PLAC8 under disease and normal conditions, in this thesis work, I identified *plac8.1* as a *PLAC8* homolog in zebrafish, a vertebrate model system amenable to various embryologic and genetic approaches. Zebrafish *plac8.1* was maternally and ubiquitously expressed until four days post fertilization when its transcript became enriched in the gut. During the process of gastrulation, Plac8.1 protein distribution gradually shifted from the cytosol to the cell membrane. At larval stages, Plac8.1 accumulated at the apical region of epithelial cells of the gut and the kidney. This dynamic gene expression and protein localization patterns suggest that Plac8.1 may have functions during zebrafish embryogenesis and organogenesis.

In the first part of this thesis, I aimed to address questions concerning the effects of high levels of *PLAC8* on cell behavior by overexpressing Plac8.1 during early embryogenesis. Embryos overexpressing Plac8.1 manifested morphological defects starting at early gastrulation. Epiboly as

well as convergence and extension gastrulation movements were delayed in *plac8.1*-overexpressing embryos, a spectrum of phenotypes resembling impaired E-cadherin function in zebrafish. Indeed, E-cadherin levels were significantly reduced in *plac8.1*-overexpressing embryos by a cell-autonomous and post-transcriptional mechanism. Similarly, PLAC8-overexpressing colon cancer cells exhibited reduced cell surface E-cadherin and many features of epithelial-mesenchymal transition (EMT). Furthermore, knockdown of *PLAC8* in colon cancer cells resulted in increased level of E-cadherin.

In the second part of this thesis, I aimed to determine the requirement for *plac8.1* function during development by employing two loss-of-function approaches. Upon injection of either of two non-overlapping antisense morpholino oligonucleotides (MOs) that effectively reduced Plac8.1 protein levels, embryos displayed an array of defects that phenocopied the class of mutants with defective cilia. Consistently, the motile cilia morphology and motility were impaired in *plac8.1* morphants. Moreover, in immunoprecipitation experiments, Plac8.1 bound Cops4, a component involved in ubiquitination regulation. Also Plac8.1 and Cops4 cooperated to regulate motile cilia morphology and motility. As a second loss-of-function approach, I generated loss-of-function allele *plac8.1*^{stl33} using Transcription Activator-Like Effector Nucleases (TALENs), a method that utilizes sequence-specific nucleases. Similar to *plac8.1* morphants, *plac8.1*^{stl33} embryos showed motile cilia morphology and beating function defects. We hypothesize that zebrafish Plac8.1 functions at the ciliary base, possibly by modulating intraflagellar transport through ubiquitination modifications.

Our *in vivo* studies of zebrafish *plac8.1* have uncovered pleiotropic functions of *plac8.1* during development. In addition, the overexpression experiments shed light on mechanisms underlying human disease. Based on the above results, I propose that Plac8.1 overexpression interferes with regulation of protein stability, whereas Plac8.1 is required for motile cilia morphogenesis and function. Common denominators of these seemingly unrelated phenotypes include the potential connection with the process of ubiquitination, and the enriched apical localization of Plac8.1. Our work can also inform studies of other members of the PLAC8 family of proteins.

CHAPTER I

INTRODUCTION

A brief overview of cancer as a multigenic disease

Cancer represents one of leading causes of death worldwide (Jemal et al., 2006; Meetoo, 2008). Carcinomas (malignant solid tumors that originate from epithelial tissues) account for over 80% of the total cancer burden in patients (statistical data from “Cancer facts and figures 2012” by American Cancer Society), and will be focused in this introduction. Environmental risk factors such as ionizing radiations and certain chemicals contribute to cancer formation (Figure 1-1, top panel). For example, tobacco smoking is closely associated with lung cancer. In fact, many tobacco combustion products and their metabolites act as mutagens to alter DNA sequences inside the cells to cause lung cancer (Hecht, 1999). In contrast to lung cancer that is closely associated with tobacco smoking, many of human cancers are not traceable to a particular environmental risk factor, suggesting other factors may also be part of carcinoma etiology (Fontham et al., 2009).

Indeed, inherited and spontaneous mutations in germ cells and somatic cells are common factors that contribute to tumorigenesis (Bertram, 2000). Despite the diversity of causes of cancers, and that cancers have been recognized as a collection of heterogeneous disorders, an abiding theme of cancer research has demonstrated that all cancer cells have multiple gene mutations (Hornberg et al., 2006; Hanahan and Weinberg, 2011). Although not all mutations in cancer cells contribute to cancer formation, highly mutated cancer genomes suggest cancer as a multigenic disease (Welch et al., 2012). Extensive studies on molecular mechanisms that create cancer over the past decades have accumulated an enormous amount of knowledge about the process of mutation accumulation as cancer develops (Rajagopalan et al., 2003; Vogelstein and Kinzler, 2004).

The malignant transformation process that converts normal cells to highly malignant cancer cells has been likened to a micro-scale evolution process (Figure 1-1). In this process, normal cells acquire mutations in various genes in a step-wise way. Each step is likely to give slight selection advantages to the cells with the mutated genes over the cells without this mutation. Then new mutations may occur within the daughter cells that derived from the previously mutated ancestors. After accumulation of

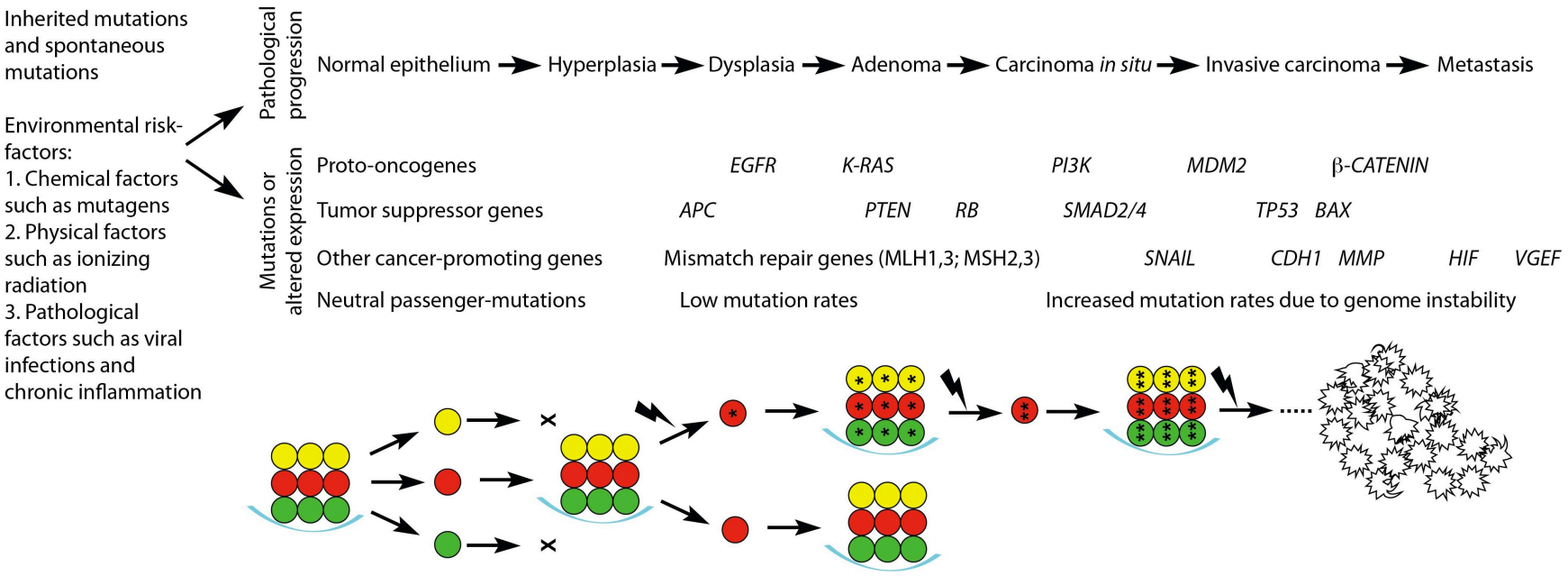

Figure 1-1. A simplified step-wise model of tumorigenesis.
Top panel: environmental factors and accumulation of mutations contribute to the pathogenesis of cancer (adapted from Rajagopalan et al., 2003).
Bottom panel: a simplified model of cancer cell evolution and progression. Clonal evolution, possible contribution of cancer stem cells (red cells), and signals from the niche (denoted by the cyan band) are incorporated to account for the heterogeneity during the path of mutation accumulation, and the heterogeneity in the final flock of highly malignant tumor cells (adapted from Magee et al., 2012).

enough genetic changes in the process spanning several years or even decades, malignant tumors may occur. For example, in colorectal cancer (one of the most frequent types of cancer in the industrialized society), initiation events are often mutations that result in the activation of the Wnt/β-catenin pathway. Loss-of-function mutations in the *ADENOMATOUS POLYPOSIS COLI* (*APC*) gene, a crucial negative regulator of the Wnt/β-catenin pathway, have been observed in about 85% of sporadic and hereditary colorectal tumors (Kinzler and Vogelstein 1996). *APC* is thought to be a gatekeeper gene for colorectal cells, and its inactivation or impairment accelerates accumulation of additional mutations. These mutations include gain-of-function mutations in the proto-oncogene *K-RAS*, and growth factor receptor and proliferation regulatory gene *EGFR*, loss-of-function mutations in genes encoding type II TGF-β receptor, and tumor suppressor gene *TP53* (Rajagopalan 2003).

During the process of cancer development, tumors are often heterogeneous, containing a mixture of cancer cells of phenotypic, functional and genetic heterogeneity (Fidler and Kripke, 1977; Fidler and Hart, 1982). These heterogeneities may be explained by at least three possibilities (Figure 1-1, bottom panel). First, several independent microevolution processes from multiple ancestor cells may take place in parallel during tumor progression. This multitude of evolution processes may result in a mixture of cells from several tribes with diverse genetic constitution (Nowell, 1976). Second, differences in microenvironments experienced by cancer cells contribute to functional and phenotypic differences even for genetically identical cells (Bissell and Hines, 2011). Third, in cancers like myeloid leukemia, certain cells referred to as cancer stem cells possess the characteristic of normal stem cells, and can ultimately give rise to diverse differentiated cancer cells (Ogawa et al., 1970; Becker and Jordan, 2011). However, for solid tumors, the cancer stem cell model is still under investigation (Quintana et al., 2008). It remains possible that all three events can contribute to the diversity and heterogeneity of cancer cells.

Despite the heterogeneity of cancer cells, one of the defining effects of accumulated mutations is deregulated growth and proliferation. Generally speaking, gain-of-function mutations in proto-oncogenes and loss-of-function mutations in tumor suppressor genes are largely responsible for deregulated growth and proliferation (Vogelstein et al., 2000; Vogelstein and Kinzler, 2004).

Normal epithelial cells respond to extracellular signals that promote or inhibit growth and proliferation, thereby maintaining tissue integrity (Cross and Dexter, 1991). In contrast, many abnormal

cells including those cells at early stages of malignant transformation often grow and proliferate independent of extracellular regulatory signals (Vogelstein and Kinzler, 2004). Gain-of-function mutations that convert proto-oncogenes to oncogenes account for multiple aspects of deregulated growth and proliferation. Many of proto-oncogenes are components of the growth factor signaling pathways (Basergar, 1994). For example, *RAS* (one of the most frequently mutated genes in cancer) encodes a cytoplasmic or membrane-tethered protein responsible for relaying growth factor signaling from the outside of cells to the cytosol (Boguski and McCormick, 1993). Gain-of-function mutations can lock the changed RAS protein in GTP bound state, a state that activates the growth factor signaling constitutively (Tabin et al., 1982; Parada et al., 1982). This unabated signaling by the constitutively active RAS protein promotes growth and proliferation even without exogenous stimuli, thereby contributing to the enlargement of tumors (Bos, 1989).

In addition to gain-of-function mutations in proto-oncogenes, loss-of-function mutations in tumor suppressor genes are also important for cancer cell growth and proliferation. Tumor suppressors genes generally function as negative regulators of cell growth and proliferation. For example, *APC* tumor suppressor is a negative regulator of the Wnt/β-catenin signaling that promotes proliferation in intestinal epithelia (Huang, et al., 1996; Kinzler and Vogelstein, 1996). *TP53* is another tumor suppressor that constitutes a crucial defense mechanism against cancer (Vogelstein et al., 2000). *TP53* encodes a ubiquitously expressed transcription factor p53 that is constantly produced, and degraded, to achieve a relatively low steady state level in normal cells (Kruse and Gu, 2009). When a cell experiences unchecked growth stimuli including those caused by *RAS* mutations, p53 degradation is blocked, giving rise to high levels of p53 proteins that translocate to the nucleus to activate responsive genes (Prives and Hall, 1999; Kruse and Gu, 2009). Depending on the nature of the responsive genes, p53 protein may activate apoptosis, the cell suicide program that is able to eliminate over-proliferating cells in a short period of time (Oren, 2003). In such a way, gain-of-function mutations in proto-oncogenes alone have limited ability to promote unrestrained proliferation in cells with properly functioning p53 (Vogelstein and Kinzler, 2004). Therefore, gain-of-function mutations in proto-oncogenes and loss-of-function mutations in tumor suppressor genes cooperate to promote growth and proliferation, which drive early phases of cancer pathological progression and formation of local adenomas or carcinomas (Figure 1-1 top panel).

At the advanced phases of cancer pathological progression, cancer cells acquire other properties in addition to proliferation and growth (Figure 1-1, top panel). These properties include invasion and metastasis that are responsible for majority of mortalities in patients with cancer (Hornberg et al., 2006; Hanahan and Weinberg, 2011). The process of invasion and metastasis entails downregulation of adhesion molecules and ensuing detachment from neighbor cells in the epithelia sheet, losing epithelial transcription program while gaining properties of mesenchymal cells to change cells shape and acquire motility (undergoing **e**pithelial-**m**esenchymal **t**ransition, or EMT), migrating to new locations and establishing tumor growth (Thiery et al., 2009; Valastyan and Weinberg, 2011). The cell behaviors underlying invasion and metastasis are caused by additional mutations or altered expression in a class of cancer-promoting genes that is difficult to be classified as proto-oncogenes or tumor suppressor genes (Luo et al., 2009). Increasing evidence has indicated that cancer cells execute many steps in the invasion and metastasis process by activating or overexpressing genes that are normally used to mediate critical steps in early embryonic development (Thiery et al., 2009). For example, upregulation of genes encoding transcription factors from the Snail family mediates both normal gastrulation cell movements and cancer metastasis (Thiery et al., 2009).

Not all genes mutated or deregulated in cancer cells have clearly defined biological functions. For example, elevated expression of *PLAC8* (*PLACENTA-SPECIFIC 8*) has been found in invasive colorectal cancer cells in human and in mice, and it is required for cancer formation in xenograft experiments (McMurray et al., 2008). However, the molecular mechanisms underlying how elevated *PLAC8* supports tumorigenesis, and the normal function of *PLAC8* remain unclear. The discovery of mutations in cancer genomes and modified gene transcription profiles in cancer cells leave open the question as to the function of the mutated or abnormally expressed genes. Understanding the function of the mutated or deregulated genes is necessary to understand mechanisms that create cancer, and to devise potential treatments for cancer patients.

In summary, cancer is a multigenic disease (Vogelstein and Kinzler, 2004). The overlap between genes crucial for embryonic development and those underlying the etiology of cancer suggests a close connection between cancer biology and developmental biology. In some cases, cancer can also be understood as developmental molecular mechanisms gone awry. Moreover, insights into the mechanisms

of tumorigenesis can be obtained from studies of normal embryonic development. Genetic studies in models organisms amenable to genetic approaches can bridge the knowledge gap between the detection of genes implicated in cancer and understanding the molecular function of these genes.

Genetic studies in model organisms

Genetics proved over and over again to be a crucial approach to understand the molecular mechanisms underlying normal development and physiology, and pathogenesis of human disease (Figure 1-2). In particular, genetic studies in model organisms can provide key insights into functions of disease genes, including genes overexpressed in cancer tissues. Both human genetics, and experimental genetics in model organisms are valuable approaches that compliment each other in important ways. Classical human genetic studies provide direct evidence of gene-disease association. *CFTR* is one of the first disease genes cloned on the basis of linkage analysis (Riordan et al., 1989). In addition, cell transformation assays and molecular approaches enabled the identification of *HRAS* mutation as the first somatic mutation found in a human bladder carcinoma cell line (Parada et al., 1982; Der, 1982; Tabin et al., 1982). These discoveries motivated functional studies on *CFTR* and *HRAS* in human cultured cells and model organisms, and disease genes-targeted therapeutics. However, due to the limited availability of naturally occurring mutations in the human population, it is challenging to understand molecular mechanism or conclusive causal relationship between genotypes and phenotypes with human genetics approaches.

In comparison, analyses with forward and reverse genetic approaches in model organisms make it possible to characterize gene functions and the underlying molecular mechanisms of disease, to establish causal relationship between genotypes and phenotypes, and to create disease models (Figure 1-2). Forward genetics is driven by phenotypes resulting from spontaneous or induced mutations, followed by gene identification via positional cloning and sequencing of candidate genes, in a way essentially similar to how human genetics approaches the phenotype-to-gene questions. While spontaneous mutations occur at low rates, Hermann Muller's discovery of the mutagenic effects of X-ray radiation in *Drosophila* alleviated the reliance on spontaneous mutations (Muller, 1946). The mutagenic effects of X-ray and other ionizing radiation, together with chemical mutagens were used in genetic

studies of *Drosophila*, bacteria, λ phage, and yeast, together establishing the forward genetics paradigm (Muller 1946; Beadle and Tatum, 1958; Jacob and Monod, 1961; Hartwell, 1978). Subsequently, using alkylating reagent ethyl methanesulfonate (EMS) based mutagenesis screens in *Drosophila*, Christiane Nüsslein-Volhard and Eric Wieschaus demonstrated the power of forward genetic screens to the complex problem of animal embryonic development. In addition to forward genetic screens in *Drosophila*, an alkylating reagent *N*-ethyl-*N*-nitrosourea (ENU) based mutagenesis and genetic screens were carried out in the zebrafish, the first vertebrate species to be employed in such large-scale forward genetic approach (Mullins, et al., 1994; Solnica-Krezel et al., 1994; Driever et al. 1996). The results of these screens were reported in the 1996 *Development* zebrafish issue, and they ushered zebrafish as an important genetic vertebrate model system.

Reverse genetics entails generating mutations in genes-of-interest, followed by analyses of the resulting mutant phenotypes. In model organisms such as the mouse, homologous recombination between the introduced and endogenous genomic DNA in embryonic stem cells affords replacing wild-type alleles with engineered constructs to perturb target gene function (Doetschman et al., 1987; Snouwaert et al., 1992). Homologous recombination based gene targeting has only recently been successfully demonstrated in the zebrafish (Bedell et al., 2012a). Another approach, known as **T**argeting **I**nduced **L**ocal **L**esions **In G**enomes (TILLING) can be used to obtain mutations in genes of interest. ENU, the mutagen of choice in forward genetic screens, is used to mutagenize spermatogonia in male fish. When such mutagenized males are crossed with wild-type females, F1 fish are generated that are heterozygous for the newly induced mutations. Then DNA samples from thousands of F1 fish are collected to construct a screening library, and target gene specific primers are used to generate amplicons. Mutations in specific genes can then be detected by CEL-1 enzyme based heteroduplex detection or by next generation sequencing. Then individual samples carrying mutations in the genes are recovered (Wienholds et al., 2003). The recovered mutations are generally point mutations including missense mutation or nonsense mutations.

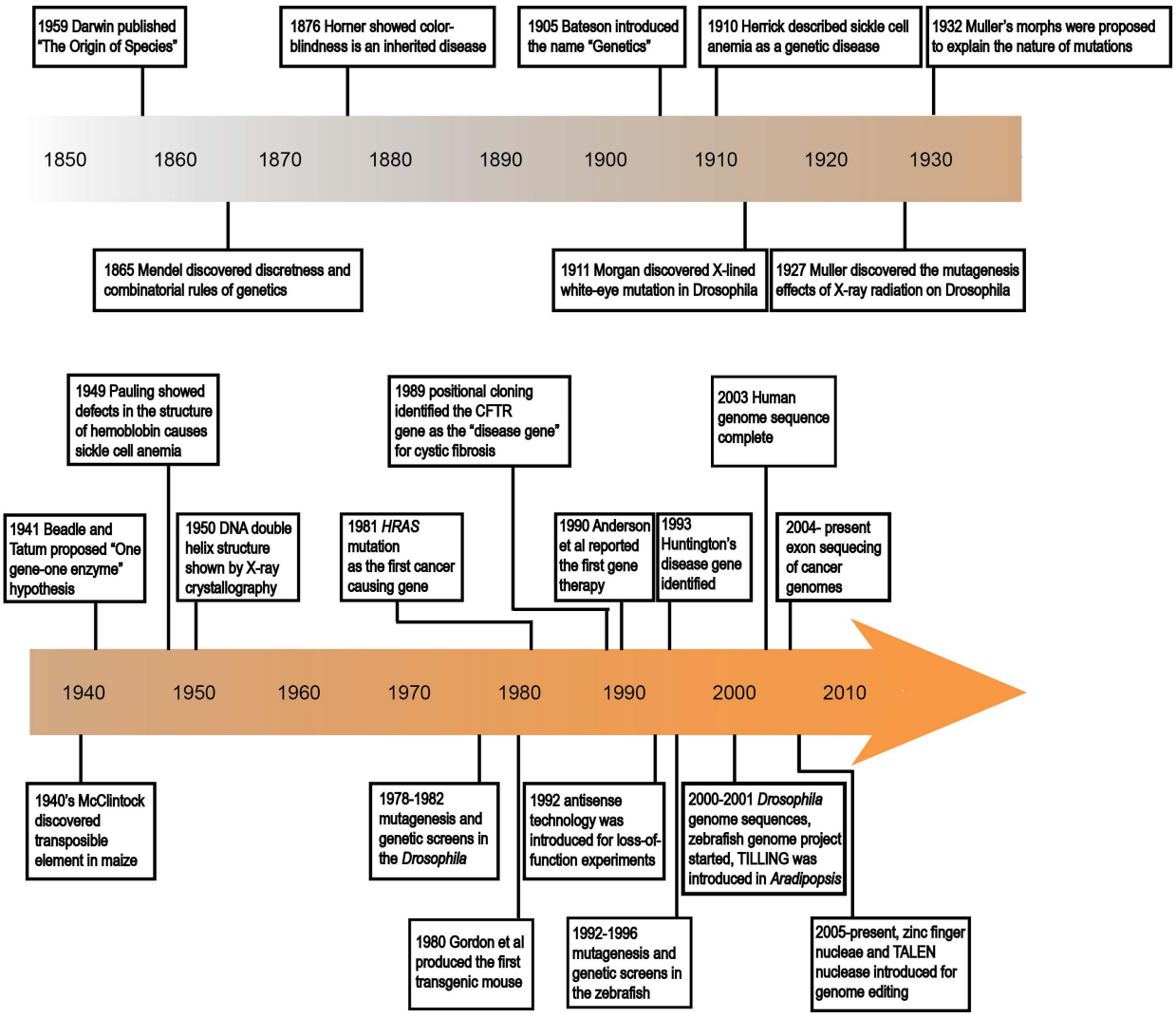

Figure 1-2. Landmarks of genetic studies in humans and model organisms

Muller's morphs offer a framework to understand the nature of mutations

In addition to pioneering X-ray induced mutagenesis, another contribution of Muller to genetics comes from the "Muller's morphs", a conceptual framework to classify different *Drosophila* mutations (Muller, 1932). Muller's morphs provided an advanced framework to interpret classical genetics, and to understand the effects of various mutations on the function of their wild-type genes. However, it must be recognized that that Muller's morphs do not form a one-to-one relationship with the underlying molecular

mechanisms (Wilkie, 1994). Therefore, it is important to understand gene function by taking perspectives from Muller's morphs, and from gene functions at the molecular level (Figure 1-3 B).

Our understanding of gene functions at the molecular level has evolved from the initial "one gene-one enzyme" hypothesis (Beadle and Tatum, 1941), to a broader view. The functions of genes are carried out by the products they encode, such as RNAs for non-protein coding genes (tRNA, rRNA, snoRNAs, microRNAs, siRNAs, piRNAs, long non-coding RNA such as Xist), or proteins of protein-coding genes. Here we only discuss protein-encoding genes, for which proteins are the units of function under many circumstances. In multicellular eukaryotes, many mechanisms regulate the form and amount of protein encoded by a gene, and thus its function. Spatio-temporally regulated gene transcription through genetic and epigenetic mechanisms, regulation of splicing isoforms, modulation of transcript stability by micro RNAs are among the factors that determine where, when, and how much protein (gene function) will be produced. Posttranslational regulations such as directed transport and localization, binding to other molecules to form complexes, post-transcriptional modification by lipid or small protein tags including ubiquitin, and stability modulation also determine the subcellular localization and amount of proteins (Walsh, 2005). In summary, the molecular function of a gene comprises its spatio-temporal expression, intracellular localization, and the molecular activity of its products (RNA or protein).

According to Muller's morphs, loss-of-function mutations are classified as *amorphic* or *hypomorphic* mutations (Figure 1-3 A). An *amorphic* mutation completely eliminates the function of the gene, whereas a *hypomorphic* mutation partially ablates the gene function to various degrees. From the molecular biology point of view, an *amorphic* mutation of a gene or equivalent condition can be generated when the RNA (for non-protein coding genes), or protein (for protein-coding genes) are completely eliminated, or when the resultant RNA (for non-protein coding genes), or protein (for protein-coding genes) are completely inactive. Similarly, a *hypomorphic* mutation of a gene or equivalent conditions can be generated when the RNA (for non-protein coding genes), or protein (for protein-coding genes) are present but at reduced quantity compared to wild-type conditions, or when the resultant RNA (for non-protein coding genes), or protein (for protein-coding genes) are only partially inactive. On the other hand, gain-of-function mutations are classified as *hypermorphic*, *antimorphic*, or *neomorphic* mutations (Figure 1-3 A). A *hypermorphic* mutation increases the normal function of the gene, by molecular mechanisms

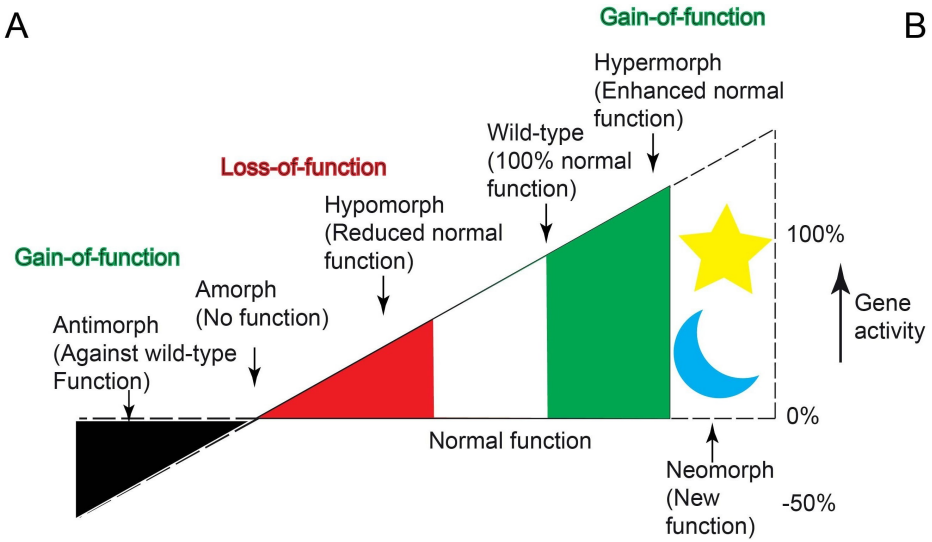

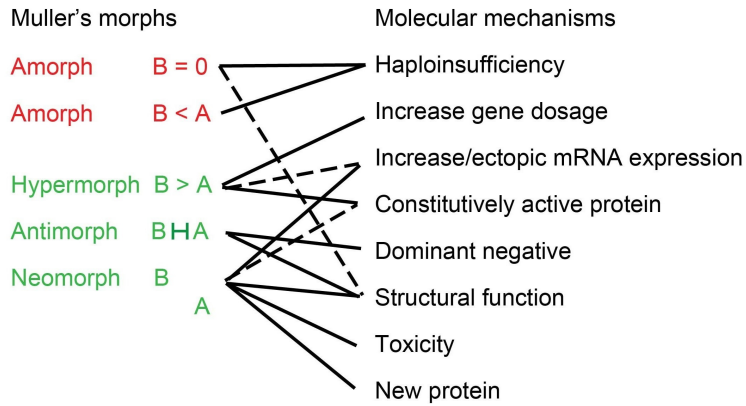

Muller's morphs	Dorminant or recessive	Gain-of-function or loss-of-function	Frequency	Function of mutated alleles	m/wild-type phenotype	m/m phenotype	m/deletion phenotype	m/duplication phenotype	Possible molecular mechanisms
Amorphic	Recessive	Loss of normal function	Common	Complete loss-of-function	Wild-type	Mutant same as m/deletion	Mutant same as m/m	wild-type	Gene deletion No transcription Non-functional RNA products
	Dominant	Loss of normal function	Uncommon	Complete loss-of-function	Mutant	Mutant	Mutant	Wild-type	No translation Non-functional protein products
Hypomorph	Recessive	Loss of normal function	Common	Partial loss-of-function	Wild-type	less severe than m/deletion	More severe than m/m	Wild-type	Point mutation, insertion or deletion mutation Reduced transcription or imparied RNA processing Reduced translation Protein products of reduced function
	Dominant	Loss of normal function	Uncommon	Partial loss-of-function	Mutant	More severe than m/wild-type	More severe than m/m	Wild-type	
Hypermorph	Dominant	Gain of normal function	Uncommon	Increased function	Mutant	More severe than m/wild-type	Less severe than m/wild-type	More severe than m/wild-type	Gene duplication Increased transcription Increased stability of RNA products Increased translation Increased stability of protein products Protein products of enhanced function
Antimorph	Dominant	Gain of function	Uncommon	Gain of function to antagonize normal function of the gene	Mutant			Less severe than duplication	Altered protein products functioning as competitive or noncompetitive inhibitor of wild proteins Improper activation of negative feedback loop
Neomorph	Dominant	Gain of function	Uncommon	Gain of unrelated new functions	Mutant	Mutant	Mutant	Mutant	Protein products of new functions

Figure 1-3. Muller's morphs.

A. Types of mutant alleles according to Muller's morphs.
B. Relationship between Muller's morphs and molecular mechanisms. Solid lines denote common connections, and dashed lines show less frequent connections (adapted from Wilkie, 1994).
Bottom panel: A table summarizing Muller's morphs, and the genetic phenotypes, and possible molecular mechanisms.

such as increasing RNA or protein expression levels, or increasing RNA or protein activity. An *antimorphic* mutation is a mutation that antagonizes the normal gene function. At the molecular level, *antimorphic* mutations can also be referred to as dominant negative mutations. These mutations interfere with normal gene functions by various mechanisms such as forming functionally inactive complexes with wild-type gene-encoded proteins. A *neomorphic* mutation causes gain-of-functions that are distinct from the normal function of the wild-type gene through ectopic RNA or protein expression, increased RNA or protein expression levels, or acquired protein functions because of altered structure. While *antimorphic, amorphic*, *hypomorphic*, and *hypermorphic* mutations form a quantitative series regarding to the function of the wild-type gene, *neomorphic* mutations indicate qualitatively new functions of the wild-type gene (Figure 1-3 A). In addition to the five mutations types, Muller commented that a combination of mutations of pleiotropic genes, genes that influence multiple phenotypes, might form complex series of phenotype spectra that are challenging to interpret with simple quantitative analyses (Muller, 1932). Proposed 12 years prior to the identification of DNA as the genetic material, the framework of Muller's morphs is still widely uses, and is applicable to diverse genetic model organisms including zebrafish.

Zebrafish as a model system to study embryonic development

During the past two decades, zebrafish has emerged as a powerful model organism for studying vertebrate development and disease (Driever et al., 1994; King, 2009; Santoriello and Zon, 2012). Adult zebrafish are small in size, and can be economically maintained in large number with fresh water aquaculture systems applicable in relatively small amounts of space. Zebrafish embryos are fertilized externally, and the rapid external development and the optical transparency of the embryos enable convenient cell labeling, *in vivo* and *in vitro* imaging (King, 2009). In addition, high fecundity (hundreds embryos from a single pair per week) and short generation time (about 2-3 months) make zebrafish a unique vertebrate system amenable to large-scale forward and reverse genetic screens. Pioneering forward genetic screens on zebrafish have uncovered many important mutants by inducing point mutations in zebrafish with ENU, followed by F2 classical genetic screens for morphologically abnormal embryos and gene identification with positional cloning (Solnica-Krezel et al., 1994; Mullins et al., 1994) (Figure 1-4). In addition to chemical based screens, retroviral insertion based screens can be performed

to identify a myriad of mutations (Lin et al., 1994; Gaiano et al., 1996). Alternatively, point mutations in genes-of-interest can be identified with reverse genetics approaches such as TILLING (Wienholds et al., 2003). Recent improvements in genome editing technology such as zinc finger nuclease, and Transcription Activator-Like Effector Nucleases (TALENs) provide additional methods to induce mutations in genes-of-interest followed by screening founder fish for germ line mutations (Meng et al., 2008; Cermak et al., 2011).

Besides forward and reverse genetic screens, injection of antisense morpholino oligonucleotides (MOs) designed to target specific gene sequences into one-cell stage zebrafish embryos represents another loss-of-function approach to interfere with gene translation or splicing (Nasevicius and Ekker, 2000). In MOs, the backbone of the nucleotide is engineered so that the morpholine ring substitute the ribose, thereby extending the stability of MO to several days *in vivo* (Hudziak et al., 1996; Moulton and Jiang, 2009). In addition, the change in the backbone renders high affinity of MO to its cognate target in a sequence specific manner, therefore having reasonably high specificity of gene interference. MOs designed to block target mRNA translation may contain sequence complementary to the 5' UTR region and/or regions spanning the translation initiation AUG site. The steric hindrance caused by tight binding of MOs to the target mRNA interferes with its translation. Alternatively, MOs can be designed to bind to exon-intron junctions of mRNA, impairing correct intron splicing, and consequently leading to frame-shifts and premature stop codons (Corey and Abrams, 2001).

Complementary to the loss-of-function experiments, gain-of-function experiments can be performed by injection of synthetic RNAs that encode proteins of interest. The injections are carried out at one-cell stage to achieve ubiquitous overexpression. Alternatively, an injection into a single cell at or after 32-cell stage can produce a mosaic expression. In addition to the transient experiments by RNA injection, transgenic fish can be generated with systems such as the *Tol2* transposase system (Kwan et al., 2007). Based on the selection of promoters and drivers, expression of the transgene can be regulated temporally and spatially (Kwan et al., 2007; Villefranc et al., 2007). Besides the genetic approaches, effects of small molecules on zebrafish development can be conveniently assessed by adding small molecules to the zebrafish larvae culture medium (Hong, 2009; Zhong and Lin et al., 2011). These research approaches

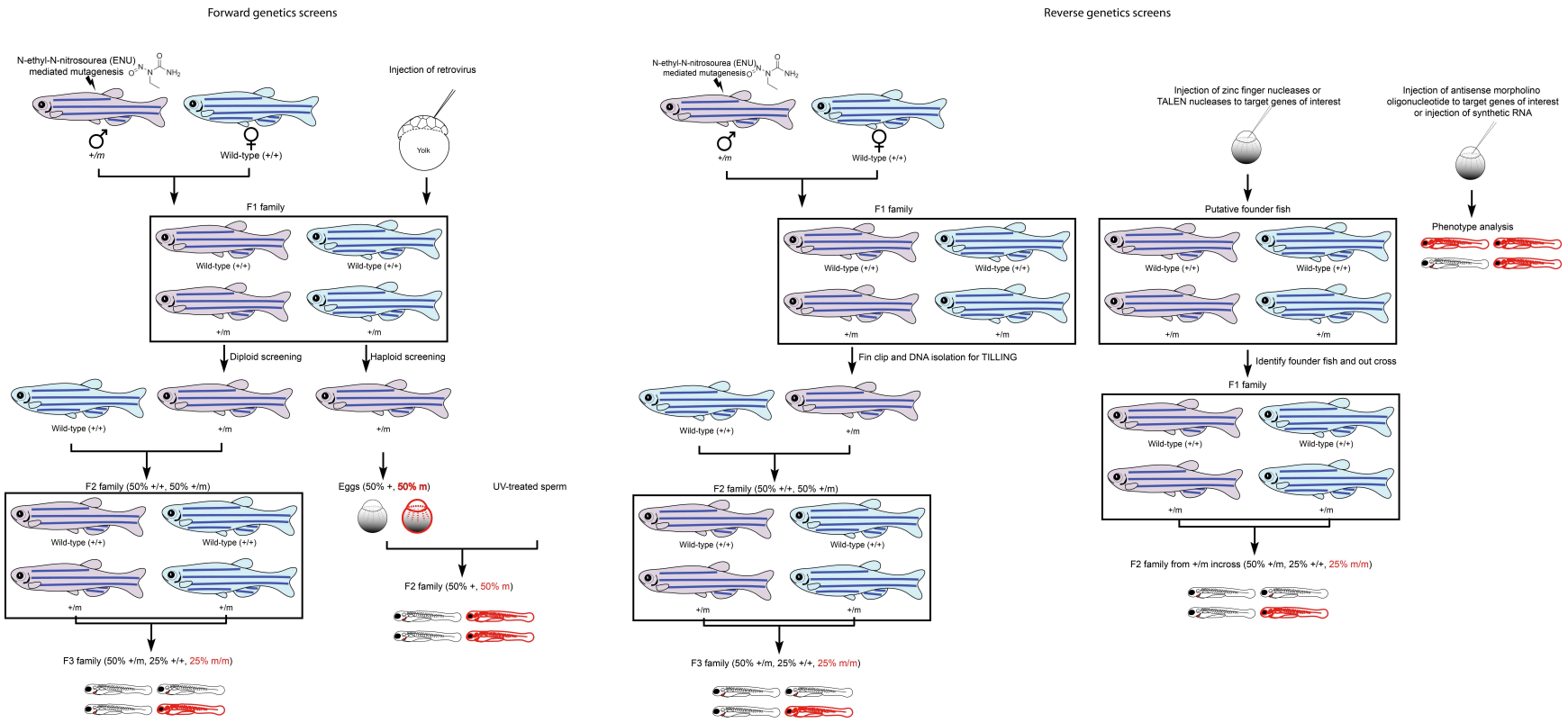

Figure 1-4. Zebrafish as a genetic model system with forward genetic and reverse genetic approaches (adapted from Santoriello and Zon, 2012).

make zebrafish a model system particularly suitable to study early developmental processes such as gastrulation. Again provide a logical lead to the next section.

Cell fate specification and morphogenetic cell movements during zebrafish gastrulation

Gastrulation is a highly orchestrated process that entails both extensive cell movements and inductive events that specify cell fates. During gastrulation, embryos form three germ layers, establish the body plans, and specify organ primordia and place them at proper locations. The combination of optical clarity of externally developing zebrafish embryos with the powerful genetic approaches makes zebrafish particularly suitable for studying the molecular genetic basis of the cell movements during gastrulation (Kimmel et al., 1989; Solnica-Krezel et al., 1996; Hammerschmidt et al., 1996). Extensive studies in zebrafish have identified three classes of gastrulation mutants: those specifically affecting cell fate specification, those specifically affecting cell migration, and those affecting both cell fates and movements. These studies, suggest that cell fate specification and cell migration can be uncoupled in zebrafish, but also uncovered genetic programs that coordinate cell fate specification and movements (Kimmel et al., 1989; Solnica-Krezel et al., 1996; Hammerschmidt et al., 1996; Mullins et al., 1996; Myers et al., 2002a,b)

Within 24 hours, zebrafish embryos develop from radial symmetric zygotes to larvae with dorsal-ventral, anterior-posterior, and left-right axes (Bisgrove et al., 1999; Long et al., 2003; Amack and Yost, 2004; Schier and Talbot, 2005). Regulated by maternally deposited protein and RNA transcripts, dorsal-ventral axis is the earliest breach of symmetry. Syntabulin-dependent transportation of maternally deposited dorsal determinant to the future dorsal side leads to stabilization of β-catenin in the nuclei at the future dorsal side (Schneider et al., 1996; Solnica-Krezel, 1999; Nojima et al., 2010). At about 3 hpf (512/1000 cell stage), zygotic transcription starts (Kane and Kimmel, 1993), and nuclear β-catenin initiates the Wnt/β-catenin signaling cascade that is essential for the formation of the Nieuwkoop center which is required for the formation of the future dorsal organizer in zebrafish (Schneider et al., 1996) (Figure 1-5 A).

At the onset of gastrulation at the shield stage, Nodal ligand gene *squint* is expressed at the margin (Dougan et al., 2003). Squint proteins relay Nodal signaling-dependent mesendodermal program across a distance of several cells, and are not just confined to the immediate neighbors (Chen and Schier,

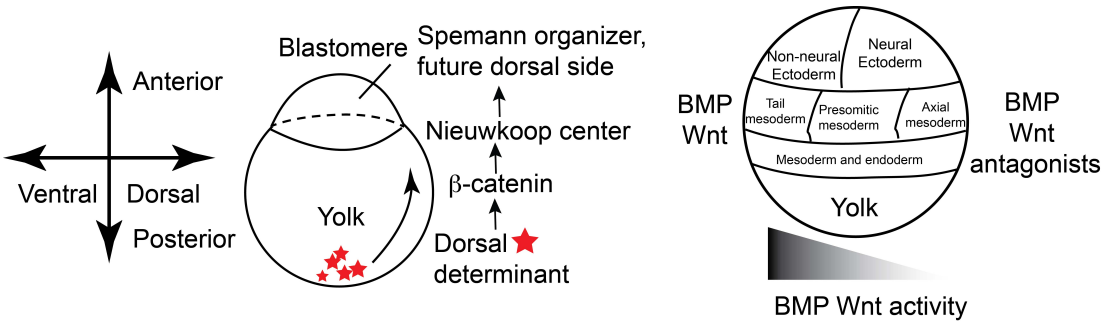

A. Dorsal-ventral axis formation by maternal and zygotic signaling molecues

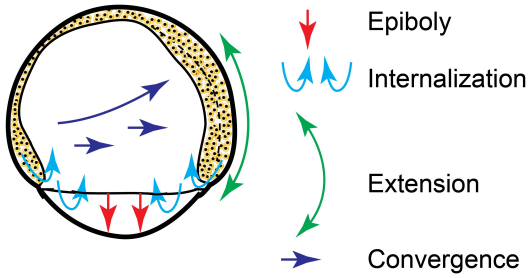

B. Morphogenetic movements during gastrulation

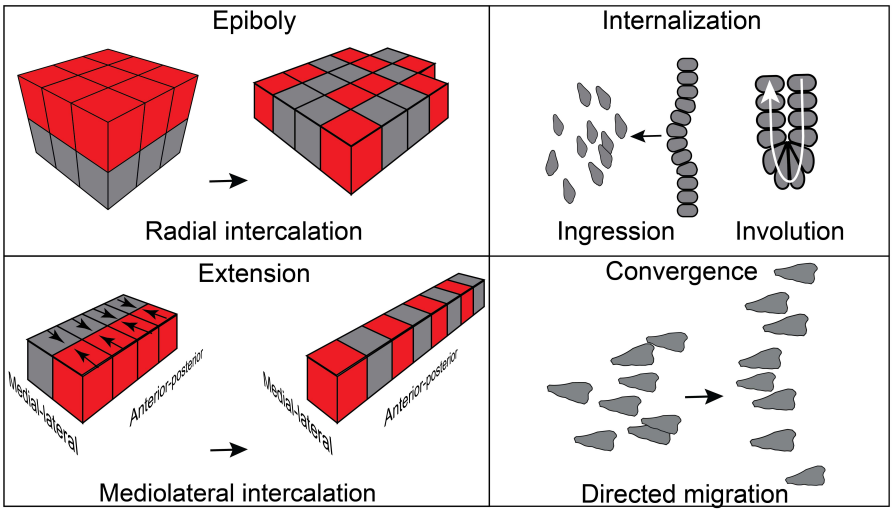

C. Cell behaviors for morphogenetic movements during gastrulation

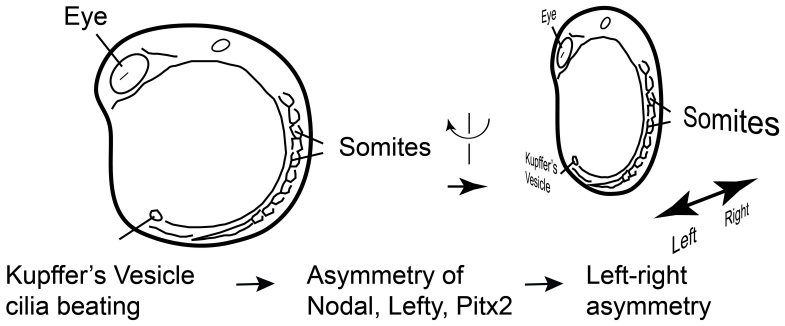

D. Left-right axis formation

Figure 1-5. Cell fate specification and morphogenetic cell movements together shape zebrafish body plan during embryonic development (diagram adapted from Solnica-Krezel, 2005, and Yin et al., 2009).
A. The maternal dorsal determinant is transported in a microtubule dependent manner to the future dorsal side, and mediating Wnt/β-catenin signaling to specify the dorsal Spemann organizer. Then the dorsal organizer antagonizes the ventral posteriorization signaling of zygotic BMP and Wnt/β-catenin molecules, contributing to the establishment of dorsal ventral patterning and cell fate specification. Other signaling events such as Nodal, FGF, and retinoid acid signaling events are omitted in the simplified diagram.
B. Morphogenetic movements in a mid-gastrulation stage zebrafish embryo.
C. Possible cellular behaviors responsible for the gastrulation cell movements.
D. A diagram depicting the role of Kupffer's vesicle and Nodal signaling molecules, and transcription factor Pitx2 in the left-right axis formation in zebrafish early embryogenesis.

2001). Thereby, the Nodal gradient along the margin-animal pole contributes to the specification of germ layers: low or no Nodal activity for the cells located far from the margin constitute the ectoderm, whereas the marginal cells that experience relatively high Nodal activity become constitute the mesendoderm, precursors of both mesoderm and endoderm (Chen and Schier, 2001; Dougan et al., 2003). On the other hand, the dorsal organizers express FGF ligands, and multiple secreted molecules that inhibit the ventral BMP and zygotic Wnt/β-catenin signaling molecules, setting up the dorsal-ventral, and anterior-posterior axes (Solnica-Krezel et al., 1995; Schneider et al., 1996; Schulte-Merker et al., 1997; Fekany-Lee et al., 2000; Hashimoto et al., 2000; Furthauer et al., 2004;). Cells located far from the dorsal organizer received high levels of BMP and Wnt/β-catenin activity, becoming the future ventral posterior mesoderm (Langdon and Mullins, 2011; Robertis, 2006) (Figure 1-5 A). The dorsal gastrula Spemann-Mangold organizer gives rise to the future dorsal and anterior midline tissues including the notochord, prechordal plate, and floor plate (Kimmel et al., 1990). Non-axial marginal cells form other types of mesoderm based on their position to the dorsal organizer and the ventral organizer (Agathon et al., 2003). The left-right axis is determined by expression of Nodal ligand *southpaw* (*spw*) specifically at the left side of lateral plate mesoderm (Essner et al., 2002). The beating of cilia in the Kupffer's vesicle, a transiently ciliated epithelium in zebrafish analogous to the node in mouse embryo, is thought to set up the lateral expression of *southpaw* (Stern, 2002; Long et al., 2003; Essner et al., 2005) (Figure 1-5 D).

During zebrafish gastrulation, four morphogenetic movements (epiboly, internalization, convergence and extension movements) cooperate with the cell fate specification to form zebrafish embryos with a typical vertebrate body plan and properly placed organ primodia (Solnica-Krezel, 2005; Yin et al., 2009; Roszko et al., 2009). Epiboly is the animal pole to vegetal pole movements to thin three germ layers, and to spread three germ layers to cover the yolk ball. Internalization tucks mesendodermal cells underneath the ectodermal cells. Convergence and extension movements narrow the embryo media-laterally, and elongate the embryo anterior-posteriorly (Figure 1-5, B).

Multiple mutations have been identified to affects cells movements. For example, E-cadherin is needed for epiboly, convergence and extension movements (Kane et al., 2005). In addition, G protein-coupled receptors (GPCR) signaling by Gα12/13, and prostaglandin also regulate epiboly indirectly

through E-cadherin (Lin et al., 2005; Lin et al., 2009; Speirs et al., 2010). These results suggest that balance E-cadherin is required for proper gastrulation movements.

Several signaling pathways also closely regulate cell movements. For example, the ventral to dorsal gradient of BMP activity coordinate convergence and extension movements (Myers et al., 2002a). Also the ventral BMP signaling-mediated cell-cell adhesion regulation is critical for lateral mesodermal cells migration (von der Hardt et al., 2007). Nodal signaling that patterns the formation of mesendoderm regulates internalization (Carmany-Rampey and Schier, 2001; Feldman et al., 2002; Schier and Talbot, 2005). Loss-of-function of Wnt/β-catenin pathway regulator Dkk1 accelerates internalization in a Wnt/β-catenin independent manner (Caneparo et al., 2007). Proper levels of Wnt/planar cell polarity (PCP) signaling is crucial for efficient convergent and extension (Topczewski et al., 2001; Jessen et al., 2002). In addition, Stat3 is hypothesized to secrete signaling molecules to regulate convergence and extension (Yamashita et al., 2002; Miyagi et al., 2004).

PLAC8 family of proteins and its implication in carcinomas

The human *PLAC8* gene was identified as encoding a putative secreted cytokine expressed in the plasmacytoid dendritic cells (PDCs) (Rissoan et al., 2002), a type of migratory antigen-presenting cells that may link innate and adaptive immunity (Colonna et al., 2004). A cysteine rich protein (16 of 117 amino acid residues are cysteine), human PLAC8 was initially named as C-15 (Rissoan et al., 2002). Similarly, the mouse Plac8, also known as Onzin, is a cysteine-rich protein with 80% sequence identity to the human PLAC8 protein. Mouse *Plac8* gene was shown to be highly expressed in the placenta (Galaviz-Hernandez et al., 2003). In addition, *Plac8* is also expressed in other tissues including the gut, lung, kidney, and the immune system (Rogulski et al., 2005; Ledford et al., 2007). *Plac8*$^{-/-}$ mice displayed defects in innate immunity (Ledford et al., 2007; Johnson et al., 2012), and brown fat differentiation anomalies (Jimenez-Preitner et al., 2011).

Several lines of evidence from cancer research have implicated elevated levels of *PLAC8* in cancer pathology. For example, *Plac8* is one of the most upregulated genes in young adult mice colon (YAMC) cells transformed by active HRAS and defective p53. Knockdown of *Plac8* in these cells or in HT29, a human colorectal cancer (CRC) cell line with mutated *TP53*, significantly reduced tumor growth

(McMurray et al., 2008), suggesting *PLAC8* was required for tumor formation. In a separate study, three-dimensional cell culture experiments with human colorectal cancer cells HCA-7 also correlated the association of high levels of PLAC8 with cellular behavior resembling cancer invasion (Coffey and Li, Vanderbilt University, unpublished results). Moreover, between SW480 and SW620 colorectal cancer cells separated from the same patient, levels of *PLAC8* transcript and levels of PLAC8 protein were higher in SW620 cells (derived from lymph node metastasis) than in SW480 cells (derived from the primary tumor) (Cunxi Li and Robert J. Coffey, unpublished results). In addition to colorectal cancer cells, invasive clones derived from the human Hs578T breast cancer cells had higher expression of *PLAC8* compared to less invasive counterparts derived from the same parental cells (Hughes et al., 2007). The transcription of *Plac8* was inhibited by Myc (Rogulski et al., 2005), and PKCε-Erk (Wu et al., 2010), and was activated by hematopoietic stem cell regulator Mies1 (Cai et al., 2012). The proposed molecular functions of PLAC8 in tumorigenesis included promoting growth, inhibiting apoptosis through Akt-Mdm2-p53 pathway (Rogulski et al., 2005), and through interaction with Phospholipid Scramblase 1 (Li et al., 2006) (Figure 1-6 D). However, the effect of PLAC8 on apoptosis varied depending on the cell types (Mourtada-Maarabouni et al., 2012), indicating the molecular function of overexpressed PLAC8 in cancer cells remains incomplete and poorly defined.

Various phylogenetic analyses showed that homologs of *PLAC8* could be identified in vertebrates, but not in invertebrates (Guo et al., 2010; Song et al., 2011; Bedell et al. 2012b) (Figure 1-6 A). On the other hand, motif analyses indicated that PLAC8 belong to a large family of proteins widely distributed in animals, plants, and algae. These proteins contain cysteine-concentrated motif such as CCXXXXCPC or CLXXXXCPC (C=cysteine, L=leucine, P=proline, and X represent any other amino acid residues), and are referred to as the PLAC8 motif-containing proteins (Song et al., 2011). One difference between PLAC8 proteins and PLAC8 motif-containing proteins is that PLAC8 motif-containing proteins tend to have a linker of variable lengths between the two PLAC8 motifs, whereas PLAC8 proteins tend to lack such linkers, and are usually of little more than 100 amino acid residues in length (Figure 1-6 B, C).

Although no developmental defects have been reported in the *Plac8*$^{-/-}$ mice (Ledford et al., 2007), the expression levels of *PLAC8* in *in vitro* fertilized cattle embryos were used to predict implantation success in cattle breeding practices (El-Sayed et al., 2006), suggesting that *PLAC8* and its related genes

might be important for embryogenesis in other species. Indeed, in zebrafish, *ponzr1*, a gene encoding for a PLAC8 motif-containing protein, is essential for kidney and pharyngeal arch development (Bedell et al., 2012b). In tomato and in maize, a *PLAC8* related gene *fruit weight 2.2* (*fw2.2*) regulates fruit cell number and fruit size (Guo et al., 2010; Libault and Stacey, 2010). AtPCR1 and AtPCR2 in *Arabidopsis thaliana* extrude metal ion including cadmium and zinc ions from plant cells (Song et al. 2011). In the algae *Chlamydomonas reinhardtii*, a PLAC8 motif-containing protein Agg2p localizes to the flagellar membrane close to the base of the flagella, and regulates phototaxis (Iomini et al., 2006). These observations suggest that these PLAC8-motif containing proteins constitute an emerging family, of which the diverse functions need to be uncovered. It is possible that in a cell type-, protein subcellular localization-, and species-dependent manner, the cysteine clusters of PLAC8-motifs contribute to diverse molecular functions by forming cysteine-divalent ion interactions, protein-protein interactions, and forming thiol-based catalytic centers (Brüne and Mohr, 2001; Leichert and Jakob, 2006; Kodali and Thorpe, 2010).

This thesis focuses on a two-pronged approach to the functional characterization of zebrafish Plac8.1, the zebrafish protein of functional similarity and highest sequence identify to human PLAC8. First, I modeled elevated levels of *PLAC8* expression in cancer by gain-of-function experiments of *plac8.1* during zebrafish embryonic development, and to provide insights in cancer cells with high levels of *PLAC8*. Second, I investigate the function of *plac8.1* in zebrafish embryogenesis by reduction of function experiments.

A

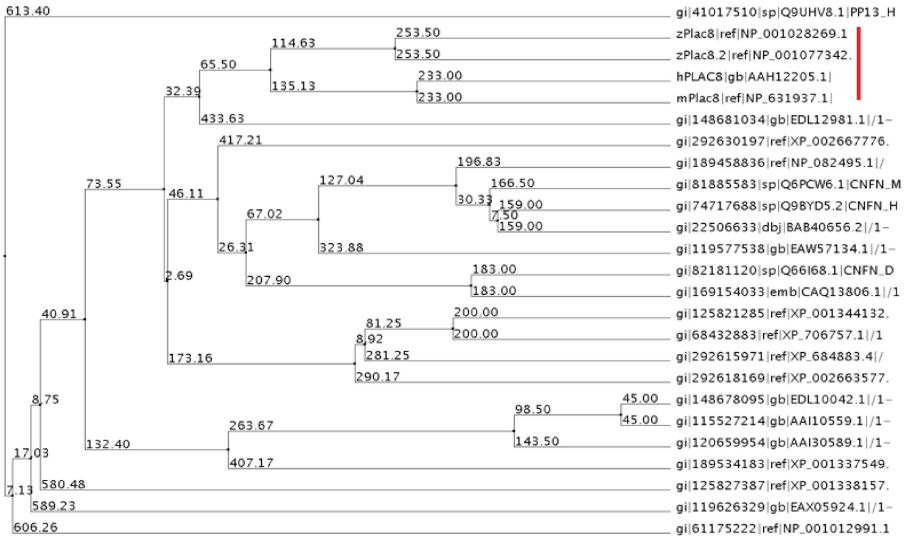
613.40
gi|41017510|sp|Q9UHV8.1|PP13_H
114.63
253.50
zPlac8|ref|NP_001028269.1
253.50
zPlac8.2|ref|NP_001077342.
65.50
233.00
hPLAC8|gb|AAH12205.1|
135.13
32.39
233.00
mPlac8|ref|NP_631937.1|
433.63
gi|148681034|gb|EDL12981.1|/1-
417.21
gi|292630197|ref|XP_002667776.
196.83
73.55
46.11
127.04
166.50
gi|189458836|ref|NP_082495.1|/
30.33
159.00
gi|81885583|sp|Q6PCW6.1|CNFN_M
67.02
7.50
159.00
gi|74717688|sp|Q9BYD5.2|CNFN_H
26.31
323.88
gi|22506633|dbj|BAB40656.2|/1-
2.69
207.90
183.00
gi|119577538|gb|EAW57134.1|/1-
183.00
gi|82181120|sp|Q66I68.1|CNFN_D
40.91
200.00
gi|169154033|emb|CAQ13806.1|/1
81.25
200.00
gi|125821285|ref|XP_001344132.
8.92
281.25
gi|68432883|ref|XP_706757.1|/1
173.16
290.17
gi|292615971|ref|XP_684883.4|/
gi|292618169|ref|XP_002663577.
8.75
45.00
gi|148678095|gb|EDL10042.1|/1-
98.50
45.00
gi|115527214|gb|AAI10559.1|/1-
263.67
132.40
143.50
gi|120659954|gb|AAI30589.1|/1-
17.03
407.17
gi|189534183|ref|XP_001337549.
7.13
580.48
gi|125827387|ref|XP_001338157.
589.23
gi|119626329|gb|EAX05924.1|/1-
606.26
gi|61175222|ref|NP_001012991.1

B

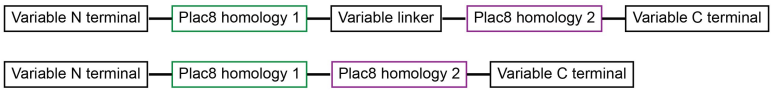
Variable N terminal
Plac8 homology 1
Variable linker
Plac8 homology 2
Variable C terminal
Variable N terminal
Plac8 homology 1
Plac8 homology 2
Variable C terminal

C

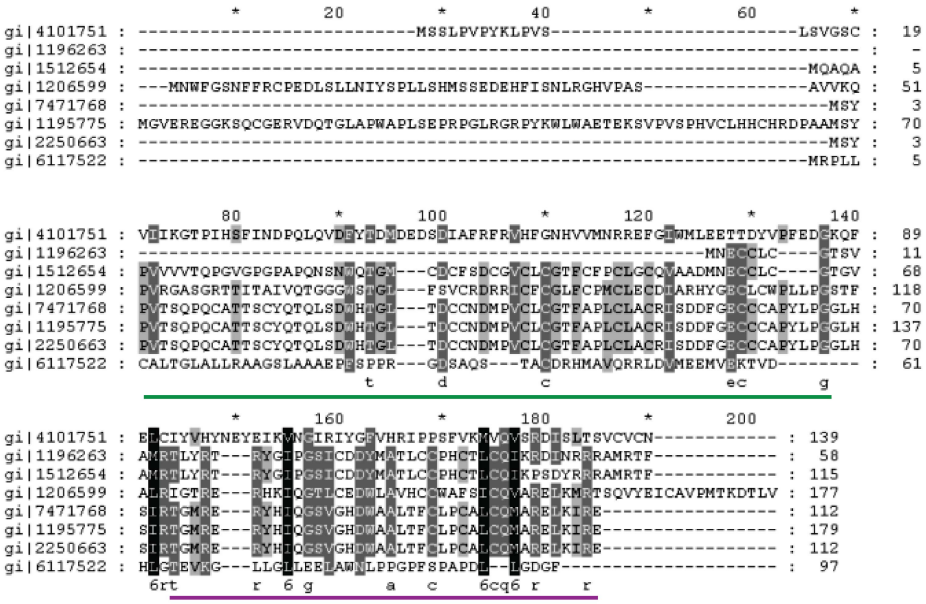
gi|4101751 : MSSLPVPYKLPVS LSVGSC : 19
gi|1196263 : - : -
gi|1512654 : MQAQA : 5
gi|1206599 : MNWFGSNFFRCPEDLSLLNIYSPLLSHMSSEDEHFISNLRGHVPAS AVVKQ : 51
gi|7471768 : MSY : 3
gi|1195775 : MGVEREGGKSQCGERVDQTGLAPWAPLSEPRPGLRGRPYKWLWAETEKSVPVSPHVCLHHCHRDPAAMSY : 70
gi|2250663 : MSY : 3
gi|6117522 : MRPLL : 5
gi|4101751 : VHIKGTPIHSFINDPQLQVDEYTDADEDSDIAFRFRVHFGNHVVMNRREFGIWMLEETTDYVPFEDEKQF : 89
gi|1196263 : MNEGCLC---STSV : 11
gi|1512654 : PVVVVTQPGVGPGAPAPQNSNTQTGT---CDCFSDCGVCLCGTFCFPCLGCQVAADMNEGCLC---STGV : 68
gi|1206599 : PVRGASGRTTITAIVQTGGGTSTGI---FSVCRDRRICFCGLFCPMCLECDIARHYGECLCWPLLPCSTF : 118
gi|7471768 : PVTSQPQCAITSCYQTQLSDTHTGI---TDCCNDMPVCLCGTFAPLCLACRISDDFGECCCAPYLPCGLH : 70
gi|1195775 : PVTSQPQCAITSCYQTQLSDTHTGI---TDCCNDMPVCLCGTFAPLCLACRISDDFGECCCAPYLPCGLH : 137
gi|2250663 : PVTSQPQCAITSCYQTQLSDTHTGI---TDCCNDMPVCLCGTFAPLCLACRISDDFGECCCAPYLPCGLH : 70
gi|6117522 : CALTGLALLRAAGSLAAAEPSSPPR---GDSAQS---TASDRHMAVQRRLDVMEEMVEKTVD : 61
gi|4101751 : EHCIYVHYNEYEIKVNGIRIYGFVHRIPPSFVKMVDVSRDDISLTSVCVCN : 139
gi|1196263 : AMRTLYRT---RYGIPGSICDDYMATLCGPHCTLCQIKRDDINRRRAMRTF : 58
gi|1512654 : AMRTLYRT---RYGIPGSICDDYMATLCGPHCTLCQIKPSDYRRRAMRTF : 115
gi|1206599 : ALRIGTRE---RHKIQGTLCEDWLAVHCGWAFSICQVARELKMRTSQVYEICAVPMTKDTLV : 177
gi|7471768 : SIRTGMRE---RYHIQGSVGHDWAALTFGLPCALCQMARELKIRE : 112
gi|1195775 : SIRTGMRE---RYHIQGSVGHDWAALTFGLPCALCQMARELKIRE : 179
gi|2250663 : SIRTGMRE---RYHIQGSVGHDWAALTFGLPCALCQMARELKIRE : 112
gi|6117522 : HEGTEVKG---LLGLLEELAWNLPPGPFSPAPDL--LGDGF : 97

D

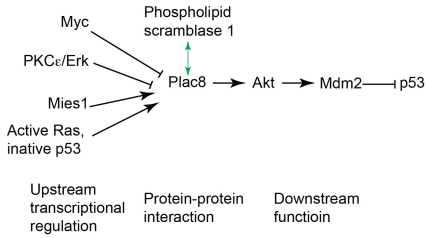
Myc
Phospholipid scramblase 1
PKCε/Erk
Plac8
Akt
Mdm2
p53
Mies1
Active Ras, inative p53
Upstream transcriptional regulation
Protein-protein interaction
Downstream functioin

Figure 1-6. PLAC8 family of cysteine-rich proteins
A. Phylogenetic analysis of the *Plac8* family genes in human, mouse and zebrafish. The vertical red bar indicates the human *PLAC8*, mouse *Plac8*, and zebrafish *plac8.1*, *plac8.2* that cluster together. B. Typical domain arrangement of Plac8 like proteins (upper panel) and members of the Plac8 family of proteins (lower panel). C. Amino acid sequence alignment of the Plac8 family of proteins in human. D. A diagram summarizing the transcriptional regulation, protein-protein interaction, and downstream signaling of Plac8 from the literature.

CHAPTER II

Excess PLAC8 promotes ERK2-dependent EMT in colon cancer

Cunxi Li[1†], Haiting Ma[2†], Zheng Cao[1], Yang Wang[1], Alina Starchenko[3], Anne Powell[1], Ramona Graves-Deal[1], Gregory D Ayers[4], Mary Kay Washington, Michael Gerdes, Lila Solnica-Krezel[2] and Robert J. Coffey[1,3,5*]

[1]Department of Medicine, Vanderbilt University Medical Center, Nashville, Tennessee 37232, [2]Department of Developmental Biology, Washington University School of Medicine, St. Louis, MO 63110, [3]Department of Cell and Developmental Biology, [4]Department of Statistics, Vanderbilt University Medical Center, Nashville, Tennessee 37232; [5]Department of Veterans Affairs Medical Center, Nashville, TN 37232

Running Title: Implicating PLAC8 in EMT

Key words: PLAC8, invasion, EMT, colon cancer, zebrafish, gastrulation

[†]Cunxi Li and Haiting Ma contributed equally to this work

Abstract

Epithelial to mesenchymal transition (EMT) is thought to be a transcriptionally driven program characterized by a cadherin switch (repression of CDH1 and expression of CDH2 mRNA), along with induction of mesenchymal genes like vimentin (VIM). PLAC8 has been implicated in colon cancer, but the mechanism is unclear and endogenous PLAC8 protein has not been studied. By combining analysis in zebrafish and humans, we show that endogenous PLAC8 localizes to the apical domain of differentiated intestinal epithelium. Excess PLAC8 in zebrafish embryos and colon cancer cells results in a post-transcriptional reduction in total and/or cell surface CDH1. PLAC8-overexpressing colon cancer cells exhibit many features of EMT, including aberrant cell motility and increased invasiveness. Despite increased *CDH1* mRNA and lack of *CDH2* mRNA, there is increased mRNA and protein expression of CDH3, VIM and ZEB1 in PLAC8-overexpressing colon cancer cells. The EMT phenotype in these cells is coupled to increased p-ERK2, and selective knockdown of ERK2 restores CDH1 levels while suppressing elevated levels of CDH3 and VIM. Knockdown of endogenous PLAC8 in colon cancer cells results in increased levels of CDH1 and decreased levels of CDH3 and p-ERK2. Using a novel multiplex immunofluorescence-based technique, we observe a correlation between PLAC8 and these EMT markers at the leading edge of a human colorectal tumor. We propose that excess PLAC8 can induce an atypical ERK2-dependent (associated) EMT in colon cancer.

Introduction

PLAC8 is a small 115-amino acid, cysteine-rich protein that was first identified in human plasmacytoid dendritic cells by subtractive hybridization analysis of gene expressed in activated monocyte-derived dendritic cells (Rissoan et al., 2002). By *in situ* hybridization, *Plac8* expression was found to be restricted to giant trophoblasts and the spongiotrophoblast layer in the placenta (Galaviz-Hernandez et al., 2003). Subsequently, *PLAC8* mRNA expression was observed in myeloid and lymphoid cells, as well as in normal and neoplastic epithelial cells (Ledford et al., 2007). *Plac8*-deficient mice have defects in innate immunity (Ledford et al., 2007) and exhibit contact hypersensitivity (Ledford et al., 2012), impaired brown and white fat differentiation and late onset obesity (Jimenez-Preitner et al., 2011). In addition, *Plac8* transcripts are upregulated in immortalized mouse colonocytes transformed by combined mutant *H-ras*

and *p53* (McMurray et al., 2008). Knockdown of endogenous *Plac8* in these cells and in a human colorectal cancer (CRC) cell line, HT-29, reduces growth of xenografts in nude mice (McMurray et al., 2008). Although PLAC8 has essential roles in normal physiology, and a possible role in CRC, the underlying molecular mechanisms and intracellular distribution of endogenous Plac8 protein have not been studied.

Herein, we show that endogenous PLAC8 localizes to the apical domain of terminally differentiated human colonic epithelium. To begin to understand the function of PLAC8, we utilized the experimental advantages provided of the zebrafish model (Santoriello and Zon, 2012). We first identified the zebrafish PLAC8 homolg, Plac8.1. It also localizes to the apical domain of the zebrafish gut, and shows a dynamic distribution pattern during embryogenesis. Overexpression of Plac8.1 in the early zebrafish embryo impaired gastrulation cell movements, phenocopying *cdh1* (encoding Cdh1) mutant defects. When overexpressed, Plac8.1 caused a post-transcriptional reduction in Cdh1 levels in zebrafish gastrulae acting in a cell-autonomous fashion. Likewise, overexpression of PLAC8 in a human CRC cell line, HCA-7, resulted in reduced functional cell surface CDH1 (despite increased mRNA expression).

EMT is thought to be a transcriptional program with repression of *CDH1* mRNA and induction of mRNA encoding for *CDH2* and mesenchymal genes like VIM as characteristic features. As mentioned above, CDH1 was regulated post-transcriptionally and CDH2 was not expressed in either parental or PLAC8-overexpressing HCA-7 cells. However, these PLAC8-overexpressing cells had increased mRNA levels of *CDH3*, linked to colon cancer progression (Park et al., 2012; Sun et al., 2011; Hardy et al., 2002), and *ZEB1* and *VIM*, along with morphological, molecular and functional features of EMT. PLAC8-overexpressing HCA-7 cells exhibited increased p-ERK2, previously shown to induce EMT (Shin et al., 2010); knockdown of ERK2, but not ERK1, in these cells increased total and cell surface CDH1 and decreased CDH3 and VIM. Knockdown of endogenous PLAC8 in colon cancer cells increased CDH1 levels while decreasing levels of CDH3 and p-ERK1/2. We propose that excess PLAC8 may promote an atypical EMT and cell invasiveness that is, at least in part, ERK2-dependent.

Results

Endogenous PLAC8 protein localizes to the apical domain of terminally differentiated human colonic epithelium. Although *Plac8* mRNA expression is increased in immortalized mouse colonocytes transformed by introduction of both mutant *H-ras* and *p53*, and knockdown of *Plac8* reduces tumor growth in xenografts (McMurray et al., 2008), how PLAC8 contributes to colonic neoplasia is unknown. To begin to address its role in CRC, we examined its distribution in both normal human colon and CRC by immunofluorescence using a commercial PLAC8-specific antibody. The specificity of this antibody was first validated by comparing the immunofluorescent staining of PLAC8-positive cells and their knockdown counterparts. PLAC8 immunofluorescence was detected in normal colon where it was found exclusively at the apical domain of fully differentiated colonic epithelium at the top of crypts in both colonocytes (Figure 2-1A, B) and goblet cells (Figure 2-2A, B). There was an abrupt decrease in immunofluorescence in epithelial cells deeper in the crypt (Figure 2-1A, B) and PLAC8 staining was absent in epithelial cells at the crypt base (Figure 2-2C, D). Staining was also observed in some scattered mononuclear cells in the stroma.

Cytosolic PLAC8 is correlated to tumor grade and linked to mucinous and medullary CRC. We next analyzed PLAC8 expression in a CRC tissue microarray (TMA) (Powell et al., 2012). All CRC cases showed the above noted expression of PLAC8 in scattered mononuclear cells in the stroma. In 49% of cases (41/84), no staining was observed in the malignant epithelium (Figure 2-2F), whereas in the remaining 51% of cases (43/84), there was membranous and/or cytosolic PLAC8 staining in the malignant epithelium (Table 2-1). Cytosolic PLAC8 staining was confined to the cytoplasm in 9 cases (11%), where it strongly correlated with higher tumor grade (p=0.0009) (Table 2-1). In typical moderately differentiated colorectal adenocarcinomas, PLAC8 localized to the apical domain similar to its distribution in normal colon (Figure 2-1C, D). As expected, CDH1 was found along the basolateral membrane of polarized normal and neoplastic epithelium (Figure 2-1A, B and D). Notably, strong cytosolic PLAC8 immunofluorescence was detected in two histological subtypes - medullary (Figure 2-1E, F) and mucinous (Figure 2-1G, H) carcinoma. In these subtypes, PLAC8 was largely cytosolic and, in areas with

prominent PLAC8 immunofluorescence, CDH1 appeared to be less membranous. All CRC cases showed the expression of PLAC8 in scattered mononuclear cells in the stroma.

Increased levels of PLAC8 are linked to tumor progression. Because the commercial PLAC8 antibody was not suitable for immunoblotting, we generated a rabbit anti-PLAC8 antibody (Methods), validated its specificity (Figure 2-3) and used it to examine a battery of human CRC cell lines cultured on plastic. In two matched CRC cell lines, PLAC8 levels were higher in the metastatic compared to primary cell lines - SW620 versus SW480 (Leibovitz et al., 1976) and KM12SM versus KM12C (Kitadai et al., 1996) (Figure 2-4A). The strongest PLAC8 signal was found in LoVo cells, a microsatellite unstable mucinous cell line (Drewinko et al., 1976). In two HCA-7 subclones, CC and SC (described below), PLAC8 levels were higher in SC than parental HCA-7 cells, whereas PLAC8 was not detected in CC (Figure 2-4A).

Culturing HCA-7 cells in type 1 collagen led to the identification of colonies with two distinct morphologies (Figure 2-4B) and markedly different levels of PLAC8 (Figure 2-4A and C): hollow cysts lined by a single layer of polarized cells enclosing a central lumen (designated cystic clones, CC) with undetectable levels of PLAC8 or solid masses with ill-defined borders and protrusions (designated spiky clones, SC) with high levels of PLAC8. When cells from these two representative cell lines CC and SC were injected subcutaneously into athymic nude mice, they retained their *in vitro* morphologies: CC formed well-differentiated, encapsulated cysts, whereas SC formed poorly differentiated tumors that invaded into adjacent skeletal muscle. Moreover, by immunofluorescence, PLAC8 was not detected in CC tumors but was present and largely cytosolic in SC tumors (Figure 2-4B, bottom two rows). Knockdown of *PLAC8* in SC cells reduced their growth in soft agar (Figure 2-4C).

Thus, PLAC8 expression appears to be context-dependent, with PLAC8 levels being higher in metastatic (SW620, KM12SM) and invasive (SC) tumors than their less aggressive counterparts (SW480, KM12C, CC). Although these studies suggest a correlation between increased PLAC8 levels and CRC progression, they leave open the question as to its cellular function and precise role in CRC.

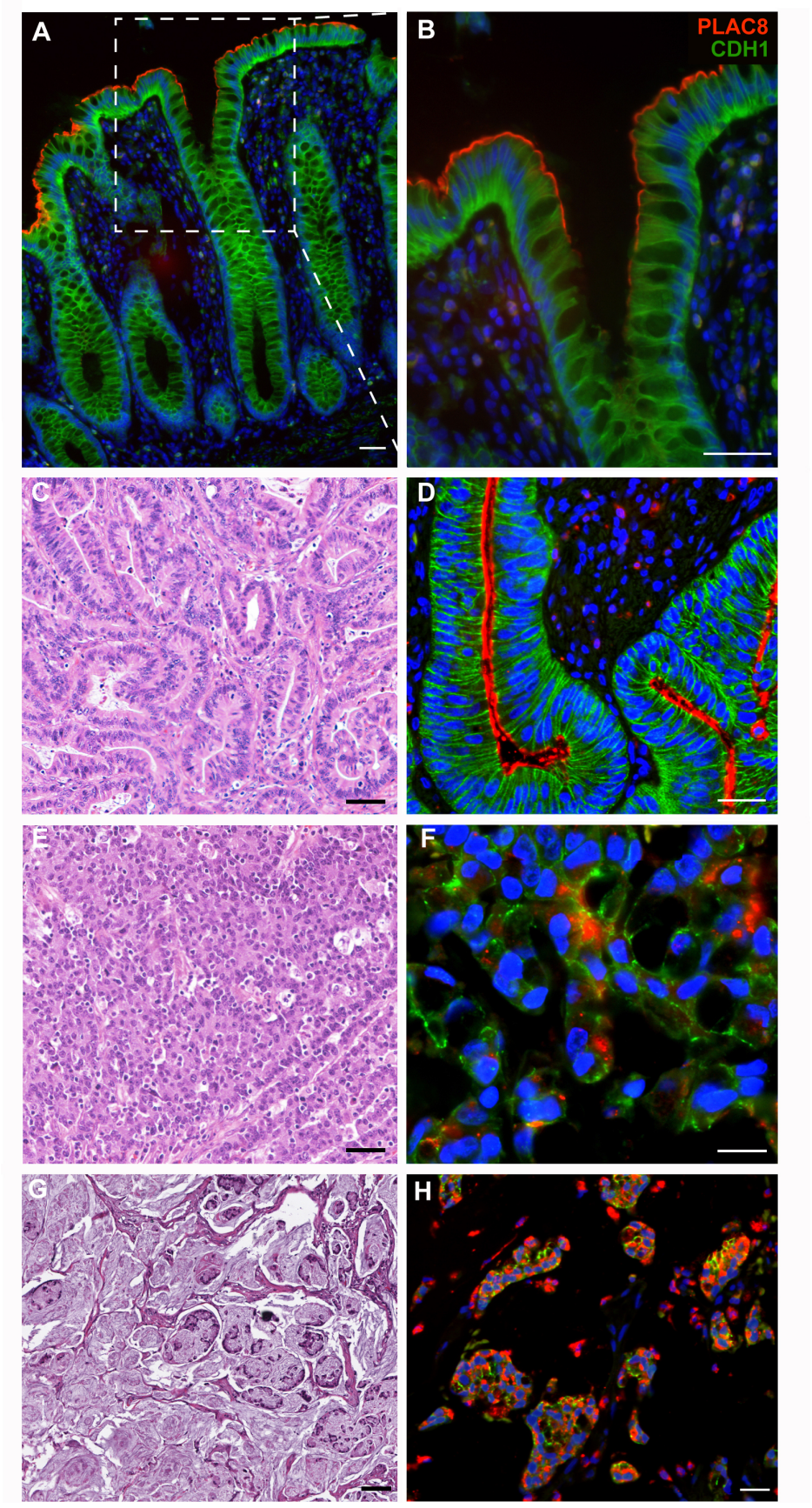
A
B
PLAC8
CDH1
C
D
E
F
G
H

Figure 2-1. PLAC8 immunofluorescence in human normal colon and CRC.
(**A** and **B**) In normal colon, PLAC8 fluorescence (red) localizes to the apical domain of differentiated colonic epithelium at the top of crypts. Boxed region in (A) is magnified in (B). Epithelial cells are outlined by CDH1 immunofluorescence (green). **(D)** In a typical moderately differentiated adenocarcinoma, PLAC8 also localizes to apical domain but immunofluorescence extends deeper into the neoplastic crypts (Figure 2-2E). **(F and H)** PLAC8 immunofluorescence is largely detected in the cytoplasm of medullary (F) and mucinous (H) adenocarcinoma**. (C, E and G)** Serial H&E-stained sections at lower magnification correspond to similar areas in (D, F and H). In all immunofluorescent panels, DAPI (blue) marks nuclei. Scale bars, 100 μm.

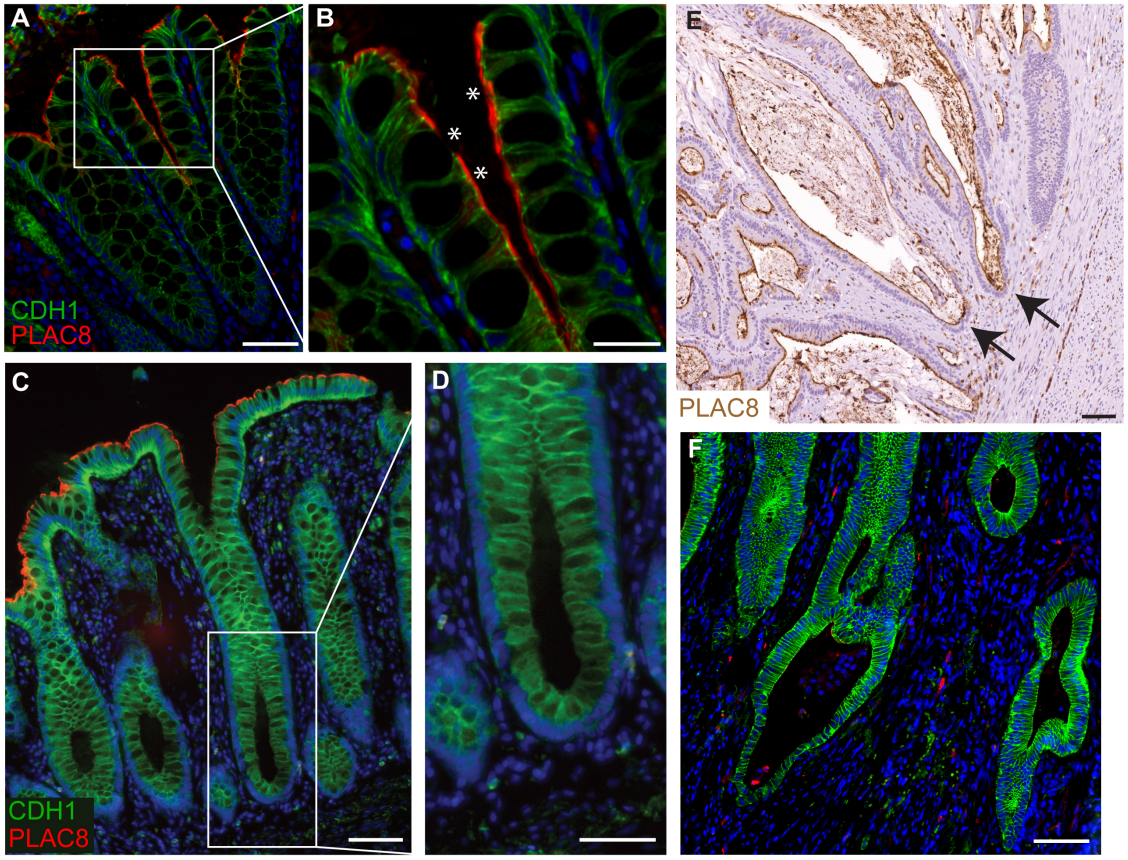
A
B
C
D
E
F
CDH1
PLAC8
CDH1
PLAC8
PLAC8

Figure 2-2. PLAC8 extends into the neoplastic crypts of adenocarcinoma.
(**A** and **B**) In normal colon, PLAC8 fluorescence (red) localizes to the apical domain of both differentiated colonic and goblet epithelia. Boxed region in (A) is magnified in (B) to show the goblet cells (asterisks). CDH1 immunofluorescence (green) was used to outline the epithelia. DAPI stained the nuclei. **(C and D)** PLAC8 does not localize to the bottom of crypts. **(E)** In a typical moderately differentiated adenocarcinoma, PLAC8 also localizes to apical domain but immunohistochemistry extends deeper into the neoplastic crypts. **(F)** PLAC8 immunofluorescence is not detected in 51% adenocarcinimas. DAPI (blue) marks nuclei. Scale bars, 100 μm.

Table 2-1. Correlation between advanced cancer grade and cytoplasmic localization of PLAC8.

Tumor Grade	# Cases/All Grades	Cytosolic PLAC8 Expression	
		# Cases / Grade	%
I	11/84	0/11	0
II	51/84	2/51	4
III	22/84	7/22	32

Statistic	Df	Chi-squared value	*p* value
Chi-square	2	14.0223	0.0009

DF, Degree of freedom

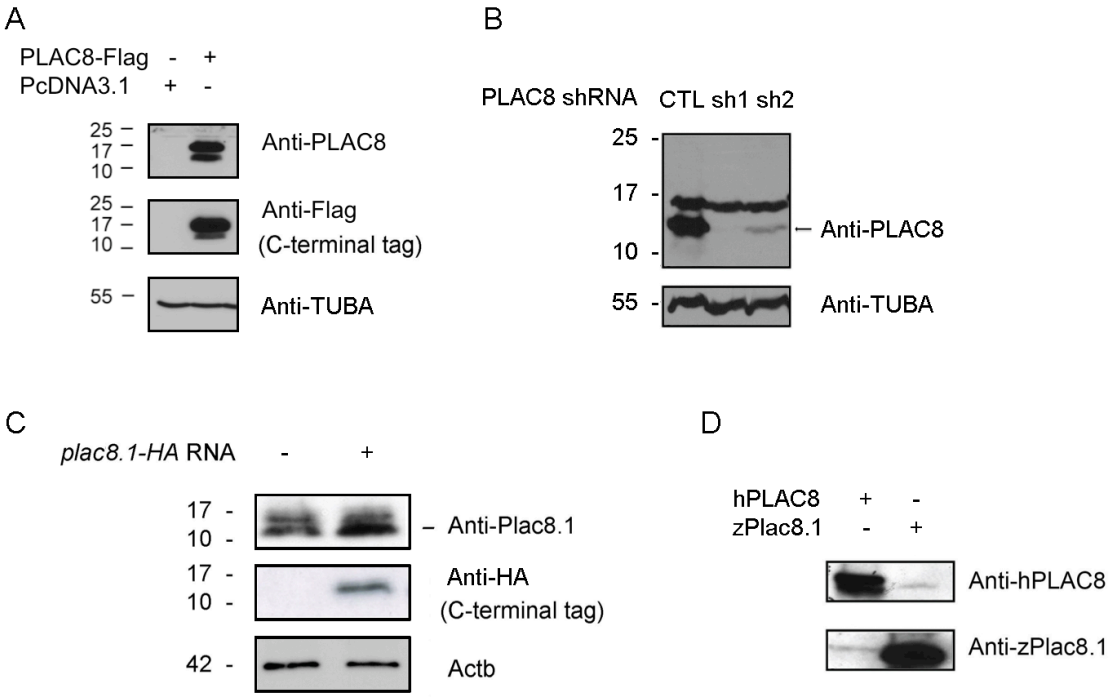
A
PLAC8-Flag - +
PcDNA3.1 + -
25
17
10
Anti-PLAC8
25
17
10
Anti-Flag
(C-terminal tag)
55
Anti-TUBA
B
PLAC8 shRNA CTL sh1 sh2
25
17
10
Anti-PLAC8
55
Anti-TUBA
C
plac8.1-HA RNA - +
17
10
Anti-Plac8.1
17
10
Anti-HA
(C-terminal tag)
42
Actb
D
hPLAC8 + -
zPlac8.1 - +
Anti-hPLAC8
Anti-zPlac8.1

Figure 2-3. Characterization of anti-PLAC8 and zPlac8 antibodies.
(A) FLAG tagged *PLAC8* cDNA and pcDNA3 vector as a control were transfected into HEK293T cells. Both affinity-purified anti-PLAC8 antibody and anti-FLAG antibody recognized the PLAC8-FLAG chimera. **(B)** PLAC8 shRNAs depleted endogenous PLAC8 from SC1 cells (arrow pointed). There is an unknown 17 Kd band detectable in SC1 cells cultured on plastic dishes, but undetectable in SC1 cells cultured in collagen gel. **(C)** Zebrafish Plac8.1-HA fused peptide was detected by both anti-Plac8.1 antibody and anti-HA antibody. **(D)** There is no obvious cross reaction between zebrafish Plac8.1 and human PLAC8 antibodies.

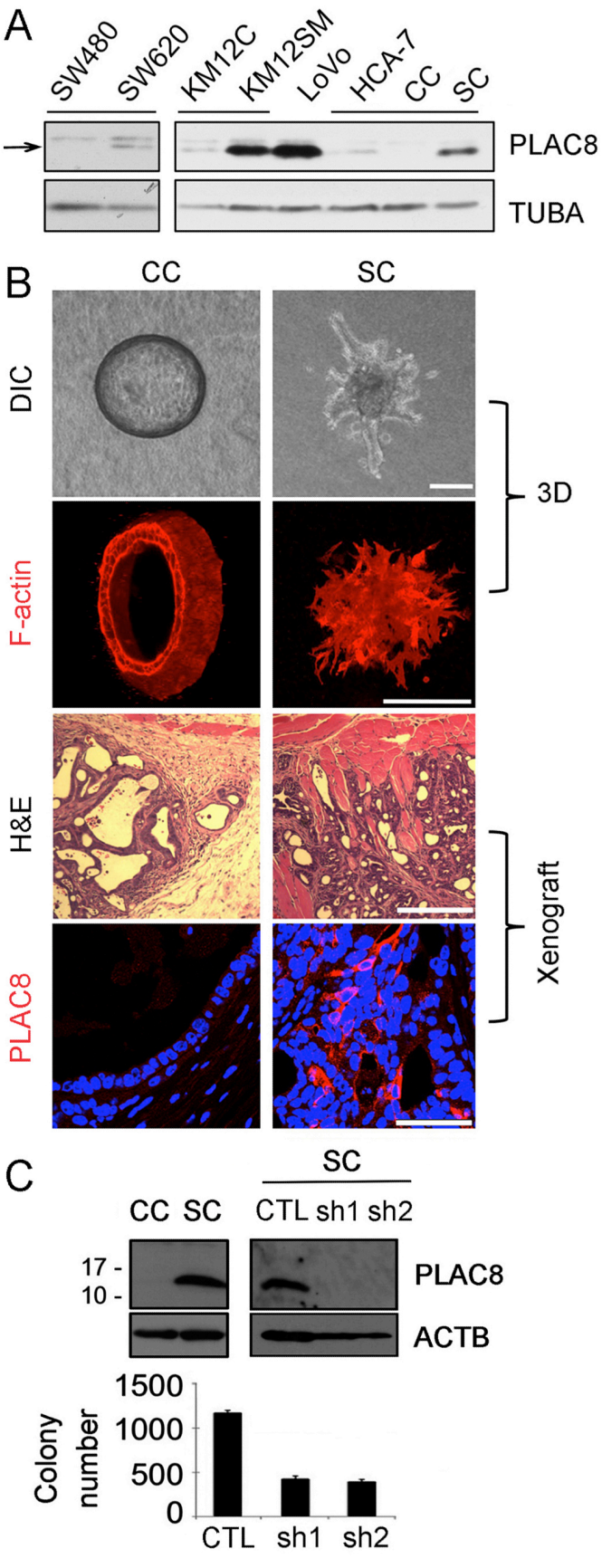
A
SW480
SW620
KM12C
KM12SM
LoVo
HCA-7
CC
SC
PLAC8
TUBA
B
CC
SC
DIC
F-actin
H&E
PLAC8
3D
Xenograft
C
SC
CC SC
CTL sh1 sh2
17 -
10 -
PLAC8
ACTB
Colony number
1500
1000
500
0
CTL
sh1
sh2

Figure 2-4. Increased PLAC8 protein is linked to tumor progression.
(**A**) By immunoblotting of CRC cell lines cultured on plastic, PLAC8 levels are higher in cells derived from metastatic tumors (SW620 and KM12SM) compared to cells derived from primary tumors (SW480 and KM12C), as well as in more invasive SC cells compared to CC or parental HCA-7 cells. (**B**) In 3D collagen culture, HCA-7 cell colonies exhibit two distinctive phenotypes, cystic clones (CC) that formed smooth-edged spheres with a clear cavity and spiky clones (SC) that grew as a solid mass with ill-defined borders and multiple protrusions. Top panels, differential interference phase contrast microscopy. Bottom panels, phalloidin-Taxas Red immunofluorescence. Scale bars, 100 μm. In xenograft experiment, CC and SC cells were subcutaneously injected into athymic nude mice for 4-8 weeks. CC cells formed well-differentiated cystic tumors with a thick fibroblastic capsule and no detectable PLAC8 immunofluorescence (left panels), whereas SC cells formed poorly differentiated tumors that invaded into skeletal muscle and exhibited strong, largely cytosolic PLAC8 immunofluorescence (bottom panels). Scale bars, 100 mm. (**C**) In 3D collagen, similar to plastic culture, PLAC8 is strongly expressed in SC cells but not detectable in CC cells by immunoblotting. PLAC8 is efficiently knocked down in SC by two stably expressing PLAC8 shRNAs (right panel). The bottom chart shows PLAC8 knockdown in these two SC cells results in decreased colony number in collagen culture. (*, $p<0.05$).

Identification and characterization of zebrafish plac8 homologs. To begin to elucidate the cellular and molecular functions of PLAC8 *in vivo*, we took advantage of the tractability afforded by the zebrafish model (Santoriello and Zon, 2012). Using the reciprocal best hits (RBH) method (Moreno-Hagelsieb and Latimer, 2008), we identified the zebrafish *zgc114201* gene that encodes a cysteine-rich protein with 44% amino acid identity (including 13 of 16 cysteines) and 62% similarity to human PLAC8 (Figure 2-5A, C). In phylogenetic analyses, this putative zebrafish Plac8 clustered with Plac8 proteins from other species (Figure 2-5E). Furthermore, analysis of the human, mouse, and zebrafish genomes revealed that *zgc114201* is a syntenic equivalent of human *PLAC8* (Figure 2-5B). We noted the second best hit, *zgc158845* (42% identity 41.5%, 56% similarity to *PLAC8*), located next to *zgc114201* (Figure 2-5B). Given their physical proximity and structural similarity, *zgc114201* and *zgc158845* likely arose via a tandem gene duplication event (Woods et al., 2000), According to the zebrafish gene nomenclature guidelines, we designated these genes *plac8.1* and *plac8.2*, respectively. Using RT-PCR, we found that *plac8.2* was expressed during early embryogenesis only at low levels, whereas *plac8.1* was prominently expressed in multiple developmental stages (Figure 2-5D). Thus, we elected to focus on *plac8.1* in this study.

Whole-mount *in situ* hybridization revealed that *plac8.1* RNA was expressed maternally and uniformly during early embryogenesis (Figure 2-6A) until four days post-fertilization (dpf), when it was upregulated in the gut and downregulated in other tissues (Figure 2-6C). To investigate Plac8.1 protein distribution, we generated a rabbit polyclonal antibody against a C-terminal peptide (Methods) and validated its specificity by immunoblotting (Figure 2-3C and D). Using this antibody, we found ubiquitous Plac8.1 immunofluorescence during gastrulation stages (Figure 2-6B, left panels). Strikingly, the intracellular distribution of Plac8.1 in mesenchymal gastrula cells changed from largely cytosolic at the onset of gastrulation to progressively enriched at the plasma membrane at later gastrula stages (Figure 2-6B). This dynamic pattern of intracellular distribution was also observed in gastrulae expressing a C-terminal fusion protein, Plac8.1-EGFP (Figure 2-7D), or Plac8.1-HA (data not shown). Given the accumulation of *Plac8.1* transcripts in the gut, we next analyzed its distribution in this organ. Like in human intestine, Plac8.1 protein was enriched at the apical surface of gut epithelial cells at 4 dpf (Figure 2-6D). Thus,

Plac8.1 intracellular distribution is dynamic and highly regulated in a developmental stage- and cell type-dependent manner.

Overexpression of plac8.1 impairs gastrulation, phenocopying cdh1 loss-of-function. To gain mechanistic insight into the effects of *plac8* overexpression, we injected various amounts of synthetic *plac8.1* RNA into one-cell stage zebrafish embryos (Figure 2-7A). Plac8.1 overexpressing embryos displayed normal morphology until gastrulation, when cells accumulated predominantly in the dorsal region of the gastrula (Figure 2-7A). Moreover, the blastoderm margin was further away from the vegetal pole in Plac8.1-overexpressing compared to uninjected control embryos. These results indicate that excess Plac8.1 impairs the epibolic movements that spread the embryonic tissues around the yolk. Accordingly, expression of the mesodermal marker *no tail* (*ntl*) (Schulte-Merker et al., 1994) at the blastoderm margin was positioned further from the vegetal pole in embryos overexpressing Plac8.1 compared to control embryos. Moreover, the *ntl* expression domain, marking dorsal forerunner cells (normally in close contact with the dorsal blastoderm margin) was separated from the deep cell margin in embryos overexpressing Plac8.1 (Figure 2-7A), a phenotype consistent with epiboly defects (Lin et al., 2009). In addition, *ntl* expression domain in the nascent chordamesoderm was shortened anteroposteriorly, but broadened mediolaterally (Figure 2-7A), suggesting that excess Plac8.1 also impairs convergence and extension gastrulation movements.

At the completion of embryogenesis, Plac8.1-overexpressing embryos manifested dorsally curved and shortened body axes, with a small fraction displaying various degrees of cyclopia (Figure 2-7A**)**. Injection of exogenous RNA encoding human PLAC8 led to a similar phenotype (data not shown). Penetrance of the defective gastrulation phenotypes described above increased in a concentration-dependent manner (Figure 2-8A), and was reduced by co-injection with a *plac8.1* antisense morpholino oligonucleotide, MO1-*plac8.1*, which inhibits translation of the injected *plac8.1* RNA (data not shown). Taken together, these data suggest the observed defects in epiboly and convergence and extension gastrulation movements are due to overexpression of Plac8.1.

A

```
zPlac8.1        ------MEVTSQP-----SAFHPQEFHSGLMSCCDDVGVCCCGLFCLPCMGCSIASDMNE 49
hPLAC8          MQAQAPVVVVTQPGVGPGPAPQNSNWQTGMCDCFSDCGVCLCGTFCFPCLGCQVAADMNE 60
                      : *.:**     .* : .::::*: .* .* *** ** **:**:**.:*:****

zPlac8.1        CCLCGLGMPMRSVYRTKYNIEGSMCNDWAATTFCFTCAACQLKRDIDIRKSNGTLKL    106
hPLAC8          CCLCGTSVAMRTLYRTRYGIPGSICDDYMATLCCPHCTLCQIKRDINRRRAMRTFKI    117
                ***** .:.**::***:*.* **:*:*: **  *  *: **:****: *::  *:*:
```

B

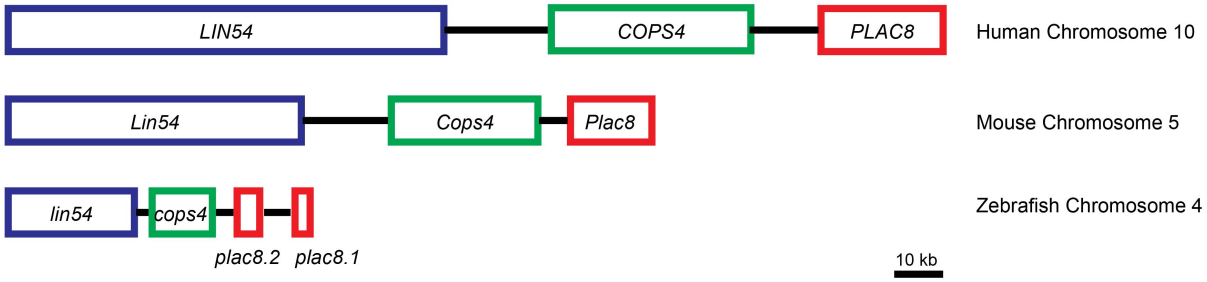

C

	Plac8.2	Human PLAC8	Mouse PLAC8
Plac8.1	75.5% 83.0%	44.4% 61.5%	43.9% 59.6%
Plac8.2	-	41.5% 55.9%	42.9% 58.0%
Human PLAC8	-	-	80.3% 85.5%

D

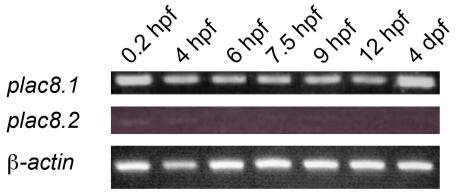

E

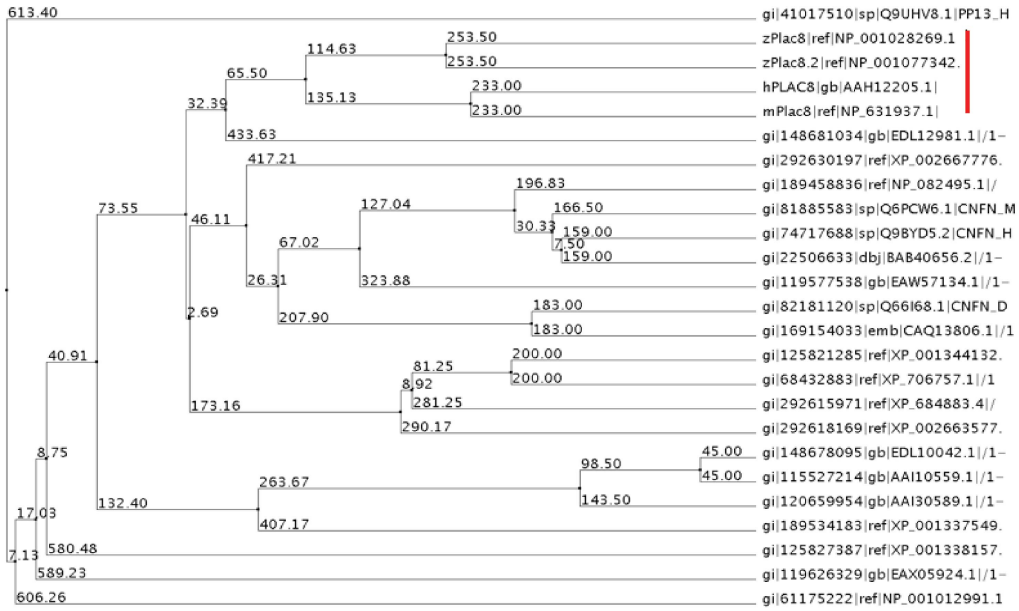

Figure 2-5. Identification of zebrafish *plac8* homologs.
(A) Amino acid sequence alignment of zebrafish Plac8.1 (zPlac8.1) and human PLAC8 (hPLAC8). Identical amino acid residues are denoted by "*"; conserved substitutions and semi-conserved substitutions are denoted by ":" and ".", respectively. (**B**) A diagram illustration of the gene arrangements of the *Plac8* loci in humans, mouse, and zebrafish. (**C**) Comparison of amino acid sequences between zebrafish Plac8.1, Plac8.2 and mammalian PLAC8 proteins. The two numbers of each box denote identity (top numbers) and similarity (bottom numbers). (**D**) Expression of zebrafish *plac8.1* and *plac8.2.* RT-PCR experiments of RNA samples extracted from zebrafish embryos at various developmental time points were performed with *plac8.1, plac8.2* and *Actb* (loading control) specific primers as labeled. (**E**) Phylogenetic analysis of Plac8 domain containing proteins from human, mouse, and zebrafish shows that the four Plac8 proteins cluster together (marked by the red line).

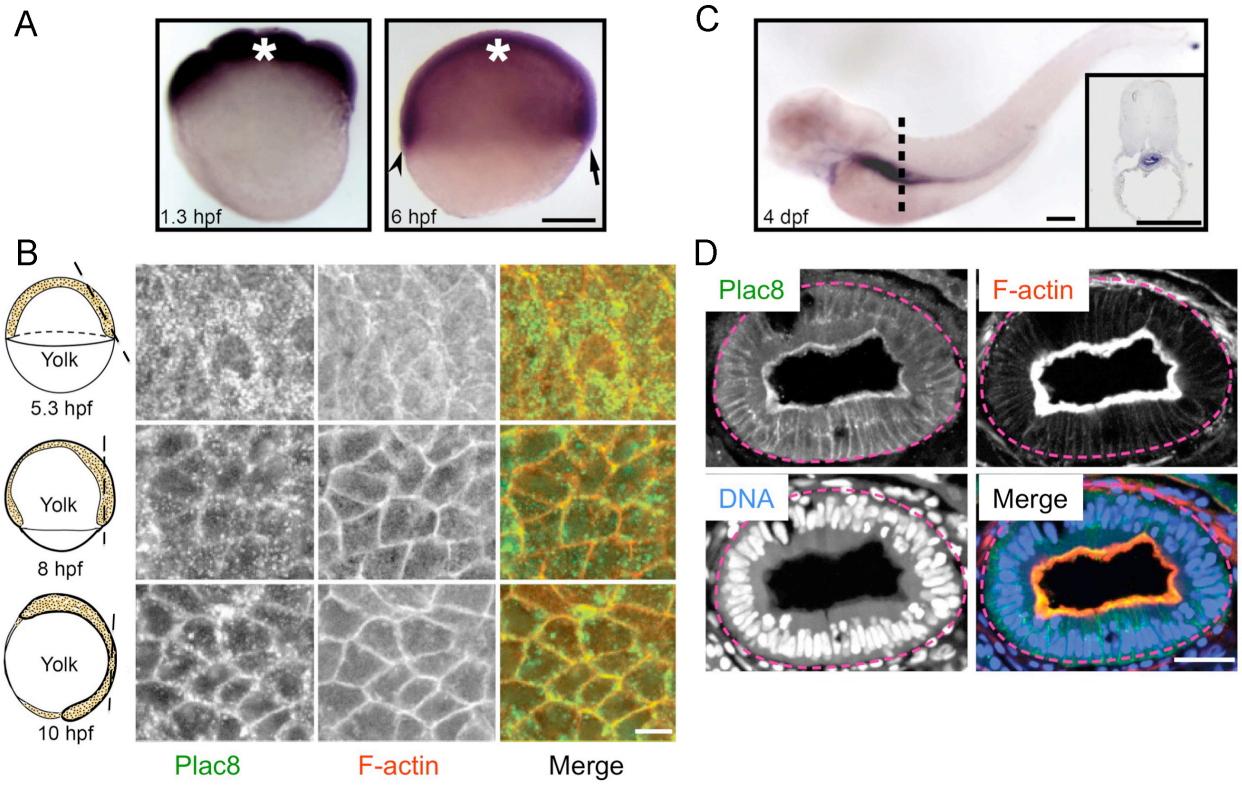
A
1.3 hpf
6 hpf
C
4 dpf
B
Yolk
5.3 hpf
Yolk
8 hpf
Yolk
10 hpf
Plac8
F-actin
Merge
D
Plac8
F-actin
DNA
Merge

Figure 2-6. Characterization of *plac8.1* RNA expression and protein localization in zebrafish embryos.

(**A**) Whole-mount *in situ* hybridization (ISH) using an anti-sense probe against full-length coding sequence of *plac8.1* on zebrafish embryos at indicated hours post-fertilization (hpf). Asterisks denote position of animal poles. The arrow and arrowhead denote future dorsal and ventral side, respectively. A sense probe showed no appreciable signal (data not shown). **(B)** Confocal immunofluorescent images of whole-mount zebrafish embryos stained with anti-Plac8.1 (green) and Texas Red-conjugated phalloidin (red, F-actin). Cartoons on left of each panel illustrate corresponding stages. The dashed lines correspond to their right section planes. **(C)** Whole-mount ISH using *plac8.1* anti-sense probe on zebrafish embryos at 4 days post-fertilization (dpf). Dashed line indicates approximate position for transverse section shown in inset with strong signal in gut. Scale bars, 100 μm. **(D)** Cryosections through the gut of embryos 4 at dpf were stained with anti-Plac8.1 antibody (green), Texas Red-conjugated phalloidin (red, F-actin) and TO-PRO-3 (blue, DNA). Scale bars, 10 μm.

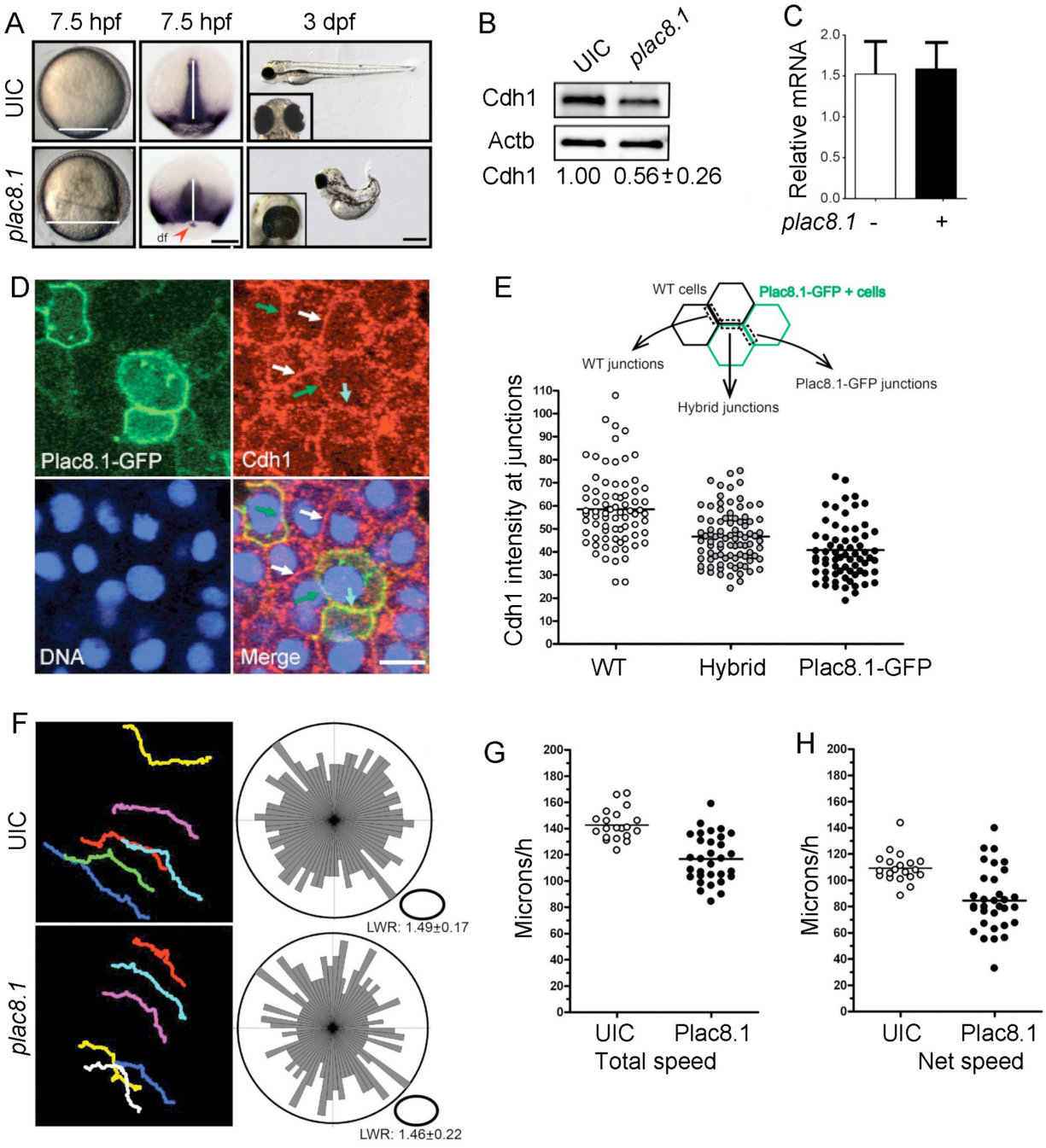
A
7.5 hpf
7.5 hpf
3 dpf
UIC
plac8.1
df
B
UIC
plac8.1
Cdh1
Actb
Cdh1 1.00 0.56±0.26
C
Relative mRNA
2.0
1.5
1.0
0.5
0.0
plac8.1 - +
D
Plac8.1-GFP
Cdh1
DNA
Merge
E
WT cells
Plac8.1-GFP + cells
WT junctions
Plac8.1-GFP junctions
Hybrid junctions
Cdh1 intensity at junctions
WT
Hybrid
Plac8.1-GFP
F
UIC
plac8.1
LWR: 1.49±0.17
LWR: 1.46±0.22
G
Microns/h
UIC
Plac8.1
Total speed
H
Microns/h
UIC
Plac8.1
Net speed

Figure 2-7. Overexpression of *plac8.1* results in cell-autonomous downregulation of E-cadherin and multiple developmental defects that phenocopy *cdh1* loss-of-function.
(**A**) Left panels: representative micrographs of uninjected control (UIC) zebrafish embryo and embryos injected with synthetic *plac8.1* RNA during gastrulation stages. Horizontal white lines denote progression of deep cell margin, and mark the diameter of the deep cell margin. Middle panels: ISH with *no tail (ntl,* zebrafish homolog of T-box containing transcription factor *Brachyury)* anti-sense probe during gastrulation stages. The vertical white lines denote the forming midline tissues, and the red arrowhead indicates the cluster of dorsal forerunner cells separated from the deep cell margin. Right panels: micrographs of uninjected control embryos and embryos overexpressing *plac8.1* RNA at 3 dpf with ventral view of eyes shown in insets. Scale bars, 100 mm. (**B**) Immunoblotting showed moderately reduced levels of Cdh1 in lysates from control or *plac8.1* overexpressing embryos at 50% epiboly stages. Average fold reduction of Cdh1, normalized to b-actin, is indicated underneath the immunoblots as mean ± standard deviation from 7 independent experiments ($p<0.01$). (**C**) qRT-PCR showed no significant change in *cdh1* RNA level in Plac8.1-EGFP overexpressing embryos compared to controls. Mean ± standard errors from three independent experiments are shown. (**D**) Representative micrographs of a cluster of cells with three types of membrane junctions: those shared by two WT cells (white arrows); those shared by two Plac8.1-EGFP overexpressing cells (cyan arrow); hybrid membrane junctions (green arrows). Scale bars, 10 mm. (**E**) Upper panel, a cartoon representation of the three types of membrane junctions. Lower panel, quantification of membrane Cdh1 intensity at different membrane junctions. (**F**) Left panels: representative paths of lateral mesodermal cells traveling during course of time lapse in UIC embryos and embryos overexpressing *plac8.1*. Right panels: orientations of the long axes of lateral mesodermal cells are plotted with length-width ratio expressed as mean ± standard error. (**G and H**) Quantification of total speeds and net speeds of lateral mesodermal cells.

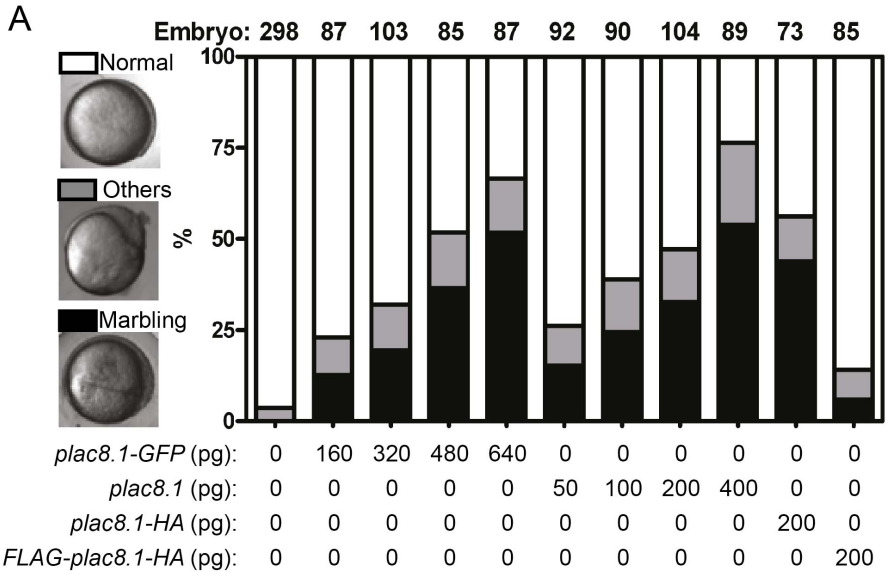
A
Embryo: 298 87 103 85 87 92 90 104 89 73 85
Normal
Others
Marbling
100
75
50
25
0
%
plac8.1-GFP (pg): 0 160 320 480 640 0 0 0 0 0 0
plac8.1 (pg): 0 0 0 0 0 50 100 200 400 0 0
plac8.1-HA (pg): 0 0 0 0 0 0 0 0 0 200 0
FLAG-plac8.1-HA (pg): 0 0 0 0 0 0 0 0 0 0 200

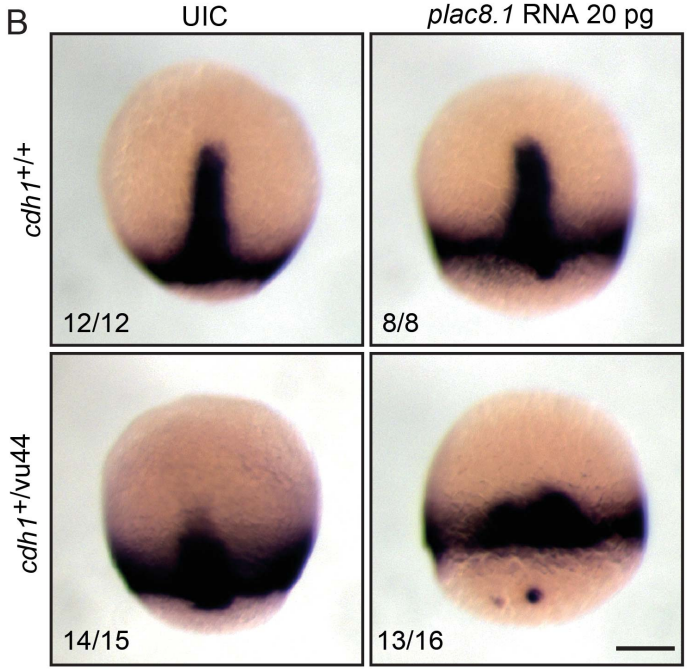
B
UIC
plac8.1 RNA 20 pg
cdh1+/+
cdh1+/vu44
12/12
8/8
14/15
13/16

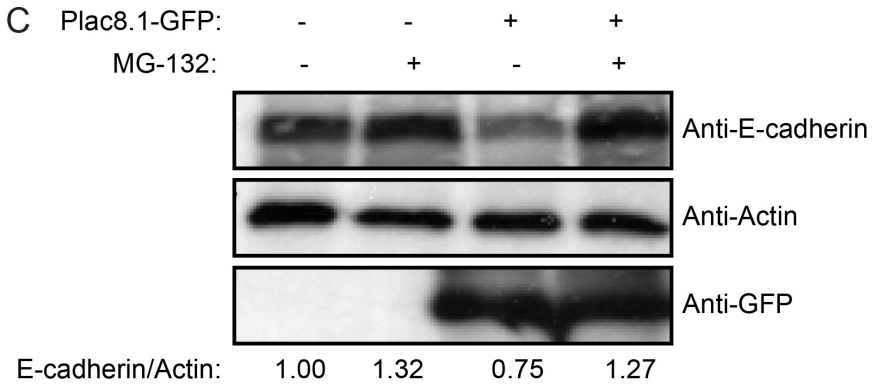
C
Plac8.1-GFP: - - + +
MG-132: - + - +
Anti-E-cadherin
Anti-Actin
Anti-GFP
E-cadherin/Actin: 1.00 1.32 0.75 1.27

Figure 2-8. The effect of Plac8.1 overexpression on zebrafish embryonic development.
(A) Quantitation of the percentage of normal embryos (normal, open bars), embryos showing the phenotype in Figure 2-7A (marbling, filled bars), or embryos showing other defects (others, gray bars). The total numbers of embryos are labeled on the top of each column. Results from three independent injection experiments are plotted. The type and amount of synthetic RNA injected are labeled at the bottom of the plot. (**B**) Expression of low dose Plac8.1 exacerbates embryonic developmental defects in *cdh1*$^{+/vu44}$ embryos. Representative micrograph of *in situ* hybridization with *ntl* probe of wild-type (top panel) or *cdh1*$^{+/vu44}$ embryos injected with 20 pg *plac8.1* RNA (bottom panel). DNA samples from embryos were extracted after *in situ* hybridization pictures were taken, followed by genotyping of the *cdh1* gene. The numbers of embryos were labeled on the lower left corner of each picture. (**C**) Downregulation of Cdh1 by Plac8.1 overexpression is partially suppressed by MG-132 treatment. Representative Western blotting of lysates from embryos injected with *plac8.1-GFP* RNA with or without MG132 treatment (50 μM). Antibodies were labeled to the right of each panel. Actb was used as a loading control. Normalized levels of Cdh1 are labeled at the bottom of each lane.

To determine the cellular basis of these gastrulation abnormalities, we characterized movements of lateral mesodermal cells in control gastrulae and embryos overexpressing Plac8.1-EGFP using Nomarski time-lapse analysis. Cells from the control and Plac8.1-EGFP-overexpressing embryos showed similar length-width ratios (LWR), suggesting that Plac8.1 overexpression does not affect cell elongation (Figure 2-7F, right panel). Also, the orientation of cell bodies of Plac8.1-EGFP -overexpressing gastrulae showed a similar pattern to controls (Figure 2-7F, right panels). Tracking the positions of representative mesodermal cells over time by time-lapse analyses revealed normal cell migration paths in Plac8.1-EGFP- overexpressing gastrulae (Figure 2-7F, left panels). However, both the total and net cell migration speeds were significantly reduced in embryos overexpressing Plac8.1-EGFP compared to control gastrulae (Figure 2-7G and H).

Plac8.1 overexpression causes cell-autonomous, post-transcriptional downregulation of Cdh1. The morphogenetic phenotypes observed in gastrulae overexpressing Plac8.1 resembled *cdh1* loss-of-function phenotypes (Lin et al., 2009; Babb and Marrs, 2004; Shimizu et al., 2005; Kane et al., 2005; McFarland et al., 2005). If Plac8.1 could influence Cdh1 function during gastrulation, embryos with reduced Cdh1 levels should be sensitive to Plac8.1 expression levels. To test this, we injected a low dose of *plac8.1* RNA (20 pg) into offspring of *cdh1*$^{vu44/+}$ parents, and monitored epiboly progression using *ntl* as a marker of the blastoderm margin. We observed that resulting progeny of three genotypes formed distinct phenotypic classes: WT gastrulae had a very mild epiboly defect, *cdh1*$^{vu44/+}$ heterozygotes manifested more severe epiboly defects (Figure 2-8B, lower right picture), and *cdh1*$^{vu44/vu44}$ homozygotes displayed the most severe phenotype (data not shown). This synergistic epiboly defect in *cdh1*$^{vu44/+}$ heterozygous embryos expressing low amounts of Plac8.1 supports the notion that Plac8.1 negatively influences *cdh1* gene expression or function.

We next examined whether Plac8.1 had an effect on *cdh1* transcriptional regulation. By quantitative RT-PCR, *cdh1* RNA levels were not significantly different between uninjected control and Plac8.1-overexpressing embryos (Figure 2-7C), suggesting that Plac8.1 represses *cdh1* post-transcriptionally. However, by immunoblotting, Cdh1 levels were reduced about 50% in gastrulae overexpressing Plac8.1

compared to control embryos (Figure 2-7B). Moreover, treatment of Plac8.1-overexpressing embryos with the proteasome inhibitor, MG-132, attenuated the reduction in Cdh1 levels (Figure 2-8C), indicating that excess Plac8.1 promotes Cdh1 proteasome-mediated degradation. To test whether Plac8.1 regulated Cdh1 levels in a cell-autonomous manner, we injected *plac8.1-EGFP* RNA into one cell of 32-cell stage embryos, and detected Cdh1 by immunofluorescence at early gastrula stage (Figure 2-7D). Measurements of the membrane Cdh1 immunofluorescence intensity revealed significantly reduced intensity at membranes shared by two Plac8.1-overexpressing cells; less, yet still significantly reduced intensity at membranes shared by one WT cell and one Plac8.1-EGFP-expressing cell compared to Cdh1 level at membranes shared by cells without excess Plac8.1-EGFP (Figure 2-7E). The Plac8.1-EGFP signal was negatively correlated with Cdh1 signals (Figure 2-7E, and regression analysis data not shown). Taken together, these studies are consistent with a model whereby excess Plac8.1 expression negatively regulates Cdh1 levels in zebrafish gastrulae in a cell-autonomous fashion, at least in part, by promoting its proteasome-mediated degradation.

Overexpression of PLAC8 in HCA-7 cells reduces cell surface CDH1 and confers an EMT phenotype. We next wished to compare the functional consequences of stably overexpressing PLAC8 in HCA-7 cells (HCA-7P8) to those observed for zebrafish. We analyzed the 2D invasive behavior of parental and HCA-7P8 cells using a previously described MAtS invasion assay (Ashby et al., 2012). Cells were seeded at high density on monomeric collagen and cell migration was analyzed upon removal of a magnetic stencil (Methods). Parental HCA-7 cells moved as a cohesive sheet, whereas HCA-7P8 cells moved unevenly and tended to detach from a common but irregular front (Figure 2-9A and Figure 2-10). The deviation ratio and number of detached cells/field were significantly greater in HCA-7P8 than those observed for parental HCA-7 cells at 8 and 24 hrs after stencil removal (Figure 2-9B). When HCA-7P8 cells were cultured in a 3D collagen matrix, they showed less membranous CDH1 by immunofluorescence, especially in cells located at the population front (Figure 2-9C). Hence, consistent with our findings in zebrafish embryos (Figure 2-7D), PLAC8 overexpressing HCA cells show altered migration and reduced membrane expression of CDH1.

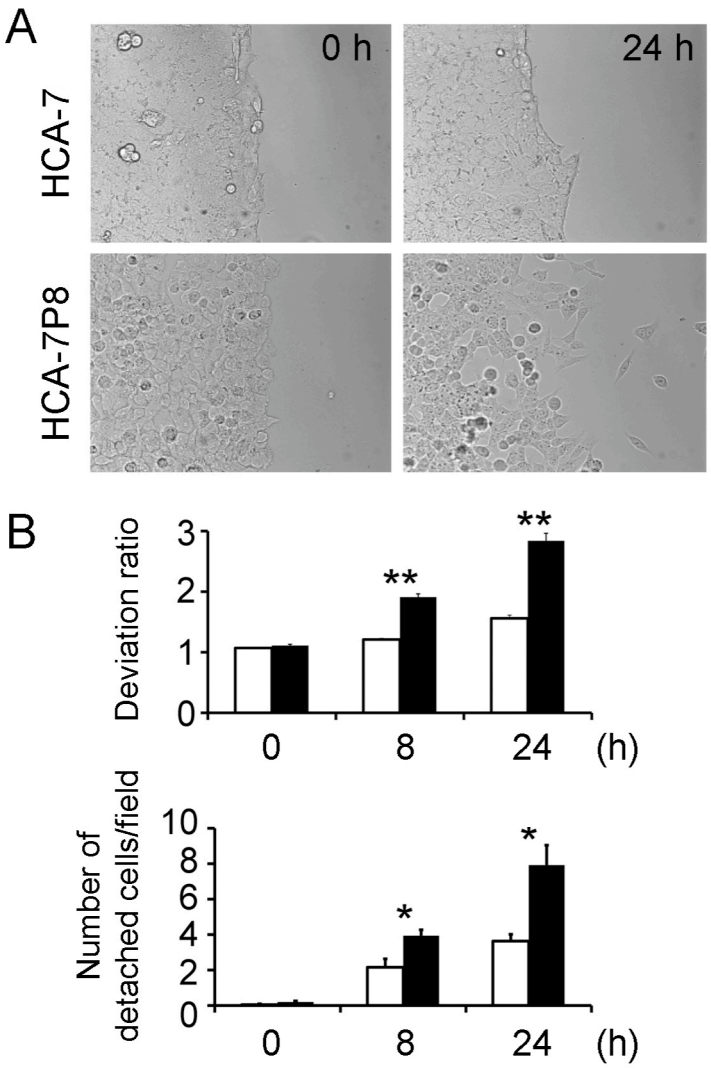
A
0 h
24 h
HCA-7
HCA-7P8
B
Deviation ratio
3
2
1
0
**
**
0
8
24
(h)
Number of detached cells/field
10
8
6
4
2
0
*
*
0
8
24
(h)
C
PLAC8
CDH1
Merge

Figure 2-9. Expression of PLAC8 enhances HCA-7 cell invasion and alters CDH1 subcellular localization.
(**A**) 2D invasive capacity was assessed by a MAtS invasion assay. After removal of a magnetically attachable stencil, cell movement of parental HCA-7 and PLAC8-overexpressing HCA-7 (HCA-7P8) cells was monitored over 24 hrs by time lapse microscopy. HCA-7 cells moved as a common front whereas HCA-7P8 cell movement was uneven and cells detached. **(B)** At 8 and 24 hrs, static images were taken and quantified by two parameters (deviation ratio and number of detached cells/field), based on 3 independent experiments performed in triplicate. Both parameters were significantly greater in PLAC8-overexpressing cells, (p<0.05). (**C**) After 15 days in 3D collagen culture, PLAC8 and CDH1 immunofluorescence were largely cytosolic in HCA-7 cells overexpressing PLAC8 (HCA-7P8). The boxed regions in the upper panels are magnified in the lower panels. Scale bars, 50 μm.

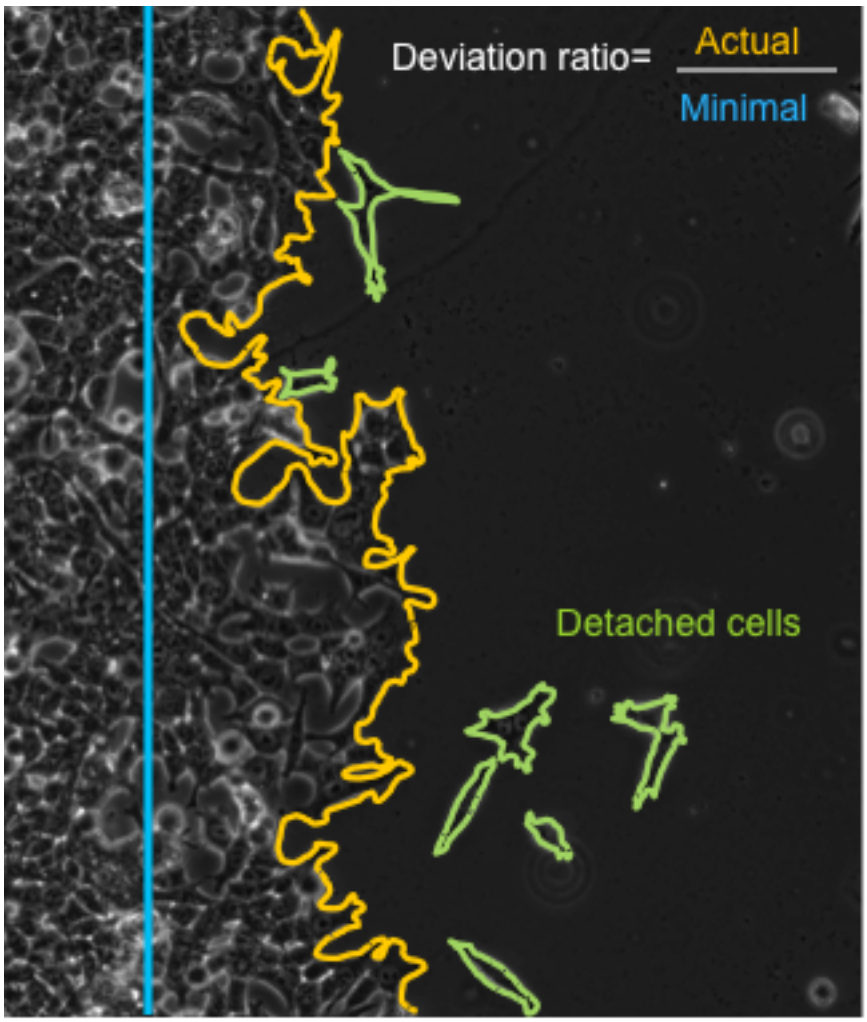
Deviation ratio=
Actual
Minimal
Detached cells

Figure 2-10. Cell migration measurement.
The blue line represents the start border after removing a stencil. Yellow line outlines the migratory edge of the cell sheet at an experimental time point. Countable detached cells are illustrated in green hollows.

HCA-7P8 cells exhibit an EMT signature. Given that PLAC8-overexpressing HCA-7 cells displayed functional and morphological features of EMT, we next examined expression of EMT-related genes using a commercial quantitative RT-PCR array (Table 2-2), followed by validation using independent quantitative RT-PCR. Consistent with a typical EMT signature (Thiery et al., 2009), *VIM* and *ZEB1* transcripts were increased by 12- and 4-fold, respectively, in HCA-7P8 compared to parental HCA-7 cells. Besides ZEB1, we did not observe increased expression of other transcriptional regulators of CDH1 (such as TWIST, SNAIL, SLUG and ZPO1) in PLAC8-overexpressing HCA-7 cells (data not shown). In contrast to transcriptional repression of *CDH1* seen in typical EMT, *CDH1* mRNA was slightly upregulated (1.4-fold) in HCA-7P8 cells, and *CDH2* transcripts were undetectable in both cells (Figure 2-11A). Interestingly, expression of *CDH3*, a cadherin linked to colon cancer progression (Sun et al., 2011), was upregulated nearly 4-fold in PLAC8-overexpressing HCA-7 cells. Although PLAC8 overexpression did not reduce *CDH1* nor increase *CDH2* RNA levels, it did result in a cadherin switch: transcriptional upregulation of *CDH3* and reduced cell surface CDH1, along with other more typical features of EMT.

To determine the post-transcriptional effects of PLAC8 on CDH1, we examined the Triton X-100-soluble and -insoluble fractions of CDH1 in parental and HCA-7P8 cells. The Triton-insoluble pool of CDH1 is thought to represent a cytoskeletal-attached, higher ordered complex of functional CDH1 at the plasma membrane (Piepenhagen and Nelson, 1993). PLAC8 overexpression reduced the insoluble pool of CDH1, which paralleled the immunofluorescence experiments and observations from zebrafish. Similar to the changes observed at the transcript level, CDH3 was increased in HCA-7P8 cells whereas it was barely detected in parental HCA-7 cells. CDH3 was mainly detected in the Triton X-100-soluble fraction.

We next examined these and other markers by immunoblotting of whole cell lysates (Figure 2-11A, left panels) and immunofluorescence (Figure 2-11A, right panels). Levels of *CDH1* and *CTNND1* were modestly reduced in PLAC8-overexpressing HCA-7 cells. By immunofluorescence, we observed less membranous and increased cytoplasmic CDH1 expression. By immunoblotting, HCA-7P8 cells expressed increased levels of VIM and ZEB1 compared to parental HCA-7 cells. VIM fluorescence was detected in approximately 10% of HCA-7P8 cells, and, when present, it had a filamentous appearance in the

Table 2-2. Gene expression in fold change using commercial human EMT qRT-PCR array.

Gene Symbol	Fold Change HCA-7P8 /HCA-7C
SERPINE1	**37.98**
PTP4A1	**34.97**
AHNAK	**28.73**
SNAI1	**26.53**
EGFR	**25.6**
GSC	**23.28**
MSN	**21.19**
ZEB2	**20.84**
VIM	**15.28**
CALD1	**12.94**
TMEM132A	**12.55**
SNAI3	**12.53**
TMEFF1	**12**
AKT1	**11.95**
FOXC2	**11.78**
GNG11	**11.69**
CDH2	**11.24**
MST1R	**10.5**
MITF	**10.03**
ERBB3	**9.86**
FZD7	**9.64**
DSP	**9.16**
WNT11	**9.04**
CDH1	**8.9**
KRT14	**8.84**
OCLN	**8.46**
F11R	**8.12**
PDGFRB	**7.97**

Gene Symbol	Fold Change HCA-7P8 /HCA-7C
COL5A2	**7.06**
SMAD2	**7.04**
MMP2	**6.52**
TGFB3	**6.12**
TSPAN13	**6.05**
ITGB1	**5.24**
VPS13A	**4.47**
SPARC	**4.35**
GSK3B	**4.33**
MMP9	**4.25**
FGFBP1	**4.14**
ZEB1	**4.09**
WNT5A	**4**
CTNNB1	**3.86**
CAMK2N1	**3.69**
PTK2	**3.57**
TGFB2	**3.49**
ITGAV	**3.43**
WNT5B	**3.18**
COL3A1	**3.08**
TCF3	**3.01**
TWIST1	**2.73**
IGFBP4	**2.63**
NOTCH1	**2.55**
TIMP1	**2.53**
BMP1	**2.48**
NUDT13	**2.47**
PPPDE2	**2.44**

Gene Symbol	Fold Change HCA-7P8 /HCA-7C
B2M	**2.3**
COL1A2	1.95
KRT7	1.88
VCAN	1.79
NODAL	1.79
SPP1	1.76
SIP1	1.72
STAT3	1.7
KRT19	1.65
PLEK2	1.53
TGFB1	1.4
JAG1	1.39
ITGA5	1.27
ACTB	1.21
RAC1	1
HPRT1	-1.17
IL1RN	-1.22
RGS2	-1.24
CAV2	-1.25
GAPDH	-1.45
FN1	-1.58
RPL13A	-1.64
DSC2	**-2.47**
ESR1	**-2.5**
TCF4	**-3.94**
MAP1B	**-4.55**
STEAP1	**-8.25**
ILK	**-41.04**

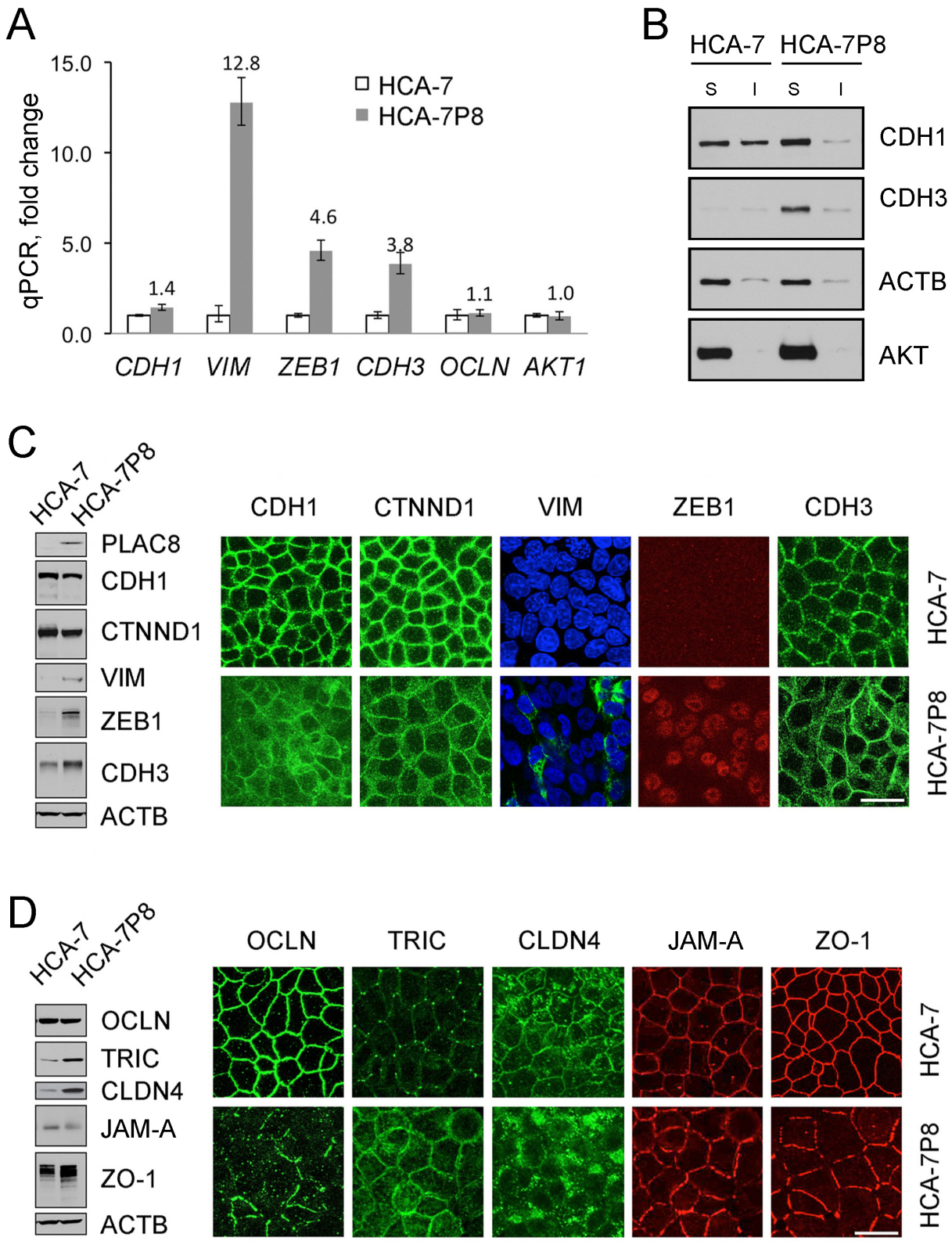
A
qPCR, fold change
15.0
10.0
5.0
0.0
HCA-7
HCA-7P8
1.4
12.8
4.6
3.8
1.1
1.0
CDH1
VIM
ZEB1
CDH3
OCLN
AKT1
B
HCA-7
HCA-7P8
S
I
S
I
CDH1
CDH3
ACTB
AKT
C
HCA-7
HCA-7P8
PLAC8
CDH1
CTNND1
VIM
ZEB1
CDH3
ACTB
CDH1
CTNND1
VIM
ZEB1
CDH3
HCA-7
HCA-7P8
D
HCA-7
HCA-7P8
OCLN
TRIC
CLDN4
JAM-A
ZO-1
ACTB
OCLN
TRIC
CLDN4
JAM-A
ZO-1
HCA-7
HCA-7P8

Figure 2-11. HCA-7P8 cells exhibit features of EMT.
(**A**) By qRT-PCR, *CDH1* was slightly upregulated (1.4-fold), whereas *ZEB1, VIM* and *CDH3* were markedly upregulated by 13-, 5- and 4- fold, respectively, in HCA-7P8 cells compared to HCA-7 cells. Expression of OCLN and AKT were not significantly changed upon expression of PLAC8. (**B**) By detergent fractionation analysis, CDH1 of HCA-7P8 cells was mostly in Triton X-100 soluble fraction. HCA-7 control cells had ~50% CDH1 insoluble, which reflected membranous CDH1. Induced CDH3 protein in HCA-7P8 cells was also predominantly soluble in Triton X-100 containing CSK buffer (Nathke et al., 1994). The ratio of soluble and insoluble ACTB in CSK buffer was consistent in both lines. AKT was totally extractable using Triton X-100. (**C**) Expression and localization of classical EMT markers were assessed by immunoblotting (left panel) and immunofluorescence (right panel). In contrast to the qRT-PCR result, CDH1 showed a modest reduction by immunoblotting in HCA-7P8 cells; it appeared less membranous and more cytoplasmic by immunofluorescence. CTNND1 was also slightly reduced in HCA-7P8 cells by immunoblotting compared to HCA-7 cells. Consistent with qRT-PCR results, VIM, ZEB1 and CDH3 protein levels were upregulated by immunoblotting. In HCA-7P8 cells, VIM immunofluorescence was heterogeneous and observed in approximately 10% of the cells; when present, it had a filamentous pattern in the cytoplasm. ZEB1 fluorescence was present uniformly and nuclear in HCA-7P8 cells. CDH3 appeared more cytoplasmic compared to HCA-7 by immunofluorescence. (**D**) Expression and localization of tight junction proteins were assessed by immunoblotting (left panels) and immunofluorescence (right panels). There was no change in OCLN protein levels by immunoblotting, but a marked reduction in membranous OCLN and ectopically-punctate cytoplasmic OCLN in HCA-7P8 cells compared to HCA-7 cells by immunofluorescence. Tricellulin (TRIC) and CLDN4 protein levels were upregulated by immunoblotting in HCA-7P8 cells and lost their distinctive localization at tricellular junctions and now appeared throughout the membrane and in the cytoplasm. Scale bars, 20 μm.

cytoplasm. ZEB1 fluorescence was detected in nuclei of all PLAC8-overexpressing cells. CDH3 levels were slightly increased in HCA-7P8 cells and CDH3 fluorescence appeared to be more cytosolic compared to parental HCA-7 cells.

Alterations in tight junction proteins have been reported in EMT and cancer progression (Soini, 2012; Masuda et al., 2010; Ohkubo and Ozawa, 2004). Although OCCLUDIN (OCLN) levels were not significantly altered by PLAC8 overexpression, it was largely delocalized from the plasma membrane and appeared as cytoplasmic puncta (Figure 2-11D, right panels). The loss of junctional OCLN led us to examine other tight junction proteins. Immunoblotting experiments revealed elevated levels of TRICELLULIN (TRIC) in HCA-7P8 compared to parental HCA-7 cells (Figure 2-11D, left panels). In contrast to the typical localization of TRIC at tricellular junctions in parental HCA-7 cells, TRIC immunofluorescence was apparent throughout the plasma membrane and in the cytoplasm of HCA-7P8 cells (Figure 2-11D, right panels). By contrast, JAM-A levels appeared reduced and additional, faster migrating ZO-1 bands were observed in HCA-7P8 cells compared to parental HCA-7 cells byimmunoblotting. In both instances, fluorescence was less uniform and reduced at the tricellular junctions in the former versus latter cells (Figure 2-11D right panels).

PLAC8 enhances phosphorylation of ERK2. To elucidate the molecular mechanism by which excess PLAC8 leads to this EMT phenotype, we examined signaling pathways known to be linked to EMT (Figure 2-12A). Although we observed no difference in total ERK1/2 levels between parental and HCA-7P8 cells, p-ERK1/2 levels were markedly increased in HCA-7P8 cells with the increase in p-ERK2 being especially prominent. There was a modest increase in total and p-AKT in HCA-7P8 cells; PLAC8 has previously been shown to increase p-AKT in myeloid cells (Rogulski et al., 2005). Likewise, we observed no difference in total and p-SRC between parental and HCA-7P8 cells. To further investigate whether ERK1 and ERK2 have same impact on the PLAC8-expressing HCA-7 cells, we separately knocked down *ERK1* and *ERK2* in comparison using lentiviral vectors (targeting sequences are listed in Table 2-3). Figure 2-12B shows their knockdown efficacy in the pool cells and consequence of representative EMT markers. shERK2, but not shERK1, upregulated CDH1. shERK2-4 had no depletion efficacy on ERK2, so

that CDH1 level was unchanged. shERK2 not only changed the EMT marker expression but also converted the protrusive features of HCA-7P8 to epithelial features with smooth edge of cell patches and cell-cell contact (Figure 2-12C). Using immunofluorescence, we clearly showed both CDH1 and CDH3 had a sharper membranous localization. ZEB1 and VIM were reduced (Figure 2-12D). At the same time, we observed ERK2 inhibitor, Pyrazolylpyrrole, could also convert HCA-7P8 cells to its parental HCA-7 cell morphology in a dosage-dependent manner (1-100 nM) and upregulated membranous CDH1 (data not shown).

Knockdown of endogenous PLAC8 in SC cells restores cell surface CDH1 in 3D culture and in xenografts. Having established the molecular and morphological effects of selectively overexpressing PLAC8 in HCA-7 cells, we returned to the study of HCA-7-derived CC (PLAC8 low) and SC (PLAC8 high) cells, and tested the consequences of knocking down *PLAC8* in SC cells (Figure 2-4C). In 3D collagen culture, levels of CDH1 and CTNND1 were similar between CC and SC cells (data not shown). However, by immunofluorescence, CDH1 was largely cytoplasmic in SC, compared to its basolateral plasma membrane distribution in CC cells (Figure 2-13A). Knockdown of PLAC8 in SC cells did not change CDH1 and CTNND1 protein levels (data not shown)**.** In 3D collagen culture, stable knockdown of *PLAC8* in SC cells resulted in restoration of CDH1 and CTNND1 plasma membrane fluorescence, compared to control CC knockdown cells (Figure 2-13B). A similar differential distribution of CDH1 was observed in CC and SC tumor xenografts, established following subcutaneous injection into athymic nude mice (Figure 2-13C). However, in tumors harvested after subcutaneous injection of SC cells stably expressing *PLAC8* shRNA, CDH1 staining was observed at the plasma membrane compared to tumors formed by SC cells expressing a control shRNA (Figure 2-13D). These results further support the significance of PLAC8 in the post-transcriptional regulation of CDH1.

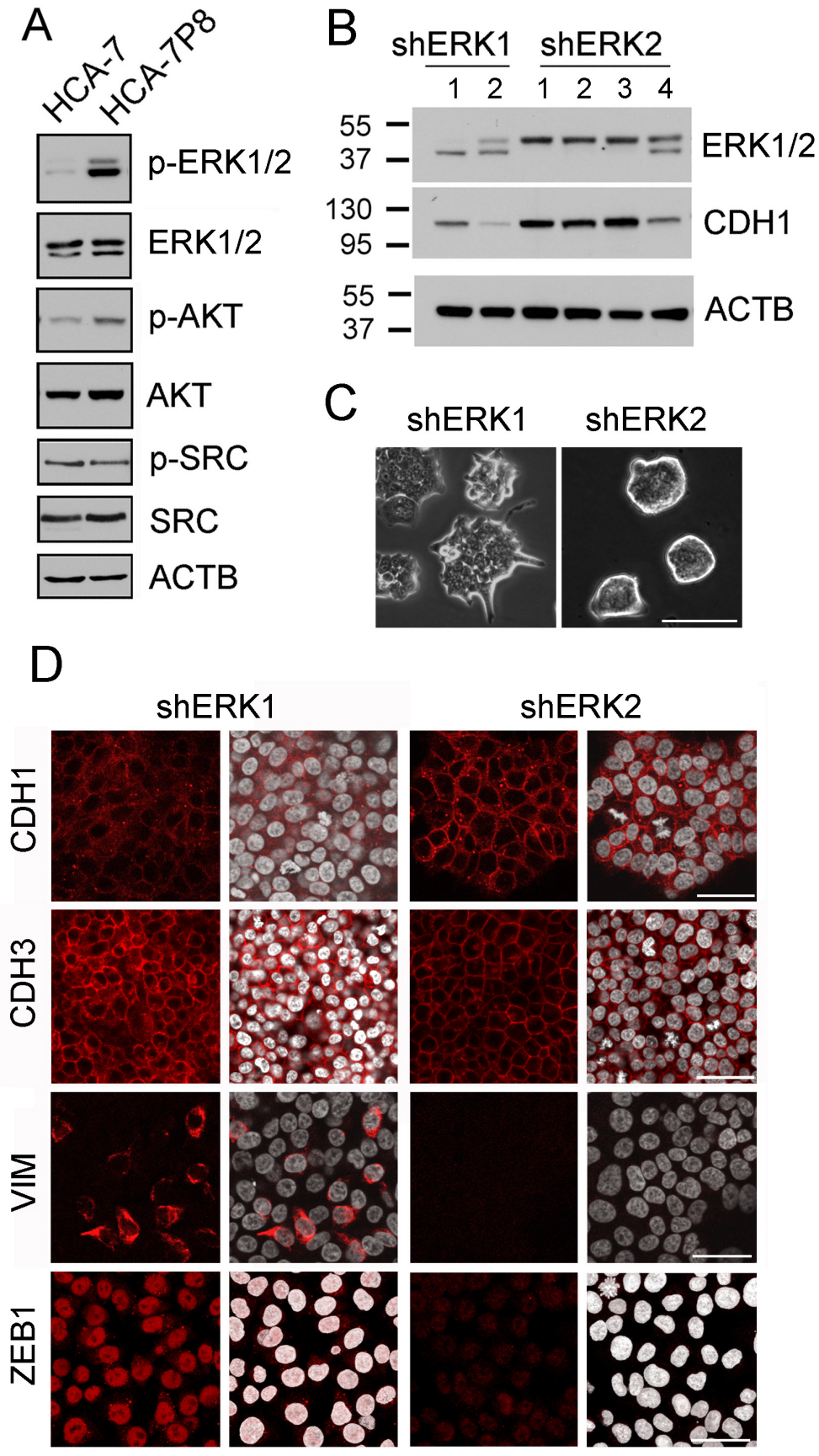
A
HCA-7
HCA-7P8
p-ERK1/2
ERK1/2
p-AKT
AKT
p-SRC
SRC
ACTB
B
shERK1
shERK2
1 2 1 2 3 4
55
37
130
95
55
37
ERK1/2
CDH1
ACTB
C
shERK1
shERK2
D
shERK1
shERK2
CDH1
CDH3
VIM
ZEB1

Figure 2-12. PLAC8 induces EMT through ERK2 activation.
(**A**) Total and activated EMT-related kinases were assessed by immunoblotting. Although both ERK1 (slower migrating, higher band) and ERK2 (faster migrating, lower band) were increased in HCA-7P8 cells, ERK2 phosphorylation was much stronger. Total ERK1/2 proteins were expressed at similar levels in HCA-7 and HCA-7P8 cells. Total and p-AKT were slightly increased, whereas total and p-SRC (Y416) were unchanged in PLAC8-overexpressing HCA-7 cells. (**B**) ERK1 and ERK2 were stably knocked-down in HCA-7P8 cells. To examine the expression level of EMT markers. shERK1-1 and shERK2-1,2,3 were sufficiently reduced their correspondence gene expression. Consequently, total CDH1 was only upregulated in ERK2-knockdown cells, but not In the ERK1-knockdown cells. (**C**) Knocking down ERK2 also reverted protrusive HCA-7P8 colonies to edge-smooth colonies, but did not ERK1, under DIC microscope. (**D**) By immunofluorescence in ERK2-knockdown HCA-7P8 cells, the expression of VIM was undetectable, and CDH1 was apparently localized at the plasma membrane. However, knocking down ERK1 from HCA-7P8 cells did not change those expression. Scale bar: 50 μm.

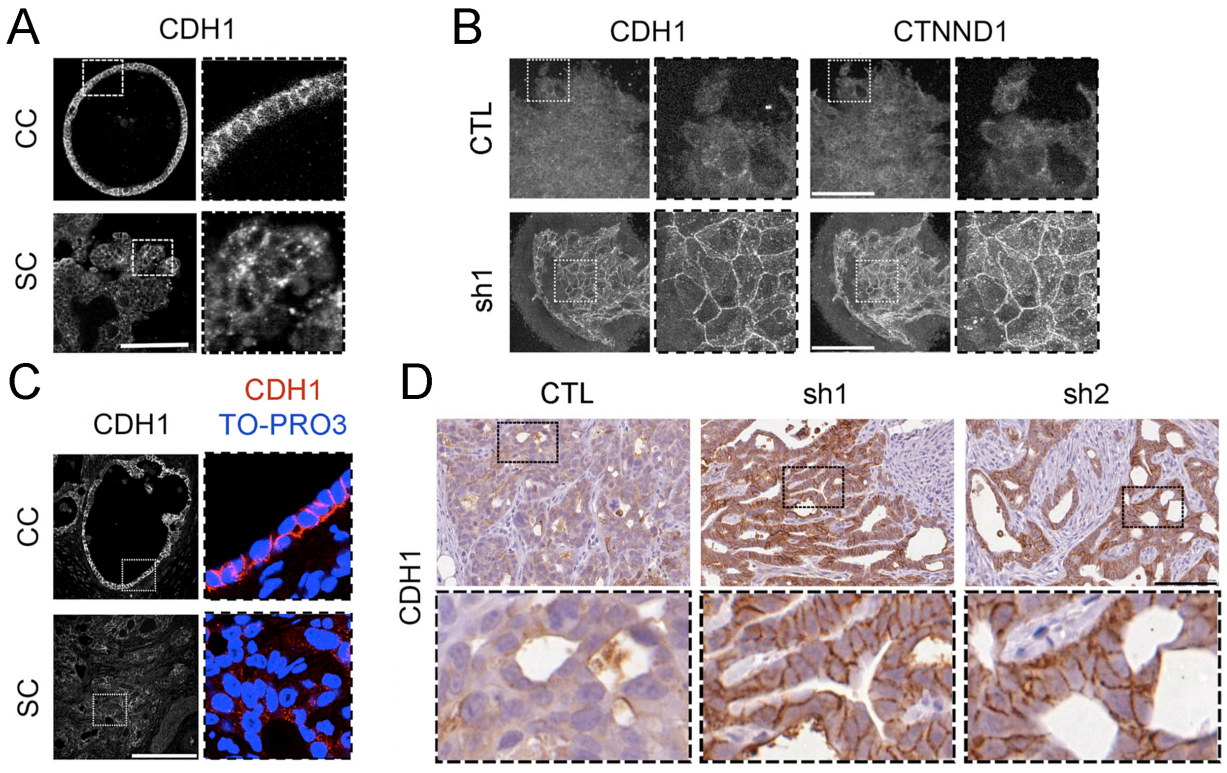
A
CDH1
CC
SC
B
CDH1
CTNND1
CTL
sh1
C
CDH1
CDH1
TO-PRO3
CC
SC
D
CTL
sh1
sh2
CDH1

Figure 2-13. Depletion of endogenous PLAC8 in SC cells restores cell surface CDH1 in 3D culture and *xenografts.*
(**A**) In 3D collagen culture, CDH1 localized to basolateral plasma membrane of CC cells, whereas CDH1 was detected diffusely in cytoplasm of SC cells. Boxed areas are magnified on right. Scale bars, 100 mm. (**B**) SC cells were stably infected with two PLAC8-specific shRNAs (sh1 and sh2) or non-targeted control (CTL). Both CDH1 and CTNND1 immunofluorescence were restored to the plasma membrane upon depleting PLAC8 from SC cells. Scale bars, 100 mm. (**C**) CC and SC cells were subcutaneously injected into athymic nude mice. After 4 weeks, CC cells formed glandular tumors with large cysts (top panel) with CDH1 (red) immunofluorescence observed at basolateral membrane. SC cells formed less differentiated tumors with reduced membranous and enhanced cytoplasmic CDH1 immunofluorescence. Boxed areas are magnified on right with nuclear contrast staining (TO-PRO3). Scale bars, 100 mm. (**E**) In xenografts from cells infected with *PLAC8-shRNAs*, CDH1 re-localized to membrane by immunofluorescence, similar to that in CC xenografts. Boxed fields are magnified in dashed boxes. Scale bars, 100 μm.

Discussion

The cross-species functional analysis of PLAC8 presented here significantly advances our understanding of the role of PLAC8 upregulation in colon cancer and implicates excess PLAC8 in an ERK2-dependent atypical EMT. We show that this small evolutionarily conserved protein has dynamic cytoplasmic and juxtamembrane distribution during zebrafish gastrulation, and is enriched in the apical domain of gut epithelia in zebrafish and mouse. Studies in zebrafish provided important insights into how excess PLAC8 may contribute to the pathogenesis of colon cancer. Overexpression of zebrafish *plac8.1* or human *PLAC8* in zebrafish embryos impaired gastrulation movements, phenocopying mutants with reduced Cdh1 levels. Excess Plac8.1 reduced levels of Cdh1 post-transcriptionally, acting in a cell-autonomous fashion. By culturing HCA-7 human CRC cell line in 3D, we identified a population of highly invasive cells in which PLAC8 is among the most upregulated genes and is largely cytosolic, and this is correlated with cytosolic CDH1 distribution. Reducing endogenous PLAC8 in these cells restores CDH1 to the cell surface. Thus, excess Plac8 in both zebrafish embryos and human colon cancer cells appears to be necessary and sufficient to post-transcriptionally modulate CDH1 level and/or its subcellular distribution. Moreover, we show that PLAC8 is overexpressed and cytosolic in a subset of CRCs, and correlate cytosolic PLAC8 with advanced histological grade, as well as medullary and mucinous histological subtypes.

The present studies do not address the precise mechanism(s) by which excess PLAC8 results in reduced total and/or cell surface CDH1. We observed that subcellular distribution of CTNND1 and CTNNB followed that of CDH1. Further, knockdown of E3-ubiquitin ligase CBLL1 (Fujita et al., 2002) failed to affect levels or distribution of CDH1 (data not shown), suggesting a mechanism other than ubiquitylation and degradation. We also did not see a change in the size of CDH1 by immunoblotting (data not shown), suggesting ectodomain cleavage-induced subcellular redistribution is not likely to play a role. We also noticed that *ILK* is greatly downregulated in HCA-7 cells overexpressing PLAC8 (Table 2-2). Since loss of *ILK* affects CDH3 (Nakrieko et al., 2008). The reduction of *ILK* transcription may at least in part explain some of the phenotypic difference between HCA-7 cells overexpressing PLAC8 and control cells. Future

studies will examine impaired delivery and/or internalization, amongst plausible mechanisms by which excess PLAC8 dysregulate CDH1 protein.

Downregulation of CDH1 is a hallmark of EMT, generally a transcriptionally driven program in which transcription factors, such as SNAI1, SNAI2, TWIST1, TWIST2, ZEB1, ZEB2 and ZPO1, cooperate to orchestrate a cadherin switch (most often repression of *CDH1* and induction of *CHD2*) and to induce expression of mesenchymal genes like VIM, and associated changes in cellular morphology and behavior (Miettinen et al., 1994; Brabletz, 2012). In addition to our analysis of SC subline of HCA-7 cell in which *PLAC8* is among most overexpressed genes, we show that stably overexpressing PLAC8 along in HCA-7 cells resulted in a post-transcriptional reduction of total and cell surface CDH1. *CDH2* transcription was not affected by PLAC8, but *CDH3* was transcriptionally upregulated, as was the mesenchymal marker *VIM*. Moreover, tight junction components (OCLN, TRIC. CLDN4) were mislocalized. Thus, excess PLAC8 expression results in conventional features of EMT, including a cadherin switch, but through unconventional post-transcriptional effects on CDH1 level and distribution. This is consistent with our observation that the only transcriptional repressor that was elevated was ZEB1, with *ZEB1* mRNA level increase by 4.6-fold in PLAC-8-overexpressing HCA-7 cells compared to parental cells. However, none of the other known *CDH1* transcription repressors we examined (TWIST1, TWIST 2, SNAI11 and SLUG) were altered, and ZEB2 not detectable. Clearly, ZEB1 by itself is not sufficient to repress *CDH1* expression in PLAC8-overexpressing HCA-7 cells.

We did observe increased mRNA expression of CDH3 in HCA-7P8 cells. In mouse models, forced expression of CDH3 under colonic epithelial specific promoter L-Fabp causes significant increase in crypt fission (Milicic et al., 2008). Expression of CDH3 (Paredes et al., 2012; Mandeville et al., 2008) in cancer cells promoted cell motility, migration and invasion, potentially by interfering with CTNND1 binding to CDH1 (Paredes et al., 2008) or promoting CTNND1 cytoplasmic accumulation (Taniuchi et al., 2005). CDH3 binding CTNND1 through the juxtamembrane domain may be crucial for induction of invasion (Paredes et al., 2004; Cheung et al., 2010) by competing CDH1 away to bind CTNND1 that has been implicated in stabilizing CDH1 (Ireton et al., 2002). Recent reports indicated alternate mechanisms to

regulate cell migration in different cell types, such as underlying cooperation with IGF1 receptor (Cheung et al., 2011) and ROBO-3 complex (Bauer et al., 2011). Increased CDH3 potentially outcompete CDH1 for the available pool of p120, thereby destabilizing cell surface E-cadherin.

Our present study points to enhanced p-ERK2 as a mediator of many of the effects of excess PLAC8. Previous studies have linked p-ERK2, but not p-ERK1, to EMT through transcriptional upregulation of ZEB1/2 and DEF motif-containing target FRA-1 (Shin et al., 2010). Here, we show that shRNA knockdown of ERK2 in PLAC-8-overexpressing HCA-7 cells, but not ERK1, increases total levels of CDH1 and restore functional cell surface CDH1. Similar results were seen with selective ERK2 inhibitor. Further experiments are required to determine precisely how excess PLAC8 enhances p-ERK2 phosphorylation.

We provide the first analysis of endogenous PLAC8 protein, showing that both human PLAC8 and zebrafish Plac8.1 localize to the subapical domain of normal differentiated gut epithelium, and a dynamic cytoplasmic and juxtamembrane distribution in the zebrafish gastrulae. It will be instructive to examine the localization of PLAC8 protein in adipocytes and dendritic cells given its requirement for brown fat differentiation and immune function, and whether it has a dynamic pattern of distribution in these cells as we observed during zebrafish gastrulation. Future studies will address the function of PLAC8 in the cytoplasmic and subapical domain: its precise localization and interacting partners. Of particular interest will be whether PLAC8 has the same partners and molecular activities when expressed at its endogenous levels and when in excess, and thus whether the effects we observed upon its overexpression in zebrafish gastrula or when upregulated in colon tumor represent hypermorphic or neomorphic activities of this protein.

This work also introduces a new 3D system for studying CRC. Pioneering work by the laboratories of Minna Bissell and Joan Brugge has shown the greater biological relevance of studying breast cancer cells in 3D rather than on plastic (Hall et al., 1982; Debnath and Brugge, 2005). Such 3D systems in CRC are much more limited and have relied largely on Caco-2 cells (Jaffe et al., 2008). HCA-7 cells form a uniform

polarizing monolayer when cultured on Transwell filters. By culturing HCA-7 cells in type 1 collagen, we observe colonies with two distinct morphologies and behaviors (manuscript in preparation). PLAC8 was one of 50 genes upregulated greater than 4-fold in SC versus CC clones (data not shown). To identify specific roles for PLAC8, we stably overexpressed it in parental HCA-7 cells and observe the EMT-like phenotype described herein. Importantly, when we selectively knockdown PLAC8 in SC1 cells, we restore cell surface CDH1 *in vitro* and *in vivo*.

In summary, our data suggest that PLAC8 is a novel factor that promotes EMT in an unconventional manner. In a subset of colon cancers, PLAC8 protein relocalizes from a subapical domain to the cytoplasm, coincident with redistribution of CDH1 from the cell surface to the cytoplasm, a hallmark of EMT, both *in vitro* and *in vivo*. Interestingly, although excess PLAC8 induces an EMT that includes changes in CDH1 localization and upregulation of *ZEB1* and *VIM*, it does not affect levels of *SNAIs* or *TWISTs*. Excess PLAC8 also results in mislocalization of tricellular TJ proteins (OCLN and TRIC) without affecting JAM1 and ZO-1 localization at bicellular TJs. More importantly, this PLAC8-induced EMT phenotype seems to be ERK2-dependent. We propose that excess PLAC8 promotes an ERK2-mediated unconventional EMT in colon cancer. Finally, using a novel multiplex immunofluorescence-based technique, we observe a correlation between PLAC8 and these EMT markers at the leading edge of a human colorectal tumor, providing *in vivo* evidence for EMT.

Methods

Plasmids, transfection and infection of human cell lines. Full-length cDNA of human *PLAC8* was obtained from Origene (Rockville, MD). Primers GGAATGCAAGCTCAGGCGCCGGTG (forward) and TGGATCCGAAGATCTTGAAAGTACGCATGGCT (reverse) were used for PCR amplification, and the product was cloned into pcDNA3.1 and pRetroX-Tight-Pur vectors with or without a FLAG-tag. For knockdown experiments, lentiviral-delivered shRNAs (TRCN0000133820 and TRCN0000133929) against *PLAC8* and control SHC005 were purchased from Sigma-Aldrich (St. Louis, MO). Plasmid transfection was mediated by Metafectene Pro (Biontex-USA, San Diego, CA) according to the manufacture's instructions. *PLAC8*-containing retrovirus was packaged in Phoenix cells; shRNA lentivirus was

enveloped in HEK293 cells co-transfected with pD8.2 and pMD packaging plasmids. Both retroviral- and lentiviral-containing media were filtered through 0.45 μm cellulose acetate syringe filters (VWR Scientific, Radnor, PA) before infection. Retroviral-*PLAC8*-infected cells were screened with 50mg/ml G418. Lentiviral-infected HCA-7 and CC cells were cultured in DMEM medium supplemented with 0.5mg/ml puromycin.

Antibody generation and other immunoassaying reagents. Anti-human PLAC8 and anti-zebrafish Plac8.1 antibodies were generated by immunizing rabbits with KLH-conjugated peptides of amino acid sequences from the C-terminus of human PLAC8 (CQIKRDINRRRAMRTFKI) or zebrafish Plac8.1 (CQLKRDIDIRKSNGTLKL), respectively (Covance Inc, Princeton, NJ). Specificity of both anti-PLAC8 and anti-Plac8.1 antibodies was confirmed using FLAG-tagged and untagged peptides. Additional validation was performed by shRNA or morpholino knockdown in mammalian cells and zebrafish, respectively (Figure 2-3). Other antibodies used in the study include: anti-PLAC8 antibody (Sigma-Aldrich, HPA040465), anti-CDH1 C-terminus antibodies (36/E-cadherin, cat#610181, and Abcam, ab40772), anti-CDH1 N-terminus antibody (LSBio, LS-B7125), anti-CDH2 (Cell Signaling Technology, cat#4061), anti-CDH3 (BD Transduction, cat#610227), anti-b-actin (ACTB, Sigma, A5316), anti-a-tubulin (TUBA, EMD Millipore, CP06), anti-MDM2 (R&D Systems, MAB1244), anti-CBLL1 (Abcam, ab91185), anti-GFP (Invitrogen, A11122), Anti-FLAG (M2, Sigma, F1804), anti-HA (12CA5) (Roche Applied Science) and anti-zebrafish Cdh1 (20). Horseradish peroxidase- and Cy3- conjugated donkey anti-mouse or anti-rabbit IgG secondary antibodies were obtained from Jackson ImmunoResearch, and Alexa 488-conjugated goat anti-mouse antibody and Alexa 568-conjugated goat anti-rabbit antibodies from Invitrogen. All other chemicals were purchased from Sigma unless otherwise stated.

Immunoblotting. Cells were lysed in either cell lysis buffer (25 mM Tris HCl, 150 mM NaCl, 0.5% Nonidet P-40, 0.5% sodium deoxycholate, 1 mM DTT and 2% BSA) or M-PER (Pierce) plus 1X protease inhibitor cocktail (Sigma, P2714). Soluble cell lysates were obtained by centrifugation. Protein concentration of soluble lysates was determined using a Micro BCA Protein Assay Kit (Pierce), followed by boiling in sample buffer. For PLAC8 immunoblotting, both tissues and cultured cells were lysed in 8 M urea SDS sample buffer (2% SDS, 0.125M TRIS-HCl, pH 6.8, 8M urea, 10% BME). Proteins were resolved on 7.5-16% SDS-PAGE gels, followed by standard Western blotting. Zebrafish embryos collected at designated

stages were manually dechorionated and homogenized in NP-40 lysis buffer (1% Nonidet P-40 [Igepal A-680), 50mM Tris-HCl pH 7.4, 150mM NaCl, 2mM EDTA, 50mM NaF and 10% glycerol). Soluble embryo lysates were obtained by centrifugation at 15,000 RPM for 5 min, followed by resolution on SDS-PAGE gels and transfer to PVDF membranes. Immunoblotting was performed with anti-zebrafish Cdh1 or anti-Actb diluted in 5% skim milk in TBST. Following HRP-conjugated secondary antibody incubation, immunoreactive signals were visualized by enhanced chemiluminescence (GE Healthcare), and data were collected and analyzed with a ChemiDoc XRS+ system equipped with Quantity One (Version 4.2.1) software (Bio-Rad Laboratories).

Immunocytochemistry. For CDH1 immunofluorescence, cells were fixed in Histochoice Tissue Fixative (Sigma, H2904) for 15 min. Cells for all other immunofluorescent assays were fixed in 4% paraformaldehyde. Cells were permeablized with 0.5% Triton X-100 for 10 min, followed by a standard immunofluorescence procedure.

Whole-mount immunofluorescence of embryos was performed as described (Topczewska et al., 2001). Briefly, embryos were collected and fixed in 4% PFA at 4°C followed by manual dechorionation. Embryos were gradually exchanged to blocking buffer (PBS, 0.1% Tween-20, 2% DMSO, 5% goat serum) and blocked for 1 hour at room temperature. Embryos were incubated overnight at 4°C in rabbit anti-zebrafish Cdh1 antibody (Babb and Marrs, 2004). They were then washed in blocking buffer 8 times, 15 minutes per wash at room temperature, and incubated with secondary antibody at 4°C overnight. Nuclei were stained with SYTO-59 and embryos were mounted in 0.75% low-melt agarose (Lonza, ME). Collection and analysis of confocal micrographs were performed on Olympus FV-500.

For cryosectioning, fixed embryos were embedded in Optimal Cutting Temperature compound (OCT, Tissue-Tek, Inc.), and 10 μm sections were obtained from a CM1950 Cryostat Microtome (Leica). Antibody staining procedures and image acquisition were similar to whole-mount immunofluorescence.

2D and 3D cell culture. HCA-7, CC and SC cells, SW480 and SW620 cells, KM12C and KM12-SM cells, LoVo cells and all derivatives were grown in Dulbecco's modified Eagle's medium (DMEM) (Corning Cellgro) at 37 °C and 5% CO. All culture media were supplemented with 10% fetal bovine serum (FBS), glutamine, nonessential amino acids, 100 U/ml penicillin and 100 mg/ml streptomycin (Hyclone, Logan, UT). For soft agar culture, cells were grown on plastic for 4 days prior to being plated in 6-well dishes in

triplicate at 0.5 x 10^4 cells/ml in 0.4% Type VII agarose (Sigma) over a hardened layer of 0.8% agarose. After 13-25 days at 37°C, and 5% CO_2, colonies were counted using the Oxford Optronix Gelcount.

3D collagen cultures were set up using three layers of collagen (PureCol, Advanced Biomatrix) in 12-well dishes. The top and bottom layers consisted of 400 ml/well of collagen diluted to 2 mg/ml in medium. The middle layers consisted of 400 ml/well of 2 mg/ml collagen in medium and contained 5000 cells/ml in triplicate. One milliliter medium was added on the top of each collagen sandwich. Medium was changed every 2 to 3 days. After 14-18 days, colonies were counted using the Oxford Optronix Gelcount. After quantification of the colony number and size, samples were either fixed in 4% paraformaldehyde for immunofluorescence or lysed for Western blotting.

MAtS invasion assay. This assay was performed as previously described (Ashby et al., 2012). Briefly, a magnetically attachable stencil was placed onto 12-well dishes, previously coated with monomeric collagen (0.1 mg/ml collagen I). HCA-7C and HCA-7P8 cells were seeded at high density. After 48 hours, the stencil was removed and cell movement was monitored by time-lapse microscopy.

Patients, TMA Construction and TMA Slide Preparation. The TMA was constructed on a manual Beecher arrayer and consisted of triplicate 1 μm cores from paraffin blocks of primary colorectal cancers from 84 patients. Cases were chosen to include a variety of CRC subtypes (mucinous, medullary and signet ring cell carcinomas) from all four cancer stages. Ten cores of normal colonic mucosa were included as controls. Freshly cut 5mm TMA paraffin sections were used for IHC.

Mouse xenografts. To investigate *in vivo* cancerous behavior, 4X10^6 cells of each subclone suspended in 100 ml PBS were subcutaneously injected in both flanks. Xenografts were separately prepared for paraffin sectioning and snap-freezed for 28-56 days.

Zebrafish strain maintenance and embryo staging. Wild-type (WT) AB*, *tp53*$^{zdf1/zdf1}$ mutant (Berghmans et al., 2005), and *sox32*$^{ta56/+}$ mutant (Kikuchi et al., 2001; Dickmeis et al., 2001) zebrafish were maintained as previously reported (Solnica-Krezel et al., 1996). Zebrafish embryos were bred naturally and staged according to morphology as previously described (Kimmel et al., 1995).

Identification and cloning of zebrafish plac8 homologs. Zebrafish *plac8* homolog candidates were identified by TLBSTN algorithm (http://blast.ncbi.nlm.nih.gov/) with human PLAC8 (accession number: AAH12205.1) and mouse Plac8 (accession number: NP_631937.1) protein sequences. The obtained

candidate genes were further screened and confirmed by syntenic analysis. As a result of the analysis, two previously uncharacterized genes from the zebrafish gene collection (ZGC), *zgc114201* and *zgc158845*, were renamed as *plac8.1* and *plac8.2*, respectively. The coding sequence of *plac8.1* was obtained from the zebrafish gene repository (Open Biosystems, Lafayette, CO) and subcloned into a pCS2 vector, yielding pCS2-*plac8.1*. Similarly, the *plac8.1* coding sequence was subcloned into pCS2 vectors with carboxyl terminal eGFP or mCherry tags, yielding pCS2-*plac8.1-EGFP* or pCS2-*plac8.1-mCherry* constructs, respectively. Using the pCS2-*plac8.1-eGFP* plasmid as a basis, pCS2-*plac8.1-mt3-eGFP* was generated using site-directed mutagenesis with the following primers: ATCGCCAGTGGCATGGGCGGGTGCTGCT-TGTGTGG (forward) and CCACACAAGCAGCACCCGCCCATGCCACTGGCGAT (reverse). Coding sequences of all constructs were completely sequenced and manually examined to ensure correct DNA sequence.

Zebrafish embryo injection. Sense-capped RNA was synthesized by the mMESSAGE mMACHINE RNA synthesis kit (Ambion, Grand Island, NY) from enzyme-treated and linearized plasmid templates. The synthesized RNA was purified and examined with both spectrometry and agarose gel electrophoresis to ensure expected molecular weight and integrity prior to injection. Embryos were injected at the one-cell stage, unless noted as mosaic injected. For mosaic injection, single cells of 32-cell stage embryos were injected.

Whole-mount in situ hybridization of zebrafish. The full-length coding sequence of *plac8.1* was used to generate digitonin-labeled sense and anti-sense RNA probes. The digitonin-labeled probe usd to detect *ntl* expression was from published studies (Schulte-Merker et al., 1994). The labeled probes were examined with spectrometry and agarose gel electrophoresis to ensure integrity and expected molecular weight. For whole-mount *in situ* hybridization, zebrafish embryos of desired stages were fixed in 4% paraformaldehyde (PFA). The subsequent steps for whole-mount *in situ* hybridization were performed according to the described protocol (Thisse and Thisse, 2008)**.** Micrographs of whole-mount embryos were collected with a Discovery V12 stereo microscope with an Axio Cam MRc camera and Axio Vision software (Carl Zeiss MicroImaging). Cryosectioning of whole-mount *in situ* hybridization samples was performed with a cryostat microtome as described before. Micrographs were collected with an Axio Z1

compound microscope with an AxioCam MRc camera and Axio Vision software (Carl Zeiss MicroImaging).

Time-lapse imaging and analysis. Multi-Z-plane differential interference contrast (DIC) time-lapse images were collected with a Quorum WaveFX-X1 spinning disc confocal system (Quorum Technologies) equipped with MetaMorph software (Molecular Devices). Zebrafish embryos were dechorinated in 0.3x Danieau at 60% epiboly (about 7 hpf). Embryos were then mounted in glass-bottom dishes (Matek) with 0.75% low-melt agarose (Lonza), with the lateral mesoderm close to the glass in order to be imaged (Sepich et al., 2005). Lateral mesoderm cells were identified and focused upon with a 10X objective before the setup of time-lapse recording. Mesodermal cells were imaged from 70% epiboly (7.5 hpf) to 75% epiboly (8 hpf) at 0.5-minute intervals for 30 min with 2 μm Z increment, using a 40X water-immersion objective. The collected time-lapse images were processed using MetaMorph software. Cell morphometric analysis and cell movement tracking were manually processed using ImageJ. Data were exported to Excel software (Microsoft). Statistical analysis and data plotting were performed with Prism software (GraphPad Software, Inc.). The angle data were plotted with the Rose.Net software (http://mypage.iu.edu/~tthomps/programs/).

RNA isolation and quantitative RT-PCR analysis. Total RNA from human cells or zebrafish embryos were extracted with Trizol Reagent (invitrogen), digested with DNase and further cleaned up using the RNeasy Mini Kit (QIAGEN). cDNA was generated with SuperScript II reverse transcriptase (Invitrogen). Quantitative RT-PCR was performed in triplicate using the StepOnePlus Real-Time PCR system (Applied Biosystems) from three independent experiments. Each 20 μl reaction, containing 0.1 μM primers (sequences see Table 2-3), 4 mM MgCl2 and EXPRESS SYBR GreenER Supermix with Premixed ROX (catalog number A10315, Invitrogen), was run under the following conditions: 50°C 2 min, 95°C 2 min; 95°C 15 s, 58°C 45 s for 45 cycles. The melting curve was verified and the results were comparatively quantified using the ΔΔCt method.

Genotyping of the cdh1^{vu44} allele. The *cdh1*^{vu44} allele and wild-type *cdh1* were distinguished by a PCR-generated Restriction fragment length polymorphism (RFLP) method. The VU44 primers used for PCR reactions listed in Table 2-3. The PCR amplification products were digested with the restriction enzyme *DdeI* before agarose gel electrophoresis. The *cdh1*^{vu44} allele gave rise to products of 104 bp and 216 bp,

whereas wild-type cdh1 gene gave rise to a single product of 310 bp.

Pharmacological treatment using MG-132. Zebrafish embryos were incubated in 24-well tissue culture dishes (20-30 embryos each well with 2 ml of solution) with 50 mM MG-132 (Calbiochem) diluted from a 100 mM stock dissolved in embryo medium (0.03% Instant Ocean solution) with 1% DMSO from dome-stage to shield stage. For vehicle control experiments, 1% DMSO in embryo medium was used. At the end of the treatments, embryos were dechrionated for further analysis.

Acknowledgments

We thank J.A. Marrs for generous gifts of antibodies; Drs. G.D. Longmore, S.K. Dutcher, P.V. Bayly, A.B. Reynolds, J.G. Patton, and J.T. Gamse, D.S. Sepich, and R.S. Gray for critical comments and discussions; E.A. Sanders, S. Canter, A. Bradshaw, H. Beck for excellent zebrafish care; Vanderbilt Antibody and Protein Resource core laboratory for generating the anti-PLAC8 and anti-Plac8.1 antibodies. This work is supported by the National Cancer Institute CA46413 and Gastrointestinal Specialized Program of Research Excellence P50CA095103 to R. J. Coffey, T32CA119925 to A. E. Powell, 5T32CA009582-25 to A. Starchenko and P30CA68485 to Vanderbilt Antibody and Protein Resource core laboratory, and GM55101 grant to L. Solnica-Krezel.

Table 2-3. Sequences of primers used in quantitative RT-PCR.

Gene	Forward primer sequence (5' to 3')	Reverse primer sequence (5' to 3')
CDH1	TGCTCTTGCTGTTTCTTCGG	TGCCCCATTCGTTCAAGTAG
CDH2	GGCAGTAAAATTGAGCCTGA	GGAGTTTTCTGGCAAGTTGA
CDH3	AAGATCTTCCCATCCAAACG	CTACAGCGAAGACACCCTCA
CDH11	CGGAATTCATTGTCAAGGTC	CCGAAAAATAGGGTTGTCCT
CDH17	ATGCAAGTTCTTTTGCCAAG	TGTGTCTCCCCTCAGTGAAT
VIM	TCCAAGTTTGCTGACCTCTC	TCAACGGCAAAGTTCTCTTC
ZEB1	GCACAACCAAGTGCAGAAGA	CATTTGCAGATTGAGGCTGA
OCLN	ATGACAAGCGGTTTTATCCA	CTCCAGCTCATCACAGGACT
AKT1	ACCTTTTCGACGCTTAACCT	TGGAGGGAAGGTTCCATATT
PLAC8	GTTTCACCATCTTGGTCAGG	CTGTAATTCCAGCACCTTGG
SNAI1	ACCCCACATCCTTCTCACTG	TACAAAAACCCACGCAGACA
SNAI2	CTTTTTCTTGCCCTCACTGC	GCTTCGGAGTGAAGAAATGC
TWIST1	GTCCGCAGTCTTACGAGGAG	CCAGCTTGAGGGTCTGAATC
TWIST2	GGGAGTGAGCACATTAGCAA	GGGCATGAGTACCCTTAGGA
ACTB	GGACTTCGAGCAAGAGATGG	AGCACTGTGTTGGCGTACAG

*All primers were first validated using standard curve method followed by melting curve before applying to experimental samples.

Sequences of other primers used in the study.

Primer name	Forward primer sequence (5' to 3')	Reverse primer sequence (5' to 3')
PLAC8 cloning primer	GGAATGCAAGCTCAGGCGCCGGTG	TGGATCCGAAGATCTTGAAAGTACGCATGGCT
VU44 genotyping primer	GGCTCAATATAACAGGCTCTGGGCAGATTC	CACTGGGGCTGATTCACGATTGCAC
plac8.1 cloning primer	TAATACGACTCACTATAGGCTCGAGTCATAATTTCAGCGTGCCGTTACTCTTTC	ATTTAGGTGACACTATACTCGAGTCATAATTTCAGCGTGCCGTTACTCTTTC
plac8.1-EGFP cloning primer	TAATACGACTCACTATAGGCTCGAGTCATAATTTCAGCGTGCCGTTACTCTTTC	GGACTAGTTAATTTCAGCGTGCCGTTACTCTTTC
plac8.1-EGFP mt2 primer	GCCAGTGACATGAACGAGGGCGGCTTGTGTGGTTTAGGC	GCCTAAACCACACAAGCCGCCCTCGTTCATGTCACTGGC
plac8.1-EGFP mt3 primer	ATCGCCAGTGGCATGGGCGGGTGCTGCTTGTGTGG	CCACACAAGCAGCACCCGCCCATGCCACTGGCGAT

CHAPTER III

Zebrafish Plac8.1 links ubiquitination regulating protein Cops4 to cilia formation and function

ABSTRACT

Overexpression of zebrafish Plac8.1, a member of a family of cysteine rich protein conserved in vertebrate, led to reduction of a key cell-cell adhesion molecule E-cadherin and defects in gastrulation cell movements (Chapter II). To examine the requirement of Plac8.1 in zebrafish embryonic development, loss-of-function studies by MO-targeting and TALEN induced mutagenesis in the *plac8.1* gene were performed. This study presents unexpected results implicating zebrafish Plac8.1 as a regulator of cilia morphogenesis and function. Cilia are microtubule-based cell surface structures that function as an organelle mediating processes ranging from receiving and integrating diverse extracellular stimuli to generating rhythmic beating motions essential for physiology. Immunofluorescence with an anti-Plac8.1 antibody showed that in ciliated epithelia, Plac8.1 was concentrated at the cell apical domain where cilia reside. Injection of MOs targeting *plac8.1* translation or splicing led to multiple phenotypes, including left-right asymmetry defects, and kidney cysts that are often associated with cilia defects. In Plac8.1 deficient embryos, cilia numbers in the Kupffer's vesicle (a ciliated epithelial tissue that initiates left-right asymmetry formation in zebrafish) and kidney ducts were significantly reduced. Moreover, cilia in kidney ducts were abnormally curled, and showed detached ciliary membranes around the ciliary axonemes. Furthermore, zebrafish embryos with deficient Plac8.1 also showed impaired beating of motile cilia in the KV, kidney, and the olfactory placode. To test the phenotypic specificity of *plac8.1* morphants, we induced *plac8.1* mutation with TALEN designed to target *plac8.1* gene, and obtained a hypomorphic allele *plac8.1*^{stl33}. Similar to *plac8.1* morphant, zebrafish *plac8.1*^{stl33} embryos displayed ventrally curved body axes, kidney cysts, cilia morphology and beating function defects. In addition, interferences of Plac8.1 did not yield detectable defects in expression of transcription factors regulating motile cilia transcription program, indicating that Plac8.1 acted downstream of, or parallel with, motile ciliary transcriptional program.

Furthermore, cilia-dependent phenotypes in *plac8.1* morphants were exacerbated by reduced expression of Cops4, an integral component of the ubiquitination-regulating complex COP9 signalosome.

Besides the functional interaction in regulating cilia formation and function, Plac8.1 showed biochemical interaction with Cops4. Collectively, these results identify Plac8.1 and Cops4 as potential new regulators of cilia. We propose that ubiquitination modification is involved in motile cilia morphology and function.

INTRODUCTION

PLAC8 is a member of cysteine-rich protein family conserved in vertebrates, and has been implicated in cancer formation and invasion, immunity, and adipose differentiation (Ledford et al., 2007; McMurray et al., 2008; Song et al., 2011; Jimenez-Preitner et al., 2011). High levels of PLAC8 have been observed in breast cancer cells and colorectal cancer cells (Hughes et al., 2007, McMurray et al., 2008). Zebrafish *plac8.1* is a homolog of human *PLAC8*, expressed maternally and zygotically in a ubiquitous fashion during early embryogenesis. Overexpression of Plac8.1 led to posttranscriptional downregulation of key cell-cell adhesion molecule E-cadherin, and defects of morphogenetic cell movements during gastrulation (Chapter II). Although gain-of-function experiments by Plac8.1 overexpression provided insights into the role of high levels of PLAC8 in cancer cells, the role of Plac8.1 in zebrafish embryogenesis has not been addressed. To examine the requirement of Plac8.1 in zebrafish embryogenesis, reduction of *plac8.1* function experiments were used in this study. Plac8.1 was highly expressed in epithelial cells with motile cilia, and that Plac8.1 was enriched at the apical domain from which cilia emanate. Wild-type embryos injected with MOs targeting *plac8.1*, or *plac8.1*^{stl33} mutant embryos showed defects in cilia formation and function. These results implicated Plac8.1 as a component regulating formation and function of cilia during zebrafish embryonic development. To investigate the mechanism by which Plac8.1 regulated cilia formation and function, we examined the functional interaction between Plac8.1 and Cops4, a Plac8.1-binding protein. Cilia-dependent phenotypes in embryos deficient in Plac8.1 were exacerbated by reduced expression of Cops4. Since Cops4 is an integral component of the ubiquitination-regulating complex COP9 signalosome, we propose that ubiquitination pathway is involved in cilia formation in zebrafish.

Cilia are highly organized cell surface structures composed of the basal body as the cellular anchor, the microtubule-based axoneme, and the ciliary membrane that are separated from the plasma membrane by periciliary diffusion barriers (Gerdes et al., 2009; Nachury et al., 2010). The cilia assembly

and function require the precise coordination of docking of functional basal bodies, axoneme growth and maintenance, and selective exchange of ciliary proteins by bidirectional microtubule motor-driven vesicular intraflagellar transport (IFT) (Gray et al., 2009; Wallingford and Mitchell, 2011; Ishikawa and Marshall 2011; Rohatgi and Snell 2010). While in invertebrates cilia are generally restricted to sensory neurons and gametes, in vertebrates, cilia are present in a wide spectrum of cells and are involved in diverse functions including generating fluid flow and motility, mediating signal transduction, and providing structural supports for sensory components (Ishikawa and Marshall 2011; Louvi and Grove, 2011). For example, cilia are essential for Hedgehog (Hh) signaling in vertebrates (Huangfu et al., 2003). In addition, platelet-derived growth factor receptor PDGFR$\alpha\alpha$ signaling, and Notch signaling in the skin are mediated by cilia, suggesting that the biological processes mediated by cilia are probably diverse (Schneider et al., 2005; Ezratty et al., 2011). Defects in cilia formation or function underlie a variety of human diseases collectively referred to as ciliopathies (Gerdes et al., 2009; Hildebrandt et al., 2011).

Mutations in multiple genes in model organisms lead to cilia defects. Comparative genomic studies and proteomic studies of cilia have identified over hundreds of molecules that are potentially involved in cilia (Li et al., 2004; Inglis et al., 2006). Zebrafish embryos with cilia defects generally manifest curved body axes in addition to many features similar to ciliopathies in human patients such as kidney cysts and malfunction, and left-right asymmetry defects (Brand et al., 1996). The cilia in zebrafish kidney are essential for kidney function (Sun et al., 2004; Zhao and Malicki, 2007). In addition, cilia in the KV function to establish the left-right embryonic axis (Essner et al., 2005; Kramer-Zucker et al., 2005). The beating of KV cilia generates left-to-right fluid flow that, like the nodal flow in the mouse embryo, leads to expression of Nodal signaling molecules in the left lateral plate mesoderm, thereby initiating a downstream gene cascade to establish left-right asymmetry (Nonaka et al., 1998; Okada et al., 2008; Essner et al., 2005; Kramer-Zucker et al., 2005; Okabe et al., 2008). As mentioned above, disruption to cilia impairs Hh signaling in the mouse embryos, as cilia are the sites where critical signal transduction molecules such as Patched and Smoothened localize and transduce signals (Huangfu et al., 2003; Corbit et al., 2005; Eggenschwiler and Anderson 2007; Goetz and Anderson 2010). Similar to the mouse, zebrafish embryos without cilia exhibit phenotypes associated with dampened Hh signaling, indicating the importance of cilia in Hh signaling transduction is conserved in vertebrates (Huang and Schier, 2009).

However, many zebrafish mutants lacking only the zygotic cilia genes' function show normal Hh signaling, probably because maternally deposited transcripts or proteins compensate for the zygotic loss of function during early embryo development (Tsujikawa and Malicki, 2004; Huang and Schier, 2009).

EXPERIMENTAL PROCEDURES

Zebrafish strain maintenance and embryo staging

Wild-type (WT) AB*, *tp53*$^{zdf1/zdf1}$ mutant (Berghmans et al., 2005), *Tg[sox17:GFP]* (Sakaguchi et al., 2006), and *Tg[cmlc2:GFP]* (Huang et al., 2003) transgenic strains of zebrafish were maintained as previously reported (Solnica-Krezel et al., 1996). Zebrafish embryos were obtained by natural breeding and staged according to morphology as previously described (Kimmel et al., 1995).

Generation of *plac8.1* mutant with transcription activator-like effector nucleases (TALENs)

TALENs targeting zebrafish *plac8.1* gene were designed to recognize the following sequences: 5'-TGACATCTCAACCGTCGG-3' (left TALEN) and 5'-TCAAGCCTGAGTGAAAT-3' (right TALEN). The left and right TAL effector repeats arrays were assembled via the REAL (Restriction Enzyme And Ligation) method (Sander et al., 2011), and cloned into pJDS74 and pJDS78 TALEN scaffolds, respectively. To generate founder fish, synthetic RNA encoding the two TALENs were injected into one-cell zebrafish embryos (70 pg for each TALEN). Samples from the injected embryos were tested for mutation efficiency, and the rest of the embryos from well-mutated batch were raised for germline mutation analysis. The mutation analysis for analysed with PCR (annealing temperature: 59 °C) of the following primers:

forward primer: (5'-GAGATGGGTAGAAAGGCATCCACCATATAACAC-3')

reverse primer: (5'-ATACGCCCACGTCATCACAGCAG-3'). Then the PCR amplicons were treated with BtsCI for 1 hour at 50 °C. Wild-type *plac8.1* gene gives rise to two bands of about 147 bp and 47 bp, and mutanted *plac8.1* alleles with the BtsCI sit altered give rise to a single band of 194 bp.

Antisense MOs and synthetic RNA injection

Antisense MOs (Gene Tools) were dissolved in distilled water and injected into one cell-stage embryos as described (Marlow et al. 2002). Two MOs were designed to target *plac8.1*. The sequence of MO1-*plac8.1* that blocks translation is: (5'-GACGGTTGAGATGTCACCTCCATGA-3'). The sequence of MO2-*plac8.1* that targets the first exon-intro boundary of *plac8.1* and prevents proper slicing of the first intron is: (5'-AATGACAGGAATCACTTACATACGC-3'). The sequence of MO-*cops4* that blocks translation is: (5'-CCGGACGCCATTTTCCTCCGCACTT-3').

The *plac8.1* coding sequence was sub-cloned into pCS2 vectors with carboxyl terminal HA, EGFP or monomeric Cherry tags, giving rise to pCS2-*plac8.1-HA*, pCS2-*plac8.1-EGFP*, or pCS2-*plac8.1-mCherry*, respectively. The PCR product from the pCS2-*plac8.1-HA* plasmid with the following primers: 5'-GAATTCATGGAAGTAACGTCACAGCCCTCGGCGTTTC-3' (forward primer), 5'-GAAACGCCGAGGGCTGTGACGTTACTTCCATGAATTC-3' (reverse primer) was cloned into a pCS2 vector with EcoRI and XhoI sites, giving rise to a rescue *plac8.1-HA* construct. To generate a construct encoding RNA lacking the MO1-*plac8.1* binding site synonymous substitutions were introduced by *in vitro* mutagenesis by QuickChange Site-Directed Mutagenesis Kit (Stratagene). To validate coding sequences of all constructs they were completely sequenced and manually examined.

Sense-capped RNAs were synthesized by the mMESSAGE mMACHINE RNA synthesis kit (Ambion) from enzyme treated and linearized *plac8.1* plasmids templates, and *arl13b-GFP* template (a gift from Brian Ciruna, University of Toronto, Canada) (Borovina et al., 2010). The synthesized RNA was purified and examined with both spectrometry and agarose gel electrophoresis to ensure expected molecular weight and integrity prior to injection.

Antibody generation, western blotting, and immunofluorescence

Anti-zebrafish Plac8.1 antibodies were generated by immunizing rabbits with KLH-conjugated with peptides of the amino acid sequence from the C terminus of zebrafish Plac8.1 (CQLKRDIDIRKSNGTLKL) (Covance). Other antibodies used in the study include: anti-HA monoclonal antibody (12CA5) (Roche Applied Science), anti-anti-zebrafish Plac8.1 antibodies were generated by immunizing rabbits with KLH-conjugated with peptides of the amino acid sequence from the C terminus of

zebrafish Plac8.1 (CQLKRDIDIRKSNGTLKL) (Covance). Other antibodies used in the study include: anti-HAlone 3E6) (Invitrogen) for immunoprecipitation.

For western blotting analysis, embryos collected at designated stages were manually dechorionated and homogenized in NP40 lysis buffer containing Nonidet P-40 (Igepal A-680) 1 %, Tris-HCl (pH 7.4) 50 mM, NaCl 150 mM, EDTA 2 mM, NaF 50 mM, and glycerol 10 %. Lysed embryos were centrifuged at 4°C for 15,000 RPM for 5 min. After centrifugation equal amounts of clear lysates were resolved on SDS-PAGE and transferred to polyvinylidene difluoride membranes. The membranes were blocked in TBST with 5% skim milk and incubated with primary antibody diluted in TBST with 5% skim milk, followed by washing and incubation with appropriate secondary horseradish persoxidase-conjugated secondary antibody (Promega). Finally, immunoreactive complexes were revealed by enhanced chemiluminescence (Amersham Biosciencs), and data were collected and analyzed with ChemiDoc XRS+ system equipped with Quantity One (Version 4.2.1) software (Bio-Rad Laboratories).

For immunoprecipitation, 40 embryos were processed in 400 μL NP-40 lysis buffer with freshly added protease inhibitors (Roche Applied Sciences) according to the above-mentioned methods. One μg of anti-GFP antibody was added to 200 μL cleared lysate, and incubated at 4°C for two hours. Then 30-50 μL protein G Sepharose resins were added to the clear lysates, followed by incubation at 4°C for two hours. The protein G Sepharose resins were washed four times at 4°C, each time with 500 μL NP40 buffer. Then equal volume 2x Laemmli sample buffers were added followed by western blotting analysis as mentioned above.

Whole-mount immunofluorescence experiments were performed as previously described (Topczewski et al., 2001). Briefly, embryos were collected and fixed in 4% paraformaldehyde for overnight at 4 °C, followed by manual dechorionation. Then embryos were changed to phosphate buffered saline (PBS) with 0.1% Tween-20. Then embryos were blocked in PBS with 5% goat serum, 2% DMSO, 0.1% Triton X-100, 0.1% Tween-20 for one hour at room temperature. Then primary antibodies were diluted in blocking buffer (1:250-1:500) and incubated overnight at 4 °C. Embryos were washed in blocking buffer for eight times, 15 minutes each time with PBS containing 0.1% Triton X-100 and 0.1% Tween-20 at room temperature. Then they were incubated with fluorophore-labeled secondary antibody (1:400) over night at 4 °C (Jackson Immuno Research Laboratories). Then embryos were washed with

PBS containing 0.1% Triton X-100 and 0.1% Tween-20 at room temperature for eight times, 15 minutes each time. After washing, SYTO-59 red (1:5,000) was used to stain DNA for 30 min, and then wash twice for 10 minutes each. Images were acquired using a Zeiss LSM 510 laser scanning inverted microscope (Carl Zeiss MicroImaging) and processed using Image J and LSM software (Zeiss MicroImagin).

Whole-mount *in-situ* hybridization (WISH)

The full-length coding sequence of *plac8.1* was used to generate digoxigenin-labeled sense and anti-sense RNA probes. Other probes include *pax2a* (Krauss et al., 1991), *foxj1* (Neugebauer et al., 2009), *southpaw* (Long et al., 2003), *insulin* (Milewski et al., 1998), *cmlc2* (Yelon et al., 1999), *foxa3* (Odenthal and Nüsslein-Volhard, 1998). The labeled probes were examined with spectrometry and agarose gel electrophoresis to ensure integrity and expected molecular weight. For WISH, zebrafish embryos of desired stages were fixed in 4% PFA. The following steps for whole-mount *in-situ* hybridization were performed according to the described protocol (Thisse and Thisse, 2008). Micrographs of whole-mount embryos were collected with a Discovery V12 stereomicroscope with an Axio Cam MRc camera and Axio Vision software (Carl Zeiss MicroImaging). Cryosectioning of WISH samples were performed with a cryostat microtome as described before (Kochakpour, 2009). Micrographs were collected with an Axio Z1 compound microscope with an AxioCam MRc camera and Axio Vision software (Carl Zeiss MicroImaging).

Cryosection and histology staining

Embryos at 3 dpf were fixed in 4% PFA dissolved in PBS overnight. Cryosectioning of whole-mount samples was performed with a cryostat microtome as described before (Kochakpour et al., 2009). Tissue slides were stained with standard hematoxylin and eosin stain (Fisher et al., 2008).

Kupffer's vesicle flow analysis

Kupffer's vesicle flow analyses were performed according to previously published methods (Neugebauer et al., 2009). Briefly, embryos at 3-5-somite stage (10.5-11 hpf) were dechorionated and mounted in 0.5% low melting point agarose in Danieau solution on a concave glass slide. Fluorescent

polystyrene beads (1 μm in diameter, Invitrogen) were injected into Kupffer's vesicle and imaged on a Zeiss Image Z1 compound microscope (Carl Zeiss MicroImaging).

Transmission electron microscopy

Zebrafish embryos of 1.5 dpf were processed for transvers section for transmission electron microscopy analysis according to previously published protocol (Jaffe et al., 2010).

High-speed time-lapse microscopy analysis

High speed time-lapse imaging of cilia beating was performed according to previously published protocol (Jaffe et al., 2010). Briefly, one-day old zebrafish embryos were anesthetized in tricaine solution (0.16%) and mounted in 1% low melting temperature agarose laterally on a 2-slide bridged cover slip. Images of the mounted embryos were acquired by using a Zeiss Image Z1 compound microscope (Carl Zeiss MicroImaging) equipped with Dragonfly Express Camera and PGR software (Point Grey Research). Lateral traces of cilia beat paths in the olfactory placode were obtained according to previous methods (Wilson et al., 2009). To examine the fluid flow generated by olfactory placode cilia, fluorescent microspheres were used as tracing reagent. Briefly, zebrafish embryos were raised in 90% hypertonic Hank's saline to suppress edema. Then four-day old zebrafish embryos were anesthetized in tricaine solution (0.16%) and mounted laterally on a 2-slide bridged cover slip, with fluorescent beads diluted to the concentration of 300 beads /μl and applied to the olfactory placode of zebrafish embryos. High-speed time-lapse imaging of fluorescent beads movements were recorded with a Zeiss Image Z1 compound microscope (Carl Zeiss MicroImaging) equipped with Dragonfly Express Camera and PGR software (Point Grey Research). The images were process with ImageJ, and data were plotted with MATLAB software package.

Acridine orange staining

Chorions of zebrafish embryos were manually removed at 36 hpf. Then acridine orange staining was performed by incubating embryos in E3 medium (5 mM NaCl, 0.17 mM KCl, 0.33 mM $CaCl_2$, 0.33 mM $MgSO_4$. 0.1% methylene blue) with 2 m 0.1% methylene blue) with 2 were manually removed at°C in

the dark. Afterwards, embryos were washed in E3 medium four times for 10 minutes in the dark before imaging with a fluorescence microscope.

Statistical analysis

Factorial ANOVA test was performed with customized SAS (SAS Institute) code to analyze interactions between *plac8.1* and *cops4* loss-of-functions. Other analyses were performed using the Prism software (GraphPad Software).

RESULTS

Expression of *plac8.1* in epithelial tissues with motile cilia

To understand the role of *plac8.1* in zebrafish development, we examined its expression pattern by using WISH. *plac8.1* transcript was ubiquitously expressed during early development until 4 dpf when its expression was enriched in the gut (Chapter II). The ciliated green algae *Chlamydomonas reinhardtii* has a protein similar to Plac8.1 (sequence alignment not shown). Furthermore, *Chlamydomonas reinhardtii* Agg2p harbors a domain similar to Plac8 and localizes to proximal flagellar membrane near the basal bodies (Iomini et al., 2006). Therefore, we examined ciliated tissues. Indeed, zebrafish *plac8.1* was expressed in the Kupffer's vesicle (a ciliated structure analogous to the mouse node) (Figure 3-1 a), kidney ducts (Figure 3-1 d), and the olfactory placode (Figure 3-1 b). In contrast, the control WISH with a labeled *plac8.1* sense probe did not yield detectable signal (Figure 3-1 c). Furthermore, transverse section of 1.5 dpf embryos showed the expression of *plac8.1* in the pronephric ducts.

Plac8.1 protein localized close to the cilia basal body at the apical domain of ciliated epithelial cells

We generated an anti-Plac8 antibody against the C-terminal peptide of the zebrafish Plac8.1 to visualize the tissue and subcellular localization of endogenous Plac8.1 during zebrafish embryogenesis. With zebrafish Plac8.1 protein expressed in *E.coli* as a positive control, we found that antibodies raised against the zebrafish Plac8.1 strongly reacted with the Plac8.1 protein, but to a much less extent reacted

to the human PLAC8 protein (Figure 3-2 b). In addition, the preimmune serum did not yield detectable signal (data not shown). To determine the antibody's specificity, we utilized two independent *plac8.1* MOs: MO1-*plac8.1*, designed to interfere with translation, and MO2-*plac8.1* designed to interfere with splicing (Figure 3-2 a). Attesting the effectiveness of MO1-*plac8.1*, its injection into zebrafish embryos interfered with the translation of *plac8.1-GFP* RNA that retains the MO1-*plac8.1* recognition sequence (Figure 3-2 e, e1, e2), but not of a mismatch construct mm*plac8.1-mCherry* RNA, in which the MO1-*plac8.1* target sequence was mutated to contain 6 mismatches (Figure 3-2 e, e3, e4). For MO2-*plac8.1*, RT-PCR experiments revealed that its injection into zebrafish embryos caused retention of the first intron in the mature RNA transcript in zebrafish embryos at 1 dpf as expected (Figure 3-2 d). Although a small amount of properly processed RNA transcript still remained, these results demonstrated that MO2-*plac8.1* was also effective. In protein lysates prepared from un-injected control embryos at 1 dpf, we detected a band of about 12 kDa, well in agreement with the theoretical molecular weight of Plac8.1. This band was reduced in the lysate from zebrafish embryos injected with MO-1, and to a lesser extent in the lysates from zebrafish embryos injected with MO-2 (Figure 3-2 c). These experiments, together with other lines of evidence (Chapter II), suggested that the 12 kDa bands were specific to Plac8.1. Moreover, both MOs were effective in reducing the levels of endogenous Plac8.1 protein at 1 dpf, with MO1-*plac8.1* more effective.

We next used the validated anti-Plac8.1 antibody to detect protein localization in zebrafish embryos with whole-mount immunofluorescence. As shown in Chapter II, the anti-Plac8.1 immunofluorescence signals localized in the cytosol of zebrafish embryos at the onset of gastrulation at the 50% epiboly stage (Figure 2-3). During the process of gastrulation, the distribution of Plac8.1 gradually shifted from the cytosol to the cell membrane while cells probably underwent an epithelialization process (Figure 2-3) (Sepich et al., 2011). In 8-10 somite-stage embryos, Plac8.1 localized at the lumen-facing apical membrane of Kupffer's vesicle (KV) cells (Figure 3-2 f-h'). These Plac8.1-positive, lumen-facing cells appeared to be the ciliated cells of the KV as indicated by their strong anti-GFP staining in *Tg [sox17:GFP]* transgenic fish embryos (Sakaguchi et al., 2006; Essner et al., 2005). In the *plac8.1* MO-1 injected embryos, however, the Plac8.1 signal was significantly reduced (Figure 3-2 f'-h'), suggesting the apical localization of the endogenous Plac8.1 protein. Furthermore, co-staining with basal body marker

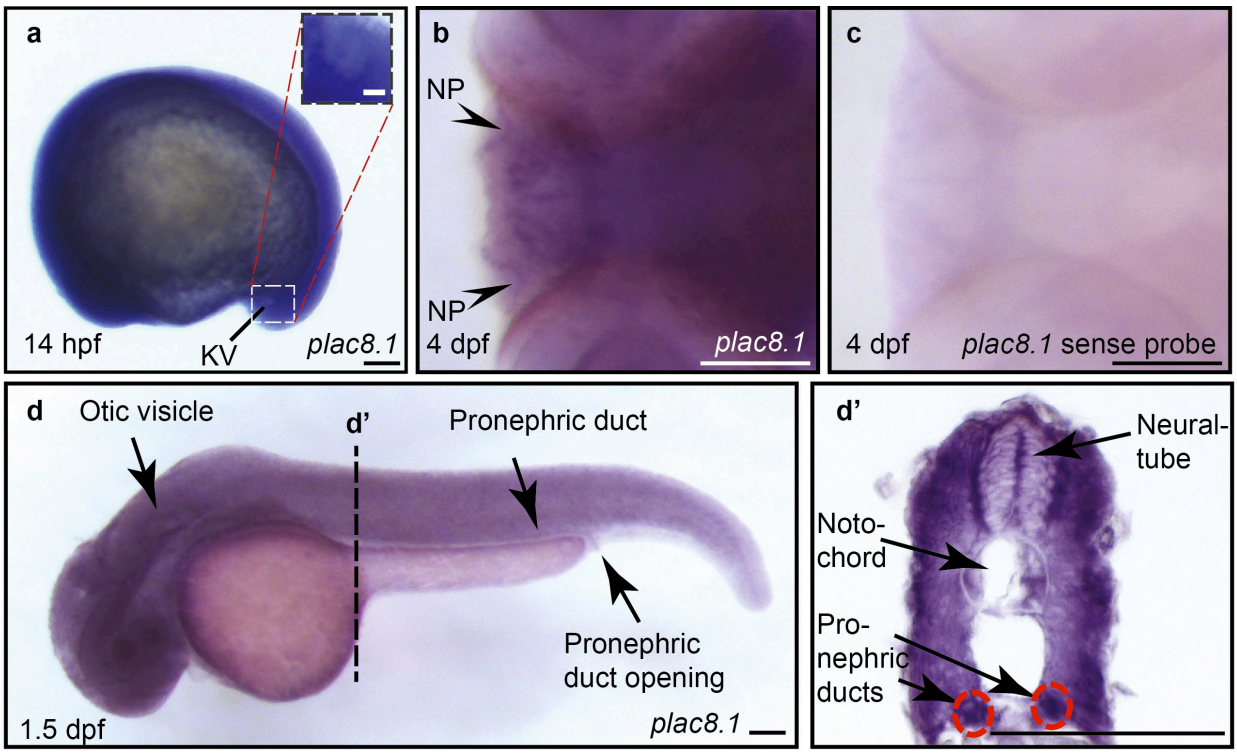

Figure 3-1. Zebrafish *plac8.1* was expressed in ciliated tissues.
a-d', Expression of *plac8.1* in the zebrafish Kupffer's Vesicle (KV) at 14 hpf (**a**), the otic vesicle and the pronephric duct at 1.5 dpf (**d**), and the nasal pit epithelium (**b** and **c**). The transverse section along the dashed line in d is shown in d'. *plac8.1* is expressed in the pronephric duct (red circles in **d'**).
Scale bars: 10 microns: the inset of **a**, other scale bars:100 microns (Figure 3-1 d'). Altogether, these experiments suggested that Plac8.1 could be required for zebrafish embryogenesis, possibility by functioning in these ciliated tissues.

γ-tubulin showed that the two proteins co-localized at the apical region of the KV cells (Figure 3-3 a-a''). In addition to the KV, we detected high levels of Plac8.1 in the kidney duct in 1 dpf zebrafish embryos (Figure 3-2 i-k'). Similar to the staining in the KV cells, Plac8.1 localized close to the apical membrane and intracellular puncta in the kidney cells (Figure 3-2 i, Figure 3-4 f). The Plac8.1 signal did not overlap completely with but localized close to acetylated tubulin signals that marked the apical cilia of kidney cells (Figure 3-2 i-k'). Also, Plac8.1 was detected at the bases of motile cilia in the zebrafish embryo kidney ducts as shown by co-staining with an anti-γ-tubulin antibody that marked the cilia basal bodies (Figure 3-3 b-b''). In contrast to wild-type control embryos, the signal was drastically reduced in MO1-*plac8.1* injected embryos at 1.5 dpf (Figure 3-2 i'-k', Figure 3-4 f'), consistent with the patterns reflecting the endogenous Plac8.1 protein distribution. These data suggested that endogenous Plac8.1 might play critical role in motile cilia function by regulating basal bodies and/or apical membranes on which motile cilia reside.

In addition, we found similar localization patterns in other ciliated cells, including the olfactory placode cells (Figure 3-10 d, and data no shown), which was consistent with WISH of 4 dpf zebrafish embryos (Figure 3-1 b). What's more, the 5' regulatory in zebrafish, mouse, and human had conserved motifs frequently found in genes functioning in olfactory system (data not shown). Moreover, Plac8.1 appeared to be enriched in the sensory hair cells of the lateral-line neuromasts (Figure 3-3 c-d''), and localized at the base of cilia (Figure 3-3 f-f'').

Since basal bodies that serve as centrosomes at the base of cilia also mediate mitosis in dividing cells, Plac8.1 might localize to mitosis spindles in dividing cells. To better explore this speculated dynamic localization pattern *in vivo*, we generated epitope-tagged Plac8.1 with C-terminal HA, EGFP or monomeric Cherry (mCherry). Irrespective of the tag utilized, Plac8.1 localized predominantly at a peripheral structure near the cell membrane, and also was found in intracellular puncta (Figure 3-4, Chapter II). Plac8.1 visualized with a C-terminal mCherry fusion also localize to the base of cilia (Figure 3-3 e-e''). These fusion proteins showed localization patterns consistent with the results obtained with the Plac8.1 antibody staining. Also these fusion proteins appeared to be functional similar to untagged Plac8.1 (Figure 3-5, 3-6, Chapter II), indicating these fusion constructs could provide dynamic information of the endogenous Plac8.1 protein. After the verification, we performed time-lapse imaging of

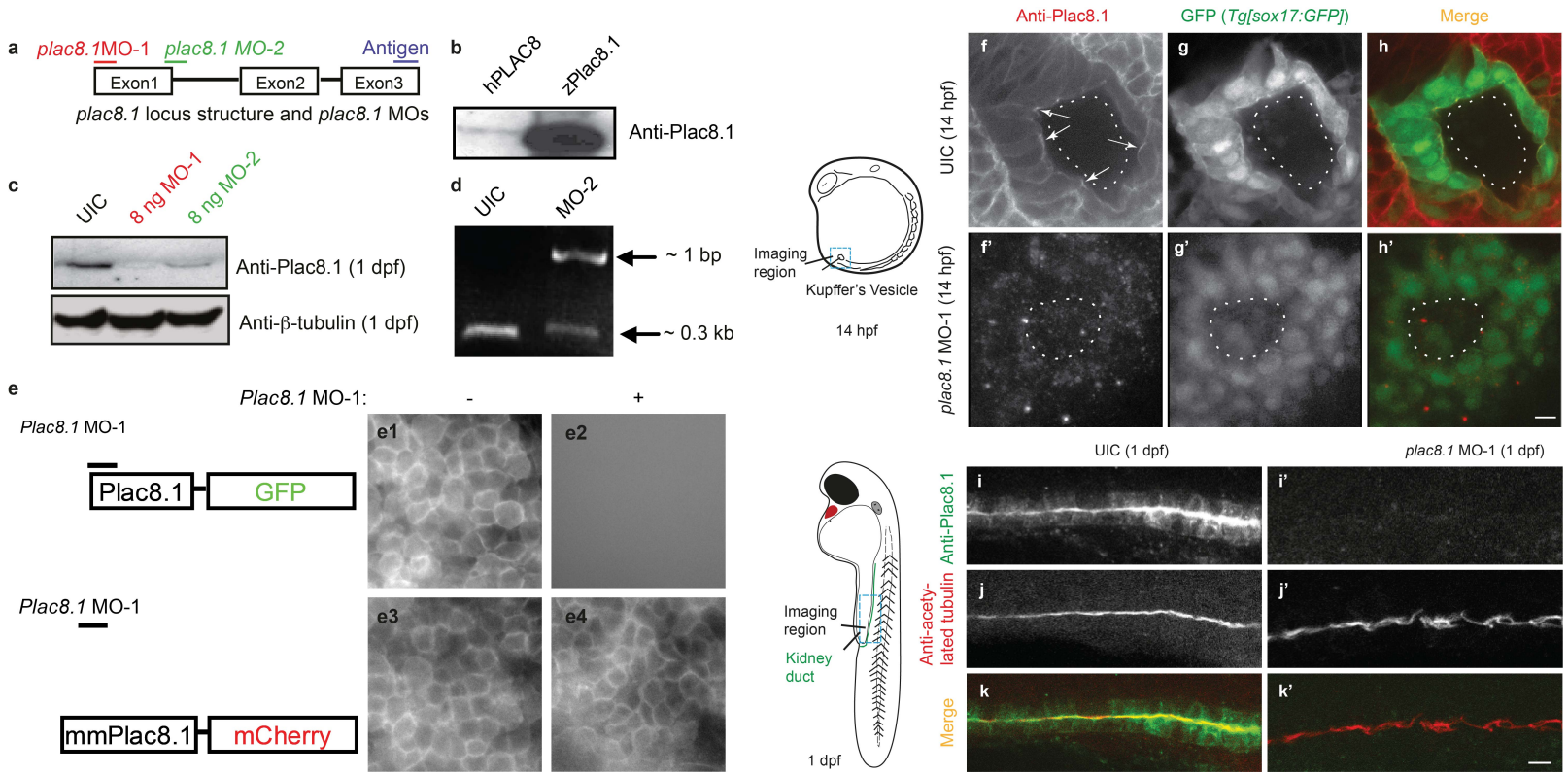

Figure 3-2. Zebrafish Plac8.1 protein enriched at the apical sided of ciliated epithelium.
a-e4. Generation and validation of reagents to perturb and to monitor Plac8.1 levels. **a.** A cartoon showing the gene structure of *plac8.1*, the targeting region of two Plac8 MOs: MO-1 and MO-2 (not drawn to scale), and the antibody recognition site marked in blue.
b. Western blotting of human PLAC8 and zebrafish Plac8.1 proteins produced in *E.coli*. **c.** Western blotting to test the effectiveness of the 2 MOs with lysates from uninjected control zebrafish embryos (UIC), or embryos injected with either MO-1 or MO-2. **d.** RT-PCR uninjected control zebrafish embryos (UIC), or embryos injected with MO-2 with *plac8.1* primers confirmed that MO-2 is effective to interfere with splicing of the first intron, leading to an extra PCR amplicon of 1 kb in size. **e.** Cartoon showing two fluorescent fusion construct of Plac8.1. The Plac8.1-GFP construct retains MO-1 binding site and was sensitive to MO-1 (**e1-e2**), whereas the mismatched *mmPlac8-mCherry* construct, which was predicted not to be sensitive to MO-1 with synonymous substitutions, and encodes the same amino acid sequences for Plac8.1, did not show sensitivity to MO-1 (**e3-e4**).
f-k' Plac8.1 protein localization overlaps with the base cilium. A cartoon illustration of a 14 hpf embryo of which the Kupffer's Vesicle (KV) images are shown to the left of **f-h'**. **f-h'**. Confocal micrograph of KV cells (ventral view) in *Tg[sox17:GFP]* embryos in which KV cells express high level GFP. In wild-type control embryos (UIC), Plac8.1 localizes to the apical of KV cells (arrows) facing the lumen of KV (dashed line). In contrast, the signal is lost in embryos with defective Plac8.1 (*plac8.1* MO-1, **f'-h'**). **i-k'**. Plac8.1 enriches to the apical membrane in the pronephric duct cells of wild-type embryos (**i-k**, cartoon illustration on the left of the confocal micrograph), and the signal is lost in Plac8.1 deficient embryos (**i'-k'**). Scale bars: 10 microns.

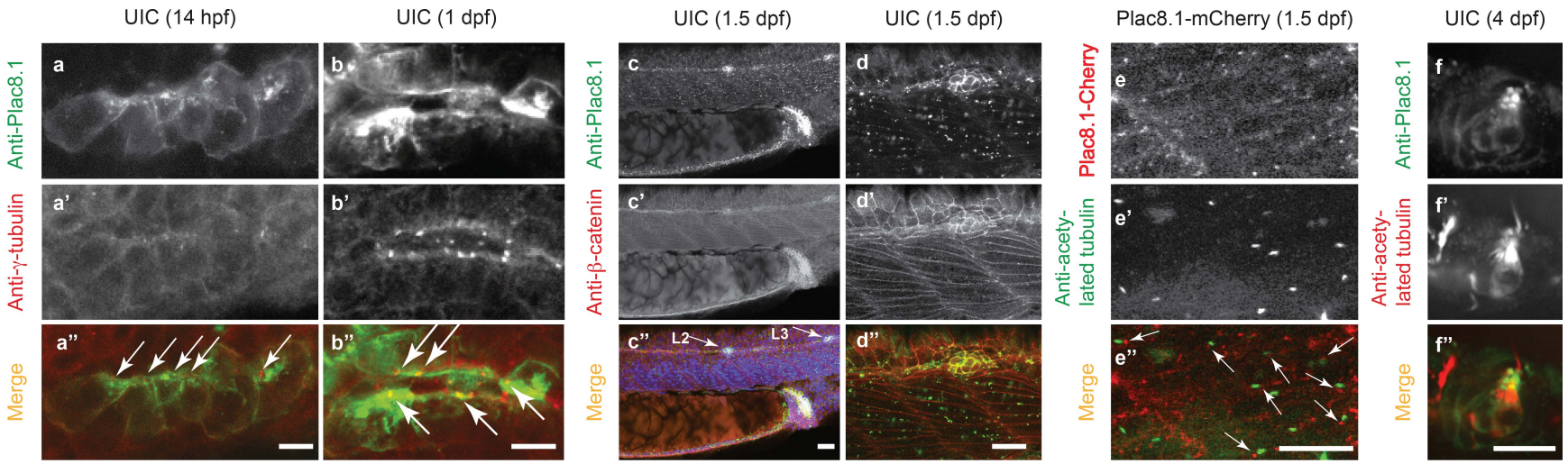

Figure 3-3. Zebrafish Plac8.1 protein localized at the base of cilia.

a-b''. The Anti-Plac8.1 staining (green), and anti-gamma-tubulin (a basal body marker) staining (red) show that Plac8.1 overlaps with gamma-tubulin in KV cells (arrows in **a''**). and in the kidney ducts (arrows in **b''**).

c-d''. In addition to kidney ducts, distribution of Plac8.1 is enriched in the lateral neuromasts (L2, L3 labeled by the arrows). Higher magnification in **c''** also shows puncta staining of Plac8.1 in the muscle.

e-e''. Plac8.1-mCherry shows similar puncta signal as the anti-Plac8.1 staining. Co-staining with an anti-acetylated tubulin antibody shows Plac8.1 at the bases of cilia (arrows in **d''**).

f-f''. Co-staining of anti-Plac8.1 and anti-acetylated tubulin antibody shows that Plac8.1 is enriched at the base of cilia of a lateral line neuromast. Scale bars: 5 microns in **e-e''**, other scale bars: 10 microns.

plac8.1-GFP RNA injected embryos. During cell division, Plac8.1 puncta concentrated to a pair of foci aligned parallel with the direction of cell division (Figure 3-4, Chapter II, and time-lapse data not shown). These data indicated that Plac8.1 might be a part of centrosome during cell division, which was in accordance with the basal body localization in cells with motile cilia.

Reduction of *plac8.1* function led to ventrally curved body axes and kidney cyst

To investigate the function of *plac8.1* during zebrafish embryogenesis, we performed loss-of-function experiments with two independent MOs. The translation blocker MO-1 interfered with the expression of *plac8.1-GFP* RNA that retained the MO-1 cognitive site but not a mismatch construct mm*plac8.1-mCherry* RNA with the MO-1 cognitive site altered with synonymous substitution (Figure 3-2 e1-e4). Tested by western blotting, both MOs reduced the 12 kDa band recognized by the anti-Plac8.1 antibody in extract from 1 dpf embryos, with MO-1 more effective (Figure 3-2 c). However, we could not find effective reduction of Plac8.1 protein during gastrulation stage (data not shown). Therefore, the *plac8.1* morphants probably present a partial loss-of-function model. Upon injection of *plac8.1* MOs, no gross morphological defects could be detected in zebrafish embryos from the blastula through segmentation stages. Starting from 1 dpf, *plac8.1* morphants showed multiple abnormalities. A ventrally curved body axis was the first apparent morphologic defect (Figure 3-4 a-a', and data not shown). Starting from 3-4 dpf, Plac8.1-deficient embryos displayed obvious pericardial edema and kidney cysts (Figure 3-4 a-a'). Transverse sectioning and histological analysis showed dilated kidney ducts in *plac8.1* morphants (Figure 3-4 b-b', and quantification in e). At later stages, multiple organs of *plac8.1* morphants displayed abnormalities, likely being secondary to kidney defect (data not shown). Titration experiments showed the penetrance of the above phenotypes increased in a dose dependent manner (Figure 3-4 d). MO1-*plac8.1*, which showed stronger potency in reducing the Plac8.1 protein level than MO2-*plac8.1* (Figure 3-2 c), caused stronger and more consistent defects (Figure 3-4 d). Therefore, we used MO1-*plac8.1* in all experiments described in this chapter unless noted otherwise.

To test if the observed phenotypes were caused specifically by loss of *plac8.1* function we performed rescue experiments. Co-injection of a synthetic *plac8.1* RNA lacking MO1-*plac8.1* binding site significantly reduced the penetrance of the phenotypes described above (Figure 3-4 d). In addition, MOs

application could lead to nonspecific phenotypes due to the apoptosis-inducing effects (Berghmans et al., 2005; Bill et al., 2009). To test this possibility, apoptosis detections with acridine orange staining (Lecoeur et al., 2002) of 1.5 dpf embryo were used. Injections of MO1-*plac8.1* only increased brain apoptosis compared to control embryos (data not shown), suggesting the body axis phenotype observed was unlikely to be caused by non-specific apoptosis upon MOs injection. Furthermore, we also injected *plac8.1* MOs into *tp53*$^{zdf1/zdf1}$ mutant embryos, which exhibit significantly reduced apoptosis associated with MOs injection (Berghmans et al., 2005). The *tp53*$^{zdf1/zdf1}$ mutant embryos injected with *plac8.1* MOs also manifested curved body axes, pericardial edema and the kidney cysts (data not shown). The titration experiments, rescue experiments, *tp53*$^{zdf1/zdf1}$ embryo experiments, and apoptosis assays strongly suggested that the phenotypes were caused by the reduction of Plac8.1 and did not result from excess apoptotic cell death.

In zebrafish, *ponzr1*, a gene with Plac8 domain, and encoding a protein with about 30% amino acid sequence identify to Plac8.1, was shown to affect expression of kidney transcription factor *pax2a* (Bedell et al., 2012), a FGF target gene (Reifers et al., 1998; Phillips et al., 2001; Hans et al., 2004). WISH experiments with a *pax2a* probe (Krauss et al., 1991) on 1 dpf zebrafish embryos revealed that loss-of-function of *plac8.1* did not alter expression of *pax2a* (Figure 3-4 c-c'), suggesting that loss-of-function of *plac8.1* did not alter cell fates of kidney duct cells, and indicating that Plac8.1 might function downstream of *pax2a*. Taken together, these results demonstrated that reduction of *plac8.1* function led to kidney cyst formation without altering cell fate specification in the kidney cells.

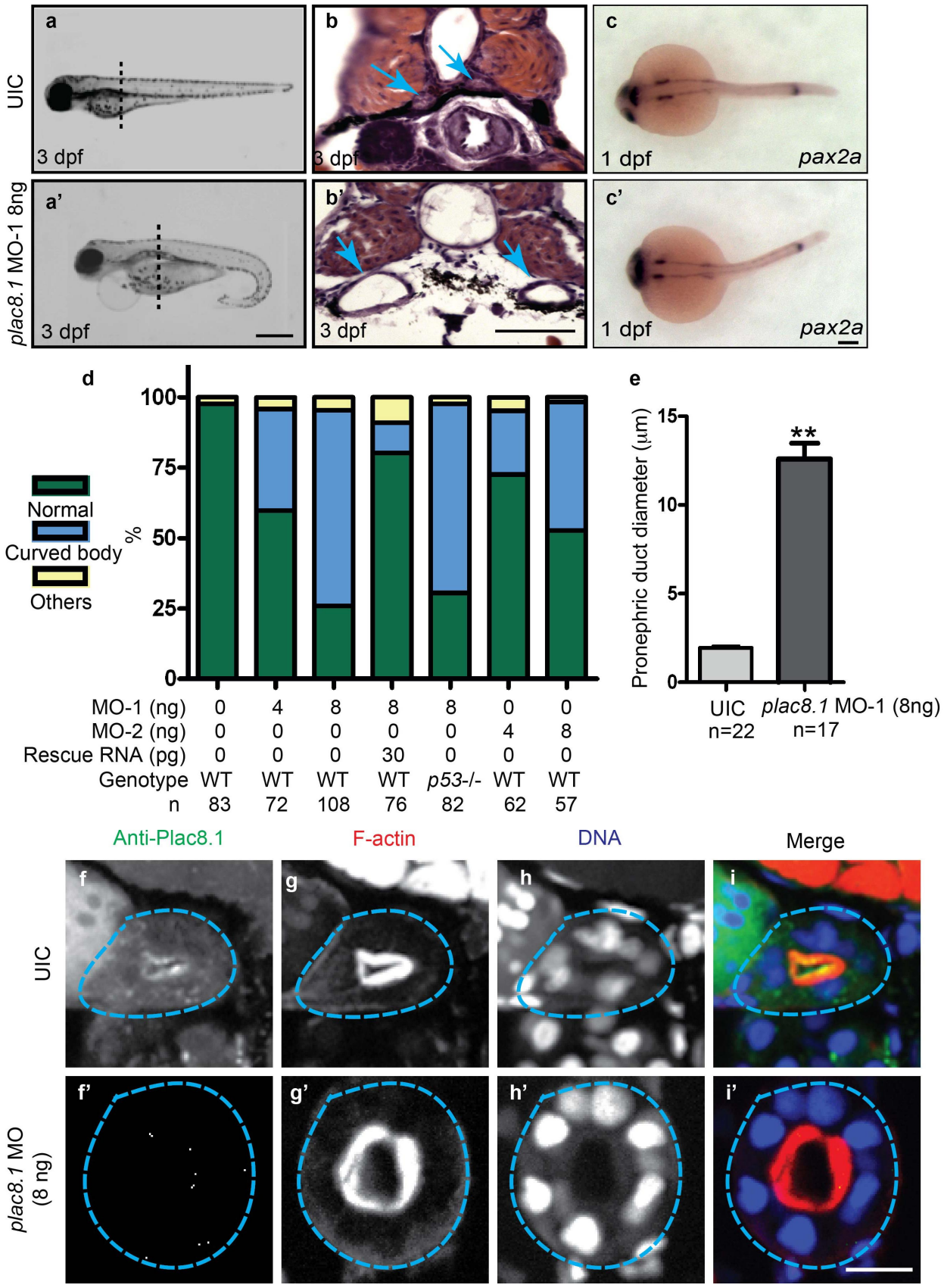
UIC
plac8.1 MO-1 8ng
a
3 dpf
b
3 dpf
c
1 dpf
pax2a
a'
3 dpf
b'
3 dpf
c'
1 dpf
pax2a
d
100
75
50
25
0
%
Normal
Curved body
Others
MO-1 (ng) 0 4 8 8 8 0 0
MO-2 (ng) 0 0 0 0 0 4 8
Rescue RNA (pg) 0 0 0 30 0 0 0
Genotype WT WT WT WT p53-/- WT WT
n 83 72 108 76 82 62 57
e
Pronephric duct diameter (μm)
15
10
5
0
**
UIC
n=22
plac8.1 MO-1 (8ng)
n=17
Anti-Plac8.1
F-actin
DNA
Merge
UIC
plac8.1 MO
(8 ng)
f
g
h
i
f'
g'
h'
i'

Figure 3-4. Reduction of *plac8.1* function resulted in body curvature and kidney cysts.
a-b'. Morphologic defects of loss-of-function of *plac8.1*. Lateral view of 3 dpf control embryos (**a**) and *plac8.1* morphants (**a'**). Transverse sections and H&E staining at the region indicated by the dashed line in **a** and **a'** are shown in **b** and **b'**. Arrows point to pronephric ducts, the diameters of which are quantified in **e**. The ** denotes $p<0.01$. **d**. Penetrance of the phenotype in **a-b'** are quantified in **d**.
c-c'. Expression of kidney transcription factor *pax2a* appeared normal as shown by the *in situ* hybridization.
f-i. Transverse section and confocal micrograph of control embryos, and *plac8.1* morphant (**f'-l'**) at 4 dpf. Cyan dashed lines outline the circumference of pronephric ducts. Scale bars: 500 microns (**a**-**b**), 50 microns (**c**-**d**), 10 microns (**f-i'**).

Reduction of *plac8.1* function led to left-right asymmetry defects

The set morphological defects observed in embryos with deficient Plac8.1, including ventrally curved body axis and kidney cysts, were also found in a battery of zebrafish mutants that in addition showed left-right asymmetry defects (Drummond, 2012). Therefore, we examined whether Plac8.1 was required for the proper establishment of left-right asymmetry by examining the expression of the Nodal ligand *southpaw* (*spw*), the earliest known marker for left-right asymmetry during zebrafish embryogenesis (Long et al., 2003). In majority of uninjected wild-type embryos, the expression of *spw* was restricted to the left side of the lateral plate mesoderm (Figure 3-5 a). However, in a dose-dependent manner, injection of MO-1 resulted in increased proportion of embryos with either absent *spw* expression (Figure 3-5 b), or expression of *spw* on the right side of the lateral plate mesoderm (Figure 3-5 c), or expression of *spw* on both sides (Figure 3-5 d). Furthermore, co-injection of MO1-*plac8.1* with the MO1-*plac8.1*-resistant *plac8.1* RNA partially rescued the aberrant *spw* expression, indicating that the defects were specific to loss-of-function of *plac8.1* (Figure 3-5 e). These results indicate that Plac8.1 is required for the normal left-side expression of *spw* in the lateral plate mesoderm (Figure e). Accordingly, WISH experiments with probes marking left-right asymmetrically placed organs including the pancreas (2 dpf, Figure 3-5 f-f'''), the liver (2 dpf, Figure 3-5 g-g'''), and the heart (2 dpf, Figure 3-5 h-h''') revealed that the laterality of these organs was also affected. Thus these results suggested that Plac8.1 is required for the left-right axis formation in zebrafish embryogenesis

Reduction of *plac8.1* function led to defects in the formation and function of cilia in the Kupffer's vesicle

Since the asymmetric expression of *spw*, and thereby proper lateral placement of internal organs depended directly on the nodal flow propelled by the beating function of the motile cilia in the Kupffer's vesicle (Essener et al., 2005; Kramer-Zucker et al., 2005), we examined the Kupffer's vesicle and the cilia that emanate from the apical sides of the cells lining it. Based on DIC imaging analysis of the area of Kupffer's vesicle, Kupffer's vesicles in *plac8.1* morphants were properly formed, and of similar size to control embryos (data not shown). In addition, analysis with the *Tg[sox17:GFP]* embryos in which the Kupffer's vesicle cells express GFP, injected with MO1-*plac8.1* had similar numbers of Kupffer's vesicle

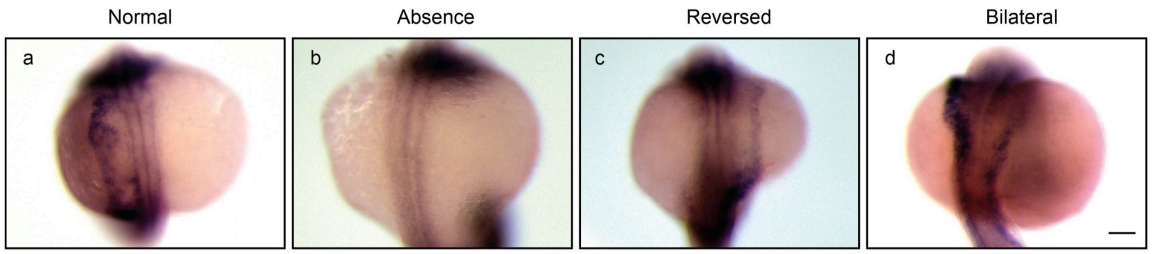

spw
19 hpf

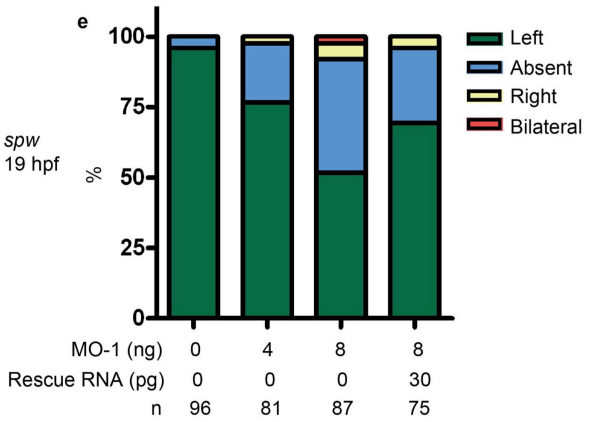

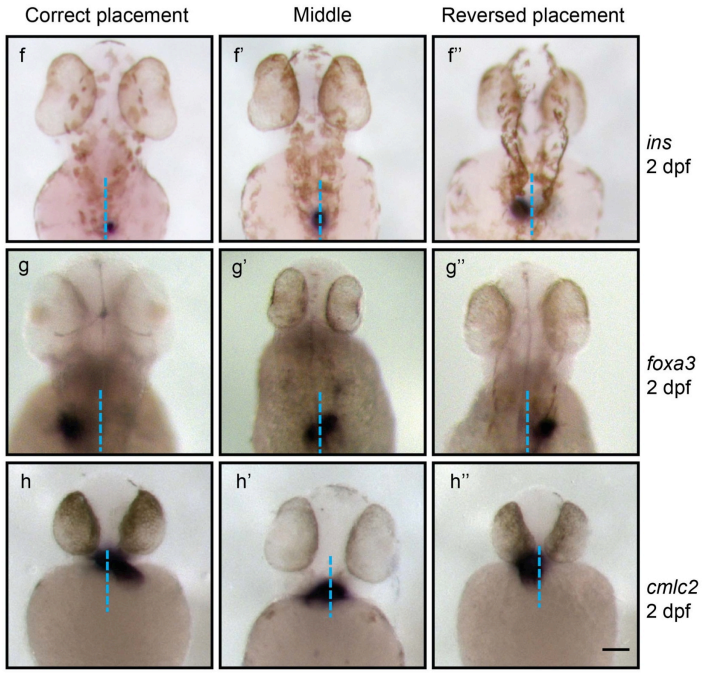

ins
2 dpf

foxa3
2 dpf

cmlc2
2 dpf

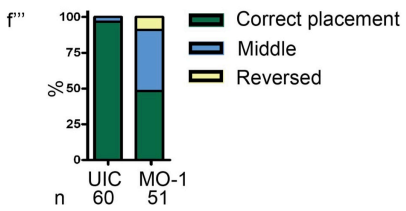

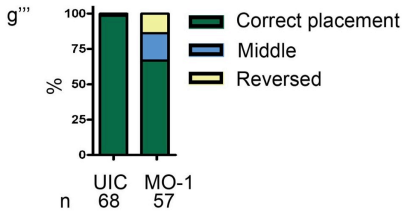

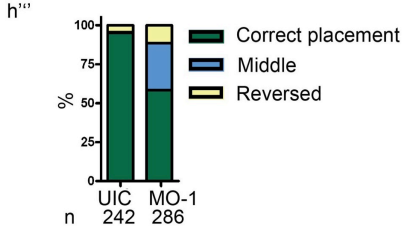

Figure 3-5. Reduction of *plac8.1* function resulted in generalized left-right asymmetry defects.

a-**d**. Dorsal view of the expression of *spw* using *in situ* hybridization. The percentage of each categories are plotted in **e**. **f**-**h'''**. Examination and quantitation of left-right asymmetrically placed organs: pancreas (**f**-**f'''**), liver (**g**-**g'''**), and heart (**h**-**h'''**). Scale bars: 50 microns.

Kupffer's vesicle cells express GFP, injected with MO1-*plac8.1* had similar numbers of Kupffer's vesicle cells compared to control embryos (Figure 3-6 e, f, g). To examine the cilia in the Kupffer's vesicle, immunofluorescence with an anti-acetylated-tubulin antibody and confocal microscopy were used. Compared with un-injected control embryos, *plac8.1* morphants had about half of the number of Kupffer's vesicle cilia (Figure 3-6 a-c). In addition, the cilia length was slightly, yet significantly reduced (Figure 3-6 d). These results indicate that ciliogenesis in the Kupffer's vesicle was affected without reducing Kupffer's vesicle cells. To test if the expression of motile ciliogenesis transcription factor *foxj1* was affected, we performed WISH with *foxj1* probe, and found no obvious defects in its expression (Figure 3-6 k, l). Therefore, reduction of *plac8.1* function affected formation of cilia in the Kupffer's vesicle, without significantly altering cell fates or transcriptional program.

To assess if the cilia-driven fluid flow in Kupffer's vesicle was normal, fluorescent microspheres were injected into the Kupffer's vesicle, and tracking experiments were performed (Essner et al., 2005). In uninjected control embryos, the beads showed robust counterclockwise rotation (Figure 3-6 h). In *plac8.1* morphants, however, the persistent flow was lost (Figure 3-6 I, quantification of the length of beads paths in j). In addition, to assess directly cilia beating, we used marker Arl13b (Borovina et al., 2010) to visualize cilia in the Kupffer's vesicle *in vivo*, and found that the cilia were almost motionless (data not shown). These results indicate that reduction of *plac8.1* function affects cilia formation and beating function in the Kupffer's vesicle, thereby affecting proper left-right asymmetry formation.

Interference with *plac8.1* expression impaired formation and function of cilia in the kidney ducts

Morphological characterization of kidney cilia in *plac8.1* morphants showed that kidney cilia formed but exhibited abnormal curled shape (Figure 3-7 b). Similar to the cilia in Kupffer's vesicle, average cilia number per 100 μm length of kidney duct was much reduced (Figure 3-7 d), whereas cilia length was slightly shorter compared to controls (Figure 3-7 e). To characterize these defects at ultrastructural level we employed transmission electron microscopy (TEM) analysis. TEM of transverse sections of kidney ducts at 1.5 dpf revealed that the ciliary membrane in the cilia of *plac8.1* morphants

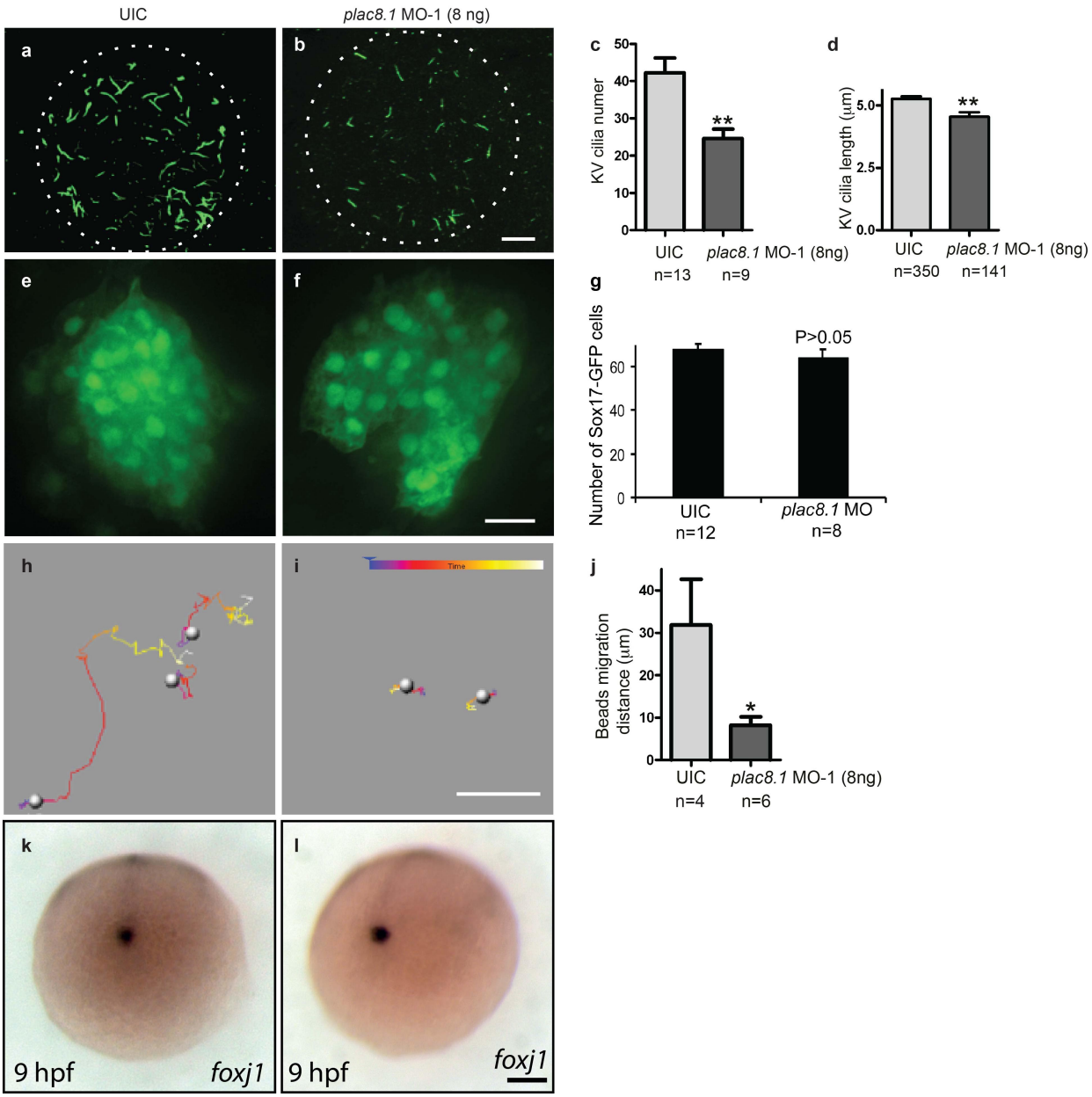

Figure 3-6. Reduction of *plac8.1* function impaired motile cilia morphology and motility in the Kupffer's vesicle.

a-**b.** Confocal micrograph of KV cilia in control embryos (**a**), and *plac8.1* morphants (**b**) shows reduced number of KV cilia in *plac8.1* morphants (quantitation in **c**). Dashed line denotes the boundary of KV. KV cilia length quantification is shown in **d**.

e-**g**. Examination of KV cells formation and shape in controls embryos (**e**) and *plac8.1* morphants (**f**). The numbers of KV cells are not significantly change (quantification in **g**).

h-**j**. Beads path tracking in the KV of control embryos (**h**), and *plac8.1* morphants (**i**) shows impaired node flow in *plac8.1* morphant (quantitation in **j**).

k-**i**. Expression of motile ciliogenesis transcription factor *foxj1* appeared normal as shown by the *in situ* hybridization.

Scale bars: 10 microns (**a-b, e-f, h**-**l**), 100 microns (**k**-**l**). ** denotes p<0.01, * denotes p<0.05.

detached from the 9+2 microtubule axonemes (Figure 3-7 g). In previously reported curled kidney cilia in the zebrafish injected with MOs targeting Cell cycle related kinase (Ccrk), similar membrane defects were also observed (Ko et al., 2010). In addition to the reduced number and abnormal morphology, the cilia in the kidney duct of *plac8.1* morphants were not as motile as those in control embryos (data not shown). Altogether, these data suggest defective morphogenesis and function of cilia in the kidney might underlie the kidney cyst formation and edema in *plac8.1* morphants (Figure 4 a'-b'). Thus, reduction of *plac8.1* function resulted in defects in both morphology and beating function of cilia in zebrafish embryo kidney ducts.

Reduction of *plac8.1* function did not affect Hh signaling

Hedgehog (Hh) signaling in mammals depends on primary cilia (Huangfu, et al., 2003; Eggenschwiler and Anderson, 2007; Goetz and Anderson, 2010). Key components of the mammalian Hedgehog (Hh) signaling pathways including the receptor Patched1, and Smoothened, in a Hh ligand dependent manner, dynamically localize at the primary cilium to mediate the Hh signal transduction cascade (Rohatgi et al., 2007). In embryos lacking cilia due to genetic inactivation of IFT component Ift88, or the IFT motor protein Kif3a, Hh signaling is defective (Murcia et al. 2000; Huangfu et al., 2003). In zebrafish, *sonic-you* (*syu*) mutations and other mutations that disrupt Hh signaling resulted in "U" shaped somites instead of chevron shaped somites typical of wild-type embryos, defects in the horizontal myoseptum, and the floor plate deficiency (Brand et al. 1996; van Eeden et al. 1996; Schauerte et al., 1998; Woods and Talbot, 2005). Similar to the mouse, zebrafish lacking cilia due to absence of both maternal and zygotic function of *ift88* gene showed dampened Hh signaling and defects including "U" shaped somites, indicating that in zebrafish cilia are also required to mediate Hh signaling cascade (Huang and Schier, 2009). My analyses of embryos injected with MO1-*plac8.1* with reduction of *plac8.1* function revealed that the somites were of the proper chevron shape with apparently normal horizontal myoseptum (Figure 3-8, a,b). In addition, immunofluorescence with anti-myosin heavy chain antibody that strongly stained slow muscle fiber of the horizontal myoseptum (Crow and Stockdale, 1986; Devoto et al., 1996) also showed that slow muscles formed normally (data not shown). Furthermore, the floor plate formed properly in embryos with reduced function of *plac8.1* (Figure 3-8, c d). These results suggest that

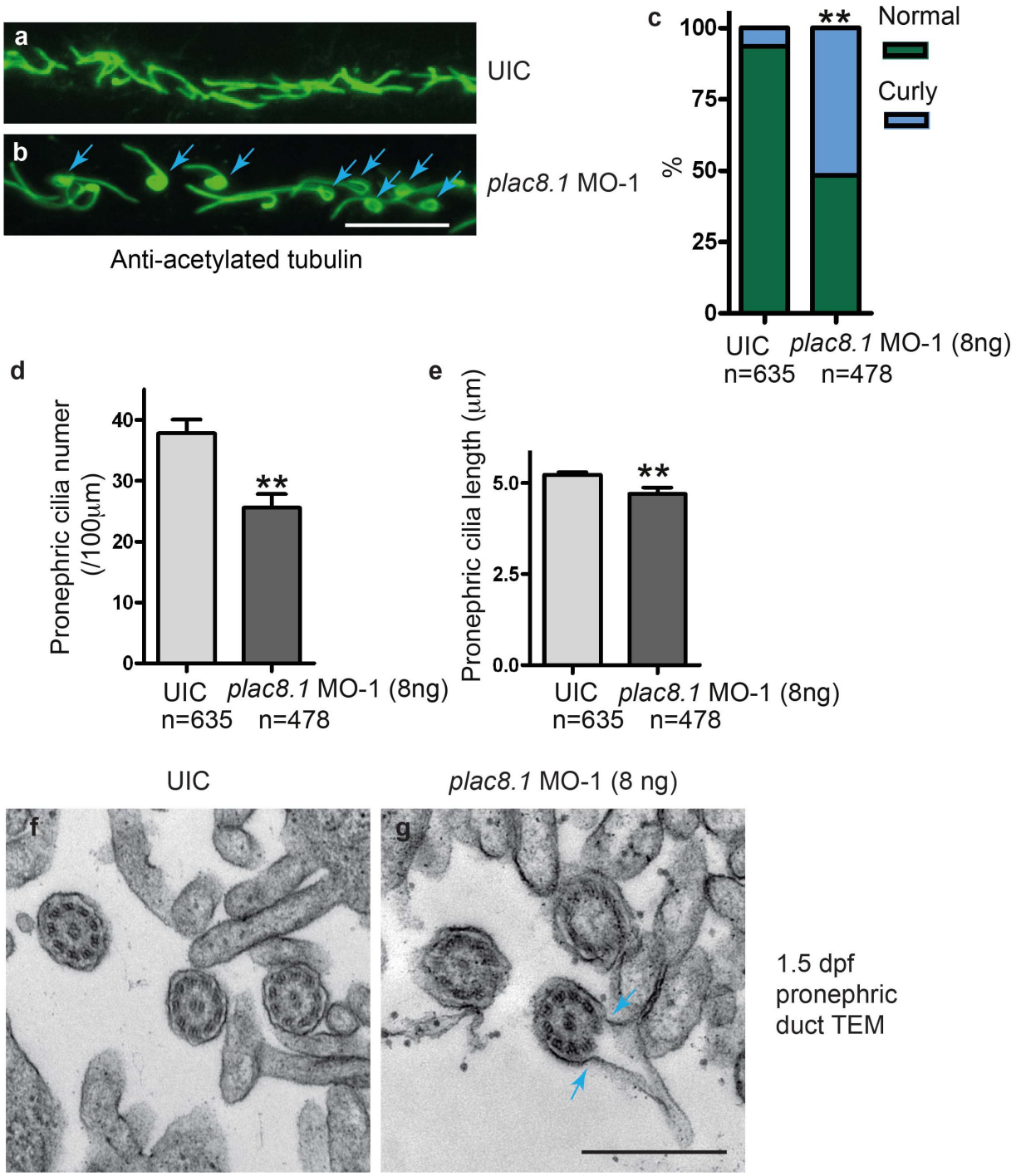

Figure 3-7. Reduction of *plac8.1* function impaired motile cilia morphology in the kidney duct. **a**-**b.** Confocal micrograph of pronephric cilia in 1.5 dpf control embryos (top panel), and *plac8.1* morphant (bottom panel). Arrows denote malformed and curled cilia in *plac8.1* morphants. **c**-**e**. Quantitation of the frequency of curly cilia (**c**), number of pronephric duct cilia over the length of 100 microns (**d**), and pronephric duct cilia length (**e**). **f**-**g**. Transverse section and transmission electron micrographs of control embryos (**f**), and *plac8.1* morphants (**g**). Arrows denote cilia membranes detached from the 9+2 microtubule structure. Scale bars: 10 microns (**a**-**b**), 500 nm (**c**-**d**), 50 microns (**d**-**d'**),

Hh signaling was not affected in this partial loss-of-function of *plac8.1* model, although it remains possible that complete loss of *plac8.1* function would result in Hh signaling defects.

Reduction of *plac8.1* function resulted in dampened cilia beating activity in the olfactory placode

In addition to test if Plac8.1 functioned in additional ciliated epithelia, we examined the olfactory placode of zebrafish embryos at 4 dpf. Zebrafish olfactory placode has motile cilia on the surface, and because of its accessibility, it is amenable to high-speed time-lapse imaging experiments (Panizzi et al., 2012). So we imaged the cilia of olfactory placode cells of zebrafish embryo where Plac8.1 is also highly expressed (Figure 3-10 d). The olfactory placode cilia in *plac8.1* morphants displayed reduced stroke amplitude compared to the controls (Figure 3-10 e). In addition, their beating frequency was dramatically reduced in the *plac8.1* morphants (Figure 3-10 f). These results, taken together with the Plac8.1 protein localization pattern in the cells with motile cilia, suggest loss-of-function of *plac8.1* specifically affect cilia morphogenesis and motility.

Plac8.1 interacted with Cops4 to regulate cilia formation and beating

To understand how Plac8.1 regulates cilia morphology and function, we examined potential Plac8.1 binding proteins. COP9 signalosome component Cops5 bound to Plac8,1 in zebrafish embryos (Chapter II, Figure 2-7). Since the gene expression pattern of *cops4* (a gene encoding another COP9 signalosome component) mirrors that of *plac8.1* (Figure 3-1) (Bradford et al., 2011), we started to test if Cops4 could interact with Plac8.1. Indeed, immunoprecipitation experiments with lysates from zebrafish embryo injected with 200 pg RNA encoding Plac8.1-EGFP showed that endogenous Cops4 was co-purified from the immunoprecipitation complex with anti-GFP antibody (Figure 3-10 a). These results suggested that Plac8.1 and Cops4 bound directly or they were in the same complex.

Composed of eight subunits (COPS1-COPS8), the COP9 signalosome is similar to the 19s lid complex of the proteasome (Wei et al., 1998; Serino et al., 1999). COP9 signalosome was initially studied in the process of *Arabidopsis thaliana* photomorphogenesis (seedling formation under light influence). COP9 signalosome has a metalloproteinase activity that removes Nedd8 modification of RING domain

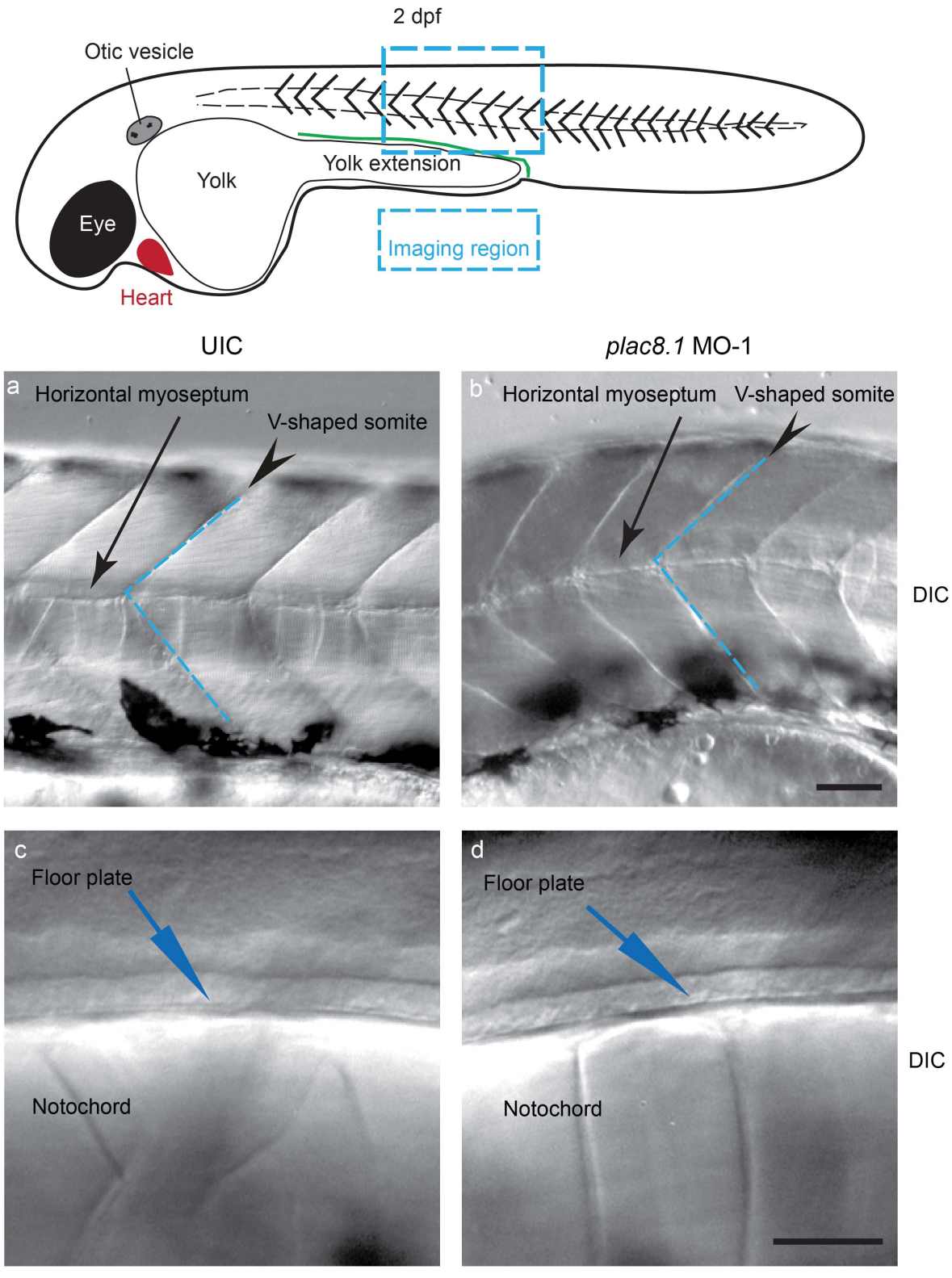
2 dpf
Otic vesicle
Yolk
Yolk extension
Eye
Imaging region
Heart
UIC
plac8.1 MO-1
a
Horizontal myoseptum
V-shaped somite
b
Horizontal myoseptum
V-shaped somite
DIC
c
Floor plate
Notochord
d
Floor plate
Notochord
DIC

Figure 3-8. No apparent Hedgehog signaling defects observed in *plac8.1* morphants.
Examination of processes depends on Hh signaing in control embryos (**a, c, e**) and *plac8.1* morphants (**b, d, f**). The “V”-shaped somites and horizontal myoseptum (**a**-**b**), floor plate formation (**c**-**d**) could not distinguish *plac8.1* morphants and control embryos.

containing E3 ubiquitin ligases, whereby modulating the stability of E3 ligase (Lyapina et al., 2001; Schwechheimer et al., 2001; Cope et al., 2002). With the capacity to remove Nedd modification (deneddylation), COP9 signalosome regulates the stability of a RING domain containing E3 ubiquitin ligase COP1 (Yi and Deng, 2005). COP1 is a master regulator of *Arabidopsis thaliana* photomorphogenesis by promoting degradation of photoreceptors and their downstream targets in dark, thereby acting as a negative regulator of seedling development in the absence of light (Yi and Deng, 2005).

Interestingly, *COP1* gene is conserved in higher plants and vertebrates. In mammalian cells, COP1 acts as an oncogenic E3 ubiquitin ligase to promote proteasome-dependent degradation of targets including tumor suppressor p53 (Dornan et al., 2004). Both overexpression and loss-of-function of *COP1* have been identified in human cancers (Marine, 2012). In addition to COP1, components of the COP9 signalosome have also been implicated in cancer. For example, the 5th subunit COPS5 promotes stability of E3 ubiquitin ligase MDM2, thereby promoting degradation of p53 (Zhang et al., 2008). Furthermore, COP9 signalosome also functions by interacting with ubiquitin ligases during DNA damage response (Hannss and Dubiel, 2011). COP9 signalosome can act either as an oncogene or as a tumor suppressor depending on their target proteins and the cellular context (Marine, 2010).

Although the COP9 signalosome components were thought to function through the function of the COP9 signalosome complex, accumulating data suggest that different components might have their specific functions, independent of the COP9 signalosome complex. For example, COPS3 promotes degradation of COP1 in mammalian cells (Yoneda-Kato et al., 2005), whereas COPS6 promotes COP1 stability (Choi et al., 2011). It is possible that the different results may originate from the distinct functions of COPS subunits in the COP9 signalosome.

Loss-of-function mutations of *COPS4* in *Arabidopsis thaliana* cause pleiotropic phenotypes including seedling development without light, and lethality shortly after seedling formation (Serino et al., 1999). However, the function of Cops4 in vertebrates has not been defined. To understand the function of *cops4* in zebrafish development, we performed loss-of-function study with MO-*cops4* that was effective in reducing Cops4 protein levels (Figure 3-9 c). In a dose dependent manner, injection of MO-*cops4* led to the ventrally curved body phenotype (Figure 3-9 a-b, and data not shown). Furthermore, similar to

plac8.1-deficient embryos, injection of MO-*cops4* resulted in a dose dependent randomization of the heart laterality (Figure e1-e3, quantification in e). Notably, in embryos with improper heart laterality, the liver was also often misplaced. Laterality defects of the heart could predict laterality defects of the liver with about 80% accuracy (Figure 3-9 f), suggesting that Cops4 deficient embryos had general left-right asymmetry disorder.

The curved body axes and left-right asymmetry phenotypes suggest that motile cilia may be defective in the embryos injected with *cops4* MO. Indeed, we observed similar cilia defects in the kidney ducts of *cops4* morphants (Figure 3-10 b middle panel). To examine if *cops4* is required for cilia motility, we used high-speed time-lapse imaging to record the cilia beating of the olfactory placode at 4 dpf. The olfactory placode cilia of *cops4* morphants beat with reduced stroke amplitude (Figure 3-10 f), and frequency compared to uninjected wild-type controls (Figure 3-10 f).

Since Plac8.1 bound to Cops4 in immunoprecipitation experiments (Figure 3-10 a), we tested if *plac8.1* and *cops4* showed functional interaction in regulating cilia morphology and activity by co-injecting low dose of MO that would result in low penetrance of phenotype when injected individually. Co-injection of MO1-*plac8.1* and MO-*cops4* resulted in much higher percentage of embryos showing ventrally curved axes than the additive effect of injecting each MO individually (Figure 3-9 d). Additionally, in the kidney ducts of embryos co-injected with low doses of MO1-*plac8.1* and MO-*cops4*, cilia were much shorter, and stretches of kidney tubes completely lacked cilia (Figure 3-10 b bottom panel). Furthermore, in embryos co-injected with low dose of *plac8.1* and *cops4* MOs, no cilia beat could be detected in the olfactory placode (Figure 3-10 f). These results support the notion that Plac8.1 and Cops4 cooperate to regulate cilia formation and beating activity, possibly by regulating ubiquitination modification and intraflagellar transport of ciliary proteins.

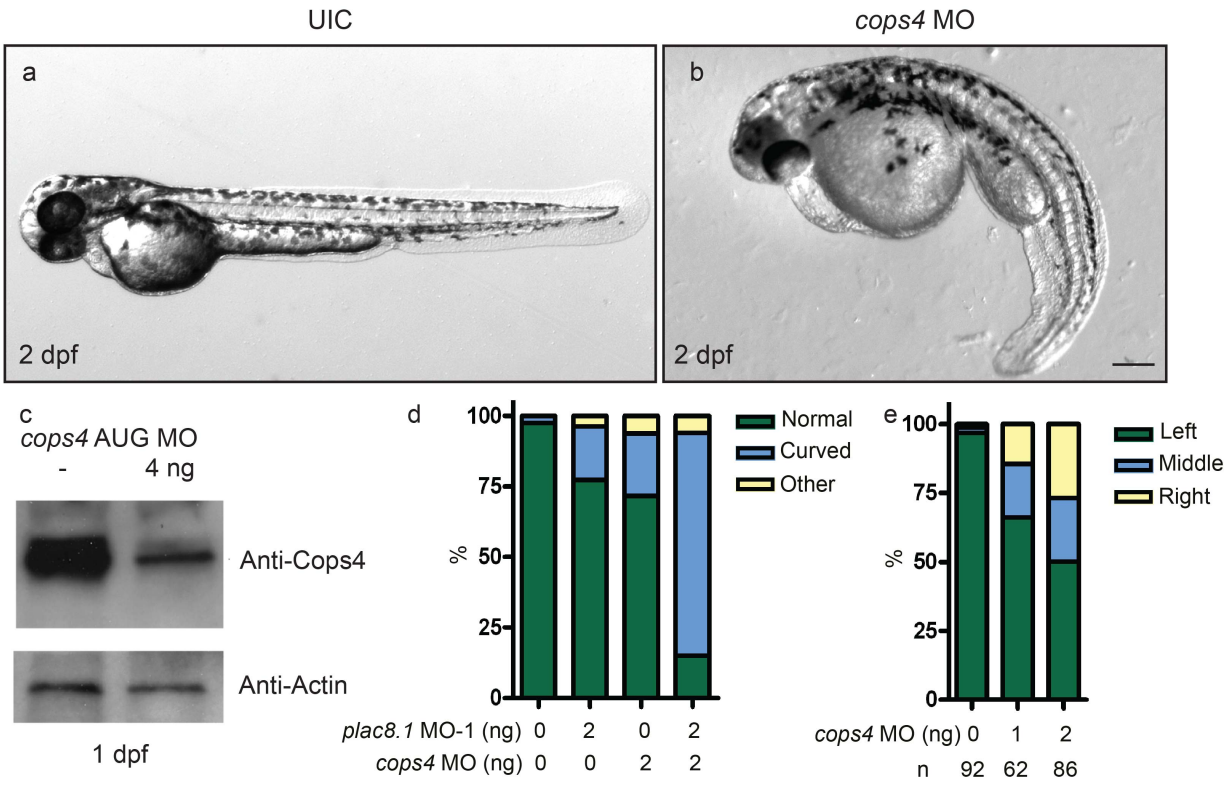

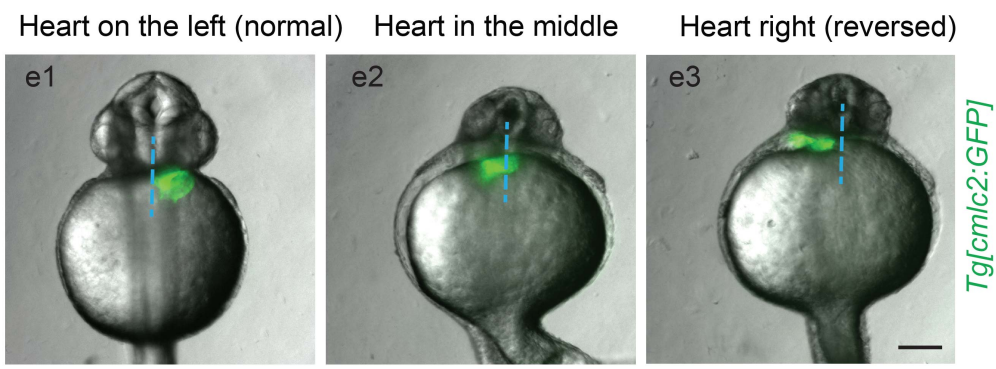

f

UIC

		Liver position	
		Correct	Misplaced
heart position	Correct	17	0
	Misplaced	0	0

Correct rate of using heart position to predict liver position: **100%**

cops4 morphant

		Liver position	
		Correct	Misplaced
heart position	Correct	27	6
	Misplaced	4	19

Correct rate of using heart position to predict liver position: **82%**

Red cells: heart position inconsistent with liver position

Figure 3-9. Reduction of *cops4* function showed similar phenotype to reduction of *plac8.1* function.
(**a, b, d**), Loss-of-function by *cops4* MO injection results embryos with ventrally curved body.
c. Western blotting showing that the *cops4* MO in reducing the protein level of Cops4.
e-e3. Loss-of-function by *cops4* results in heart laterality defects.
f. General organ laterality defects in *cops4* morphants as indicated by the high association rate of heart and liver (82%). Scale bars: 100 microns.

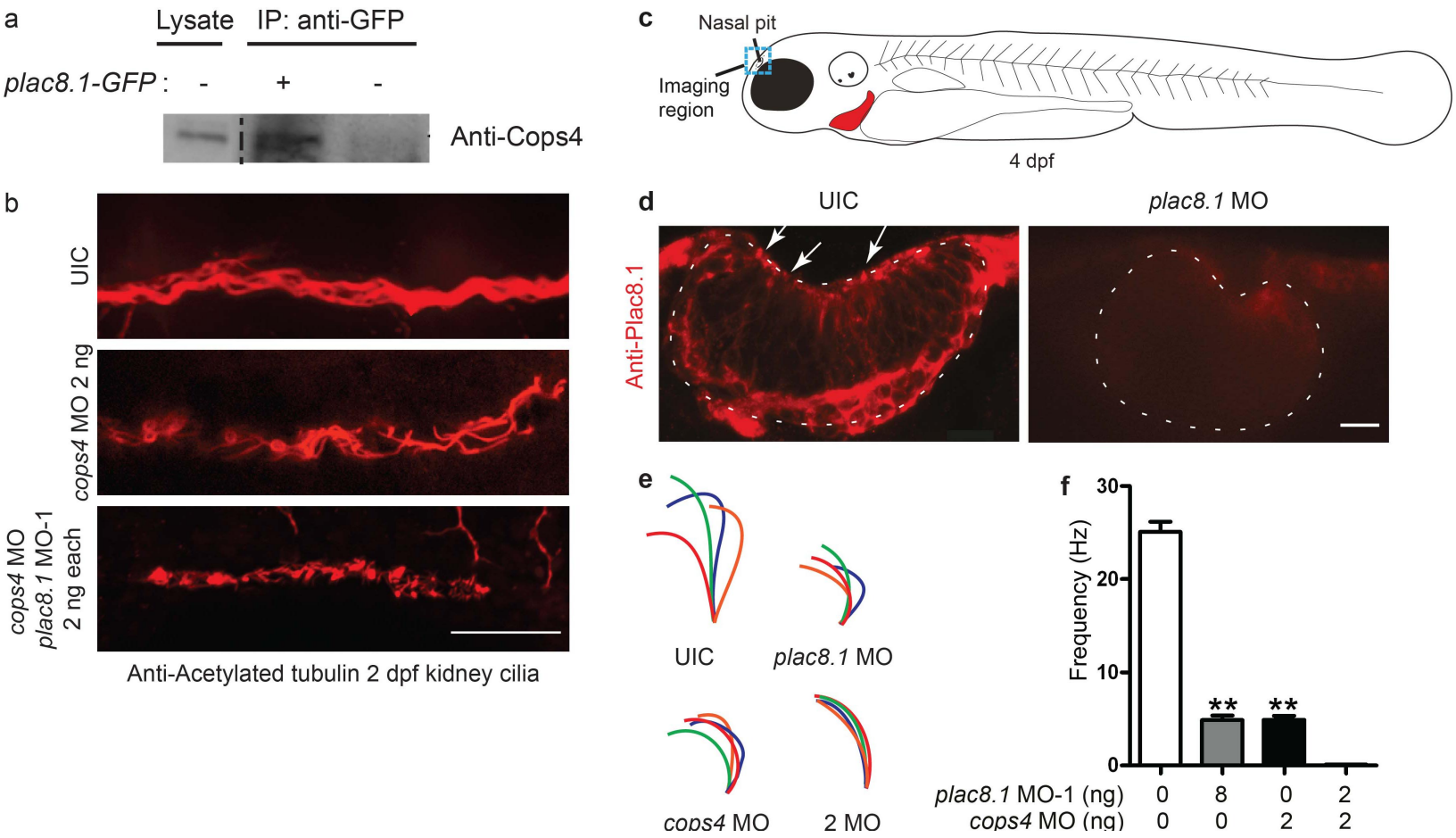

Figure 3-10, Plac8.1 bound and cooperated with Cops4 to regulate motile cilia morphology and motility.
a. Immunoprecipitation shows that Cops4 interact with Plac8.1-GFP protein.
b. Pronephric duct cilia morphology defects in *cops4* morphants, and functional interaction with loss-of-function of *plac8.1*.
c-d. Plac8.1 localizes to the base of cilia of nasal pit epithelium (cartoon illustration in **c**). Plac8.1 can be found at the apical surface of nasal pit cells of wild-type embryos (**d**, left panel), but not Plac8.1 deficient embryos (**d**, right panel). Nasal pits are outlined by the dashed line.
e-f. Lateral trace of nasal pit cilia beating waveform in control embryos, and embryos injected with *plac8.1* morpholino (8 ng), *cops4* MO (4 ng), or two morpholinos (2 ng each). Cilia beating frequencies are quantified in **f**.
Scale bars: 10 microns.

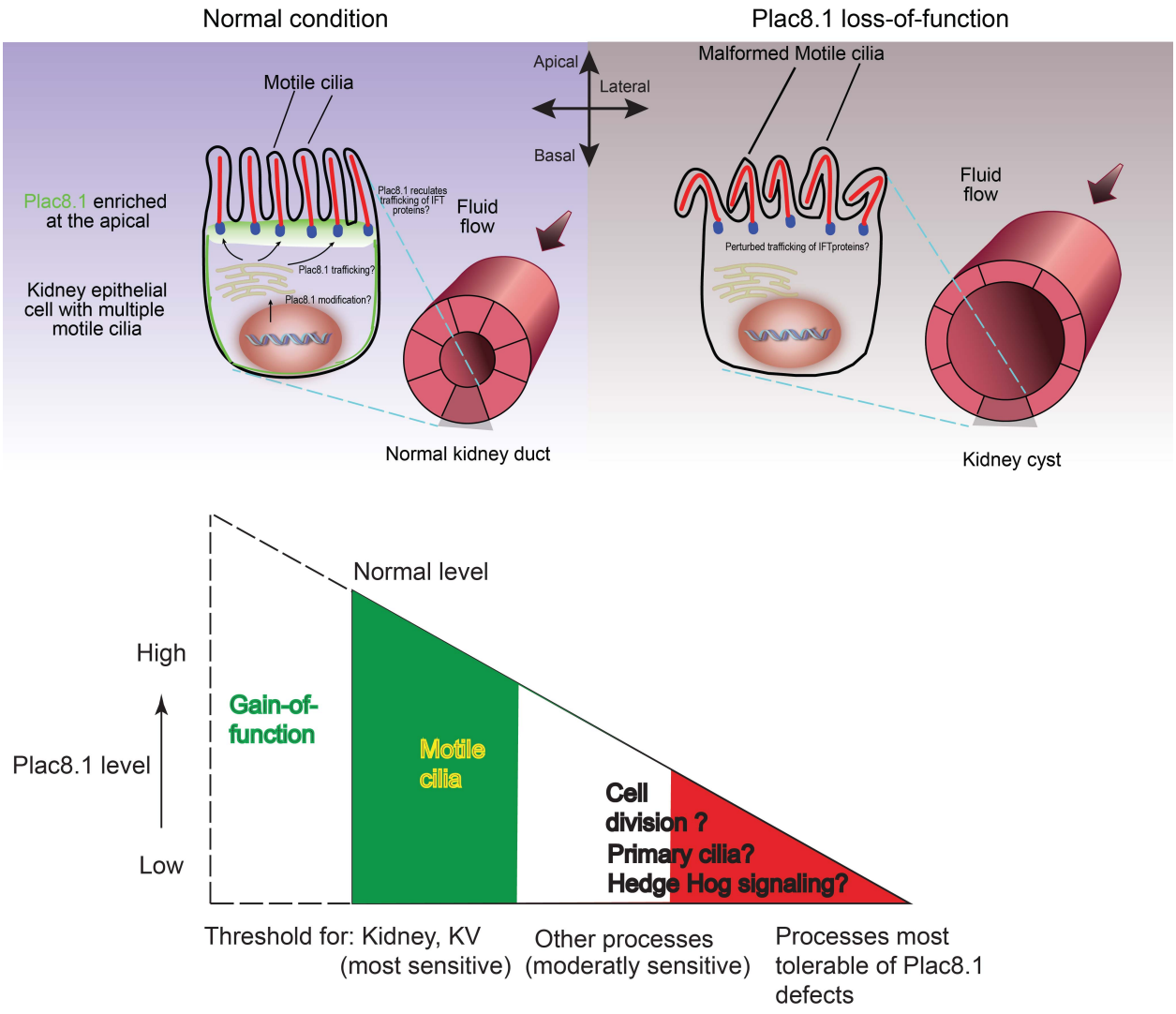

Figure 3-11. Summary of the reduction of *plac8.1* function study.
Top panel: a model of how Plac8.1 functions in motile cilia morphology and function. Bottom panel: a model to understand the pleiotropic effect of *plac8.1*.

Targeted disruption of *plac8.1* using transcription activator-like effector nucleases (TALENs)

To generate *plac8.1* mutant embryos, we used customized transcription activator-like effector nucleases (TALENs) that have been used to induce gene-specific mutations in zebrafish germline cells, thereby generating heritable mutations in target genes (Huang et al., 2011). TALENs are constructed by fusing the TAL effector DNA binding domain and FokI catalytic domain (Sanjana et al., 2012). Unlimited gene sequence specificities of customized TALEN are achieved by arranging the 34-amino acid DNA biding modules according to target sequences and a simple cipher (Boch et al., 2009; Moscou and Bogdanove, 2009). When introduced into cells, including zygotes, TALENs bind to their cognate sequences in target genes, enable dimer formation of FokI catalytic domains, and thus enable them to introduce double stand DNA breaks. The generated DNA breaks trigger DNA repair processes that may result in sequence changes, including insertions, deletions, or point mutations (Miller et al., 2011).

We designed a pair of TALENs to target the first exon of *plac8.1* (Figure 3-12, top panel). To optimize TALEN efficacy and specificity according to empirical guidelines (Miller et al., 2011), we designed the TALEN target to include an 18-nucleotide sequence and a 17-nucleotide sequence separated by a 16 nucleotides space (Figure 3-12, top panel). After injection of synthetic RNAs encoding the *plac8.1* TALEN pair, zebrafish founder embryos showed dose-dependent increase of mutations in the *plac8.1* gene, suggesting the *plac8.1* TALEN pair was effective in targeting the *plac8.1* gene (Figure 3-12, bottom panel).

To identify founder fish with germline transmission of *plac8.1* mutation, we screened 219 potential founder fish by crossing them with wild-type fish. For each potential founder fish, 20 or more offspring embryos were genotyped with *plac8.1* specific primer and BtsCI digestion. One founder fish was identified to give rise to germ line transmission (Figure 3-13 a). The rest embryos of the clutch were raised to adulthood as potential F1. To identify F1 fish carrying *plac8.1* mutation, parts of fin tissues were resected for the aforementioned genotyping method. The mutant sequences were cloned by PCR amplification and subcloning into pCR2.1 vectors for Sanger sequencing analysis. One allele *plac8.1*^{stl33} was identified with five-nucleotide insertion and four point mutations in the first exon (Figure 3-13 b-d). Based on the DNA sequence changes, the resultant Plac8.1 protein is predicted to be of 20 amino acid residues followed by two consecutive stop codons due to the frameshift mutation (Figure 3-13 e). Furthermore, Western

blotting analysis showed that Plac8.1 protein was barely detectable from lysates from *plac8.1*^{stl33} embryos (Figure 3-14 a). Taken together, these data suggest that the *plac8.1*^{stl33} allele is a strong loss-of-function allele, if not a complete loss-of-function allele.

Offspring of *plac8.1*$^{stl33/+}$ zebrafish incross showed normal morphology by 1 dpf. From 1-3 dpf, about a quarter of embryos (395/1489) displayed ventrally curved body axes, edema, and kidney cysts (Figure 3-14 b, and data not shown), a phenotype spectrum consistent with the loss-of-function phenotype of *plac8.1* morphants. Since *plac8.1* morphants showed motile cilia morphology and function defects, we focused on the Kupffer's vesicle and the olfactory placode, two tissues with motile cilia. Similar to *plac8.1* morphants, the number and length of motile cilia in the Kupffer's vesicle were significantly reduced compared to wild-type siblings (Figure 3-15 a-d). To assess cilia beating function, we introduced fluorescent beads to the olfactory placode, and recorded beads movements with time-lapse fluorescent microscopy. In wild-type siblings, the velocities of the fluorescent beads were the highest at the center of the olfactory placode center, and decreased from the center to the peripheral (Figure 3-15 e). In *plac8.1*^{stl33} mutants, the velocities were significantly reduced (Figure 3-15 f). Taken together, these results demonstrated the cilia morphology and beating function defects in zebrafish embryos with loss-of-function of *plac8.1*.

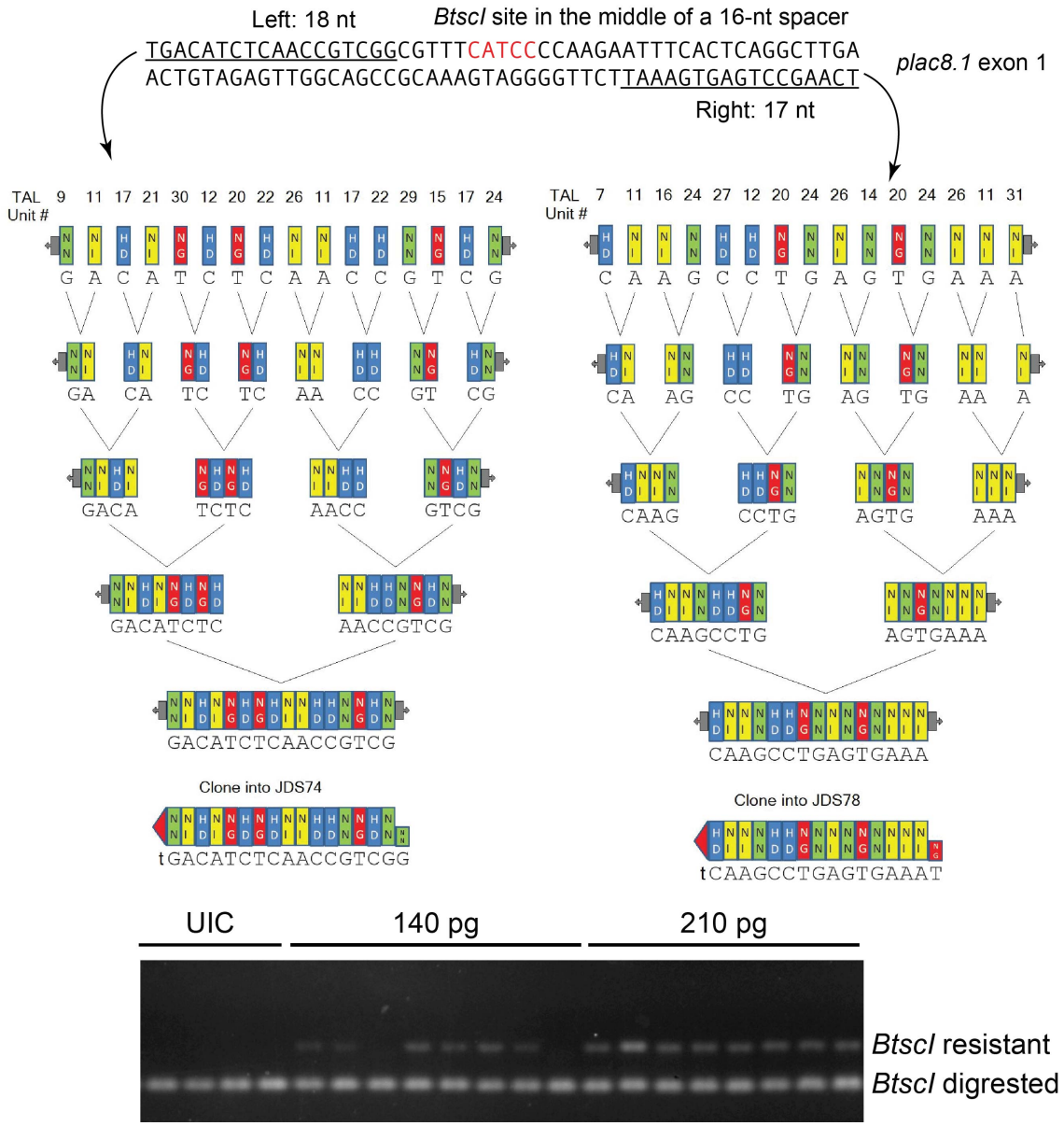

Figure 3-12. Generating and testing a pair of TALEN nucleases to target *plac8.1*.
Top panel: the design and assembly of *plac8.1* exon 1 targeting TALEN nucleases. The sequence recognized by the left arm and the right arm are underlined. The restriction enzyme *BtscI* recognition site is in red.
Bottom panel: detection of mutations in founder embryos injected with different amount of RNA encoding for the *plac8.1* TALEN pair. testing the efficacy of *plac8.1* exon 1 targeting TALEN nucleases.

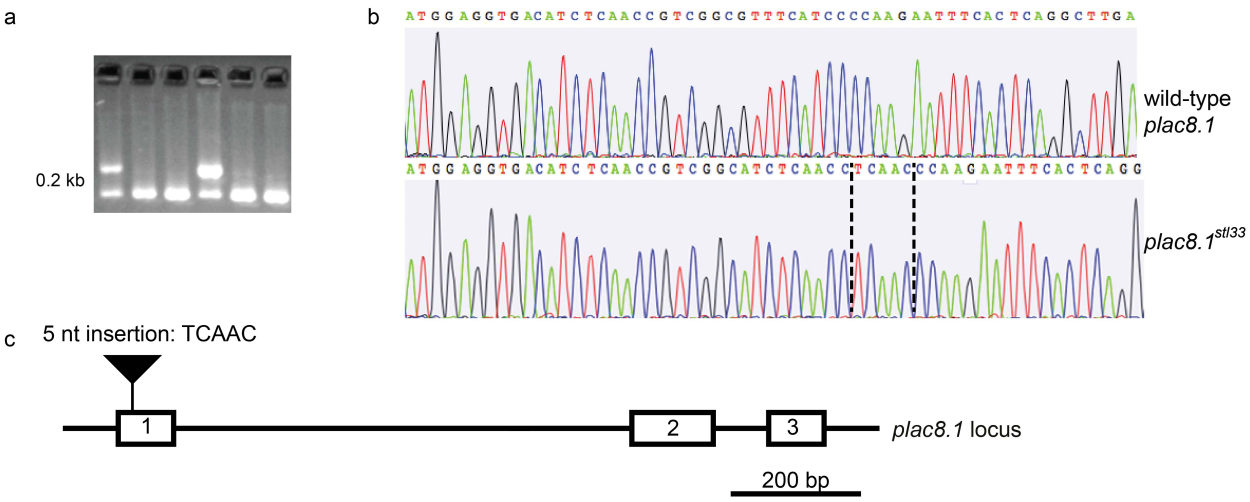

d

```
plac8.1     ATGGAGGTGACATCTCAACCGTCGGCGTTTCATCC-----CCAAGAATTTCACTCAGGCT 55
plac8.1stl33 ATGGAGGTGACATCTCAACCGTCGGCATCTCAACCTCAACCCAATAATTTCACTCAGGCT 60
             **************************.* ***:**     **** ***************
```

e

```
Plac8.1 (a.a. 1-20):
atggaggtgacatctcaaccgtcggcgtttcatccccaagaatttcactcaggcttgatg
 M  E  V  T  S  Q  P  S  A  F  H  P  Q  E  F  H  S  G  L  M
Plac8.1stl33:
atggaggtgacatctcaaccgtcggcatctcaacctcaaccaataatttcactcaggcttgatga
 M  E  V  T  S  Q  P  S  A  S  Q  P  Q  P  N  N  F  T  Q  A  -  -
```

Figure 3-13. TALEN-induced *plac8.1*^{stl33} mutant allele is a five-nucleotide insertion in *plac8.1* gene. a. An agarose gel showing separation of BtsCI digestion products of DNA fragments amplified by PCR from the genomic DNA of offspring embryos from a founder fish with *plac8.1* specific primers. The PCR amplicons from wild-type *plac8.1* gene are digested with BtsCI, whereas those from *plac8.1*^{stl33} mutant allele are not. b. Chromatograms of wide-type (top), and the mutant *plac8.1*^{stl33} (bottom) alleles indicating five-nucleotide insertion (dashed lines). c. A cartoon showing the position of the 5bp insertion (denoted by the triangle) on the gene structure of *plac8.1*. d. DNA sequence alignment of the wild-type *plac8.1* gene (top) and the mutant *plac8.1* gene (bottom). The dashed line marks the insertion, and three point mutations are marked in red. e. Amino acid sequences of the wild-type Plac8.1 protein (amino acid 1-20) and the peptide translated from the *plac8.1*^{stl33} allele (bottom). The altered nucleotides and amino acid residues are marked in red, the 5-nucleotide insertion is marked in green, and two consecutive premature stop codons are marked by "-".

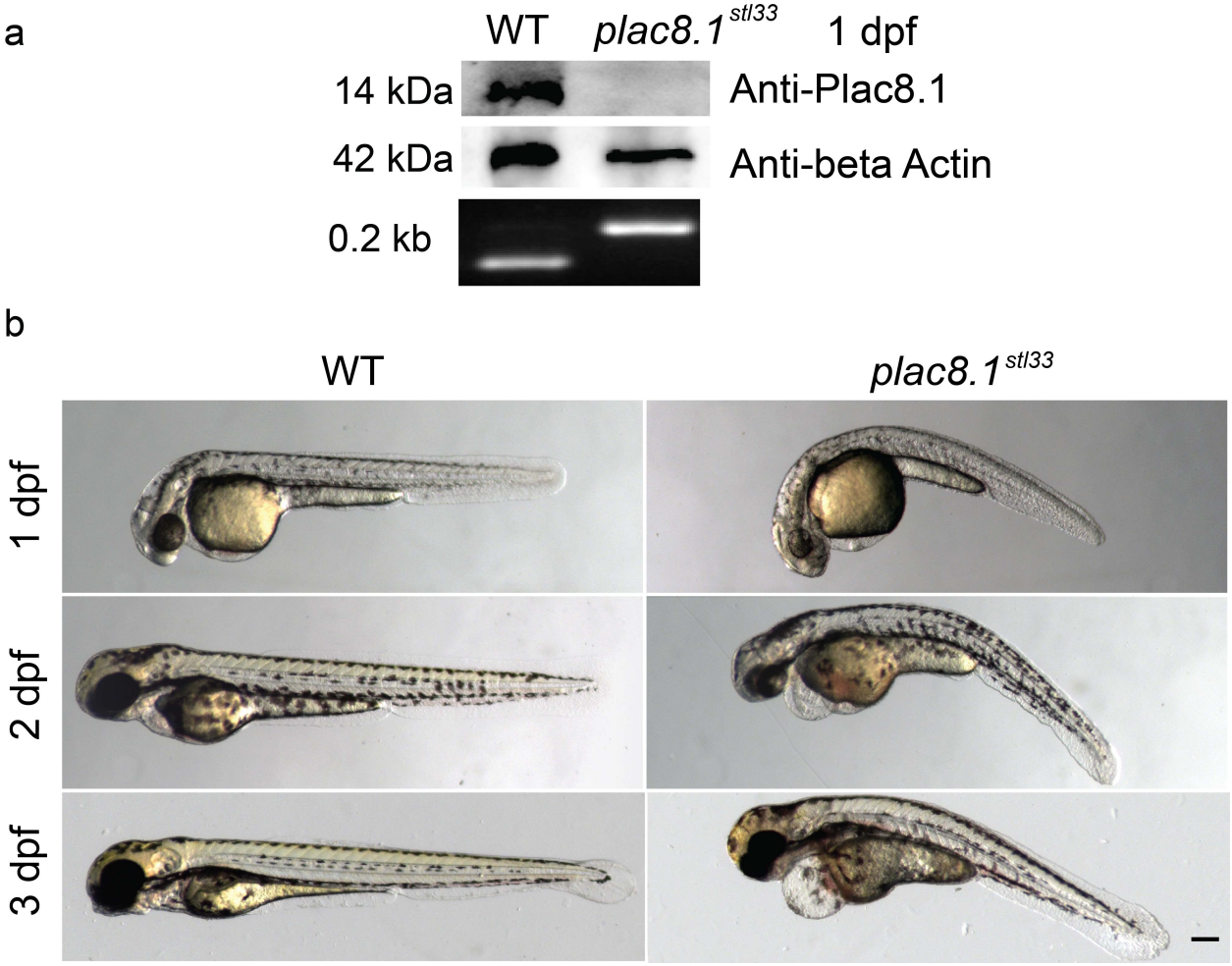

Figure 3-14. Characterization of *plac8.1*^{stl33} mutant embryos.
a. Western blotting analysis of Plac8.1 protein levels in wild-type embryos (left lanes) and *plac8.1*^{stl33} embryos (right lanes) at 1dpf. In plac8.1 mutant embryos, Plac8.1 protein level is barely detectable (top panel), whereas loading control Beta Actin shows similar levels to wild-type embryos (middle panel). Genotypes of the samples are confirmed by testing DNA from tail tissues dissected from embryos (bottom panel). b. Morphologic defects of *plac8.1*^{stl33} embryos (right panels) as compared to wild-type siblings (left panels). Scale bar: 100 μm.

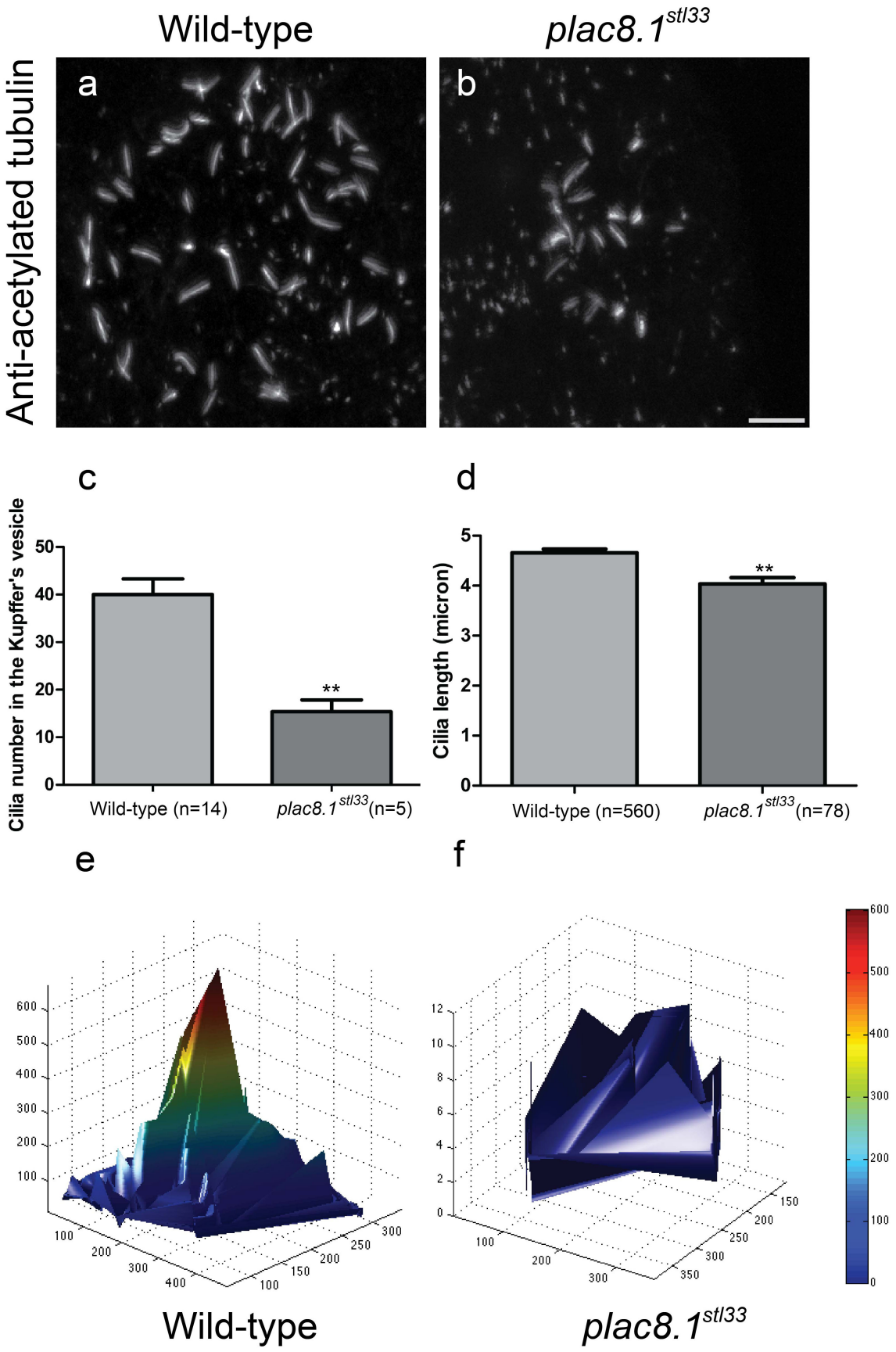
Wild-type
plac8.1stl33
Anti-acetylated tubulin
a
b
c
d
Cilia number in the Kupffer's vesicle
Wild-type (n=14)
plac8.1stl33(n=5)
Cilia length (micron)
Wild-type (n=560)
plac8.1stl33(n=78)
**
e
f
Wild-type
plac8.1stl33

Figure 3-15. Cilia morphology and function defects in *plac8.1*^{stl33} embryos
a-b. Confocal micrographs of the cilia in the Kupffer's vesicle in *plac8.1*^{stl33} embryos (b) compared to wild-type embryos (a). c. Quantification of the number of cilia in the Kupffer's vesicle. d. Comparison of Kupffer's vesicle cilia length in wild-type and *plac8.1*^{stl33} mutant. ** denotes $p<0.01$, Student's t-test. e-f. Representative heat maps of fluid movement speed (Z axis, and color coded) plotted over the surface of olfactory placode (X-Y axes) to quantify of fluid dynamics generated by motile cilia of the olfactory placode in wild-type embryos (e) and *plac8.1*^{stl33} embryos (f).

DISCUSSION

The function of zebrafish Plac8.1, an orthologous protein of human PLAC8, has been evaluated by reduction of function experiments in the zebrafish embryogenesis. In wild-type embryos, Plac8.1 protein was enriched to the apical domain of ciliated epithelial cells, and overlapping with the base of the cilium. Embryos injected with MOs targeting *plac8.1* translation or splicing, and *plac8.1*^{stl33} embryos exhibited strongly reduced Plac8.1 protein level, with an array of phenotypes often resulting from defective cilia. Indeed, Plac8.1-deficient embryos displayed decreased number and shorter cilia, impaired cilia beating, indicating *plac8.1* is required for cilia morphogenesis, beating activity, and function. Mechanistically, we identified Cops4 as a likely link between Plac8.1, cilia and COP9 signalosome. First, Plac8.1 interacted biochemically with Cops4, and reduction of Cops4 expression exacerbated defects of Plac8.1-deficient embryos in cilia formation and function. Since Cops4 is a component of the COP9 signalosome that regulates E3 ubiquitin ligases activities, we propose a molecular mechanism for Plac8.1 function whereby Plac8.1 modulates COP9 signalosome, thereby modulating ubiquitination and intraflagellar transport of ciliary proteins crucial for cilia formation and function.

In this study, MOs-mediated gene interference, and *plac8.1*-directed mutagenesis by TALENs were used as loss-of-function approaches. The rescue experiments by MO-insensitive RNA and immunofluorescence and confocal microscopy to monitor the Plac8.1 level in the Kupffer's vesicle, kidney duct and olfactory placode, and similar phenotypes between the morphants and *plac8.1*^{stl33} mutants strongly suggest Plac8.1 is required in cilia formation and function in these ciliated tissues.

With maternal load of *plac8.1* RNA and Plac8.1 protein, both morphants and *plac8.1*^{stl33} mutants may represent a hypomorphic model. Despite the limitation of the hypomorphic condition, this study of hypomorhic model of *plac8.1* provided valuable insights into the function of Plac8.1 in the Kupffer's vesicle, kidney duct, and the olfactory placode. If amorphic condition of *plac8.1* leads to early lethality, analysis of relatively late phenotype would be challenging to perform.

Localization of Plac8.1 protein

Endogenous Plac8.1 protein is enriched at the apical region of polarized epithelial cells in the kidney ducts (Figure 3-2, 3-4), and in the intestine (Figure 2-3). It is possible that post-translation modification and/or protein-protein interaction are responsible for its localization pattern. Plac8.1 protein may be modified in the Golgi, loaded in vesicles and directed targeted to the apical region. Alternatively, Plac8.1 bind to proteins localized to the apical domain, or apical proteins stabilize Plac8.1.

No evidence of altered cell fates upon reduction of *plac8.1* function

Previous studies in preadipocyte cell lines showed that mouse Plac8 is required for brown adipose tissue differentiation through the capacity of Plac8 to induce CCAAT/Enhancer Binding Proteins β (Jimenez-Preitner et al., 2011). In addition, zebrafish *ponzr1*, a gene encoding Plac8 onzin related protein 1 (Ponzr1) that shares about 30% amino acid sequence identity to Plac8.1, is required for proper expression of *pax2a* in developing kidney and normal kidney function (Bedell et al., 2012a). These results suggest that Plac8 and related proteins might be required for proper cell fate specification. To test if the various defects described here in Plac8.1-deficient embryos could be due to altered cell fates, we examined the Kupffer's vesicle and the kidney ducts, two regions showing cilia defects. WISH analyses showed no obvious difference in the expression of *foxj1*, a master regulator of motile ciliogenesis in zebrafish (Yu et al., 2008; Stubbs et al., 2008). Furthermore, embryos with reduced Plac8.1 expression showed comparable number of Kupffer's vesicle cells to control embryos as observed using *Tg[sox17:GFP]* transgenic line, indicating proper expression of *sox17*. In the kidney ducts, expression of *pax2a* in Plac8.1-deficient embryos was similar to control embryos. These results suggest that cell fate alternation was less likely to be responsible for the Kupffer's vesicle or the kidney phenotypes in embryos with reduced function of *plac8.1*. Moreover, Plac8.1 may have functions distinct from Ponzr1. An N-terminal EBFP tagged mouse Plac8 was shown to localize to the nucleus when overexpressed in Cos7 cells (Rogulski et al., 2005). However, we could not observe localization of endogenous Plac8.1 in the nucleus, arguing against the possibility the Plac8.1 act directly in the nucleus to modulate cell fate specification. Whether complete loss of *plac8.1* function changes cell fates remains an open question.

Comparison between functions of zebrafish *plac8.1* and mouse *Plac8*

Zebrafish embryos with reduction of *plac8.1* function showed normal morphology by 1 dpf. However, they developed kidney cysts and edema at later stage, and could not survive to adulthood. Therefore, zebrafish *plac8.1* is essential for zebrafish embryogenesis. By contrast, *Plac8* knockout mice display impaired innate immunity and defects in brown adipose tissue formation without showing any developmental abnormalities (Ledford et al., 2007; Jimenez-Preitner et al., 2011). This difference can be accounted for by multiple possibilities. First, it is possible that mouse *Plac8* mediates functions that are completely different from those of zebrafish *plac8.1*. Second, given the role of intraflagellar transport in immune synapse, it is possible that, the immunity defects in *Plac8* knockout mice and cilia defects in zebrafish *plac8.1* morphants embryos, both reflect a conserved molecular function in intraflagellar transport (Finetti et al, 2009; Finetti et al., 2011). Third, the reported *Plac8*$^{-/-}$ mouse allele could not completely rule out the possibility that mouse Plac8 is required for development. For instance, strain backgrounds may affect the expressivities of phenotypes in mice (Hosking et al., 2009).

Possible function of Plac8.1 in ciliogenesis and cilia beating

One of the first lines of genetic evidence showing a wide spectrum of seeming unrelated disorders spanning several organ systems can be traceable to mutations that lead to structurally altered cilium comes from the *Ift88*^{Tg737} mouse, also know as the Oak Ridge Polycystic Kidney (ORPK) mouse (Moyer et al., 1994). IFT88 is a component of the intraflagella trafficking (IFT) complex B that is essential for cilia formation. In addition to *Ift88*, researches in the last two decades have revealed that mutations in a series of genes that normally function for cilia or basal body are responsible for a growing number of disorders collectively refereed as ciliopathy (Hildebrandt et al., 2011). Among the most common phenotypes of ciliopathies are left-right asymmetry defects, and kidney cysts. Reduction of *plac8.1* function by MO targeting resulted in pleiotropic developmental abnormality ascribable to defective cilia. Indeed, both cilia formation and function were impaired upon reduction of *plac8.1* function. Consistent with the apical localization of basal body and motile cilia, Plac8.1 protein is enriched on the apical domain of tissues of motile cilia including the Kupffer's vesicle and the kidney ducts, and also on the apical domain of other ciliated cells including the cells of the olfactory placode. The reduction of *plac8.1* function

data, and Plac8.1 protein localization pattern are consistent with the notion that Plac8.1 is essential for cilia formation and function. However, the exact molecular mechanism of how Plac8.1 acts in ciliogenesis and cilia function remains to be elucidated.

Extensive studies have demonstrated that both basal body docking and intraflagellar transport are required for ciliogenesis. Ciliogenesis is initiated by the formation of basal bodies through docking the mother centriole onto the apical membranes (Ishikawa and Marshall, 2011). Basal bodies function as templates for axoneme, regulating orientation of cilia, and are strictly required for formation of cilia (Dutcher, 2003; Marshall, 2008). For example, loss-of-function of *inturned* in multiciliated cells in *Xenopus* impaired GTPase Rho-mediated apical actin assembly and basal body docking, resulted in ciliogenesis defects (Park et al., 2008). Because the centrioles are also involved in the organization of mitotic spindle poles during mitosis and cytokinesis, formation of cilia or ciliogenesis often anti-correlates with cell division. In quiescent polarized epithelia, centrioles dock to the apical membrane to form basal bodies. When cells undergo mitosis, cilia retract and centrioles duplicate in synchrony with the genome, and then function as centrosomes which nucleate the formation of the mitotic spindle (Nigg and Raff, 2009). Thus centrosomes are critical for both cell cycle progression and cilia formation. Kif24 has been shown to regulate the transition between basal body and centriole in accordance with cell cycle (Kobayashi et al. 2011). In addition, loss-of-function of cell cycle related protein including Cdc14b (Clement et al., 2011), cell cycle related kinase Ccrk (Ko et al., 2009) are linked to cilia defects, although whether their function in cilia is dependent of their function in cell cycle remains to be further determined. Because the curve cilia, and membrane detachment phenotypes in *plac8.1* morphants are similar to the phenotype in *ccrk* morphant, we tested if the protein levels of Ccrk in wild-type zebrafish embryos and *plac8.1* morphants. However, the anti-Ccrk antibody was not working in zebrafish (data not shown). Additionally, we do not have conclusive evidence of basal body docking defects in *plac8.1* morphants with transmission electron microscopy analyses (data not shown).

The detachment of ciliary membrane and axoneme in *plac8.1* morphants might be caused by IFT defects (Hou et al., 2004; Qin et al., 2001; Tran et al., 2008). GFP tagged ciliary protein Arl13b (Borovina et al., 2009) localization in cilia seemed normal in *plac8.1* morphants (data not show). However, a systemic survey of ciliary protein is needed to test location of other proteins selectively localized to ciliary.

In zebraish, the homodimeric Ccdc103 protein functions as an adaptor to bind to Dynin arms, and the mutation of *ccdc103* led to dynine arm defects and cilia motility defects (Panizzi et al., 2012). In *plac8.1* loss-of-function, Dynin arms in the kidney cilia seemed intact. However, it is possible MO might lead to mosaicism, or the phenotype may have different expressivity. Therefore, Dynin defects remain a possible reason for defective motility in *plac8.1* morphants.

In zebrafish, defective FGF signaling affects cilia function (Neugebauer et al., 2009). However, FGF signaling controls cilia length, not number (Neugebauer et al., 2009). In addition, the expression of FGF signaling target *pax2a* appeared normal in *plac8.1* morphants, suggesting FGF singnaling might be intact in loss-of-function of *plac8.1*.

Plac8.1 and signaling events connected with cilia

Cilia have emerged as a key signaling center to mediate the Hh pathway in vertebrates including zebrafish (Huangfu et al., 2003; Eggenschwiler and Anderson, 2007; Huang and Schier, 2009; Goetz and Anderson, 2010). In Plac8.1-deficient embryos, we could not obtain evidence of altered Hh signaling (Figure 3-8). This is consistent with many zygotic mutants with defective cilia genes that exhibit no signs of Hh signaling defects. For example, *ift57* and *ift172* mutants show cilia defects without Hh defects (Lunt et al., 2009). It is possible that maternal Plac8.1 protein is sufficient to mediate Hh signaling, thereby uncoupling zygotic cilia defects and Hh phenotype.

In contrast to the close association between cilia and Hh signaling, the connections between cilia and Wnt/PCP, and between cilia and Wnt/β-catenin pathway are subtle, and seem to be highly context dependent (Wallingford and Mitchell, 2010). Both the core PCP components and PCP effectors are shown to play a role in ciliogenesis, however, whether their role in basal body docking and cilia formation presents the PCP pathway in general, or multiple functions of Dvl and Prickle remains to be determined (Park et al., 2008; Gray et al., 2009; Wallingford and Mitchell, 2011). Also kinocilia defects caused by conditional mutation of *Ift88* in the cochlea also disrupt the organization of actin-based stereocilia, a typical phenotype for PCP mutants, suggesting a role of kinocilia in PCP in the cochlea (Jones et al., 2008). For the connection between cilia and Wnt/β-catenin pathway, the first piece of evidence comes from ciliopathy protein Inversin (Inv, or Nephrocystin2). When cotransfected, Inv abrogate the function of

Dvl, to activate a Wnt/β-catenin response report construct, indicating that cilia might function by dampening Wnt/β-catenin pathway, rather than potentiating it like for Hh signaling (Huangfu, et al., 2003; Simons et al., 2005; Eggenschwiler and Anderson, 2007). In zebrafish, loss-of-function of *seahorse* leads to defective cilia function and elevated Wnt/β-catenin signaling (Kishimoto et al., 2008). Furthermore, *seahorse* is required for proper convergence and extension gastrulation movements that are governed by the Wnt/PCP pathway (Jessen et al., 2002; Roszko et al., 2009; Topczewski et al., 2001). Different from *seahorse* mutant, *plac8.1* morphants showed normal morphology before showing ventrally curved body axis, arguing against the role of *plac8.1* in the Wnt/β-catenin signaling that function in embryo patterning, or the Wnt/PCP pathway that regulates convergence and extension movements. However, it is possible that maternal Plac8.1 proteins compensate for the function needed during early developmental stages.

Cops4 implicated ubiquitination pathway in ciliogenesis and function

Dynamic and tightly regulated ciliary localization of various receptor and signal transducers are essential for cilia to function as a tunable antenna to receive and process diverse extracellular signals (Wallingford and Mitchell, 2010). Despite the extensive studies of cilia and gatekeeping mechanisms, how ciliary proteins are regulated to cooperate with the gatekeeping mechanisms is largely unknown. It has been proposed that selective modification of ciliary protein via phosphorylation or ubiquitination may provide an instructive signal for dynamic localization either for cilia entry or for cilia exit (Nachury et al., 2010). In addition, ubiquitination modification is involved in cilia disassembly in the green algae *Chlamydomonas reinhardtii* (Huang et al., 2009).

Plac8.1 bound to ubiqutination regulating protein Cops4, a component of the COP9 signalosome that regulates protein ubiquitination through regulating Nedd8 cleaving from E3 ubiquitin ligases (Lyapina et al., 2001; Schwechheimer et al., 2001; Cope et al., 2002). Furthermore, plac8.1 and cops4 showed functional interaction in regulating cilia formation and function (Figure 3-9, 3-10). These results suggest that improper ubiquitination modification might affect cilia formation and function. It is possible that the ubiquitination of ciliary proteins in the cytosol could serve as a signal to direct modified proteins to cilia. Alternatively, it is also possible that Cops4 is protein of multiple functions, and its involvement in cilia

formation may not necessarily suggest the connection between ubiquitination and cilia formation. This study provides an entry point to studying the functions of Plac8.1 and Cops4 in zebrafish development, and to investigating the possible connections between protein modification such as ubiquitination and cilia formation in zebrafish.

Plac8.1 and left-right asymmetry formation

The left-right asymmetry in vertebrates is established by left-right asymmetry in gene activity during the process of embryogenesis. The posteriorly tilted motile cilia in the node of mouse, or in the Kupffer's vesicle of zebrafish embryo, generate right-to-left flow that results in activation of the Nodal ligand gene expression on the left side of lateral plate mesoderm and formation of left-right asymmetry (Nonaka et al., 1998; Essner, et al., 2002; Essner et al., 2005; Kramer-Zucker et al., 2005; Hirokawa et al., 2009, Wallingford, 2010). Left-right laterality defects can be caused by mutations that resulted in defects ciliogenesis (Clement et al., 2011), compromised cilia beating (Panizzi et al., 2012), or impaired positioning of cilia (Borovina et al., 2009; Song et al., 2010). In addition, Notch activity regulates left-right asymmetry by inducing *Nodal* expression, and is independent of cilia formation or function in zebrafish, chick, and mouse (Krebs et al., 2003; Raya et al., 2003).

In zebrafish embryos with reduction of *plac8.1* function, the number of motile cilia was significantly reduced, and the beating of cilia was dampened (ciliary dyskinesia). Consistently, the nodal flow and left-biased expression of Nodal ligand were compromised. Therefore, the deficiencies in ciliogenesis and cilia motility are likely contributing factors to the left-right asymmetry defects. Furthermore, increased Notch activity in zebrafish leads to left-right asymmetry defects (Raya et al., 2003). In addition, Notch signaling acts as an upstream positive regulator of PLAC8 transcription in T cell acute lymphoblastic leukemia cells (Riz et al., 2010). In turn, whether reduction of *plac8.1* function alters Notch activity remains to be tested.

Plac8.1 and kidney cysts formation

A previous forward genetic screen has demonstrated that mutations in genes that normally function in cilia often result in cystic kidney in zebrafish (Sun et al., 2004). The results of loss-of-function

of *plac8.1* studies are consistent with this notion. Plac8.1 deficient embryos exhibited cystic kidney formation, ciliogenesis defects, and ciliary dyskinesia. Furthermore, endogenous Plac8.1 appeared to associate closely with the base of cilia in multiple ciliated epithelia, suggesting that Plac8.1 may contribute to cilia formation and function.

Not all zebrafish with kidney cysts manifest cilia defects. For example, in zebrafish embryos with loss-of-function of *arhgef11* (encoding a RhoGEF) manifested kidney cysts without obvious cilia formation or motility defects. Instead, the polarized distribution of F-actin was affected (Panizzi et al., 2007). In the kidney ducts of Plac8.1 deficient embryos, apical F-actin was comparable to control embryos, suggesting apical-basal polarity of kidney duct epithelial cells were not grossly affected.

Furthermore, zebrafish mutant *cup*$^{tc321/tc321}$ showed kidney cysts without cilia defects (Schottenfeld et al., 2007). The *cup*$^{tc321/tc321}$ is a null allele of the zebrafish *pkd2*, a gene encoding for a cation channel Polycystin2 that localizes to cilia. Loss-of-function mutations in the human ortholog of *pkd2* account for about 15% of late onset polycystic kidney disease that exhibit autosomal dominant segregation within affected families, however, somatic inactivation of the wild-type allele are speculated be the driving force of kidney cysts formation (Mochizuki et al., 1996; Wu et al., 1997; Wu et al., 2000; Hildebrandt et al., 2011). Similar to Plac8.1, Zebrafish Pkd2 protein localized to cell membranes of kidney duct cells, and various sensory cells including the mechanosensory cells of the lateral line, and cells of the olfactory placodes (Obara, 2006). However, one striking difference between *pkd2* mutant embryos and Plac8.1 deficient embryos is that *pkd2* mutants showed dorsally curved body axes, instead of ventrally curved body axes in *plac8.1* morphants (Schottenfeld et al., 2007). Injection of *plac8.1* morphant into *pkd2* mutant embryos seemed to reduce dorsal curvature (data not shown). These lines of information indicate that *plac8.1* loss-of-function are unlikely to cause kidney cyst directly through *pkd2* loss-of-function. Still, it may be informative to test if ciliary localization of Pkd2 is affected in Plac8.1 deficient embryos.

In addition to Polycystin proteins and other ciliary proteins, Notch signaling is implicated in kidney development. Furthermore, Notch signaling suppresses cyst formation by organizing oriented cell division, thereby maintaining the monolayer epithelial structure while the tissue proliferates (Verdeguer et al., 2009; Surendran et al., 2010; Barak et al., 2012). In contrast, zebrafish *mind bomb* mutant showed

impaired Notch singling, but did not manifest kidney cysts (Haddon et al., 1998). Notch pathway in zebrafish regulates multiciliated cells (MCCs) and transporting epithelial cells so that they are separated in a “salt-and-pepper” fusion, suggestive of lateral inhibition (Liu et al, 2007). Interestingly, loss-of-function experiments by down egulating Notch ligand *jagged 2* rescued *double bubble* mutant that lacks motile cilia (Liu et al, 2007). The results of this study showed that plac8.1 is required for kidney function during development. However, whether Plac8.1 is required to maintain cilia and kidney function remains an open question. Furthermore, it would be informative to examine if *jagged 2* downregulating rescues loss-of-function of *plac8.1*. Since we did not have evidence of cell fata change by altered Plac8.1 expression, it is likely that Plac8.1 is downstream of the transcription factors, and possible acting as a permissive factor to enable ciliogenesis. As to whether Plac8.1 is sufficient for ciliogenesis, it remains to be tested with an expression system of temporal control, because Plac8.1 overexpression resulted in early developmental defects that complicate analyses of ciliated tissues at later stages (Chapter II).

ACKNOWLEDGEMENTS

We thank Drs. G.D. Longmore, S.K. Dutcher, P.V. Bayly, R. Kopan, A.B. Reynolds, J.G. Patton, J.T. Gamse, and A.M. Krezel, all L.S.-K. laboratory members, in particular Drs. D.S. Sepich, and R.S. Gray for critical comments and discussions. We acknowledge excellent fish care by E.A. Sanders, S.C. Canter, A. Bradshaw, H. Beck. We thank R.H. Carnahan and other members of Vanderbilt Antibody and Protein Resource core laboratory for the help with generating the anti-PLAC8, and anti-Plac8.1 antibodies. The Vanderbilt Antibody and Protein Resource is supported by the Vanderbilt Institute of Chemical Biology and the Vanderbilt Ingram Cancer Center (P30 CA68485). This work is supported by GM55101 grant to LSK.

CHAPTER IV

Discussion and future directions

In this thesis, I examined the function of the zebrafish *plac8.1* gene with both gain-of-function and loss-of-function experiments. The gain-of-function experiments were motivated by two sets of observations about human PLAC8. First, multiple independent studies implicated elevated levels of PLAC8 in the pathogenesis of cancer (Grate, 2005; Hughes et al., 2007; McMurray et al., 2008). However, the activity of overexpressed PLAC8 *in vivo* remained undefined. Second, *PLAC8* is among the most upregulated genes in invasive colorectal cancer SC cells compared to the less invasive counterpart CC cells (Chapter II). Gain of *plac8.1* function in zebrafish resulted in post-transcriptional downregulation of E-cadherin and defective gastrulation cell movements. On the other hand, loss-of-function experiments were performed using antisense oligonucleotides and TALEN-mediated germline mutation in *plac8.1* to assess its requirement in zebrafish embryogenesis. Loss of *plac8.1* function led to defects in motile cilia formation and activity. It is interesting to note that gain-of-function and loss-of-function phenotypes of mouse *Plac8* also appear distinct. Overexpression of *Plac8* in cancer cells promotes cancer formation in xenograft assays (McMurray et al., 2008), whereas mice with inactivated *Plac8* show impaired host defense, late onset obesity, and defects in brown fat differentiation (Jimenez-Preitner et al., 2011). Whether these seemingly unrelated phenotypes are linked at the molecular level remains to be examined.

The vertebrate-specific *PLAC8* homologs encode a class of cysteine-rich proteins with poorly defined molecular function. Zebrafish, a vertebrate model system amenable to embryologic and genetic approaches, presents an opportunity to conduct *in vivo* functional characterization of Plac8. During my studies, I identified *plac8.1* as a *PLAC8* homolog in zebrafish and characterized expression of its transcripts and protein localization patterns. I also examined the function of *plac8.1* during zebrafish embryogenesis by overexpressing Plac8.1 (gain-of-function studies in Chapter II), and by injecting MOs targeting *plac8.1* and generating *plac8.1*^{stl33} mutant with TALEN (loss-of-function studies in Chapter III). In addition to sequence homology and conserved synteny, several lines of evidence suggested zebrafish *plac8.1* is an ortholog of mouse *Plac8* and human *PLAC8*. For example, when

overexpressed in zebrafish gastrulae, the zebrafish Plac8.1 and human PLAC8 produced a similar morphological phenotypes and reduced E-cadherin levels. Furthermore, both Plac8.1 and PLAC8 activated Akt signaling (Rogulski et al., 2005). Moreover, RNA transcripts of both *plac8.1* and *Plac8* were expressed abundantly in intestine and kidney in zebrafish and mice, and both Plac8.1 and human PLAC8 proteins localized to apical domains of intestinal epithelial cells (Chapter II).

In Chapter II, I addressed the role of high levels of Plac8.1 *in vivo* by overexpressing Plac8.1 in zebrafish embryos. Excess Plac8.1, in a concentration-dependent manner, caused morphologic defects suggestive of defective gastrulation movements. By analyzing expression of cell type-specific genes and migration of mesodermal cells by time-lapse microscopy, I showed that epibolic, as well as convergence and extension gastrulation cell movements, were impaired in Plac8.1-overexpressing embryos. Impairment of epiboly, anterior migration of chordamesoderm, convergence and extension due to loss or reduction of E-cadherin expression and/or activity in zebrafish gastrulae was observed in several other studies (Babb and Marrs, 2004; Kane et al., 2005; Montero et al., 2005; Shimizu et al., 2005; Solnica-Krezel, 2006; Hammerschmidt and Wedlich, 2008; Lin et al., 2009), underscoring the requirement for precise regulation of E-cadherin levels and activity in various gastrulation cell movements. Similar to embryos with reduced E-cadherin function, Plac8.1 overexpressing embryos exhibited epiboly defects, and anteroposteriorly shortened and mediolaterally broadened chordamesdermal tissue indicative of impaired convergence and extension movements (Figure 2-5, A). In addition, Plac8.1 overexpressing embryos showed mild defects in the slow convergence movements of the lateral mesodermal cells towards the dorsal midline (Figure 2-5), which is also observed in *cdh1* mutant embryos (McFarland et al., 2005).

Since embryos overexpressing Plac8.1 showed phenotype similar to zebrafish *cdh1/E-cadherin* mutant embryos, I hypothesized that Plac8.1 overexpression led to gastrulation defects in part through inhibiting E-cadherin function. In support of this hypothesis, E-cadherin levels were significantly reduced in Plac8.1-overexpressing gastrulae at the shield stage (Figure 2-4). Moreover, Plac8.1 overexpression enhanced epiboly defects of $cdh1^{+/-}$ heterozygous mutant embryos. Using a similar strategy, Gα12/13 was shown to antagonize E-cadherin function (Fang et al., 2009). Furthermore, the transcript levels of *cdh1* were not significantly reduced upon Plac8.1 overexpression,

suggesting a post-transcriptional mechanism of E-cadherin downregulation. Preliminary data suggest that proteasomal degradation of E-cadherin may contribute, at least in part, to its Plac8.1-mediated downregulation.

Interestingly, results from the Coffey laboratory (Vanderbilt University Medical Center) show that the model for the cellular and molecular activity of overexpressed Plac8 based on zebrafish experiments appears also to apply to mammalian cells. A human colorectal cancer cell line, HCA-7, formed two distinct morphologies when cultured in 3D collagen. Epithelial CC expressed undetectable levels of PLAC8, whereas SC with ill-defined borders and protrusions expressed high levels of PLAC8, suggesting the cells with high levels of PLAC8 might be more invasive (Figure 2-2, B). Consistently, xenografts of SC cells expressing high PLAC8 levels showed reduced membrane E-cadherin, which was also observed in zebrafish embryos overexpressing Plac8.1 (Figure 2-8, D). Difference did exist, however, in that SC cells redistributed E-cadherin from the plasma membrane to the cytoplasm with only a modest decrease in E-cadherin protein levels (data not shown). In summary, we propose a consensus model from studies in zebrafish and in human cancer cells whereby high levels of Plac8 homologous proteins reduce E-cadherin activity.

In Chapter III, I focused on loss-of-function studies. The *plac8.1*-targeting MOs that effectively reduced Plac8.1 protein levels produced a set of common phenotypes suggestive of cilia defects (Drummond, 2012). Rescue experiments where MO-resistant Plac8.1 encoding RNA was injected into *plac8.1* morphants suggested the cilia phenotypes resulted specifically from interference with *plac8.1* function. In addition, *plac8.1* mutant embryos lacking its zygotic function displayed similar phenotypes, including ventrally curved body axes, kidney cysts, reduction of cilia number and length in the Kupffer's vesicle, and compromised cilia beating in the olfactory placode.

I provided several lines of evidence in support of cilia defects in *plac8.1*-deficient zebrafish embryos. First, in Plac8.1-deficient embryos, motile cilia numbers in the Kupffer's vesicle were significantly reduced, whereas cell numbers in the Kupffer's vesicle were not significantly changed. These results are consistent with defects in ciliogenesis rather than cell proliferation. Second, cilia numbers in the kidney ducts were also reduced in the embryos injected with MO1-*plac8.1*.compared to control embryos. Third, cilia in kidney ducts were abnormally curled and exhibited detached

membranes around the ciliary axonemes. Finally, zebrafish embryos with deficient Plac8.1 also showed impaired beating of motile cilia in the Kupffer's vesicle, kidney, and nasal pit.

In summary, the *in vivo* studies on zebrafish *plac8.1* uncovered pleiotropic functions of *plac8.1* during development. In addition, the overexpression experiments shed light on mechanisms underlying human disease. These results suggest that Plac8.1 overexpression interferes with the function of E-cadherin and zebrafish gastrulation, whereas Plac8.1 is required for motile cilia morphogenesis and function (Figure 4-1). This work represents the first functional characterization of zebrafish Plac8.1.

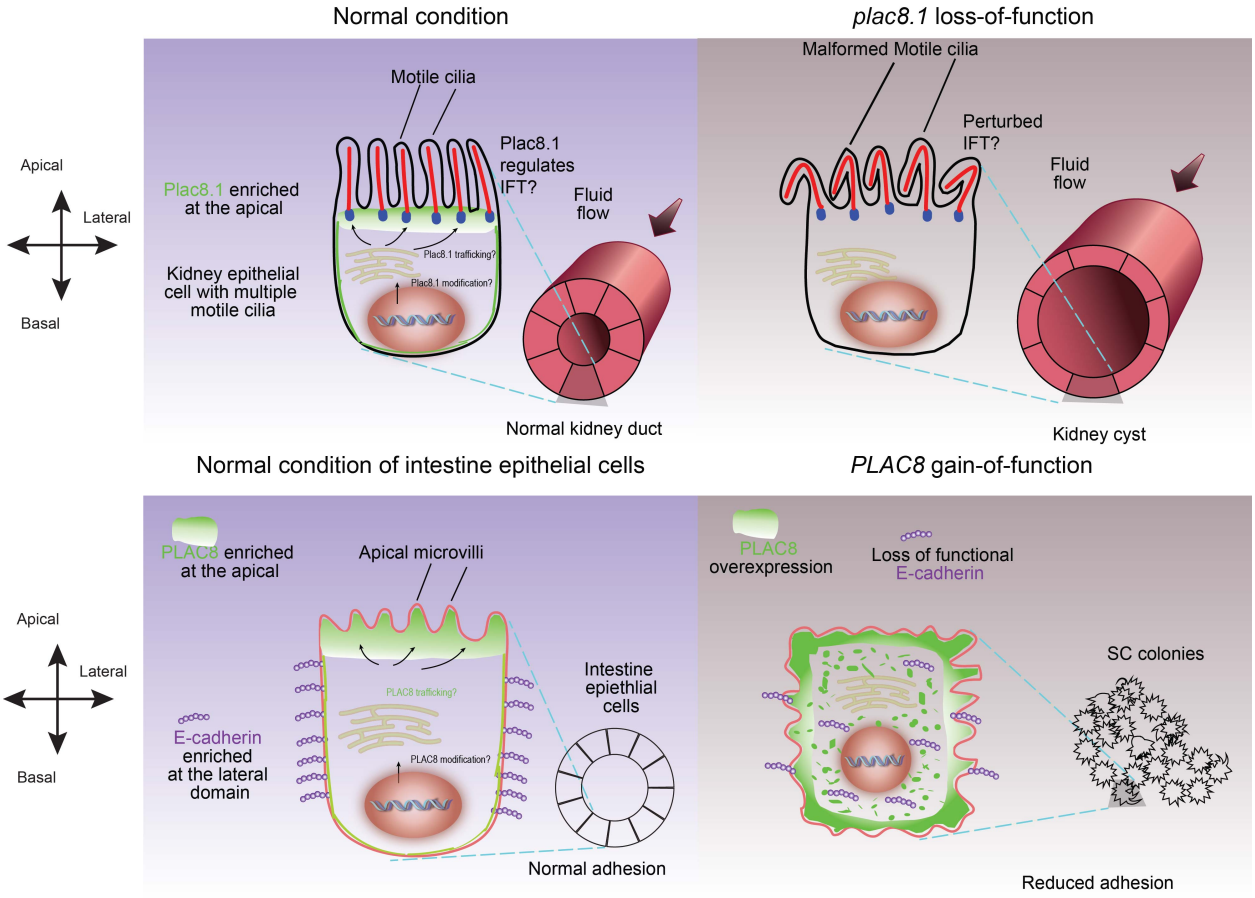

Figure 4-1 Schematic overview of findings from this study.
Top panel: a model of how Plac8.1 functions in motile cilia morphology and function. Bottom: panel: a model of the role of PLAC8 overexpression in the conversion from CC clones to SC clones.

Overexpression of zebrafish Plac8.1 leads to E-cadherin degradation and gastrulation movements defects

Chapter II demonstrated that overexpression of Plac8.1 led to reduction of E-cadherin levels and gastrulation cell movements defects. Vertebrate gastrulation entails four evolutionarily conserved morphogenetic movements (epiboly, internalization, convergence, and extension) to generate three germ layers, and to properly place organ primordia in the developing body plan (Solnica-Krezel and Sepich, 2012). A variety of cell behaviors including directed migration, radial and mediolateral intercalation, and cell shape change underlie these morphogenetic movements. Previous studies with molecular genetic approaches and *in vivo* tracking of cell movements in zebrafish gastrulae have demonstrated that anomalies of E-cadherin-mediated cell-cell adhesion affect all modes of morphogenetic cell movements (Hammerschmidt and Wedlich, 2008; Solnica-Krezel, 2006). For example, zebrafish *cdh1*/*E-cadherin* mutants or morphants exhibit defects in epiboly, internalization, convergence, and extension (Babb and Marrs, 2004; Kane et al., 2005; McFarland et al., 2005; Montero et al., 2005; Shimizu et al., 2005). Functional inhibition of E-cadherin activity without altering protein levels of E-cadherin also leads to epiboly defects (Lin et al., 2009). In addition to decreased E-cadherin level or activity, elevated E-cadherin levels (due to destabilization of the Snail transcription repressor upon dampened prostaglandin $G\beta\gamma$ signaling) also impairs epiboly, internalization, convergence, and extension movements, indicating balanced E-cadherin-mediated cell-cell adhesion is required for gastrulation movements (Speirs et all, 2010). Moreover, the ventral to dorsal BMP activity gradient instructs formation of a reverse gradient of E-cadherin-mediated cell-cell adhesiveness that is crucial for the dorsal convergence of cells in the lateral region of the zebrafish gastrula (van der Hardt et al., 2007). Finally, *cdh1/ E-cadherin*/ RNA was proposed to form a descending gradient in zebrafish blastula from the superficial to deep layer, and the resultant E-cadherin gradient to guide the polarized radial intercalation of the cells from the deep to the superficial layer (Kane et al., 2005). Cells with impaired E-cadherin function fail, in a cell-autonomous manner, to maintain their position after intercalation into superficial layers, or maintain a flattened morphology typical of the superficial layer. These results suggested that radial intercalation guided by E-cadherin-dependent cell shape changes contributes to epiboly movements (Kane et al., 2005).

Since in the process of tumorigenesis, reduction or loss of cell adhesion represents an initiating event for the invasion-metastasis cascade, genes overexpressed during tumor metastasis might have effects on cell-cell adhesion when overexpressed in zebrafish embryos (Thiery et al., 2009; Valastyan and Weinberg 2011). For example, study of Liv1, a zebrafish homologoue of a Zinc transporter associated with breast cancer, showed that Liv1 promotes E-cadherin downregulation through Snail transcription factor - based transcriptional repression (Yamashita et al., 2004). Plac8.1 gain-of-function experiments in Chapter II resulted in zebrafish gastrulation cell movements defects, at least partially through E-cadherin degradation. Similarly, human colorectal cancer cells expressing high levels of PLAC8 also exhibited compromised adhesion ascribable to attenuated E-cadherin membrane localization (Chapter II). Therefore, zebrafish gastrulation affords an efficient *in vivo* platform for functional studies of genes involved in the regulation of cell-cell adhesion in normal development and in the cancer invasion-metastasis cascade. In addition to studies of cell adhesion during gastrulation, zebrafish embryogenesis can be used as a "living test tube" for assessing the nature of mutated or deregulated genes involved in disease (Santoriello and Zon, 2012).

Zebrafish *plac8.1* is required for cilia morphogenesis and function

Among the first cellular organelles described by Leeuwenhoek, vertebrate cilia have emerged as a focus of scientific research after years of scientific obscurity as an apparently useless vestigial structure (Wallingford and Mitchell, 2011). The research on cilia formation and function is concerned with two questions. First, what are the processes and regulatory mechanisms for cilia formation and maintenance? Second, what signaling pathways and biological processes do cilia participate in? A simplified answer to the first question is that docking of functional basal bodies to the cell membrane (predominantly the apical membrane) and a process named intraflagellar trafficking (IFT), dependent on small GTPase Rab-based vesicle trafficking, are required to build and maintain a cilium, and to functionalize it with the components necessary for its specific activities. A simplified answer to the second question, supported by many lines of evidence, is that vertebrate cilia are indispensible for Hedgehog (Hh) signaling. However, additional data demonstrate a possible link between cilia and Wnt signaling pathways. Moreover, emerging evidence suggests that cilia are involved in PDGF, Notch, and potentially other signaling cascades.

Belonging to a large and diverse class of human disorders, collectively referred to as the ciliopathies, cilia malfunctions are commonly associated with left-right asymmetry defects, organ cyst formation (with kidney cysts, sensory neuropathy, and infertility being common) (Hildebrandt, 2011). Zebrafish mutants with loss-of-function of genes involved in cilia formation or function exhibit a similar spectrum of phenotypes including kidney cysts and left-right asymmetry defects. Since many functions mediated by cilia are conserved in vertebrates, zebrafish, a vertebrate species, provides a powerful genetic system to provide insights into the functional conservation of cilia during evolution. In this study, reduction-of-function of *plac8.1* resulted in a phenotype consistent with cilia defects in zebrafish, providing evidence for a role of *plac8.1* in cilia formation and function.

Understanding the function of Plac8.1 according to Muller's morphs

Biological functions of a gene can be inferred from analyzing phenotypes upon perturbations of the gene expression and/or function. The differences between wild-type controls and individuals with increased or reduced level of gene function can implicate the gene in a specific biological process, and suggest its activity in this process. Simple phenotypes versus pleiotropic phenotypes (affecting multiple traits) can indicate whether the gene has a single or many biochemical activities, or whether it has a simple or complex expression pattern. On the other hand, considering the range of phenotypes resulting from different gene perturbations according to Muller's morphs can help understand both native function of a gene, and the functional consequence of specific gene perturbations (Muller, 1932). According to Muller, gene mutations cause broadly either loss or gain of its wild-type function. Mutant alleles that cause a partial loss of gene function are hypomorphic, in contrast to amorphic mutations that completely eliminate its function. In the category of gain-of-function mutations, Muller distinguished hypermorphic alleles, which produce increased levels of the normal gene function, neomorphic alleles that acquired new function, and finally antimorphic alleles, which not only lack but can also antagonize the wild-type gene activity (Muller, 1932).

In this study, loss- and gain-of-function of *plac8.1* resulted in unrelated morphologic phenotypes. On the one hand, loss of-*plac8.1* function led to left-right asymmetry and kidney defects due to cilia abnomalies, likely representing a hypomorphic condition, since Plac8.1 protein levels were reduced in

plac8.1 morphants and mutants. On the other hand, gain-of-function experiments by injecting RNA encoding Plac8.1 resulted in gastrulation defects likely reflecting a neomorphic condition by gaining the capacity to promote degradation of E-cadherin, either due to ectopic location and/or novel protein interactions of the overexpressed protein.

Future directions

This study of zebrafish Plac8.1 opens new areas for future research. For example, it is important to understand the regulation of *plac8.1* and *PLAC8* by examining the signaling pathways that act upstream of *plac8.1* and *PLAC8* to regulate its transcription, translation, protein localization and activity. One practical approach to start probing this question is to carry out an *in silico* survey of *Plac8* transcription by analyzing genomic data deposited in databases such as the Gene Expression Omnibus (GEO) database. Based on the query results from the *in silico* survey, hypotheses can be generated for experimental tests. In addition to the upstream regulators, it is also important to know the downstream effectors of *Plac8* homologs. Microarray or deep sequencing-based analyses of transcriptional changes in *plac8.1* mutant and overexpressing embryos and wild-type controls will provide crucial information regarding molecules downstream of Plac8.1. In addition, proteomic studies can be carried out to identify binding partners of Plac8/PLAC8.

In addition to the functional studies of Plac8.1 in zebrafish embryogenesis, biochemical study of the structural properties of Plac8.1 may provide insights into its function. Therefore, it is crucial to purify Plac8.1 and PLAC8 proteins, possibly with heterologous expression system such as *E.coli* strains optimized for producing cysteine-rich proteins. The purified protein can be used for structural studies with approaches including X-ray crystallography. Furthermore, the relatively low molecular weights of Plac8 proteins make it possible to use nuclear magnetic resonance (NMR) spectroscopy to obtain dynamic structural information.

REFERENCE

Agathon, A., Thisse, C., and Thisse, B. (2003). The molecular nature of the zebrafish tail organizer. Nature *424*, 448-452.

Aguilar, R.C., and Wendland, B. (2003). Ubiquitin: not just for proteasomes anymore. Curr Opin Cell Biol *15*, 184-190.

Alessi, D.R., Andjelkovic, M., Caudwell, B., Cron, P., Morrice, N., Cohen, P., and Hemmings, B.A. (1996). Mechanism of activation of protein kinase B by insulin and IGF-1. EMBO J *15*, 6541-6551.

Alexander, J., and Stainier, D.Y. (1999). A molecular pathway leading to endoderm formation in zebrafish. Curr Biol *9*, 1147-1157.

Amack, J.D., and Yost, H.J. (2004). The T box transcription factor no tail in ciliated cells controls zebrafish left-right asymmetry. Curr Biol *14*, 685-690.

Ashby, W.J., and Zijlstra, A. (2012). Established and novel methods of interrogating two-dimensional cell migration. Integr Biol (Camb) *4*:1338-1350.

Babb, S.G., and Marrs, J.A. (2004). E-cadherin regulates cell movements and tissue formation in early zebrafish embryos. Dev Dyn *230*, 263-277.

Barak, H., Preger-Ben Noon, E., and Reshef, R. (2012). Comparative spatiotemporal analysis of Hox gene expression in early stages of intermediate mesoderm formation. Dev Dyn *241*, 1637-1649.

Barth, A.I., Nathke, I.S., and Nelson, W.J. (1997). Cadherins, catenins and APC protein: interplay between cytoskeletal complexes and signaling pathways. Curr Opin Cell Biol *9*, 683-690.

Baserga, R. (1994). Oncogenes and the strategy of growth factors. Cell *79*, 927-930.

Bauer, K., Dowejko, A., Bosserhoff, A.K., Reichert, T.E., and Bauer, R. (2011). Slit-2 facilitates interaction of P-cadherin with Robo-3 and inhibits cell migration in an oral squamous cell carcinoma cell line. Carcinogenesis *32*:935-943.

Baum, B., Settleman, J., and Quinlan, M.P. (2008). Transitions between epithelial and mesenchymal states in development and disease. Semin Cell Dev Biol *19*, 294-308.

Beadle, G.W., and Tatum, E.L. (1941). Genetic Control of Biochemical Reactions in Neurospora. Proc Natl Acad Sci U S A *27*, 499-506.

Beadle, D.J. and Tatum, E.L. (1958). Nobel Lecture.

Bech-Otschir, D., Kraft, R., Huang, X., Henklein, P., Kapelari, B., Pollmann, C., and Dubiel, W. (2001). COP9 signalosome-specific phosphorylation targets p53 to degradation by the ubiquitin system. EMBO J *20*, 1630-1639.

Becker, M.W., and Jordan, C.T. (2011). Leukemia stem cells in 2010: current understanding and future directions. Blood Rev *25*, 75-81.

Bedell, V.M., Person, A.D., Larson, J.D., McLoon, A., Balciunas, D., Clark, K.J., Neff, K.I., Nelson, K.E., Bill, B.R., Schimmenti, L.A*., et al.* (2012a). The lineage-specific gene ponzr1 is essential for zebrafish pronephric and pharyngeal arch development. Development *139*, 793-804.

Bedell, V.M., Wang, Y., Campbell, J.M., Poshusta, T.L., Starker, C.G., Krug, R.G., 2nd, Tan, W., Penheiter, S.G., Ma, A.C., Leung, A.Y*., et al.* (2012b). In vivo genome editing using a high-efficiency

TALEN system. Nature *491*, 114-118.

Berghmans, S., Murphey, R.D., Wienholds, E., Neuberg, D., Kutok, J.L., Fletcher, C.D., Morris, J.P., Liu, T.X., Schulte-Merker, S., Kanki, J.P.*, et al.* (2005). tp53 mutant zebrafish develop malignant peripheral nerve sheath tumors. Proc Natl Acad Sci U S A *102*, 407-412.

Bertram, J.S. (2000). The molecular biology of cancer. Mol Aspects Med *21*, 167-223.

Berx, G., and Van Roy, F. (2001). The E-cadherin/catenin complex: an important gatekeeper in breast cancer tumorigenesis and malignant progression. Breast Cancer Res *3*, 289-293.

Bill, B.R., Petzold, A.M., Clark, K.J., Schimmenti, L.A., and Ekker, S.C. (2009). A primer for morpholino use in zebrafish. Zebrafish *6*, 69-77.

Bisgrove, B.W., Essner, J.J., and Yost, H.J. (1999). Regulation of midline development by antagonism of lefty and nodal signaling. Development *126*, 3253-3262.

Bissell, M.J., and Hines, W.C. (2011). Why don't we get more cancer? A proposed role of the microenvironment in restraining cancer progression. Nat Med *17*, 320-329.

Boch, J., Scholze, H., Schornack, S., Landgraf, A., Hahn, S., Kay, S., Lahaye, T., Nickstadt, A., and Bonas, U. (2009). Breaking the code of DNA binding specificity of TAL-type III effectors. Science *326*, 1509-1512.

Boguski, M.S., and McCormick, F. (1993). Proteins regulating Ras and its relatives. Nature *366*, 643-654.

Boisvieux-Ulrich, E., Laine, M.C., and Sandoz, D. (1990). Cytochalasin D inhibits basal body migration and ciliary elongation in quail oviduct epithelium. Cell Tissue Res *259*, 443-454.

Borovina, A., Superina, S., Voskas, D., and Ciruna, B. (2010). Vangl2 directs the posterior tilting and asymmetric localization of motile primary cilia. Nat Cell Biol *12*, 407-412.

Bos, J.L. (1989). ras oncogenes in human cancer: a review. Cancer Res *49*, 4682-4689.

Bradford, Y., Conlin, T., Dunn, N., Fashena, D., Frazer, K., Howe, D.G., Knight, J., Mani, P., Martin, R., Brabletz, T. (2012). To differentiate or not--routes towards metastasis. Nat Rev Cancer *12*:425-436.

Brand, M., Heisenberg, C.P., Warga, R.M., Pelegri, F., Karlstrom, R.O., Beuchle, D., Picker, A., Jiang, Y.J., Furutani-Seiki, M., van Eeden, F.J.*, et al.* (1996). Mutations affecting development of the midline and general body shape during zebrafish embryogenesis. Development *123*, 129-142.

Bremnes, R.M., Veve, R., Hirsch, F.R., and Franklin, W.A. (2002). The E-cadherin cell-cell adhesion complex and lung cancer invasion, metastasis, and prognosis. Lung Cancer *36*, 115-124.

Brune, B., and Mohr, S. (2001). Protein thiol modification of glyceraldehyde-3-phosphate dehydrogenase and caspase-3 by nitric oxide. Curr Protein Pept Sci *2*, 61-72.

Cacheiro, N.L., Wilkinson, J.E., and Woychik, R.P. (1994). Candidate gene associated with a mutation causing recessive polycystic kidney disease in mice. Science *264*, 1329-1333.

Cai, M., Langer, E.M., Gill, J.G., Satpathy, A.T., Albring, J.C., Kc, W., Murphy, T.L., and Murphy, K.M. (2012). Dual actions of Meis1 inhibit erythroid progenitor development and sustain general hematopoietic cell proliferation. Blood *120*, 335-346.

Candille, S.I., Kaelin, C.B., Cattanach, B.M., Yu, B., Thompson, D.A., Nix, M.A., Kerns, J.A., Schmutz, S.M., Millhauser, G.L., and Barsh, G.S. (2007). A -defensin mutation causes black coat color in domestic

dogs. Science *318*, 1418-1423.

Caneparo, L., Huang, Y.L., Staudt, N., Tada, M., Ahrendt, R., Kazanskaya, O., Niehrs, C., and Houart, C. (2007). Dickkopf-1 regulates gastrulation movements by coordinated modulation of Wnt/beta catenin and Wnt/PCP activities, through interaction with the Dally-like homolog Knypek. Genes Dev *21*, 465-480.

Cano, A., Perez-Moreno, M.A., Rodrigo, I., Locascio, A., Blanco, M.J., del Barrio, M.G., Portillo, F., and Nieto, M.A. (2000). The transcription factor snail controls epithelial-mesenchymal transitions by repressing E-cadherin expression. Nat Cell Biol *2*, 76-83.

Carmany-Rampey, A., and Schier, A.F. (2001). Single-cell internalization during zebrafish gastrulation. Curr Biol *11*, 1261-1265.
Carver, E.A., Jiang, R., Lan, Y., Oram, K.F., and Gridley, T. (2001). The mouse snail gene encodes a key regulator of the epithelial-mesenchymal transition. Mol Cell Biol *21*, 8184-8188.

Cermak, T., Doyle, E.L., Christian, M., Wang, L., Zhang, Y., Schmidt, C., Baller, J.A., Somia, N.V., Bogdanove, A.J., and Voytas, D.F. (2011). Efficient design and assembly of custom TALEN and other TAL effector-based constructs for DNA targeting. Nucleic Acids Res *39*, e82.

Chen, Y., and Schier, A.F. (2001). The zebrafish Nodal signal Squint functions as a morphogen. Nature *411*, 607-610.

Cheung, L.W., Mak, A.S., Cheung, A.N., Ngan, H.Y., Leung, P.C., and Wong, A.S. (2011). P-cadherin cooperates with insulin-like growth factor-1 receptor to promote metastatic signaling of gonadotropin-releasing hormone in ovarian cancer via p120 catenin. Oncogene *30*:2964-2974.

Cheng, J.C., Miller, A.L., and Webb, S.E. (2004). Organization and function of microfilaments during late epiboly in zebrafish embryos. Dev Dyn *231*, 313-323.

Cheung, L.W., Leung, P.C., and Wong, A.S. (2010). Cadherin switching and activation of p120 catenin signaling are mediators of gonadotropin-releasing hormone to promote tumor cell migration and invasion in ovarian cancer. Oncogene *29*:2427-2440.

Chiang, A.C., and Massague, J. (2008). Molecular basis of metastasis. N Engl J Med *359*, 2814-2823.
Choi, H.H., Gully, C., Su, C.H., Velazquez-Torres, G., Chou, P.C., Tseng, C., Zhao, R., Phan, L., Shaiken, T.,

Ciechanover, A. (1994). The ubiquitin-proteasome proteolytic pathway. Cell *79*, 13-21.

Clement, A., Solnica-Krezel, L., and Gould, K.L. (2011). The Cdc14B phosphatase contributes to ciliogenesis in zebrafish. Development *138*, 291-302.

Colonna, M., Trinchieri, G., and Liu, Y.J. (2004). Plasmacytoid dendritic cells in immunity. Nat Immunol *5*, 1219-1226.

Cooper, M.S., and D'Amico, L.A. (1996). A cluster of noninvoluting endocytic cells at the margin of the zebrafish blastoderm marks the site of embryonic shield formation. Dev Biol *180*, 184-198.

Cope, G.A., Suh, G.S., Aravind, L., Schwarz, S.E., Zipursky, S.L., Koonin, E.V., and Deshaies, R.J. (2002). Role of predicted metalloprotease motif of Jab1/Csn5 in cleavage of Nedd8 from Cul1. Science *298*, 608-611.

Corbit, K.C., Aanstad, P., Singla, V., Norman, A.R., Stainier, D.Y., and Reiter, J.F. (2005). Vertebrate Smoothened functions at the primary cilium. Nature *437*, 1018-1021.

Corey, D.R., and Abrams, J.M. (2001). Morpholino antisense oligonucleotides: tools for investigating

vertebrate development. Genome Biol *2*, REVIEWS1015.

Craige, B., Tsao, C.C., Diener, D.R., Hou, Y., Lechtreck, K.F., Rosenbaum, J.L., and Witman, G.B. (2010). CEP290 tethers flagellar transition zone microtubules to the membrane and regulates flagellar protein content. J Cell Biol *190*, 927-940.

Cross, D.A., Alessi, D.R., Cohen, P., Andjelkovich, M., and Hemmings, B.A. (1995). Inhibition of glycogen synthase kinase-3 by insulin mediated by protein kinase B. Nature *378*, 785-789.

Cross, M., and Dexter, T.M. (1991). Growth factors in development, transformation, and tumorigenesis. Cell *64*, 271-280.

Crow, M.T., and Stockdale, F.E. (1986). Myosin expression and specialization among the earliest muscle fibers of the developing avian limb. Dev Biol *113*, 238-254.

Davis, M.A., Ireton, R.C., and Reynolds, A.B. (2003). A core function for p120-catenin in cadherin turnover. J Cell Biol *163*, 525-534.

Debnath, J., and Brugge, J.S. (2005). Modelling glandular epithelial cancers in three-dimensional cultures. Nat Rev Cancer *5*:675-688.

de Herreros, A.G., Peiro, S., Nassour, M., and Savagner, P. (2010). Snail family regulation and epithelial mesenchymal transitions in breast cancer progression. J Mammary Gland Biol Neoplasia *15*, 135-147.

De Robertis, E.M. (2006). Spemann's organizer and self-regulation in amphibian embryos. Nat Rev Mol Cell Biol *7*, 296-302.

Devoto, M., Lozito, A., Staffa, G., D'Alessandro, R., Sacquegna, T., and Romeo, G. (1986). Segregation analysis of migraine in 128 families. Cephalalgia *6*, 101-105.

Dickmeis, T., Mourrain, P., Saint-Etienne, L., Fischer, N., Aanstad, P., Clark, M., Strahle, U., and Rosa, F. (2001). A crucial component of the endoderm formation pathway, CASANOVA, is encoded by a novel sox-related gene. Genes Dev *15*, 1487-1492.

Dishinger, J.F., Kee, H.L., Jenkins, P.M., Fan, S., Hurd, T.W., Hammond, J.W., Truong, Y.N., Margolis, B., Martens, J.R., and Verhey, K.J. (2010). Ciliary entry of the kinesin-2 motor KIF17 is regulated by importin-beta2 and RanGTP. Nat Cell Biol *12*, 703-710.

Doetschman, T., Gregg, R.G., Maeda, N., Hooper, M.L., Melton, D.W., Thompson, S., and Smithies, O. (1987). Targetted correction of a mutant HPRT gene in mouse embryonic stem cells. Nature *330*, 576-578.

Dornan, D., Wertz, I., Shimizu, H., Arnott, D., Frantz, G.D., Dowd, P., O'Rourke, K., Koeppen, H., and Dixit, V.M. (2004). The ubiquitin ligase COP1 is a critical negative regulator of p53. Nature *429*, 86-92.

Dougan, S.T., Warga, R.M., Kane, D.A., Schier, A.F., and Talbot, W.S. (2003). The role of the zebrafish nodal-related genes squint and cyclops in patterning of mesendoderm. Development *130*, 1837-1851.

Drewinko, B., Romsdahl, M.M., Yang, L.Y., Ahearn, M.J., and Trujillo, J.M. (1976). Establishment of a human carcinoembryonic antigen-producing colon adenocarcinoma cell line. Cancer Res *36*:467-475.

Driever, W., Solnica-Krezel, L., Schier, A.F., Neuhauss, S.C., Malicki, J., Stemple, D.L., Stainier, D.Y., Zwartkruis, F., Abdelilah, S., Rangini, Z.*, et al.* (1996). A genetic screen for mutations affecting embryogenesis in zebrafish. Development *123*, 37-46.

Driever, W., Stemple, D., Schier, A., and Solnica-Krezel, L. (1994). Zebrafish: genetic tools for studying

vertebrate development. Trends Genet *10*, 152-159.

Drummond, I.A. (2012). Cilia functions in development. Curr Opin Cell Biol *24*, 24-30.

Dutcher, S.K. (2003). Elucidation of basal body and centriole functions in Chlamydomonas reinhardtii. Traffic *4*, 443-451.

Eddins, M.J., Carlile, C.M., Gomez, K.M., Pickart, C.M., and Wolberger, C. (2006). Mms2-Ubc13 covalently bound to ubiquitin reveals the structural basis of linkage-specific polyubiquitin chain formation. Nat Struct Mol Biol *13*, 915-920.

Eggenschwiler, J.T., and Anderson, K.V. (2007). Cilia and developmental signaling. Annu Rev Cell Dev Biol *23*, 345-373.

El-Sayed, A., Hoelker, M., Rings, F., Salilew, D., Jennen, D., Tholen, E., Sirard, M.A., Schellander, K., and Tesfaye, D. (2006). Large-scale transcriptional analysis of bovine embryo biopsies in relation to pregnancy success after transfer to recipients. Physiol Genomics *28*, 84-96.

Essner, J.J., Amack, J.D., Nyholm, M.K., Harris, E.B., and Yost, H.J. (2005). Kupffer's vesicle is a ciliated organ of asymmetry in the zebrafish embryo that initiates left-right development of the brain, heart and gut. Development *132*, 1247-1260.

Essner, J.J., Vogan, K.J., Wagner, M.K., Tabin, C.J., Yost, H.J., and Brueckner, M. (2002). Conserved function for embryonic nodal cilia. Nature *418*, 37-38.

Ezratty, E.J., Stokes, N., Chai, S., Shah, A.S., Williams, S.E., and Fuchs, E. (2011). A role for the primary cilium in Notch signaling and epidermal differentiation during skin development. Cell *145*, 1129-1141.

Fan, S., Hurd, T.W., Liu, C.J., Straight, S.W., Weimbs, T., Hurd, E.A., Domino, S.E., and Margolis, B. (2004). Polarity proteins control ciliogenesis via kinesin motor interactions. Curr Biol *14*, 1451-1461.

Fekany-Lee, K., Gonzalez, E., Miller-Bertoglio, V., and Solnica-Krezel, L. (2000). The homeobox gene bozozok promotes anterior neuroectoderm formation in zebrafish through negative regulation of BMP2/4 and Wnt pathways. Development *127*, 2333-2345.

Feldman, B., Concha, M.L., Saude, L., Parsons, M.J., Adams, R.J., Wilson, S.W., and Stemple, D.L. (2002). Lefty antagonism of Squint is essential for normal gastrulation. Curr Biol *12*, 2129-2135.

Fidler, I.J., and Hart, I.R. (1982). Biological diversity in metastatic neoplasms: origins and implications. Science *217*, 998-1003.

Fidler, I.J., and Kripke, M.L. (1977). Metastasis results from preexisting variant cells within a malignant tumor. Science *197*, 893-895.

Finetti, F., Paccani, S.R., Riparbelli, M.G., Giacomello, E., Perinetti, G., Pazour, G.J., Rosenbaum, J.L., and Baldari, C.T. (2009). Intraflagellar transport is required for polarized recycling of the TCR/CD3 complex to the immune synapse. Nat Cell Biol *11*, 1332-1339.

Finetti, F., Paccani, S.R., Rosenbaum, J., and Baldari, C.T. (2011). Intraflagellar transport: a new player at the immune synapse. Trends Immunol *32*, 139-145.

Fontham, E.T., Thun, M.J., Ward, E., Portier, K.M., Balch, A.J., Delancey, J.O., and Samet, J.M. (2009). American Cancer Society perspectives on environmental factors and cancer. CA Cancer J Clin *59*, 343-351.

Fujita, Y., Krause, G., Scheffner, M., Zechner, D., Leddy, H.E., Behrens, J., Sommer, T., and Birchmeier,

W. (2002). Hakai, a c-Cbl-like protein, ubiquitinates and induces endocytosis of the E-cadherin complex. Nat Cell Biol *4*, 222-231.

Fukasawa, K. (2007). Oncogenes and tumour suppressors take on centrosomes. Nat Rev Cancer *7*, 911-924.

Furthauer, M., Van Celst, J., Thisse, C., and Thisse, B. (2004). Fgf signalling controls the dorsoventral patterning of the zebrafish embryo. Development *131*, 2853-2864.

Gaiano, N., Amsterdam, A., Kawakami, K., Allende, M., Becker, T., and Hopkins, N. (1996). Insertional mutagenesis and rapid cloning of essential genes in zebrafish. Nature *383*, 829-832.

Galaviz-Hernandez, C., Stagg, C., de Ridder, G., Tanaka, T.S., Ko, M.S., Schlessinger, D., and Nagaraja, R. (2003). Plac8 and Plac9, novel placental-enriched genes identified through microarray analysis. Gene *309*, 81-89.

Geng, X., Speirs, C., Lagutin, O., Inbal, A., Liu, W., Solnica-Krezel, L., Jeong, Y., Epstein, D.J., and Oliver, G. (2008). Haploinsufficiency of Six3 fails to activate Sonic hedgehog expression in the ventral forebrain and causes holoprosencephaly. Dev Cell *15*, 236-247.

Gerdes, J.M., Davis, E.E., and Katsanis, N. (2009). The vertebrate primary cilium in development, homeostasis, and disease. Cell *137*, 32-45.

Gladfelter, A.S., Pringle, J.R., and Lew, D.J. (2001). The septin cortex at the yeast mother-bud neck. Curr Opin Microbiol *4*, 681-689.

Goetz, S.C., and Anderson, K.V. (2010). The primary cilium: a signalling centre during vertebrate development. Nat Rev Genet *11*, 331-344.

Grate, L.R. (2005). Many accurate small-discriminatory feature subsets exist in microarray transcript data: biomarker discovery. BMC Bioinformatics *6*, 97.

Gray, R.S., Abitua, P.B., Wlodarczyk, B.J., Szabo-Rogers, H.L., Blanchard, O., Lee, I., Weiss, G.S., Liu, K.J., Marcotte, E.M., Wallingford, J.B.*, et al.* (2009). The planar cell polarity effector Fuz is essential for targeted membrane trafficking, ciliogenesis and mouse embryonic development. Nat Cell Biol *11*, 1225-1232.

Guo, M., Rupe, M.A., Dieter, J.A., Zou, J., Spielbauer, D., Duncan, K.E., Howard, R.J., Hou, Z., and Simmons, C.R. (2010). Cell Number Regulator1 affects plant and organ size in maize: implications for crop yield enhancement and heterosis. Plant Cell *22*, 1057-1073.

Haddon, C., Jiang, Y.J., Smithers, L., and Lewis, J. (1998). Delta-Notch signalling and the patterning of sensory cell differentiation in the zebrafish ear: evidence from the mind bomb mutant. Development *125*, 4637-4644.

Haffter, P., Granato, M., Brand, M., Mullins, M., Hammerschmidt, M., Kane, D., Odenthal, J., van Eeden, F., Jiang, Y., Heisenberg, C., Kelsh, R., Furutani-Seiki, M., Vogelsang, E., Beuchle, D., Schach, U., Fabian, C., and Nüsslein-Volhard, C. (1996). The identification of genes with unique and essential functions in the development of the zebrafish, Danio rerio. Development *123*, 1-36.

Hall, H.G., Farson, D.A., and Bissell, M.J. (1982). Lumen formation by epithelial cell lines in response to collagen overlay: a morphogenetic model in culture. Proc Natl Acad Sci U S A *79*:4672-4676.

Hammerschmidt, M., Pelegri, F., Mullins, M.C., Kane, D.A., Brand, M., van Eeden, F.J., Furutani-Seiki, M., Granato, M., Haffter, P., Heisenberg, C.P.*, et al.* (1996). Mutations affecting morphogenesis during gastrulation and tail formation in the zebrafish, Danio rerio. Development *123*, 143-151.

Hammerschmidt, M., and Wedlich, D. (2008). Regulated adhesion as a driving force of gastrulation movements. Development *135*, 3625-3641.

Hanahan, D., and Weinberg, R.A. (2011). Hallmarks of cancer: the next generation. Cell *144*, 646-674.

Hannss, R., and Dubiel, W. (2011). COP9 signalosome function in the DDR. FEBS Lett *585*, 2845-2852.
Hans, S., Liu, D., and Westerfield, M. (2004). Pax8 and Pax2a function synergistically in otic specification, downstream of the Foxi1 and Dlx3b transcription factors. Development *131*, 5091-5102.

Hardy, R.G., Tselepis, C., Hoyland, J., Wallis, Y., Pretlow, T.P., Talbot, I., Sanders, D.S., Matthews, G., Morton, D., and Jankowski, J.A. (2002). Aberrant P-cadherin expression is an early event in hyperplastic and dysplastic transformation in the colon. Gut *50*:513-519.

Harel, A., and Forbes, D.J. (2004). Importin beta: conducting a much larger cellular symphony. Mol Cell *16*, 319-330.

Hartwell, L.H. (1978). Cell division from a genetic perspective. J Cell Biol *77*, 627-637.

Hashimoto, H., Itoh, M., Yamanaka, Y., Yamashita, S., Shimizu, T., Solnica-Krezel, L., Hibi, M., and Hirano, T. (2000). Zebrafish Dkk1 functions in forebrain specification and axial mesendoderm formation. Dev Biol *217*, 138-152.

Heasman, J., Crawford, A., Goldstone, K., Garner-Hamrick, P., Gumbiner, B., McCrea, P., Kintner, C., Noro, C.Y., and Wylie, C. (1994). Overexpression of cadherins and underexpression of beta-catenin inhibit dorsal mesoderm induction in early Xenopus embryos. Cell *79*, 791-803.

Hecht, S.S. (1999). Tobacco smoke carcinogens and lung cancer. J Natl Cancer Inst *91*, 1194-1210.

Heisenberg, C., Tada, M., Rauch, G., Saúde, L., Concha, M., Geisler, R., Stemple, D., Smith, J., Wilson, S. (2000). Silberblick/Wnt11 mediates convergent extension movements during zebrafish gastrulation. Nature *405*, 76-81.

Hetfeld, B.K., Helfrich, A., Kapelari, B., Scheel, H., Hofmann, K., Guterman, A., Glickman, M., Schade, R., Kloetzel, P.M., and Dubiel, W. (2005). The zinc finger of the CSN-associated deubiquitinating enzyme USP15 is essential to rescue the E3 ligase Rbx1. Curr Biol *15*, 1217-1221.

Hicke, L., Schubert, H.L., and Hill, C.P. (2005). Ubiquitin-binding domains. Nat Rev Mol Cell Biol *6*, 610-621.

Hildebrandt, F., Benzing, T., and Katsanis, N. (2011). Ciliopathies. N Engl J Med *364*, 1533-1543.

Hirokawa, N., Tanaka, Y., and Okada, Y. (2009). Left-right determination: involvement of molecular motor KIF3, cilia, and nodal flow. Cold Spring Harb Perspect Biol *1*, a000802.

Hochstrasser, M. (1996). Ubiquitin-dependent protein degradation. Annu Rev Genet *30*, 405-439.

Hong, C.C. (2009). Large-scale small-molecule screen using zebrafish embryos. Methods Mol Biol *486*, 43-55.

Hornberg, J.J., Bruggeman, F.J., Westerhoff, H.V., and Lankelma, J. (2006). Cancer: a Systems Biology disease. Biosystems *83*, 81-90.

Hosking, B., Francois, M., Wilhelm, D., Orsenigo, F., Caprini, A., Svingen, T., Tutt, D., Davidson, T., Browne, C., Dejana, E.*, et al.* (2009). Sox7 and Sox17 are strain-specific modifiers of the lymphangiogenic defects caused by Sox18 dysfunction in mice. Development *136*, 2385-2391.

Hou, Y., Pazour, G.J., and Witman, G.B. (2004). A dynein light intermediate chain, D1bLIC, is required for retrograde intraflagellar transport. Mol Biol Cell *15*, 4382-4394.

Hu, Q., Milenkovic, L., Jin, H., Scott, M.P., Nachury, M.V., Spiliotis, E.T., and Nelson, W.J. (2010). A septin diffusion barrier at the base of the primary cilium maintains ciliary membrane protein distribution. Science *329*, 436-439.

Huang, C.J., Tu, C.T., Hsiao, C.D., Hsieh, F.J., and Tsai, H.J. (2003). Germ-line transmission of a myocardium-specific GFP transgene reveals critical regulatory elements in the cardiac myosin light chain 2 promoter of zebrafish. Dev Dyn *228*, 30-40.

Huang, J., Papadopoulos, N., McKinley, A.J., Farrington, S.M., Curtis, L.J., Wyllie, A.H., Zheng, S., Willson, J.K., Markowitz, S.D., Morin, P.*, et al.* (1996). APC mutations in colorectal tumors with mismatch repair deficiency. Proc Natl Acad Sci U S A *93*, 9049-9054.

Huang, K., Diener, D.R., and Rosenbaum, J.L. (2009). The ubiquitin conjugation system is involved in the disassembly of cilia and flagella. J Cell Biol *186*, 601-613.

Huang, P., and Schier, A.F. (2009). Dampened Hedgehog signaling but normal Wnt signaling in zebrafish without cilia. Development *136*, 3089-3098.

Huang, P., Xiao, A., Zhou, M., Zhu, Z., Lin, S., and Zhang, B. (2011). Heritable gene targeting in zebrafish using customized TALENs. Nat Biotechnol *29*, 699-700.

Huangfu, D., Liu, A., Rakeman, A.S., Murcia, N.S., Niswander, L., and Anderson, K.V. (2003). Hedgehog signalling in the mouse requires intraflagellar transport proteins. Nature *426*, 83-87.

Hudziak, R.M., Barofsky, E., Barofsky, D.F., Weller, D.L., Huang, S.B., and Weller, D.D. (1996). Resistance of morpholino phosphorodiamidate oligomers to enzymatic degradation. Antisense Nucleic Acid Drug Dev *6*, 267-272.

Hughes, L., O'Brien, S.L., Gallagher, W.M., and McDonnell, S. (2007). DNA microarray-based transcriptomic profiling of an isogenic cell culture model of breast tumour cell invasion. Anticancer Res *27*, 1353-1359.

Inbal, A., Kim, S.H., Shin, J., and Solnica-Krezel, L. (2007). Six3 represses nodal activity to establish early brain asymmetry in zebrafish. Neuron *55*, 407-415.

Inglis, P.N., Boroevich, K.A., and Leroux, M.R. (2006). Piecing together a ciliome. Trends Genet *22*, 491-500.

Iomini, C., Li, L., Mo, W., Dutcher, S.K., and Piperno, G. (2006). Two flagellar genes, AGG2 and AGG3, mediate orientation to light in Chlamydomonas. Curr Biol *16*, 1147-1153.

Ireton, R.C., Davis, M.A., van Hengel, J., Mariner, D.J., Barnes, K., Thoreson, M.A., Anastasiadis, P.Z., Matrisian, L., Bundy, L.M., Sealy, L., et al. (2002). A novel role for p120 catenin in E-cadherin function. J Cell Biol *159*:465-476.

Ishikawa, H., and Marshall, W.F. (2011). Ciliogenesis: building the cell's antenna. Nat Rev Mol Cell Biol *12*, 222-234.

Jacob, F., and Monod, J. (1961). Genetic regulatory mechanisms in the synthesis of proteins. J Mol Biol *3*, 318-356.

Jaffe, A.B., Kaji, N., Durgan, J., and Hall, A. (2008). Cdc42 controls spindle orientation to position the apical surface during epithelial morphogenesis. J Cell Biol *183*:625-633.

Jaffe, K.M., Thiberge, S.Y., Bisher, M.E., and Burdine, R.D. (2010). Imaging cilia in zebrafish. Methods Cell Biol *97*, 415-435.

Jemal, A., Siegel, R., Ward, E., Murray, T., Xu, J., Smigal, C., and Thun, M.J. (2006). Cancer statistics, 2006. CA Cancer J Clin *56*, 106-130.

Jessen, J.R., Topczewski, J., Bingham, S., Sepich, D.S., Marlow, F., Chandrasekhar, A., and Solnica-Krezel, L. (2002). Zebrafish trilobite identifies new roles for Strabismus in gastrulation and neuronal movements. Nat Cell Biol *4*, 610-615.

Jimenez-Preitner, M., Berney, X., and Thorens, B. (2012). Plac8 is required for White Adipocyte Differentiation in vitro and Cell Number Control in vivo. PLoS One *7*, e48767.

Jimenez-Preitner, M., Berney, X., Uldry, M., Vitali, A., Cinti, S., Ledford, J.G., and Thorens, B. (2011). Plac8 is an inducer of C/EBPbeta required for brown fat differentiation, thermoregulation, and control of body weight. Cell Metab *14*, 658-670.

Johnson, R.M., Kerr, M.S., and Slaven, J.E. (2012). Plac8-dependent and inducible NO synthase-dependent mechanisms clear Chlamydia muridarum infections from the genital tract. J Immunol *188*, 1896-1904.

Jones, C., and Chen, P. (2008). Primary cilia in planar cell polarity regulation of the inner ear. Curr Top Dev Biol *85*, 197-224.

Kalluri, R., and Weinberg, R.A. (2009). The basics of epithelial-mesenchymal transition. J Clin Invest *119*, 1420-1428.

Kane, D.A., and Kimmel, C.B. (1993). The zebrafish midblastula transition. Development *119*, 447-456.

Kane, D.A., McFarland, K.N., and Warga, R.M. (2005). Mutations in half baked/E-cadherin block cell behaviors that are necessary for teleost epiboly. Development *132*, 1105-1116.

Kikuchi, Y., Agathon, A., Alexander, J., Thisse, C., Waldron, S., Yelon, D., Thisse, B., and Stainier, D.Y. (2001). casanova encodes a novel Sox-related protein necessary and sufficient for early endoderm formation in zebrafish. Genes Dev *15*, 1493-1505.

Kim, B.C., Lee, H.J., Park, S.H., Lee, S.R., Karpova, T.S., McNally, J.G., Felici, A., Lee, D.K., and Kim, S.J. (2004). Jab1/CSN5, a component of the COP9 signalosome, regulates transforming growth factor beta signaling by binding to Smad7 and promoting its degradation. Mol Cell Biol *24*, 2251-2262.

Kim, S.K., Shindo, A., Park, T.J., Oh, E.C., Ghosh, S., Gray, R.S., Lewis, R.A., Johnson, C.A., Attie-Bittach, T., Katsanis, N.*, et al.* (2010). Planar cell polarity acts through septins to control collective cell movement and ciliogenesis. Science *329*, 1337-1340.

Kimmel, C.B., Ballard, W.W., Kimmel, S.R., Ullmann, B., and Schilling, T.F. (1995). Stages of embryonic development of the zebrafish. Dev Dyn *203*, 253-310.

Kimmel, C.B., Kane, D.A., Walker, C., Warga, R.M., and Rothman, M.B. (1989). A mutation that changes cell movement and cell fate in the zebrafish embryo. Nature *337*, 358-362.

Kimmel, C.B., Warga, R.M., and Schilling, T.F. (1990). Origin and organization of the zebrafish fate map. Development *108*, 581-594.

King, A. (2009). Researchers find their Nemo. Cell *139*, 843-846.

Kinzler, K.W., and Vogelstein, B. (1996). Lessons from hereditary colorectal cancer. Cell *87*, 159-170.

Kishimoto, N., Cao, Y., Park, A., and Sun, Z. (2008). Cystic kidney gene seahorse regulates cilia-mediated processes and Wnt pathways. Dev Cell *14*, 954-961.

Kitadai, Y., Radinsky, R., Bucana, C.D., Takahashi, Y., Xie, K., Tahara, E., and Fidler, I.J. (1996). Regulation of carcinoembryonic antigen expression in human colon carcinoma cells by the organ microenvironment. Am J Pathol *149*:1157-1166.

Knodler, A., Feng, S., Zhang, J., Zhang, X., Das, A., Peranen, J., and Guo, W. (2010). Coordination of Rab8 and Rab11 in primary ciliogenesis. Proc Natl Acad Sci U S A *107*, 6346-6351.

Ko, H.W., Norman, R.X., Tran, J., Fuller, K.P., Fukuda, M., and Eggenschwiler, J.T. (2010). Broad-minded links cell cycle-related kinase to cilia assembly and hedgehog signal transduction. Dev Cell *18*, 237-247.

Kobayashi, T., Tsang, W.Y., Li, J., Lane, W., and Dynlacht, B.D. (2011). Centriolar kinesin Kif24 interacts with CP110 to remodel microtubules and regulate ciliogenesis. Cell *145*, 914-925.

Kochakpour, N. (2009). Immunofluorescent microscopic study of meiosis in zebrafish. Methods Mol Biol *558*, 251-260.

Kodali, V.K., and Thorpe, C. (2010). Quiescin sulfhydryl oxidase from Trypanosoma brucei: catalytic activity and mechanism of a QSOX family member with a single thioredoxin domain. Biochemistry *49*, 2075-2085.

Koppen, M., Fernandez, B.G., Carvalho, L., Jacinto, A., and Heisenberg, C.P. (2006). Coordinated cell-shape changes control epithelial movement in zebrafish and Drosophila. Development *133*, 2671-2681.

Kramer-Zucker, A.G., Olale, F., Haycraft, C.J., Yoder, B.K., Schier, A.F., and Drummond, I.A. (2005). Cilia-driven fluid flow in the zebrafish pronephros, brain and Kupffer's vesicle is required for normal organogenesis. Development *132*, 1907-1921.

Krauss, S., Johansen, T., Korzh, V., and Fjose, A. (1991). Expression of the zebrafish paired box gene pax[zf-b] during early neurogenesis. Development *113*, 1193-1206.

Krebs, L.T., Iwai, N., Nonaka, S., Welsh, I.C., Lan, Y., Jiang, R., Saijoh, Y., O'Brien, T.P., Hamada, H., and Gridley, T. (2003). Notch signaling regulates left-right asymmetry determination by inducing Nodal expression. Genes Dev *17*, 1207-1212.

Kruse, J.P., and Gu, W. (2009). Modes of p53 regulation. Cell *137*, 609-622.

Kwan, K.M., Fujimoto, E., Grabher, C., Mangum, B.D., Hardy, M.E., Campbell, D.S., Parant, J.M., Yost, H.J., Kanki, J.P., and Chien, C.B. (2007). The Tol2kit: a multisite gateway-based construction kit for Tol2 transposon transgenesis constructs. Dev Dyn *236*, 3088-3099.

Kwok, S.F., Staub, J.M., and Deng, X.W. (1999). Characterization of two subunits of Arabidopsis 19S proteasome regulatory complex and its possible interaction with the COP9 complex. J Mol Biol *285*, 85-95.

Langdon, Y.G., and Mullins, M.C. (2011). Maternal and zygotic control of zebrafish dorsoventral axial patterning. Annu Rev Genet *45*, 357-377.

Lange, S.S., Takata, K., and Wood, R.D. (2011). DNA polymerases and cancer. Nat Rev Cancer *11*, 96-110.

Latimer, A., Appel, B. (2006). Notch signaling regulates midline cell specification and proliferation in zebrafish. Dev Biol *298*, 392-402.

Lecoeur, H. (2002). Nuclear apoptosis detection by flow cytometry: influence of endogenous endonucleases. Exp Cell Res *277*, 1-14.

Ledford, J.G., Kovarova, M., and Koller, B.H. (2007). Impaired host defense in mice lacking ONZIN. J Immunol *178*, 5132-5143.

Leibovitz, A., Stinson, J.C., McCombs, W.B., 3rd, McCoy, C.E., Mazur, K.C., and Mabry, N.D. (1976). Classification of human colorectal adenocarcinoma cell lines. Cancer Res *36*:4562-4569.

Leichert, L.I., and Jakob, U. (2006). Global methods to monitor the thiol-disulfide state of proteins in vivo. Antioxid Redox Signal *8*, 763-772.

Li, J.B., Gerdes, J.M., Haycraft, C.J., Fan, Y., Teslovich, T.M., May-Simera, H., Li, H., Blacque, O.E., Li, L., Leitch, C.C.*, et al.* (2004). Comparative genomics identifies a flagellar and basal body proteome that includes the BBS5 human disease gene. Cell *117*, 541-552.

Li, Y., Rogulski, K., Zhou, Q., Sims, P.J., and Prochownik, E.V. (2006). The negative c-Myc target onzin affects proliferation and apoptosis via its obligate interaction with phospholipid scramblase 1. Mol Cell Biol *26*, 3401-3413.

Libault, M., and Stacey, G. (2010). Evolution of FW2.2-like (FWL) and PLAC8 genes in eukaryotes. Plant Signal Behav *5*, 1226-1228.

Lin, F., Chen, S., Sepich, D.S., Panizzi, J.R., Clendenon, S.G., Marrs, J.A., Hamm, H.E., and Solnica-Krezel, L. (2009). Galpha12/13 regulate epiboly by inhibiting E-cadherin activity and modulating the actin cytoskeleton. J Cell Biol *184*, 909-921.

Lin, F., Sepich, D.S., Chen, S., Topczewski, J., Yin, C., Solnica-Krezel, L., and Hamm, H. (2005). Essential roles of G{alpha}12/13 signaling in distinct cell behaviors driving zebrafish convergence and extension gastrulation movements. J Cell Biol *169*, 777-787.

Lin, S., Gaiano, N., Culp, P., Burns, J.C., Friedmann, T., Yee, J.K., and Hopkins, N. (1994). Integration and germ-line transmission of a pseudotyped retroviral vector in zebrafish. Science *265*, 666-669.

Liu, Y., Pathak, N., Kramer-Zucker, A., and Drummond, I.A. (2007). Notch signaling controls the differentiation of transporting epithelia and multiciliated cells in the zebrafish pronephros. Development *134*, 1111-1122.

Loeb, L.A., and Monnat, R.J., Jr. (2008). DNA polymerases and human disease. Nat Rev Genet *9*, 594-604.

Long, S., Ahmad, N., and Rebagliati, M. (2003). The zebrafish nodal-related gene southpaw is required for visceral and diencephalic left-right asymmetry. Development *130*, 2303-2316.

Louvi, A., and Grove, E.A. (2011). Cilia in the CNS: the quiet organelle claims center stage. Neuron *69*, 1046-1060.

Luise, C., Capra, M., Donzelli, M., Mazzarol, G., Jodice, M.G., Nuciforo, P., Viale, G., Di Fiore, P.P., and Confalonieri, S. (2011). An atlas of altered expression of deubiquitinating enzymes in human cancer. PLoS One *6*, e15891.

Lunt, S.C., Haynes, T., and Perkins, B.D. (2009). Zebrafish ift57, ift88, and ift172 intraflagellar transport mutants disrupt cilia but do not affect hedgehog signaling. Dev Dyn *238*, 1744-1759.

Luo, J., Solimini, N.L., and Elledge, S.J. (2009). Principles of cancer therapy: oncogene and non-oncogene addiction. Cell *136*, 823-837.

Lyapina, S., Cope, G., Shevchenko, A., Serino, G., Tsuge, T., Zhou, C., Wolf, D.A., Wei, N., and Deshaies, R.J. (2001). Promotion of NEDD-CUL1 conjugate cleavage by COP9 signalosome. Science *292*, 1382-1385.

MacGurn, J.A., Hsu, P.C., and Emr, S.D. (2012). Ubiquitin and membrane protein turnover: from cradle to grave. Annu Rev Biochem *81*, 231-259.

Mandeville, J.A., Silva Neto, B., Vanni, A.J., Smith, G.L., Rieger-Christ, K.M., Zeheb, R., Loda, M., Libertino, J.A., and Summerhayes, I.C. (2008). P-cadherin as a prognostic indicator and a modulator of migratory behaviour in bladder carcinoma cells. BJU Int *102*:1707-1714.

Marine, J.C. (2012). Spotlight on the role of COP1 in tumorigenesis. Nat Rev Cancer *12*, 455-464.

Marlow, F., Zwartkruis, F., Malicki, J., Neuhauss, S.C., Abbas, L., Weaver, M., Driever, W., and Solnica-Krezel, L. (1998). Functional interactions of genes mediating convergent extension, knypek and trilobite, during the partitioning of the eye primordium in zebrafish. Dev Biol *203*, 382-399.

Marshall, W.F. (2008). Basal bodies platforms for building cilia. Curr Top Dev Biol *85*, 1-22.
McCrea, P.D., Brieher, W.M., and Gumbiner, B.M. (1993). Induction of a secondary body axis in Xenopus by antibodies to beta-catenin. J Cell Biol *123*, 477-484.

Masuda, R., Semba, S., Mizuuchi, E., Yanagihara, K., and Yokozaki, H. (2010). Negative regulation of the tight junction protein tricellulin by snail-induced epithelial-mesenchymal transition in gastric carcinoma cells. Pathobiology *77*:106-113.

McFarland, K.N., Warga, R.M., and Kane, D.A. (2005). Genetic locus half baked is necessary for morphogenesis of the ectoderm. Dev Dyn *233*, 390-406.

McMurray, H.R., Sampson, E.R., Compitello, G., Kinsey, C., Newman, L., Smith, B., Chen, S.R., Klebanov, L., Salzman, P., Yakovlev, A.*, et al.* (2008). Synergistic response to oncogenic mutations defines gene class critical to cancer phenotype. Nature *453*, 1112-1116.

Meetoo, D. (2008). Chronic diseases: the silent global epidemic. Br J Nurs *17*, 1320-1325.

Meng, X., Noyes, M.B., Zhu, L.J., Lawson, N.D., and Wolfe, S.A. (2008). Targeted gene inactivation in zebrafish using engineered zinc-finger nucleases. Nat Biotechnol *26*, 695-701.

Miettinen, P.J., Ebner, R., Lopez, A.R., and Derynck, R. (1994). TGF-beta induced transdifferentiation of mammary epithelial cells to mesenchymal cells: involvement of type I receptors. J Cell Biol *127*:2021-2036.

Milewski, W.M., Duguay, S.J., Chan, S.J., and Steiner, D.F. (1998). Conservation of PDX-1 structure, function, and expression in zebrafish. Endocrinology *139*, 1440-1449.

Milicic, A., Harrison, L.A., Goodlad, R.A., Hardy, R.G., Nicholson, A.M., Presz, M., Sieber, O., Santander, S., Pringle, J.H., Mandir, N., et al. (2008). Ectopic expression of P-cadherin correlates with promoter hypomethylation early in colorectal carcinogenesis and enhanced intestinal crypt fission in vivo. Cancer Res *68*:7760-7768.

Miller, J.C., Tan, S., Qiao, G., Barlow, K.A., Wang, J., Xia, D.F., Meng, X., Paschon, D.E., Leung, E., Hinkley, S.J.*, et al.* (2011). A TALE nuclease architecture for efficient genome editing. Nat Biotechnol *29*, 143-148.

Miyagi, C., Yamashita, S., Ohba, Y., Yoshizaki, H., Matsuda, M., and Hirano, T. (2004). STAT3 noncell-autonomously controls planar cell polarity during zebrafish convergence and extension. J Cell Biol *166*, 975-981.

Mochizuki, T., Wu, G., Hayashi, T., Xenophontos, S.L., Veldhuisen, B., Saris, J.J., Reynolds, D.M., Cai, Y., Gabow, P.A., Pierides, A.*, et al.* (1996). PKD2, a gene for polycystic kidney disease that encodes an integral membrane protein. Science *272*, 1339-1342.

Montero, J.A., Carvalho, L., Wilsch-Brauninger, M., Kilian, B., Mustafa, C., and Heisenberg, C.P. (2005). Shield formation at the onset of zebrafish gastrulation. Development *132*, 1187-1198.

Moreno-Hagelsieb, G., and Latimer, K. (2008). Choosing BLAST options for better detection of orthologs as reciprocal best hits. Bioinformatics *24*, 319-324.

Moscou, M.J., and Bogdanove, A.J. (2009). A simple cipher governs DNA recognition by TAL effectors. Science *326*, 1501.

Moulton, J.D., and Jiang, S. (2009). Gene knockdowns in adult animals: PPMOs and vivo-morpholinos. Molecules *14*, 1304-1323.

Mourtada-Maarabouni, M., Watson, D., Munir, M., Farzaneh, F., and Williams, G.T. (2012). Apoptosis suppression by candidate oncogene PLAC8 is reversed in other cell types. Curr Cancer Drug Targets. Moyer, J.H., Lee-Tischler, M.J., Kwon, H.Y., Schrick, J.J., Avner, E.D., Sweeney, W.E., Godfrey, V.L.,

Moxon, S.A.*, et al.* (2011). ZFIN: enhancements and updates to the Zebrafish Model Organism Database. Nucleic Acids Res *39*, D822-829.

Mukhopadhyay, D., and Riezman, H. (2007). Proteasome-independent functions of ubiquitin in endocytosis and signaling. Science *315*, 201-205.

Muller, F.L., Colla, S., Aquilanti, E., Manzo, V.E., Genovese, G., Lee, J., Eisenson, D., Narurkar, R., Deng, P., Nezi, L.*, et al.* (2012). Passenger deletions generate therapeutic vulnerabilities in cancer. Nature *488*, 337-342.

Muller, H.J. (1932). Further studies on the nature and causes of gene mutations. In: Proceedings of the sixth international congress of genetics. Brooklyn Botanic Gardens, Wisconsin, 1932:213-55.

Muller, H.J. (1946). Nobel Lecture.

Mullins, M.C., Hammerschmidt, M., Haffter, P., and Nusslein-Volhard, C. (1994). Large-scale mutagenesis in the zebrafish: in search of genes controlling development in a vertebrate. Curr Biol *4*, 189-202.

Murcia, N.S., Richards, W.G., Yoder, B.K., Mucenski, M.L., Dunlap, J.R., and Woychik, R.P. (2000). The Oak Ridge Polycystic Kidney (orpk) disease gene is required for left-right axis determination. Development *127*, 2347-2355.

Myers, D.C., Sepich, D.S., and Solnica-Krezel, L. (2002a). Bmp activity gradient regulates convergent extension during zebrafish gastrulation. Dev Biol *243*, 81-98.

Myers, D.C., Sepich, D.S., and Solnica-Krezel, L. (2002b). Convergence and extension in vertebrate gastrulae: cell movements according to or in search of identity? Trends Genet *18*, 447-455.

Nachury, M.V., Loktev, A.V., Zhang, Q., Westlake, C.J., Peranen, J., Merdes, A., Slusarski, D.C., Scheller, R.H., Bazan, J.F., Sheffield, V.C.*, et al.* (2007). A core complex of BBS proteins cooperates with the GTPase Rab8 to promote ciliary membrane biogenesis. Cell *129*, 1201-1213.

Nachury, M.V., Seeley, E.S., and Jin, H. (2010). Trafficking to the ciliary membrane: how to get across the periciliary diffusion barrier? Annu Rev Cell Dev Biol *26*, 59-87.

Nakrieko, K. A., Welch, I., Dupuis, H., Bryce, D., Pajak, A., St Arnaud, R., Dedhar, S., D'Souza, S. J. and Dagnino, L. (2008). Impaired hair follicle morphogenesis and polarized keratinocyte movement upon conditional inactivation of integrin-linked kinase in the epidermis. Mol Biol Cell *19*, 1462-73.

Nandadasa, S., Tao, Q., Menon, N.R., Heasman, J., and Wylie, C. (2009). N- and E-cadherins in Xenopus are specifically required in the neural and non-neural ectoderm, respectively, for F-actin assembly and morphogenetic movements. Development *136*, 1327-1338.

Nasevicius, A., and Ekker, S.C. (2000). Effective targeted gene 'knockdown' in zebrafish. Nat Genet *26*, 216-220.

Nathke, I.S., Hinck, L., Swedlow, J.R., Papkoff, J., and Nelson, W.J. (1994). Defining interactions and distributions of cadherin and catenin complexes in polarized epithelial cells. J Cell Biol *125*:1341-1352.

Nelson, W.J., and Nusse, R. (2004). Convergence of Wnt, beta-catenin, and cadherin pathways. Science *303*, 1483-1487.

Neugebauer, J.M., Amack, J.D., Peterson, A.G., Bisgrove, B.W., and Yost, H.J. (2009). FGF signalling during embryo development regulates cilia length in diverse epithelia. Nature *458*, 651-654.

Nieto, M.A. (2011). The ins and outs of the epithelial to mesenchymal transition in health and disease. Annu Rev Cell Dev Biol *27*, 347-376.

Nieto, M.A., Sargent, M.G., Wilkinson, D.G., and Cooke, J. (1994). Control of cell behavior during vertebrate development by Slug, a zinc finger gene. Science *264*, 835-839.

Nigg, E.A., and Raff, J.W. (2009). Centrioles, centrosomes, and cilia in health and disease. Cell *139*, 663-678.

Nishimura, T., and Takeichi, M. (2009). Remodeling of the adherens junctions during morphogenesis. Curr Top Dev Biol *89*, 33-54.

Nojima, H., Rothhamel, S., Shimizu, T., Kim, C.H., Yonemura, S., Marlow, F.L., and Hibi, M. (2010).

Syntabulin, a motor protein linker, controls dorsal determination. Development *137*, 923-933.

Nonaka, S., Tanaka, Y., Okada, Y., Takeda, S., Harada, A., Kanai, Y., Kido, M., and Hirokawa, N. (1998). Randomization of left-right asymmetry due to loss of nodal cilia generating leftward flow of extraembryonic fluid in mice lacking KIF3B motor protein. Cell *95*, 829-837.

Nowell, P.C. (1976). The clonal evolution of tumor cell populations. Science *194*, 23-28.
Obara, T., Mangos, S., Liu, Y., Zhao, J., Wiessner, S., Kramer-Zucker, A.G., Olale, F., Schier, A.F., and

Drummond, I.A. (2006). Polycystin-2 immunolocalization and function in zebrafish. J Am Soc Nephrol *17*, 2706-2718.

Oda, H., Tsukita, S., and Takeichi, M. (1998). Dynamic behavior of the cadherin-based cell-cell adhesion system during Drosophila gastrulation. Dev Biol *203*, 435-450.

Odenthal, J., and Nusslein-Volhard, C. (1998). fork head domain genes in zebrafish. Dev Genes Evol *208*, 245-258.

Ogawa, M., Fried, J., Sakai, Y., Strife, A., and Clarkson, B.D. (1970). Studies of cellular proliferation in human leukemia. VI. The proliferative activity, generation time, and emergence time of neutrophilic granulocytes in chronic granulocytic leukemia. Cancer *25*, 1031-1049.

Ohkubo, T., and Ozawa, M. (2004). The transcription factor Snail downregulates the tight junction components independently of E-cadherin downregulation. J Cell Sci *117*:1675-1685.

Okabe, N., Xu, B., and Burdine, R.D. (2008). Fluid dynamics in zebrafish Kupffer's vesicle. Dev Dyn *237*, 3602-3612.

Okada, Y., Takeda, S., Tanaka, Y., Izpisua Belmonte, J.C., and Hirokawa, N. (2005). Mechanism of nodal flow: a conserved symmetry breaking event in left-right axis determination. Cell *121*, 633-644.

Oren, M. (2003). Decision making by p53: life, death and cancer. Cell Death Differ *10*, 431-442.
Palombella, V.J., Rando, O.J., Goldberg, A.L., and Maniatis, T. (1994). The ubiquitin-proteasome pathway is required for processing the NF-kappa B1 precursor protein and the activation of NF-kappa B. Cell *78*, 773-785.

Pan, J., You, Y., Huang, T., and Brody, S.L. (2007). RhoA-mediated apical actin enrichment is required for ciliogenesis and promoted by Foxj1. J Cell Sci *120*, 1868-1876.

Panizzi, J.R., Becker-Heck, A., Castleman, V.H., Al-Mutairi, D.A., Liu, Y., Loges, N.T., Pathak, N., Austin-Tse, C., Sheridan, E., Schmidts, M.*, et al.* (2012). CCDC103 mutations cause primary ciliary dyskinesia by disrupting assembly of ciliary dynein arms. Nat Genet *44*, 714-719.

Paredes, J., Correia, A.L., Ribeiro, A.S., Milanezi, F., Cameselle-Teijeiro, J., and Schmitt, F.C. (2008). Breast carcinomas that co-express E- and P-cadherin are associated with p120-catenin cytoplasmic localisation and poor patient survival. J Clin Pathol *61*:856-862.

Paredes, J., Figueiredo, J., Albergaria, A., Oliveira, P., Carvalho, J., Ribeiro, A.S., Caldeira, J., Costa, A.M., Simoes-Correia, J., Oliveira, M.J., et al. (2012). Epithelial E- and P-cadherins: role and clinical significance in cancer. Biochim Biophys Acta *1826*:297-311.

Paredes, J., Stove, C., Stove, V., Milanezi, F., Van Marck, V., Derycke, L., Mareel, M., Bracke, M., and Schmitt, F. (2004). P-cadherin is up-regulated by the antiestrogen ICI 182,780 and promotes invasion of human breast cancer cells. Cancer Res *64*:8309-8317.

Parada, L.F., Tabin, C.J., Shih, C., and Weinberg, R.A. (1982). Human EJ bladder carcinoma oncogene is homologue of Harvey sarcoma virus ras gene. Nature *297*, 474-478.

Park, J., Park, E., Han, S.W., Im, S.A., Kim, T.Y., Kim, W.H., Oh, D.Y., and Bang, Y.J. (2012). Down-regulation of P-cadherin with PF-03732010 inhibits cell migration and tumor growth in gastric cancer. Invest New Drugs *30*,1404-1412.

Park, T.J., Mitchell, B.J., Abitua, P.B., Kintner, C., and Wallingford, J.B. (2008). Dishevelled controls apical docking and planar polarization of basal bodies in ciliated epithelial cells. Nat Genet *40*, 871-879.

Phillips, B.T., Bolding, K., and Riley, B.B. (2001). Zebrafish fgf3 and fgf8 encode redundant functions required for otic placode induction. Dev Biol *235*, 351-365.

Pickart, C.M. (2001). Ubiquitin enters the new millennium. Mol Cell *8*, 499-504.

Piepenhagen, P.A., and Nelson, W.J. (1993). Defining E-cadherin-associated protein complexes in epithelial cells: plakoglobin, beta- and gamma-catenin are distinct components. J Cell Sci *104* (Pt 3):751-762.

Powell, A.E., Wang, Y., Li, Y., Poulin, E.J., Means, A.L., Washington, M.K., Higginbotham, J.N., Juchheim, A., Prasad, N., Levy, S.E., et al. (2012). The pan-ErbB negative regulator Lrig1 is an intestinal stem cell marker that functions as a tumor suppressor. Cell *149*:146-158.

Prives, C., and Hall, P.A. (1999). The p53 pathway. J Pathol *187*, 112-126.

Qin, H., Rosenbaum, J.L., and Barr, M.M. (2001). An autosomal recessive polycystic kidney disease gene homolog is involved in intraflagellar transport in C. elegans ciliated sensory neurons. Curr Biol *11*, 457-461.

Quintana, E., Shackleton, M., Sabel, M.S., Fullen, D.R., Johnson, T.M., and Morrison, S.J. (2008). Efficient tumour formation by single human melanoma cells. Nature *456*, 593-598.

Rajagopalan, H., Nowak, M.A., Vogelstein, B., and Lengauer, C. (2003). The significance of unstable chromosomes in colorectal cancer. Nat Rev Cancer *3*, 695-701.

Raya, A., Kawakami, Y., Rodriguez-Esteban, C., Buscher, D., Koth, C.M., Itoh, T., Morita, M., Raya, R.M., Dubova, I., Bessa, J.G.*, et al.* (2003). Notch activity induces Nodal expression and mediates the establishment of left-right asymmetry in vertebrate embryos. Genes Dev *17*, 1213-1218.

Reifers, F., Bohli, H., Walsh, E.C., Crossley, P.H., Stainier, D.Y., and Brand, M. (1998). Fgf8 is mutated in zebrafish acerebellar (ace) mutants and is required for maintenance of midbrain-hindbrain boundary development and somitogenesis. Development *125*, 2381-2395.

Rijsewijk, F., Schuermann, M., Wagenaar, E., Parren, P., Weigel, D., and Nusse, R. (1987). The Drosophila homolog of the mouse mammary oncogene int-1 is identical to the segment polarity gene wingless. Cell *50*, 649-657.

Riordan, J.R., Rommens, J.M., Kerem, B., Alon, N., Rozmahel, R., Grzelczak, Z., Zielenski, J., Lok, S., Plavsic, N., Chou, J.L.*, et al.* (1989). Identification of the cystic fibrosis gene: cloning and characterization of complementary DNA. Science *245*, 1066-1073.

Rissoan, M.C., Duhen, T., Bridon, J.M., Bendriss-Vermare, N., Peronne, C., de Saint Vis, B., Briere, F., and Bates, E.E. (2002). Subtractive hybridization reveals the expression of immunoglobulin-like transcript 7, Eph-B1, granzyme B, and 3 novel transcripts in human plasmacytoid dendritic cells. Blood *100*, 3295-3303.

Riz, I., Hawley, T.S., Luu, T.V., Lee, N.H., and Hawley, R.G. (2010). TLX1 and NOTCH coregulate transcription in T cell acute lymphoblastic leukemia cells. Mol Cancer *9*, 181.

Rodrigo-Brenni, M.C., Foster, S.A., and Morgan, D.O. (2010). Catalysis of lysine 48-specific ubiquitin chain assembly by residues in E2 and ubiquitin. Mol Cell *39*, 548-559.

Rogulski, K., Li, Y., Rothermund, K., Pu, L., Watkins, S., Yi, F., and Prochownik, E.V. (2005). Onzin, a c-Myc-repressed target, promotes survival and transformation by modulating the Akt-Mdm2-p53 pathway. Oncogene *24*, 7524-7541.

Rohatgi, R., Milenkovic, L., and Scott, M.P. (2007). Patched1 regulates hedgehog signaling at the primary cilium. Science *317*, 372-376.

Rohatgi, R., and Snell, W.J. (2010). The ciliary membrane. Curr Opin Cell Biol *22*, 541-546.

Rohde, L.A., and Heisenberg, C.P. (2007). Zebrafish gastrulation: cell movements, signals, and mechanisms. Int Rev Cytol *261*, 159-192.

Rosenzweig, R., Osmulski, P.A., Gaczynska, M., and Glickman, M.H. (2008). The central unit within the 19S regulatory particle of the proteasome. Nat Struct Mol Biol *15*, 573-580.

Roszko, I., Sawada, A., and Solnica-Krezel, L. (2009). Regulation of convergence and extension movements during vertebrate gastrulation by the Wnt/PCP pathway. Semin Cell Dev Biol *20*, 986-997.

Saha, A., and Deshaies, R.J. (2008). Multimodal activation of the ubiquitin ligase SCF by Nedd8 conjugation. Mol Cell *32*, 21-31.
Sakaguchi, T., Kikuchi, Y., Kuroiwa, A., Takeda, H., and Stainier, D.Y. (2006). The yolk syncytial layer regulates myocardial migration by influencing extracellular matrix assembly in zebrafish. Development *133*, 4063-4072.

Sander, J.D., Cade, L., Khayter, C., Reyon, D., Peterson, R.T., Joung, J.K., Yeh, J.R. (2011). Targeted gene disruption in somatic zebrafish cells using engineered TALENs. Nat Biotechnol *29*, 697-698.

Sanjana, N.E., Cong, L., Zhou, Y., Cunniff, M.M., Feng, G., and Zhang, F. (2012). A transcription activator-like effector toolbox for genome engineering. Nat Protoc *7*, 171-192.

Santoriello, C., and Zon, L.I. (2012). Hooked! Modeling human disease in zebrafish. J Clin Invest *122*, 2337-2343.

Satir, P., and Christensen, S.T. (2007). Overview of structure and function of mammalian cilia. Annu Rev Physiol *69*, 377-400.

Schauerte, H.E., van Eeden, F.J., Fricke, C., Odenthal, J., Strahle, U., and Haffter, P. (1998). Sonic hedgehog is not required for the induction of medial floor plate cells in the zebrafish. Development *125*, 2983-2993.

Scheffner, M., Nuber, U., and Huibregtse, J.M. (1995). Protein ubiquitination involving an E1-E2-E3 enzyme ubiquitin thioester cascade. Nature *373*, 81-83.

Schier, A.F., and Talbot, W.S. (2005). Molecular genetics of axis formation in zebrafish. Annu Rev Genet *39*, 561-613.

Schneider, L., Clement, C.A., Teilmann, S.C., Pazour, G.J., Hoffmann, E.K., Satir, P., and Christensen, S.T. (2005). PDGFRalphaalpha signaling is regulated through the primary cilium in fibroblasts. Curr Biol *15*, 1861-1866.

Schneider, S., Steinbeisser, H., Warga, R.M., and Hausen, P. (1996). Beta-catenin translocation into nuclei demarcates the dorsalizing centers in frog and fish embryos. Mech Dev *57*, 191-198.

Schottenfeld, J., Sullivan-Brown, J., and Burdine, R.D. (2007). Zebrafish curly up encodes a Pkd2 ortholog that restricts left-side-specific expression of southpaw. Development *134*, 1605-1615.

Schulte-Merker, S., Lee, K.J., McMahon, A.P., and Hammerschmidt, M. (1997). The zebrafish organizer requires chordino. Nature *387*, 862-863.

Schwechheimer, C. (2004). The COP9 signalosome (CSN): an evolutionary conserved proteolysis regulator in eukaryotic development. Biochim Biophys Acta *1695*, 45-54.

Schwechheimer, C., and Deng, X.W. (2001). COP9 signalosome revisited: a novel mediator of protein degradation. Trends Cell Biol *11*, 420-426.

Schwechheimer, C., Serino, G., Callis, J., Crosby, W.L., Lyapina, S., Deshaies, R.J., Gray, W.M., Estelle, M., and Deng, X.W. (2001). Interactions of the COP9 signalosome with the E3 ubiquitin ligase SCFTIRI in mediating auxin response. Science *292*, 1379-1382.

Schweitzer, K., Bozko, P.M., Dubiel, W., and Naumann, M. (2007). CSN controls NF-kappaB by deubiquitinylation of IkappaBalpha. EMBO J *26*, 1532-1541.

Sepich, D.S., Calmelet, C., Kiskowski, M., and Solnica-Krezel, L. (2005). Initiation of convergence and extension movements of lateral mesoderm during zebrafish gastrulation. Dev Dyn *234*, 279-292.

Sepich, D.S., Myers, D.C., Short, R., Topczewski, J., Marlow, F., and Solnica-Krezel, L. (2000). Role of the zebrafish trilobite locus in gastrulation movements of convergence and extension. Genesis *27*, 159-173.

Sepich, D.S., Usmani, M., Pawlicki, S., and Solnica-Krezel, L. (2011). Wnt/PCP signaling controls intracellular position of MTOCs during gastrulation convergence and extension movements. Development *138*, 543-552.

Serino, G., Tsuge, T., Kwok, S., Matsui, M., Wei, N., and Deng, X.W. (1999). Arabidopsis cop8 and fus4 mutations define the same gene that encodes subunit 4 of the COP9 signalosome. Plant Cell *11*, 1967-1980.

Shimizu, T., Yabe, T., Muraoka, O., Yonemura, S., Aramaki, S., Hatta, K., Bae, Y.K., Nojima, H., and Hibi, M. (2005). E-cadherin is required for gastrulation cell movements in zebrafish. Mech Dev *122*, 747-763.

Shin, S., Dimitri, C.A., Yoon, S.O., Dowdle, W., and Blenis, J. (2010). ERK2 but not ERK1 induces epithelial-to-mesenchymal transformation via DEF motif-dependent signaling events. Mol Cell *38*:114-127.

Siekmann, A.F., and Lawson, N.D. (2007). Notch signalling limits angiogenic cell behaviour in developing zebrafish arteries. Nature *445*, 781-784.

Simons, M., Gloy, J., Ganner, A., Bullerkotte, A., Bashkurov, M., Kronig, C., Schermer, B., Benzing, T., Cabello, O.A., Jenny, A.*, et al.* (2005). Inversin, the gene product mutated in nephronophthisis type II, functions as a molecular switch between Wnt signaling pathways. Nat Genet *37*, 537-543.

Smith, S.C., and Theodorescu, D. (2009). Learning therapeutic lessons from metastasis suppressor proteins. Nat Rev Cancer *9*, 253-264.

Soini, Y. (2012). Tight junctions in lung cancer and lung metastasis: a review. Int J Clin Exp Pathol *5*:126-136.

Snouwaert, J.N., Brigman, K.K., Latour, A.M., Malouf, N.N., Boucher, R.C., Smithies, O., and Koller, B.H. (1992). An animal model for cystic fibrosis made by gene targeting. Science *257*, 1083-1088.

Solnica-Krezel, L. (1999). Pattern formation in zebrafish--fruitful liaisons between embryology and genetics. Curr Top Dev Biol *41*, 1-35.

Solnica-Krezel, L. (2005). Conserved patterns of cell movements during vertebrate gastrulation. Curr Biol *15*, R213-228.

Solnica-Krezel, L. (2006). Gastrulation in zebrafish -- all just about adhesion? Curr Opin Genet Dev *16*, 433-441.

Solnica-Krezel, L., Schier, A.F., and Driever, W. (1994). Efficient recovery of ENU-induced mutations from the zebrafish germline. Genetics *136*, 1401-1420.

Solnica-Krezel, L., and Driever, W. (1994). Microtubule arrays of the zebrafish yolk cell: organization and function during epiboly. Development *120*, 2443-2455.

Solnica-Krezel, L., and Sepich, D.S. (2012). Gastrulation: making and shaping germ layers. Annu Rev Cell Dev Biol *28*, 687-717.

Solnica-Krezel, L., Stemple, D.L., and Driever, W. (1995). Transparent things: cell fates and cell movements during early embryogenesis of zebrafish. Bioessays *17*, 931-939.

Solnica-Krezel, L., Stemple, D.L., Mountcastle-Shah, E., Rangini, Z., Neuhauss, S.C., Malicki, J., Schier, A.F., Stainier, D.Y., Zwartkruis, F., Abdelilah, S.*, et al.* (1996). Mutations affecting cell fates and cellular rearrangements during gastrulation in zebrafish. Development *123*, 67-80.

Song, H., Hu, J., Chen, W., Elliott, G., Andre, P., Gao, B., and Yang, Y. (2010). Planar cell polarity breaks bilateral symmetry by controlling ciliary positioning. Nature *466*, 378-382.

Song, W.Y., Hortensteiner, S., Tomioka, R., Lee, Y., and Martinoia, E. (2011). Common functions or only phylogenetically related? The large family of PLAC8 motif-containing/PCR genes. Mol Cells *31*, 1-7.

Spain, B.H., Bowdish, K.S., Pacal, A.R., Staub, S.F., Koo, D., Chang, C.Y., Xie, W., and Colicelli, J. (1996). Two human cDNAs, including a homolog of Arabidopsis FUS6 (COP11), suppress G-protein- and mitogen-activated protein kinase-mediated signal transduction in yeast and mammalian cells. Mol Cell Biol *16*, 6698-6706.

Speirs, C.K., Jernigan, K.K., Kim, S.H., Cha, Y.I., Lin, F., Sepich, D.S., DuBois, R.N., Lee, E., and Solnica-Krezel, L. (2010). Prostaglandin Gbetagamma signaling stimulates gastrulation movements by limiting cell adhesion through Snai1a stabilization. Development *137*, 1327-1337.

Stern, C.D. (2002). Embryology: fluid flow and broken symmetry. Nature *418*, 29-30.

Stubbs, J.L., Oishi, I., Izpisua Belmonte, J.C., and Kintner, C. (2008). The forkhead protein Foxj1 specifies node-like cilia in Xenopus and zebrafish embryos. Nat Genet *40*, 1454-1460.

Sun, L., Hu, H., Peng, L., Zhou, Z., Zhao, X., Pan, J., Sun, L., Yang, Z., and Ran, Y. (2011). P-cadherin promotes liver metastasis and is associated with poor prognosis in colon cancer. Am J Pathol *179*:380-390.

Sun, Z., Amsterdam, A., Pazour, G.J., Cole, D.G., Miller, M.S., and Hopkins, N. (2004). A genetic screen in zebrafish identifies cilia genes as a principal cause of cystic kidney. Development *131*, 4085-4093.

Surendran, K., Selassie, M., Liapis, H., Krigman, H., and Kopan, R. (2010). Reduced Notch signaling leads to renal cysts and papillary microadenomas. J Am Soc Nephrol *21*, 819-832.

Tabin, C.J., Bradley, S.M., Bargmann, C.I., Weinberg, R.A., Papageorge, A.G., Scolnick, E.M., Dhar, R., Lowy, D.R., and Chang, E.H. (1982). Mechanism of activation of a human oncogene. Nature *300*, 143-149.

Takeichi, M. (1987). [Cellular and molecular basis for tissue construction: role of cadherins in selective cell adhesion]. Seikagaku *59*, 1-9.

Taniuchi, K., Nakagawa, H., Hosokawa, M., Nakamura, T., Eguchi, H., Ohigashi, H., Ishikawa, O., Katagiri, T., and Nakamura, Y. (2005). Overexpressed P-cadherin/CDH3 promotes motility of pancreatic cancer cells by interacting with p120ctn and activating rho-family GTPases. Cancer Res *65*:3092-3099.

Thiery, J.P., Acloque, H., Huang, R.Y., and Nieto, M.A. (2009). Epithelial-mesenchymal transitions in development and disease. Cell *139*, 871-890.

Thiery, J.P., and Sleeman, J.P. (2006). Complex networks orchestrate epithelial-mesenchymal transitions. Nat Rev Mol Cell Biol *7*, 131-142.

Thisse, C., and Thisse, B. (2008). High-resolution in situ hybridization to whole-mount zebrafish embryos. Nat Protoc *3*, 59-69.

Tomoda, K., Yoneda-Kato, N., Fukumoto, A., Yamanaka, S., and Kato, J.Y. (2004). Multiple functions of Jab1 are required for early embryonic development and growth potential in mice. J Biol Chem *279*,

43013-43018.

Topczewski, J., Sepich, D.S., Myers, D.C., Walker, C., Amores, A., Lele, Z., Hammerschmidt, M., Postlethwait, J., and Solnica-Krezel, L. (2001). The zebrafish glypican knypek controls cell polarity during gastrulation movements of convergent extension. Dev Cell *1*, 251-264.

Tran, P.V., Haycraft, C.J., Besschetnova, T.Y., Turbe-Doan, A., Stottmann, R.W., Herron, B.J., Chesebro, A.L., Qiu, H., Scherz, P.J., Shah, J.V.*, et al.* (2008). THM1 negatively modulates mouse sonic hedgehog signal transduction and affects retrograde intraflagellar transport in cilia. Nat Genet *40*, 403-410.

Tsujikawa, M., and Malicki, J. (2004). Intraflagellar transport genes are essential for differentiation and survival of vertebrate sensory neurons. Neuron *42*, 703-716.

Valastyan, S., and Weinberg, R.A. (2011). Tumor metastasis: molecular insights and evolving paradigms. Cell *147*, 275-292.

van Eeden, F.J., Granato, M., Schach, U., Brand, M., Furutani-Seiki, M., Haffter, P., Hammerschmidt, M., Heisenberg, C.P., Jiang, Y.J., Kane, D.A.*, et al.* (1996). Mutations affecting somite formation and patterning in the zebrafish, Danio rerio. Development *123*, 153-164.

Verdeguer, F., Le Corre, S., Fischer, E., Callens, C., Garbay, S., Doyen, A., Igarashi, P., Terzi, F., and Pontoglio, M. (2010). A mitotic transcriptional switch in polycystic kidney disease. Nat Med *16*, 106-110.

Vieira, O.V., Gaus, K., Verkade, P., Fullekrug, J., Vaz, W.L., and Simons, K. (2006). FAPP2, cilium formation, and compartmentalization of the apical membrane in polarized Madin-Darby canine kidney (MDCK) cells. Proc Natl Acad Sci U S A *103*, 18556-18561.

Villefranc, J.A., Amigo, J., and Lawson, N.D. (2007). Gateway compatible vectors for analysis of gene function in the zebrafish. Dev Dyn *236*, 3077-3087.

Vogelstein, B., and Kinzler, K.W. (2004). Cancer genes and the pathways they control. Nat Med *10*, 789-799.

Vogelstein, B., Lane, D., and Levine, A.J. (2000). Surfing the p53 network. Nature *408*, 307-310.

von Arnim, A.G. (2003). On again-off again: COP9 signalosome turns the key on protein degradation. Curr Opin Plant Biol *6*, 520-529.

von der Hardt, S., Bakkers, J., Inbal, A., Carvalho, L., Solnica-Krezel, L., Heisenberg, C.P., and Hammerschmidt, M. (2007). The Bmp gradient of the zebrafish gastrula guides migrating lateral cells by regulating cell-cell adhesion. Curr Biol *17*, 475-487.

Wallingford, J.B. (2010). Planar cell polarity signaling, cilia and polarized ciliary beating. Curr Opin Cell Biol *22*, 597-604.

Wallingford, J.B., and Mitchell, B. (2011). Strange as it may seem: the many links between Wnt signaling, planar cell polarity, and cilia. Genes Dev *25*, 201-213.

Walsh, C. (2005). Posttranslational Modification of Proteins: Expanding Nature's Inventory. Roberts and Company Publishers. 1st edition. ISBN-13: 978-0974707730.

Wang, J., Yuan, Y., Zhou, Y., Guo, L., Zhang, L., Kuai, X., Deng, B., Pan, Z., Li, D., and He, F. (2008). Protein interaction data set highlighted with human Ras-MAPK/PI3K signaling pathways. J Proteome Res *7*, 3879-3889.

Ward, P.S., Patel, J., Wise, D.R., Abdel-Wahab, O., Bennett, B.D., Coller, H.A., Cross, J.R., Fantin, V.R.,

Hedvat, C.V., Perl, A.E.*, et al.* (2010). The common feature of leukemia-associated IDH1 and IDH2 mutations is a neomorphic enzyme activity converting alpha-ketoglutarate to 2-hydroxyglutarate. Cancer Cell *17*, 225-234.

Warga, R.M., and Kimmel, C.B. (1990). Cell movements during epiboly and gastrulation in zebrafish. Development *108*, 569-580.

Wei, N., and Deng, X.W. (1999). Making sense of the COP9 signalosome. A regulatory protein complex conserved from Arabidopsis to human. Trends Genet *15*, 98-103.

Wei, N., and Deng, X.W. (2003). The COP9 signalosome. Annu Rev Cell Dev Biol *19*, 261-286.

Wei, N., Serino, G., and Deng, X.W. (2008). The COP9 signalosome: more than a protease. Trends Biochem Sci *33*, 592-600.

Wei, N., Tsuge, T., Serino, G., Dohmae, N., Takio, K., Matsui, M., and Deng, X.W. (1998). The COP9 complex is conserved between plants and mammals and is related to the 26S proteasome regulatory complex. Curr Biol *8*, 919-922.

Wei, Q., Zhang, Y., Li, Y., Zhang, Q., Ling, K., and Hu, J. (2012). The BBSome controls IFT assembly and turnaround in cilia. Nat Cell Biol *14*, 950-957.

Weissman, A.M. (2001). Themes and variations on ubiquitylation. Nat Rev Mol Cell Biol *2*, 169-178.

Welch, J.S., Ley, T.J., Link, D.C., Miller, C.A., Larson, D.E., Koboldt, D.C., Wartman, L.D., Lamprecht, T.L., Liu, F., Xia, J.*, et al.* (2012). The origin and evolution of mutations in acute myeloid leukemia. Cell *150*, 264-278.

Wickliffe, K.E., Lorenz, S., Wemmer, D.E., Kuriyan, J., and Rape, M. (2011). The mechanism of linkage-specific ubiquitin chain elongation by a single-subunit E2. Cell *144*, 769-781.

Wienholds, E., van Eeden, F., Kosters, M., Mudde, J., Plasterk, R.H., and Cuppen, E. (2003). Efficient target-selected mutagenesis in zebrafish. Genome Res *13*, 2700-2707.

Wiens, C.J., Tong, Y., Esmail, M.A., Oh, E., Gerdes, J.M., Wang, J., Tempel, W., Rattner, J.B., Katsanis, N., Park, H.W.*, et al.* (2010). Bardet-Biedl syndrome-associated small GTPase ARL6 (BBS3) functions at or near the ciliary gate and modulates Wnt signaling. J Biol Chem *285*, 16218-16230.

Wilkie, A.O. (1994). The molecular basis of genetic dominance. J Med Genet *31*, 89-98.

Wilson, C.W., Nguyen, C.T., Chen, M.H., Yang, J.H., Gacayan, R., Huang, J., Chen, J.N., and Chuang, P.T. (2009). Fused has evolved divergent roles in vertebrate Hedgehog signalling and motile ciliogenesis. Nature *459*, 98-102.

Woods, I.G., Kelly, P.D., Chu, F., Ngo-Hazelett, P., Yan, Y.L., Huang, H., Postlethwait, J.H., and Talbot, W.S. (2000). A comparative map of the zebrafish genome. Genome Res *10*, 1903-1914.

Woods, I.G., and Talbot, W.S. (2005). The you gene encodes an EGF-CUB protein essential for Hedgehog signaling in zebrafish. PLoS Biol *3*, e66.

Wu, G., Mochizuki, T., Le, T.C., Cai, Y., Hayashi, T., Reynolds, D.M., and Somlo, S. (1997). Molecular cloning, cDNA sequence analysis, and chromosomal localization of mouse Pkd2. Genomics *45*, 220-223.

Wu, G., and Somlo, S. (2000). Molecular genetics and mechanism of autosomal dominant polycystic kidney disease. Mol Genet Metab *69*, 1-15.

Wu, S.F., Huang, Y., Hou, J.K., Yuan, T.T., Zhou, C.X., Zhang, J., and Chen, G.Q. (2010). The downregulation of onzin expression by PKCepsilon-ERK2 signaling and its potential role in AML cell differentiation. Leukemia *24*, 544-551.

Wu, S.Y., Shin, J., Sepich, D.S., and Solnica-Krezel, L. (2012). Chemokine GPCR Signaling Inhibits beta-Catenin during Zebrafish Axis Formation. PLoS Biol *10*, e1001403.

Yamashita, S., Miyagi, C., Carmany-Rampey, A., Shimizu, T., Fujii, R., Schier, A.F., and Hirano, T. (2002). Stat3 Controls Cell Movements during Zebrafish Gastrulation. Dev Cell *2*, 363-375.

Yamashita, S., Miyagi, C., Fukada, T., Kagara, N., Che, Y.S., and Hirano, T. (2004). Zinc transporter LIVI controls epithelial-mesenchymal transition in zebrafish gastrula organizer. Nature *429*, 298-302.

Yang, J., Mani, S.A., Donaher, J.L., Ramaswamy, S., Itzykson, R.A., Come, C., Savagner, P., Gitelman, I., Richardson, A., and Weinberg, R.A. (2004). Twist, a master regulator of morphogenesis, plays an essential role in tumor metastasis. Cell *117*, 927-939.

Yang, J.Y., Zong, C.S., Xia, W., Wei, Y., Ali-Seyed, M., Li, Z., Broglio, K., Berry, D.A., and Hung, M.C. (2006). MDM2 promotes cell motility and invasiveness by regulating E-cadherin degradation. Mol Cell Biol *26*, 7269-7282.

Yasui, W., Oue, N., Aung, P.P., Matsumura, S., Shutoh, M., and Nakayama, H. (2005). Molecular-pathological prognostic factors of gastric cancer: a review. Gastric Cancer *8*, 86-94.

Yelon, D., Horne, S.A., and Stainier, D.Y. (1999). Restricted expression of cardiac myosin genes reveals regulated aspects of heart tube assembly in zebrafish. Dev Biol *214*, 23-37.

Yi, C., and Deng, X.W. (2005). COP1 - from plant photomorphogenesis to mammalian tumorigenesis. Trends Cell Biol *15*, 618-625.

Yin, C., Ciruna, B., and Solnica-Krezel, L. (2009). Convergence and extension movements during vertebrate gastrulation. Curr Top Dev Biol *89*, 163-192.

Yoneda-Kato, N., Tomoda, K., Umehara, M., Arata, Y., and Kato, J.Y. (2005). Myeloid leukemia factor 1 regulates p53 by suppressing COP1 via COP9 signalosome subunit 3. EMBO J *24*, 1739-1749.

Yu, X., Ng, C.P., Habacher, H., and Roy, S. (2008). Foxj1 transcription factors are master regulators of the motile ciliogenic program. Nat Genet *40*, 1445-1453.

Zalik, S.E., Lewandowski, E., Kam, Z., and Geiger, B. (1999). Cell adhesion and the actin cytoskeleton of the enveloping layer in the zebrafish embryo during epiboly. Biochem Cell Biol *77*, 527-542.

Zhang, X.C., Chen, J., Su, C.H., Yang, H.Y., and Lee, M.H. (2008). Roles for CSN5 in control of p53/MDM2 activities. J Cell Biochem *103*, 1219-1230.

Zhao, C., and Malicki, J. (2007). Genetic defects of pronephric cilia in zebrafish. Mech Dev *124*, 605-616.

Zhao, R., Yeung, S.C., Chen, J., Iwakuma, T., Su, C.H., Chen, B., Qu, C., Zhang, F., Chen, Y.T., Lin, Y.L.*, et al.* (2011). Subunit 6 of the COP9 signalosome promotes tumorigenesis in mice through stabilization of MDM2 and is upregulated in human cancers. J Clin Invest *121*, 851-865.

Zhong, H., and Lin, S. (2011). Chemical screening with zebrafish embryos. Methods Mol Biol *716*, 193-205.

HAITING MA

Department of Developmental Biology
Washington University in St. Louis
660 South Euclid Street, St. Louis, MO 63110
United States
Email: haiting.ma@wustl.edu

EDUCATION

Jul 2010—present: PhD candidate, Department of Developmental, Regenerative, and Stem Cell Biology, Washington University in St. Louis, USA. Thesis mentors: Dr. Lilianna Solnica-Krezel and Dr. Robert. J. Coffey.

Aug 2007—Jun 2010: PhD candidate, Department of Biology, Vanderbilt University, USA. Thesis mentors: Dr. Lilianna Solnica-Krezel and Dr. Robert. J. Coffey.

Sep 2004—May 2007 MSc: Department of Biochemistry, Schulich School of Medicine and Dentistry, the University of Western Ontario, Canada. Thesis mentor: Dr. Shawn S. C. Li.

Sep 2000—July 2004 BS in Biotechnology: College of Life Sciences, Nankai University, China. Thesis mentor: Dr. Laijun Xing and Dr. Qi Zhang.

PUBLICATIONS AND MANUSCRIPTS

1. Terence J. Van Raay, Nicholas J. Fortino, Bryan W. Miller, **Haiting Ma**, Garnet Lau, Cunxi Li, Jeffery L. Franklin, Liliana Attisano, Lilianna Solnica-Krezel, Robert J. Coffey. Naked1 antagonizes Wnt signaling by preventing nuclear accumulation of β−catenin. **PLoS One. (2011) 6(4):e18650.**

2. Chenggang Wu*, **Haiting Ma***, Kevin R. Brown, Matt Geisler, Lei Li, Eve Tzeng, Christina Y. H. Jia, Igor Jurisica and Shawn S.-C. Li. Systematic identification of SH3 domain-mediated human protein-protein interactions by peptide array target screening. **Proteomics 7 (2007):1775-1785.** (* denotes equal contributions).

3. Qi Zhang, Mingchun Li, **Haiting Ma**, Ying Sun, Laijun Xing. Identification and characterization of a novel Δ6-fatty acid desaturase gene from *Rhizopus arrhizus*. **FEBS Letters 556 (2004): 81-85.**

4. Qi Zhang, Mingchun Li, Ying Sun, **Haiting Ma**, Laijun Xing, Hongyan Sun, Yong Ren. Influence of sequence modification flanking AUG codon on Δ6-fatty acid desaturase gene expression. **Acta Microbiologica Sinica 44 (2004): 536-539.**

5. Qi Zhang, Mingchun Li, Hongyan Sun, Ying Sun, **Haiting Ma**, Laijun Xing. “Progress on molecular biology of Δ6-fatty acid desaturases.” **Chinese Journal of Biotechnology 20 (2004): 319-324.**

6. Qi Zhang, Mingchun Li, Ying Sun, **Haiting Ma**, Yong Ren, Laijun Xing. Cloning and heterologous expression of a novel Δ6-fatty acid desaturase gene from *Rhizopus arrhizus* NK030037. **Yi Chuan Xue Bao 31 (2004): 740-749.**

SOLICITED PEER-REVIEW

PLoS ONE

PRESENTATION AT MEETINGS AND SYMPOSIA

1. **Haiting Ma**, Cunxi Li, Robert J Coffey, Lilianna Solnica-Krezel. Zebrafish *placenta-specific 8.1* (*plac8.1*) links ubiquitination regulating protein Cops4 to motile cilia morphogenesis and function. Selected talk, Society for Developmental Biology 71st Annual Meeting. Montreal, QC, Canada.

2. **Haiting Ma**. Connection of ubiquitination regulating protein Cops4 to motile cilia morphogenesis and function revealed by zebrafish *placenta-specific 8.1* (*plac8.1*). 20th Annual Developmental Biology Retreat. 2012. Washington University in St. Louis.

3. **Haiting Ma**. Plac8.1 affects motile cilia and cell adhesion during zebrafish embryogenesis. Apr 4, 2012. Developmental biology research forum, Washington University in St. Louis.

4. **Haiting Ma**, Cunxi Li, Robert J Coffey, Lilianna Solnica-Krezel. Zebrafish *placenta-specific 8.1* (*plac8.1*) is required for motile cilia morphogenesis and function. Poster presentation, Society for Developmental Biology 70th Annual Meeting. Chicago, IL.

5. **Haiting Ma**. Zebrafish *placenta-specific 8.1* (*plac8.1*) is required for motile cilia morphogenesis and function. 19th Annual Developmental Biology Retreat. 2011. Washington University in St. Louis. Winning the **Viktor Hamburger Award** for the best student talk.

6. **Haiting Ma**. Functional characterization of zebrafish *placenta-specific 8.1* (*plac8.1*). Apr 13, 2012. Developmental biology research forum, Washington University in St. Louis.

7. **Haiting Ma**, Cunxi Li, Robert J Coffey, Lilianna Solnica-Krezel. Zebrafish *placenta-specific 8.1* (*plac8.1*) is required for motile cilia morphogenesis and activity. Feb 26, 2011. The sixteenth annual graduate student research symposium, Washington University in St. Louis.

8. **Haiting Ma**, Cunxi Li, Robert J Coffey, Lilianna Solnica-Krezel. 2010. Zebrafish *placenta-specific 8* (*plac8*) homolog is required for motile cilia activity, and its overexpression results in gastrulation defects. Oral presentation. The 9th international meeting on zebrafish development and genetics. Madison, WI.

9. **Haiting Ma**. Functional characterization of zebrafish homolog of *placenta specific 8* (*plac8*). Mar 26, 2010. Invited talk, Vanderbilt University the 24th graduate student research symposium.

10. Terry Van Raay, **Haiting Ma**, Nicholas J. Fortino, Cunxi Li, Jeffery L. Franklin, Lilianna Solnica-Krezel, Robert J. Coffey. 2010. Naked1 Antagonizes Wnt Signaling by Preventing Nuclear Accumulation of β-catenin. Poster presentation. The 9th international meeting on zebrafish development and genetics. Madison, WI.

11. Nanbing (Jade) Li, **Haiting Ma**, Seok-Hyung Kim, Diane Sepich, Taylur Ma, Kathryn Helde, Cecilia Moens, Lilianna Solnica-Krezel. 2010. Morphogenic defects in maternal zytotic *dachsous1* mutants. Poster presentation. The 9th international meeting on zebrafish development and genetics. Madison, WI.

12. **Haiting Ma**, Cunxi Li, Robert J Coffey, Lilianna Solnica-Krezel. 2009. Zebrafish homolog of *placenta specific 8* (*plac8*) may be required for cilia function. Poster presentation, Program of Developmental Biology of Vanderbilt University retreat. Buchanan, TN.

13. **Haiting Ma**, Seok-Hyung Kim, Nanbing Li, Diane Sepich, Taylur Ma, Kathryn Helde, Cecilia Moens, Lilianna Solnica-Krezel. 2009. Role of *dachsous1* (*dchs1*), a protocadherin gene during early embryonic development of zebrafish. Poster presentation, Society for Developmental Biology 68th Annual Meeting. San Francisco, CA.

14. **Haiting Ma**, Terence J. Van Raay, Lilianna Solnica-Krezel, Robert J. Coffey. 2008. Characterization of potential protein-protein interaction of zebrafish Naked Cuticle (Nkd1) and β-catenin. Poster presentation, Vanderbilt University Department of Biological Science retreat, Nashville, TN.

15. **Haiting Ma**, Chenggang Wu, Eve Tzeng, Shawn S.C. Li. 2007. Characterization of interaction of phospholipase C (PLC)-γ1 SH3 domain with hematopoietic progenitor kinase-1 (HPK1). Poster presentation, University of Western Ontario Department of Biochemistry retreat, London, Ontario.

SELECTED SCHOLARSHIPS AND ACADEMIC AWARDS

June 2011	Victor Hamburger award for best student talk. Washington University in St. Louis Program of Developmental Biology retreat.
July 2009	Vanderbilt University graduate school travel grant.
2005-2006	Western Graduate Research Scholarship (WGRS).
2004-2005	International Graduate Student Scholarship (IGSS) and Special University Scholarship (SUS).
2003-2004	The First-Class Scholarship of Nankai University; "Bao-steel" Scholarship (endowed by Bao-steel Education Fund).
2002-2003	National Scholarship (the First-Class).

EXPERIENCE

Apr 2011- Dec 2011	Student consultant for the BALSA group at Washington University in St. Louis.
Sep 2007-Apr 2009	Volunteering at Vanderbilt University Hospital burn center, emergency room and Red Cross at Nashville
March 26, 2010	Chair of the session "Cell signaling in normal and diseased conditions." at Vanderbilt University the 24th graduate student research symposium.
Jan 2009- Nov 2009	Teaching assistant for Biological Sciences 111 at Vanderbilt University.
Sep 2004-Nov 2004	Teaching assistant for Medical Genetics 400 at University of Western Ontario.